Immunological and Biosynthetic Studies of the Human Pyruvate Dehydrogenase Complex

UNIVERSITY
of
GLASGOW

Hiba Saeed Ahmed Bagader Al-Amodi

Division of Biochemistry & Molecular Biology, IBLS
University of Glasgow

A thesis submitted for the degree of
Doctor of Philosophy

This thesis is dedicated to my husband
&
to the fulfilment of our dream

Declaration

I hereby declare that the work presented in this thesis in my own, except where otherwise cited or acknowledged. No part of this thesis has been presented for any other degree.

Hiba Al-Amodi

August, 2007

Acknowledgements

In the first instance, I would like to acknowledge my deep gratitude to the Lord Almighty Allah for his everlasting favors upon me. I could not have reached this stage without my faith in him.

Next, I must thank the Ministry of Higher Education of Saudi Arabia who funded my PhD and also all members of the Saudi Arabian Cultural Bureau for their continuous administrative support.

I would like to take this opportunity to give a big and a great thanks to my supervisor Prof Gordon Lindsay for his guidance also helping me to remain focused and calm throughout the many trying times during the last four years which have been instrumental in the success of this project and for proof reading my thesis. Your practical and emotional support is very much appreciated.

The following people deserve a word of thanks for their important contribution to my work: Prof. Freda K. Stevenson, University of Southampton; Prof. Ben Luisi, University of Cambridge; and the team headed by Dr. Alison Ashcroft at the Astbury Centre for Structural Molecular Biology, University of Leeds.

I owe a very special thanks to my husband Abdullah for his tremendous patience, understanding and ongoing encouragement during the entire period of my study. This thesis would be incomplete without a mention of his support. He was my own "soul out of my soul," who kept my spirits up when the muses failed me. If he had not persisted with his words of wisdom and hope I fear I may have given up at some point.

I am also greatly indebted to my parents and all my brothers and sisters, especially my twin sister Hala, although they can not be with me in person I have no doubt they have been with me in spirit with their good wishes and prayers.

Last but not least, I would like to extend my thanks also to all my friends and colleagues, past and present in L233 and L232.

Abstract

The human pyruvate dehydrogenase multi-enzyme complex (PDC) catalyses the oxidative decarboxylation of pyruvate, transferring the resultant acetyl group to coenzyme A. It belongs to the family of 2-oxoacid dehydrogenase complexes that includes the 2-oxoglutarate dehydrogenase (OGDC) and branched-chain 2-oxoacid dehydrogenase complexes (BCOADC). Each assembly consists of multiple copies of three distinct component enzymes termed E1, E2 and E3. Human PDC also contains an accessory subunit (E3BP) that mediates stable E3 integration into the E2 'core' of the complex. Human E2-PDC consists of the following domains: two tandemly-repeated, amino-terminal lipoyl domains in each of which the lipoic acid cofactor is attached covalently in amide linkage to a specific lysine residue; an E1-binding domain and a carboxy-terminal catalytic core domain. E3BP, an E2-related polypeptide, consists of a single lipoyl domain, an E3-binding domain and a carboxy-terminal region with no known enzymatic function.

Primary biliary cirrhosis (PBC) is a chronic autoimmune liver disease in which inflammatory infiltration of the intrahepatic bile ducts leads to damage of the biliary epithelial cells followed by fibrosis, cirrhosis and ultimately liver failure. The disease is characterised by the presence of antimitochondrial antibodies (AMA), the production of which occurs at a very early stage of the disease. The major mitochondrial autoantigens have been identified as key constituents of the 2-OADCs, primarily the E2 and E3BP subunits of human PDC. AMA to these polypeptides are present in the serum of more than 95% of patients with PBC.

PD1 and PD2 are monoclonal antibodies (mAbs) secreted by individual patient-derived hybridomas (IgG/λ) that interact with a common lipoylation-dependent epitope found on both E2 and E3BP lipoyl domains although the precise antigenic determinant has not been fully defined to date. To address this issue, three amino acid residues adjacent to the lipoylated lysine residue of the inner lipoyl domain of E2-PDC, ILD-PDC were mutated systematically to the equivalent residues found in the non-reactive lipoyl domain of *Arabidopsis thaliana* plastid E2-PDC. In parallel, the non-reactive lipoyl domain of the E2 enzyme of the human 2-oxoglutarate dehydrogenase complex, LD-OGDC was mutated at several amino acids around the lipoylated lysine residue to the equivalent residues found in the reactive lipoyl domains of E2 and E3BP-PDC in attempts to restore the level of Ab recognition to that of the ILD-PDC. These studies

have permitted us to determine the key residues involved in PD1 and PD2 recognition and also their influence on the extent of lipoylation.

By using Western blot analysis and ELISA for ILD-PDC and LD-OGDC mutants, the epitope recognized by these mAbs was located to the C-terminal side of the key lipoyl-lysine residue of the domain. Interestingly, there was no specific amino acid, apart from the lipoyl-lysine, that could be considered as essential to Ab recognition but there was a cumulative effect of multiple mutations. Native gel analysis permitted us to study the lipoylation status of these mutants through the separation of lipoylated and non-lipoylated domains. These studies have confirmed that, apart from the lipoyl-lysine residue, there is no specific motif or individual residue that is essential for lipoylation. These data were all consistent with the hypothesis that a precise structural cue involving the presentation of the lipoyl-lysine residue at the tip of a type I β-turn was a prerequisite for recognition by the lipoylating enzyme(s).

The lipoylation status of the various domains was confirmed by subjecting all mutants to modification using mPEG maleimide, a thiol group reagent (M_r 5000). In contrast to a previous report, it was observed that the minor holodomain form (20%) of wild type ILD-PDC produced in *E. coli* in the absence of exogenous lipoic acid represented octanoylated rather than lipoylated domain as it was not amenable to mPEG maleimide (mPEG) modification. Q-TOF mass spectrophotometry was employed for confirmation of the identity of the octanoylated ILD-PDC produced *in vivo*. Moreover, it was realized that PD1 and PD2 do not interact exclusively with lipoylated ILD-PDC as the octanoylated domain, lacking the dithiolane ring, also gave a signal of equivalent intensity on Western blotting. However, modification of lipoamide thiols of ILD-PDC with bulky substituents, mPEG, 4-hydroxy-2-nonenal, N-ethylmaleimide and iodoacetamide yielded modified forms of the ILD that were undetectable when probed with these mAbs. It is suggested that this loss of recognition is not attributable to the importance of the dithiols in Ab recognition *per se* but rather to the fact that these substituents may block or mask the epitope from Ab recognition as a result of steric hindrance.

In an attempt to investigate the hypothesis that PBC could be induced by aberrant modification of the lipoyl-lysine residue via natural metabolites or xenobiotic agents serving as substrates for *E. coli* LplA ligase, the non-lipoylated domain of human ILD-PDC (produced in the absence of the exogenous lipoic acid) was modified *in vitro* with

various lengths of saturated fatty acids (C2-C14) and related compounds. These included a branched-chain fatty acid (C8), valproic acid, a common anti-epileptic drug causing steatosis and an unsaturated aliphatic compound, trans-2-nonenoic acid, closely related in structure to a major lipid peroxidation product, 4-hydroxynonenal. It was shown that *E. coli* lipoyl LplA ligase has a broad substrate specificity that was not exclusive to 8-carbon substrates; it can incorporate a range of saturated fatty acids of varying chain length (C6 to C12) and also branched or unsaturated compounds with variable degrees of efficiency.

Western blot analysis was employed to study the cross reactivity between these modified ILD-PDC domains and mAb PD1 or PD2. Incorporation of a fatty acid with a minimal chain length of 8-carbon atoms (octanoate) was necessary to elicit restoration of mAb cross-reactivity. Similar responses were induced by modification with decanoate and dodecanoate as well as valproate and trans-2-nonenoic acid.

Interestingly, trans-2-nonenoic acid is a close relative of the major lipid peroxidation product, 4-hydroxynonenal that can be readily converted to 4-hydroxy trans-2-nonenoic acid *in vivo*. This compound is potentially a suitable substrate for the bacterial lipoylation system. Thus, it is proposed that oxidative stress could lead to aberrant modification of nascent non-lipoylated E2 components by this route resulting in neoantigen formation. Chronic or severe exposure to oxidative stress may also promote energy depletion by causing PDC malfunction and metabolic damage. These events may render modified PDC neoantigens accessible to the immune system, there breaking tolerance and initiating an autoimmune response against native lipoylated E2 and/or E3BP. However, the question as to why AMA are targeted mostly to E2 and E3BP-PDC is still an enigma.

The second part of the thesis involved biosynthetic studies of the E2, E3BP and E3 enzymes of the PDC and the role(s) of their N-terminal presequences (matrix targeting signals) in the regulation of protein expression/folding. A variety of precursor constructs of human PDC were engineered to carry out this work. Thus, pre-E2, its N-terminal truncated form and pre-E3BP containing elongated presequences (53-86 amino acids) as well as pre-E3 housing a standard length presequence (35 amino acids) were cloned into pET-14b. In addition, the work was extended to study the behaviour of the hybrid precursors, pE2-E3 and pE3-E2 cloned into the same plasmid.

The general findings of this study were as follows: firstly, comparing the levels of expression of each precursor to its mature form through small-scale protein inductions in *E. coli* at different temperatures, it was observed that both types of presequence as well as the nature of mature protein affect the level of protein expression. Therefore, it was noticed that both types of presequence had no significant effect on the level of protein expression when they were linked to the mature E3 whereas the negative effect of these presequences was apparent when they were linked to mature E2 or E3BP. Secondly, comparing the solubility of precursors with their mature forms, both extended and standard presequences markedly reduced the solubility of precursor constructs by inducing the production of inclusion bodies although the effect appeared to be more marked with the former. Thirdly, on decreasing the rate of the protein synthesis by growing *E. coli* cultures at lower temperatures, it was possible to minimise the formation of insoluble protein aggregates and achieve partial or indeed complete solubility of precursor forms in some cases. Fourthly, these precursors appeared to retain the ability to fold correctly or at least to initiate the correct folding pathway. Thus both soluble and insoluble fractions of E2 and E3BP precursors contained lipoylated domains as judged by their ability to cross-react with PD2, an indication that these N-terminally located domains had adopted their native conformations.

These observations were consistent with the view that N-terminal mitochondrial targeting sequences markedly reduced the rate of protein folding rather than suppressing the folding process completely. In this scenario, precursors would exist as nascent folding intermediates for longer periods compared to their mature equivalents and so would be more prone to aggregation and degradation as observed in this study. Further experiments are planned to test this hypothesis.

Table of Contents

Declaration ..... **I**

Acknowledgements ..... **II**

Abstract ..... **III**

Table of Contents ..... **VII**

List of Tables ..... **XIV**

List of Figures ..... **XV**

Abbreviations ..... **XIX**

Chapter 1 Introduction **1**

1.1 The 2-oxoacid dehydrogenase complexes **2**

1.1.1 Catalytic mechanism 4

1.1.2 Complex organisation 4

1.1.2.1 Pyruvate dehydrogenase (E1) 6

1.1.2.2 Dihydrolipoamide acetyltransferase (E2) 10

1.1.2.2.1 The peripheral subunit binding domain (PSBD) 12

1.1.2.2.2 The C-terminal domain (CD) 13

1.1.2.2.3 The linker regions (LR) 15

1.1.2.3 Dihydrolipoamide dehydrogenase (E3) 16

1.1.2.4 E3-binding protein (E3BP) 17

1.1.3 Regulation of the pyruvate dehydrogenase complex 20

1.1.4 Protein targeting 24

1.1.5 Genetic defects in OADCs 28

1.2 Immunity and autoimmunity: an overview **30**

1.2.1 Primary biliary cirrhosis: an overview 32

1.2.2 Autoantibodies and their autoantigens 36

1.2.3 Nuclear autoantigens in PBC 37

1.2.4 Identification of the M2 mitochondrial antigens 38

1.2.4.1 AMA and the 2-oxoacid dehydrogenase complexes 41

1.2.4.2 Enzyme inhibitory properties of antimitochondrial antibodies 43

1.2.4.3 T-cell responses and PBC 44

1.2.4.4 Biliary epithelial cells and PBC 46

1.2.4.5 Selective targeting of bile ducts in PBC 50

1.2.4.6 Molecular mimicry and PBC 53
1.3 Aims of this thesis....56
Chapter 2 Materials and Methods 58
2.1 Molecular biology materials....59
2.1.1 Chemicals 59
2.1.2 Enzymes....59
2.1.3 Synthetic oligonucleotides....59
2.1.3.1 Oligonucleotides for precursor cloning of human PDC....59
2.1.3.1.1 Oligonucleotides used for subcloning pre-E2, N-terminal pre-E2 truncate and its mature form 59
2.1.3.1.2 Oligonucleotides for pre-E3 cloning....60
2.1.3.1.3 Oligonucleotides for pre-E3BP cloning....60
2.1.3.1.4 Oligonucleotides for pE2-E3 cloning 60
2.1.3.1.5 Oligonucleotides for pE3-E2 cloning 61
2.1.3.2 Oligonucleotides for cloning the lipoyl domains of *Arabidopsis thaliana (A. thaliana)* 61
2.1.3.2.1 Oligonucleotides used for cloning the lipoyl domain of *A. thaliana* plastic E2-PDC 61
2.1.3.2.2 Oligonucleotides used for cloning the inner lipoyl domain of *A. thaliana* mitochondrial E2-PDC 62
2.1.3.3 Oligonucleotide primers for site-directed mutagenesis....62
2.1.3.3.1 Oligonucleotides for human ILD-E2 mutations 62
2.1.3.3.2 Oligonucleotides for human LD-OGDC mutations....63
2.1.4 Bacterial strains 64
2.1.4.1 For molecular biology techniques....64
2.1.4.2 For protein expression....64
2.1.5 Plasmid vectors....65
2.1.6 Molecular biology kits....65
2.1.7 Gel documentation....66
2.1.8 Nucleotide accession numbers....66
2.2 Molecular biology methods 66
2.2.1 Bacterial media 66
2.2.2 Bacterial cell storage 67
2.2.3 Initiating bacterial growth 67
2.2.4 Preparation of chemically competent *E. coli* cells 67
2.2.5 Transformation of chemically competent *E. coli* by heat shock 67
2.2.5.1 Transformation of competent *E. coli* with plasmid DNA 68
2.2.5.2 Transformation of competent *E. coli* with ligated plasmid....68

2.2.5.3 Transformation of *E. coli* XL-1 Blue chemically competent cells 68
2.2.5.4 Transformation of one shot TOP10 competent cells with ligated plasmid 68
2.3 DNA techniques.....69
2.3.1 Agarose gel electrophoresis.....69
2.3.2 Polymerase chain reaction (PCR).....69
2.3.2.1 Amplification of E2, E3, E3BP precursors, N-terminal pre-E2 truncate and its mature form 70
2.3.2.2 Amplification of LD and ILD of *A thaliana* chloroplastic and mitochondrial E2-PDC.....71
2.3.3 TOPO TA vector cloning 72
2.3.4 Restriction digestion.....73
2.3.4.1 Restriction digestion of plasmids.....73
2.3.4.2 Restriction digestion of PCR Products.....73
2.3.4.2.1 Restriction endonuclease digestion of E2, E3, E3BP precursors, N-terminal pre-E2 and E2 truncates as well as presequences of E2 and E3 73
2.3.4.2.2 Restriction endonuclease digestion of *A. thaliana* chloroplastic LD- and mitochondrial ILD-PDC and pGEX-2T vector 74
2.3.5 PCR Based mutagenesis of ILD-PDC and LD-OGDC 74
2.3.6 DNA isolation and purification from agarose 75
2.3.7 Determination of DNA size.....76
2.3.8 Ligation of Digested Plasmids and PCR products.....76
2.3.9 Plasmid Propagation and Purification 76
2.3.10 DNA preparation for sequencing.....77
2.3.11 Protein overexpression 77
2.3.11.1 Small scale over-expression of precursor and mature proteins of various constructs of human PDC as well as N-terminal E2-PDC truncate and its LD form of *A. thaliana* plastid.....77
2.3.11.2 Large scale over-expression of E3, *LplA*, and lipoyl domain constructs of E2-PDC and E2-OGDC as well as LDS of human E3BP, Atpt LD-PDC and Atmt ILD-PDC.....78
2.3.12 Bacterial cell disruption.....79
2.4 Protein Materials 80
2.4.1 Chemicals 80
2.4.1.1 Chemicals for modification of the lipoamide cofactor of ILD-PDC 80
2.4.1.2 Chemicals for modification of the lipoyl-lysine residue of ILD-PDC.....80
2.4.1.3 General chemicals 80
2.4.2 Enzymes.....81
2.4.3 Antibodies.....81
2.4.4 Biological tissues.....81

2.4.5 Equipments 82
2.4.6 Spectrophotometric equipment 82
2.4.7 Dialysis, buffer exchange and protein concentration 82
2.5 Protein methods 83
2.5.1 Solubilisation of expressed fusion proteins 83
2.5.2 Protein purification 84
2.5.2.1 Purification of GST-fusion proteins 84
2.5.2.2 Cleavage of GST-tag 84
2.5.2.3 Metal chelate chromatography 85
2.5.2.3.1 Preparation for metal chelate chromatography 85
2.5.2.3.2 His-Tag purification of human E3 85
2.5.2.4 Anion exchange chromatography 86
2.5.2.5 Gel filtration 86
2.5.3 Enzyme assays 87
2.5.3.1 Dihydrolipoamide dehydrogenase (E3) activity 87
2.5.3.2 PDC activity 88
2.5.4 Protein analysis 88
2.5.4.1 SDS-Polyacrylamide Gel Electrophoresis (SDS-PAGE) 88
2.5.4.1.1 SDS-PAGE Buffers 88
2.5.4.1.2 SDS-PAGE 89
2.5.4.2 Discontinuous non-denaturing gel electrophoresis 90
2.5.5 Estimation of protein concentration 91
2.5.6 Immunoblotting 91
2.5.6.1 Enhanced chemiluminescence (ECL™) for detection of specific antigens (Western Blot) 91
2.5.6.2 Immunodetection with Anti-His antibodies or Anti-HisHRP conjugates (chemiluminescent method) 92
2.5.6.3 Stripping and preparing the membrane 93
2.5.7 Measurement of antibody titre against different lipoyl domain constructs by enzyme-linked immunoabsorbent assay (ELISA) 93
2.5.8 Modification of the lipoamide cofactor 94
2.5.8.1 mPEG maleimide, N-ethylmaleimide (NEM) and iodoacetamide modification 94
2.5.8.2 HNE modification 95
2.5.9 Modification of the lipoyl-lysine residue 95
2.5.10 Quadrupole-time of flight (Q-TOF) Mass spectrometry 96
2.5.10.1 Electrospray ionisation (ESI) mass spectrometry 97
2.5.10.2 Sample preparation 99
2.5.10.3 Identification of the lipoyl domain substituent 99

Chapter 3 Investigation of the molecular basis of patient derived monoclonal antibody interactions with E2 and E3BP lipoyl domains of the human pyruvate dehydrogenase complex..... 104

3.1 Section 1 105

3.1.1 Aims of this section 106

3.1.2 RESULTS 106

3.1.2.1 PCR amplification of lipoyl domains of *A. thaliana* E2-PDCs 106

3.1.2.2 Cloning of LDs of *Arabidopsis thaliana* E2-PDCs.....107

3.1.2.3 Protein expression 110

3.1.2.4 GST-tag purification of LDs from various sources.....110

3.1.2.5 Investigation into the reactivity of different wild type LDs with mAb PD2.....110

3.1.2.6 Checking the lipoylation of LD-GST fusion proteins by methoxy poly (ethylene glycol) maleimide (mPEG maleimide) modification 115

3.1.2.7 Checking the lipoylation of the chloroplastic *A. thaliana* E2-PDC didomain.....117

3.2 Section 2 121

3.2.1 Aims of this section 121

3.2.2 RESULTS 123

3.2.2.1 Generation of the ILD-PDC mutants 123

3.2.2.2 Expression and purification of the mutant constructs 123

3.2.2.3 Checking the cross reactivity of ILD-PDC mutants with mAbs PD1 and PD2.....126

3.2.2.4 Checking the lipoylation of ILD mutants.....126

3.2.2.5 Comparison of the cross reactivity between mAbs PD1 and PD2 and mutated constructs of ILD-PDC by ELISA 130

3.3 Section 3 137

3.3.1 Aims of this section 137

3.3.2 RESULTS 139

3.3.2.1 Generation of LD-OGDC mutant constructs and checking the cross reactivities of these mutants with mAbs PD1 and PD2 139

3.3.2.1.1 Mutation of the two residues differing in LD-OGDC in the highly conserved central block 139

3.3.2.1.2 Mutation of single conserved N- and C-terminal residues located outside the central block differing in LD-OGDC.....142

3.3.2.1.3 Multiple mutations involving residues inside and outside of the central core.....142

3.3.2.1.4 Additional mutations of LD-OGDC in the C-terminal region adjacent to the central block.....143

3.3.2.2 Checking the lipoylation of LD-OGDC mutants 147

3.3.2.3 Determining the cross reactivity between mAbs PD1 and PD2 and mutated constructs of LD-OGDC by ELISA 148

3.4 Discussion 153

3.4.1 Cross reactivity and lipoylation states of wt ILD-PDC and its mutant K173Q in the presence and absence of exogenous lipoate 154

3.4.2 Cross reactivity and lipoylation states of ILD-PDC mutants 155

3.4.3 Cross reactivity and lipoylation states of LD-OGDC mutant constructs 158

3.4.4 Concluding remarks 162

Chapter 4 Investigation of the effect of chemical modification of the lipoic acid prosthetic group and the lipoyl lysine residue on mAbs recognition 165

4.1 Section 1 166

4.1.1 Chemical compounds and PBC 167

4.1.2 Aims of this chapter 170

4.1.3 RESULTS 171

4.1.3.1 Determination of the extent to which the dithiolane ring of the lipoate cofactor of the ILD-PDC constitutes an important part of the antibody recognition site 171

4.1.3.1.1 Methoxy poly (ethylene glycol) maleimide (mPEG maleimide) modification 171

4.1.3.1.1.1 Modification of bPDC with mPEG maleimide 171

4.1.3.1.1.2 Modification of recombinant ILD with mPEG maleimide 172

4.1.3.1.2 4-hydroxy-2-nonenal (HNE) modification 172

4.1.3.1.2.1 Modification of bPDC with HNE 172

4.1.3.1.2.2 Modification of recombinant ILD-E2 with NHE 173

4.1.3.1.3 N-ethylmaleimide (NEM) modification 180

4.1.3.1.3.1 Modification of bovine PDC with NEM 180

4.1.3.1.3.2 Modification of recombinant ILD-E2 with NEM 180

4.1.3.1.4 Modification of recombinant ILD-E2 with iodoacetamide 181

4.1.4 Discussion 186

4.2 Section 2 188

4.2.1 The lipoyl domain 188

4.2.1.1 Structure of the Lipoyl Domain 188

4.2.2 The lipoic acid moiety 190

4.2.3 RESULTS 194

4.2.3.1 Overexpression and purification of *E. coli* LplA 194

4.2.3.2 Incorporation of various fatty acids and related compounds into ILD-E2 *in vitro* using *E. coli* LplA ligase 194

4.2.4 Discussion 206

Chapter 5 Molecular cloning and overexpression of E2, E3BP and E3 precursors as well as preliminary folding studies of E2 and E3BP precursors of human pyruvate dehydrogenase complex 213

5.1 Introduction.....214

5.2 Aims of this study.....217

5.3 RESULTS 218

5.3.1 General strategy for cloning E2, E3BP, E3 precursors, the N-terminal truncate of mature E2 and its precursor, pE2-E3 and pE3-E2 218

5.3.1.1 PCR amplification.....218

5.3.1.2 Ligation, transformation and identification of clones.....220

5.3.2 Overexpression of precursor proteins at different temperatures 230

5.3.3 Checking the solubility of recombinant E2, E3BP and E3 constructs by immunoblotting 236

5.3.4 Checking the folding of precursors using immunoblot analysis 243

5.4 Discussion.....248

Chapter 6 General discussion 253

References 260

Appendices 289

List of Tables

1-1 Summary of reported prevalence of familial primary biliary cirrhosis 35
1-2 Characteristics of mitochondrial antigens in PBC 40
3-1 Alignment of E2 and E3BP lipoyl domains from various species 122
3-2 Alignment of E2 and E3BP lipoyl domains from various species 138
5-1 Comparison of M_r values of mature and precursor forms of constituent subunits of human PDC, OGDC and BCOADC 216

List of Figures

Chapter 1

Figure 1-1 Location of the 2-oxoacid dehydrogenase complexes in cellular energy metabolism 3

Figure 1-2 Reaction mechanism of pyruvate dehydrogenase complex 5

Figure 1-3 Structure of the octahedral and icosahedral E2 inner cores of PDC 7

Figure 1-4 Three dimensional structure of E1 from the human pyruvate dehydrogenase complex 9

Figure 1-5 Domain organisation of the E2 and E3BP components from the 2-oxoacid dehydrogenase complexes 11

Figure 1-6 Schematic representation of the peripheral subunit binding domain of *B. stearothermophilus* E2-PDC 14

Figure 1-7 Structure of human dihydrolipoamide dehydrogenase (E3) 18

Figure 1-8 Regulatory mechanisms for pyruvate dehydrogenase by feedback inhibition and covalent modification via a protein phosphorylation/ dephosphorylation system 23

Figure 1-9 Schematic overview of import of preproteins into mitochondria 27

Chapter 2

Figure 2-1 Basic diagram for a mass spectrometer 97

Figure 2-2 Q-TOF mass spectrometry in MS mode 98

Figure 2-3 Mass spectra of ILD-PDC plus lipoate 101

Figure 2-4 Mass spectra of ILD-PDC K173Q 102

Figure 2-5 Mass spectra of ILD-PDC minus lipoate 103

Chapter 3

Figure 3-1 Amplification products of chloroplastic and mitochondrial lipoyl domains of *A. thaliana* E2-PDC 108

Figure 3-2 Restriction digestion of putative positive colonies showing the presence of inserts of the expected sizes 109

Figure 3-3 Overexpression of ILD and LD of mitochondrial and chloroplastic E2-PDC from *A. thaliana* expressed as GST fusion proteins 112

Figure 3-4 Solubilities of LDs of plant mitochondrial and chloroplastic E2-PDC expressed as GST fusion proteins 113

Figure 3-5 The reactivities of various wild type lipoyl domains (LDs) with mAb PD2 114

Figure 3-6 mPEG-maleimide modification (gel shift assay) of different lipoyl domain GST fusion constructs 116

Figure 3-7 Cross reactivities of different wild type LDs with mAb PD2 119

Figure 3-8 mPEG-maleimide modification (gel shift assay) of different thrombin cleaved LDs 120

Figure 3-9 Overexpression of single (E168V), double (T171S:T175D), and triple (E168V:T171S:T175D) ILD mutants 124

Figure 3-10 Solubility assessment of single (E168V), double (T171S:T175D) and triple (E168V:T171S:T175D) mutants of human ILD-PDC-GST-fusion proteins 125

Figure 3-11 Immunoblotting of the recombinant ILD-PDC mutants with mAb PD2 132

Figure 3-12 Checking the lipoylation of ILD-PDC mutants using non-denaturing PAGE analysis 133

Figure 3-13 Checking the lipoylation of mutant ILD constructs of PDC by native PAGE 134

Figure 3-14 mPEG maleimide modified ILD-PDC mutants on SDS-PAGE analysis 135

Figure 3-15 Binding of mAb PD2 to mutant ILD-PDC constructs detected by ELISA 136

Figure 3-16 Overexpression of T44A, S45T and T44A:S45T mutants of LD-OGDC 140

Figure 3-17 Solubility assessment of LD-OGDC T44A:S45T expressed as a GST-fusion protein 141

Figure 3-18 Immunoblotting of recombinant LDs-OGDC T44A, S45T, T44A:S45T, D33G, P49E and D33G:P49E constructs with mAb PD2 144

Figure 3-19 Immunoblotting of the recombinant S45T:P49E, T44A:S45T:P49E, D33G:T44A:S45T and D33G:T44A:S45T:P49E LD-OGDC constructs with mAb PD2 145

Figure 3-20 Immunoblotting of the recombinant LD-OGDC mutant constructs with mAb PD2 146

Figure 3-21 Checking the lipoylation of LD-OGDC mutants using native PAGE analysis 149

Figure 3-22 Checking the lipoylation of LD-OGDC mutants using mPEG maleimide modification 150

Figure 3-23 Checking the lipoylation of LD-OGDC-GST mutants using mPEG maleimide modification 151

Figure 3-24 Binding of mAb PD2 to mutant constructs of LD-OGDC detected by ELISA 152

Chapter 4

Figure 4-1 Activity of bovine PDC after modification with mPEG maleimide 174

Figure 4-2 Modification of bovine PDC with mPEG maleimide: effect on enzyme recognition by PD2 175

Figure 4-3 Modification of human ILD-E2 with mPEG maleimide: effect on recognition by PD2 176

Figure 4-4 Activity of bovine PDC after modification with increasing concentrations of HNE 177

Figure 4-5 Modification of bovine PDC with HNE: effect on autoantibody recognition 178

Figure 4-6 Modification of human ILD-PDC with HNE: effect on recognition by PD2 179

Figure 4-7 Activity of bovine PDC after modification with NEM 182

Figure 4-8 Modification of bovine PDC with NEM: effect on PD2 recognition 183

Figure 4-9 Modification of human ILD-E2 with NEM: effect on PD2 recognition 184

Figure 4-10 Modification of human ILD-E2 with iodoacetamide: effect on recognition by PD2 185

Figure 4-11 Schematic representation of the three-dimensional structure of the inner lipoyl domain from human E2-PDC 189

Figure 4-12 Complementary pathways of protein lipoylation in *E. coli* 192

Figure 4-13 Overexpression of *E. coli* lipoyl ligase 197

Figure 4-14 Solubility assessment of *E. coli* lipoyl ligase after overexpression at various temperatures 198

Figure 4-15 Post-translational modification of the human ILD-PDC *in vitro* by octanoic and decanoic acids 199

Figure 4-16 Post-translational modification of the human ILD-E2 *in vitro* by hexanoic acid 200

Figure 4-17 Post-translational modification of the human ILD-E2 *in vitro* by fatty acids of varying chain length 203

Figure 4-18 Post-translational modification of the human ILD-E2 *in vitro* with valproate as a substrate 204

Figure 4-19 Post-translational modification of the human ILD-PDC *in vitro* with trans-2-nonenoic acid 205

Figure 4-20 Hypothetical scheme reflecting the mechanism by which biological compounds may break tolerance and induce PBC 211

Figure 4-21 hypothetical scheme reflecting the mechanism by which microorganism infection or biological compounds may break the tolerance to native E2-PDC 212

Chapter 5

Figure 5-1 Nucleotide sequence of EST IMAGE clone 2394617 obtained from BLAST search matched against chromosome 11 clone RP11-708L7 219

Figure 5-2 Amino acid sequence of the deduced E2-PDC presequence btained from BLAST search 219

Figure 5-3 PCR products of full length pre-E2, N-terminal pre-E2 truncate and its mature form 223

Figure 5-4 Restriction digestion of plasmids of pre-E2, N-terminal pre-E2 truncate and its mature form 224

Figure 5-5 PCR amplification of presequences and mature forms of E2 and E3 225
Figure 5-6 Restriction digestion of pE2-E3 plasmids 226
Figure 5-7 Restriction digestion of pE3-E2 plasmids 227
Figure 5-8 PCR amplification and restriction digestion of pre-E3 plasmids 228
Figure 5-9 PCR amplification and restriction digest of pre-E3BP plasmids 229
Figure 5-10 Overexpression of E2 precursor, mature E2 and their N-terminal truncated forms 232
Figure 5-11 Overexpression of hybrid pE2-E3 and pE3-E2 at various temperatures .. 233
Figure 5-12 Overexpression of pre-E3 and its mature form at various temperatures ... 234
Figure 5-13 Overexpression of pre-E3BP and its mature form at various temperatures 235
Figure 5-14 Western blot analysis of pre-E2 and its mature form expressed in *E. coli* to check solubility at different temperatures 238
Figure 5-15 Western blot analysis of the N-terminal pre-E2 truncate and its mature E2 form to check the solubility at various temperatures 239
Figure 5-16 Western blot analysis of pE2-E3 and pE3-E2 expressed in *E. coli* to check solubility at various temperatures 240
Figure 5-17 Western blot analysis of pre-E3 and its mature form expressed in *E. coli* at various temperatures 241
Figure 5-18 Western blot analysis of pre-E3BP and its mature form expressed in *E. coli* at various temperatures 242
Figure 5-19 Western blot analysis of pre-E2 and its mature form expressed in *E. coli* at various temperatures 244
Figure 5-20 Western blot analysis of N-terminal pre-E2 truncate and its mature form expressed in *E. coli* at various temperatures 245
Figure 5-21 Western blot analysis of pE3-E2 expressed in *E. coli* at various temperatures 246
Figure 5-22 Western blot analysis of pre-E3BP and its mature form expressed at various temperatures 247
Figure 5-23 Aggregation of non-native protein chains as a side-reaction of the productive folding process 251

Abbreviations

Ab	Antibody
ALDH	aldehyde dehydrogenase
AMA	anti-mitochondrial antibodies
Amp	Ampicillin
AMP	adenine monophosphate
Amu	atomic mass unit
API	atmospheric pressure ionisation
approx.	approximately
APS	ammonium persulphate
ATP	adenine triphosphate
BCAA	branched chain amino acids
BCOADC	branched chain 2-oxoacid dehydrogenase complex
BEC	biliary epithelial cell
Bpdc	bovine pyruvate dehydrogenase complex
BSA	bovine serum albumin
BSO	buthionine sulfoximine
CD	circular dichroism
CD	catalytic domain
CoA	coenzyme A
CTL	cytotoxic T lymphocyte
CVHC	chronic viral hepatitis C
Da	Daltons
DHL	Dihydrolipoamide
DTT	Dithiothreitol
E1	pyruvate decarboxylase
E2	dihydrolipoamide acetyltransferase
E3	dihydrolipoamide dehydrogenase
E3BP	dihydrolipoamide dehydrogenase-binding protein
ECL	enhanced chemiluminescence

EDTA	ethylenediaminetetra-acetate
ELISA	enzyme-linked immunoabsorbent assay
EtBr	ethidium bromide
FAD	flavin adenine dinucleotide
GFC	gel filtration chromatography
GMP	guanine monophosphate
GST	glutathione S-transferase
GTP	guanine triphosphate
HNA	4-hydroxy tran-2-nonenoic acid
HNE	4-hydroxy-2-nonenal
HRP	horse radish peroxidase
Ig	Immunoglobulin
ILD	inner lipoyl domain
IPTG	isopropyl-thio-b-D-galactopyranoside
LA	lipoic acid
LA	lactic acidosis
LAE	lipoate-activating enzyme
LB	Luria broth
LD	lipoyl domain
LplA	lipoate-protein ligase A
LT	lipoyl-AMP:*N*$^{\epsilon}$-lysine lipoyltransferase
mAb	monoclonal antibody
MCP	micro-channel plate
MES	2-(N-morpholino) ethane sulfonic acid
Min	Minutes
MOPS	3-[N-Morpholino] propanesulphonate
mPEG	methoxy poly (ethylene glycol)
MPP	mitochondrial-processing peptidase
NAD^+	oxidized form of nicotinamide adenine dinucleotide
NADH	reduced form of nicotinamide adenine dinucleotide
NEM	N-ethylmaleimide

NMR	Nuclear magnetic resonance
OGDC	2-oxoglutarate dehydrogenase complex
OLD	outer lipoyl domain
PAGE	polyacrylamide gel electrophoresis
PBC	primary biliary cirrhosis
PCR	polymerase chain reaction
PBS	phosphate buffered saline
PSBD	peripheral subunit binding domain
PD	patient-derived
PDC	pyruvate dehydrogenase complex
PMSF	Phenymethylsulphonyl fluoride
ROS	reactive oxygen species
SDS	sodium dodecyl sulphate
Sec	Seconds
SPR	surface plasmon resonance
TAE	tris-acetate-EDTA
TBS	tris-buffered saline
TCA	tri-carboxylic acid
TCA cycle	tricarboxylic acid cycle
TEMED	NNN'N' –tetramethylethylenediamine
TFA	trifluoroacetic acid
TMB	3,3' ,5,5' tetramethylbenzamidine
ThDP	Thiamine diphosphate
TIM	translocases of inner mitochondrial membranes
TOM	translocases of outer mitochondrial membranes
Tris	2-amino-2-(hydroxymethyl)-1,3-propandiol
UV	Ultraviolet
v/v	volume to volume
w/v	weight to weight
Wt	wild-type
XM-ligase	xenobiotic/medium-chain fatty acid CoA ligase

Chapter 1

Introduction

1.1 The 2-oxoacid dehydrogenase complexes

The mitochondrial 2-oxoacid dehydrogenase complexes (M_r values 5-10x10^6) are members of the thiamine diphosphate (ThDP)-requiring family of multienzyme assemblies located in the mitochondrial matrix. In most organisms, there are three types of 2-oxoacid dehydrogenase complexes (OADCs): the pyruvate dehydrogenase complex (PDC), the 2-oxoglutarate dehydrogenase complex (OGDC) and the branched-chain 2-oxoacid dehydrogenase complex (BCOADC) (Pettit *et al.*, 1973; Perham, 1991). Each complex occupies a key position in intermediary metabolism and functions at a strategic point in the primary pathways of energy production linking glycolysis (PDC) with the citric acid cycle (OGDC) or in amino acid catabolism (BCOADC) as shown in Figure 1-1.

PDC catalyses the irreversible step in carbohydrate utilization by converting pyruvate to acetyl CoA which enters the TCA cycle or is used in biosynthetic pathways (Koike & Koike, 1976; Rahmatullah *et al.*, 1989; Maeng *et al.*, 1994). OGDC is required for converting 2-oxoglutarate to succinyl CoA and serves at a key regulatory point in determining flux through the Krebs cycle (Koike, 1974). BCOADC catalyzes the irreversible step in the catabolism of the essential branched-chain amino acids (BCAA) i.e. valine, leucine and isoleucine and is also involved in the degradation of threonine and methionine (Stanley & Perham, 1980; Milne *et al.*, 2002). Moreover, defects in these complexes are implicated in a variety of metabolic, genetic and autoimmune disorders including lactic acidosis, maple syrup urine disease and primary biliary cirrhosis (Patel & Harris, 1995; Yeaman *et al.*, 2000; Nellis & Danner, 2001; Milne *et al.*, 2002).

Each complex is composed of multiple copies of three major enzymes consisting of a central core, composed of either 24 or 60 E2 subunits that are responsible for E1 and E3 binding. The E1 and E2 components are distinct for each complex and are encoded by separate genes while the E3 component, at least in mammals, is common to all three complexes and is encoded by a single gene. In the mammalian, yeast and nematode PDCs, an additional subunit was identified in the 1980s and originally termed protein X (De Marcucci & Lindsay, 1985; Jilka *et al.*, 1986).

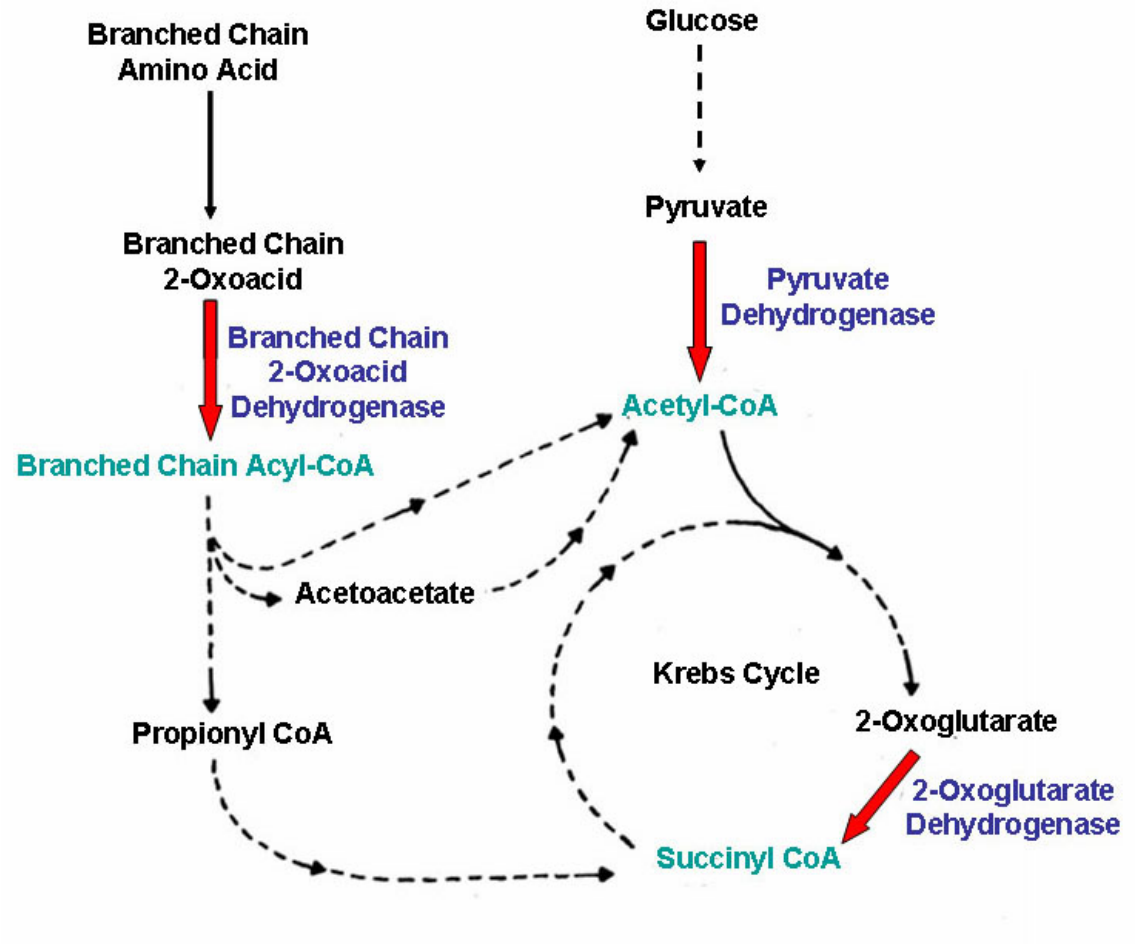

Figure 1-1 Location of the 2-oxoacid dehydrogenase complexes in cellular energy metabolism
Enzymes are shown in blue and their products in green. Red arrows represent the reactions of these complexes

This polypeptide has since been found to mediate the stable association of E3 with the E2:X core and has been renamed E3-binding protein (E3BP) (Rahmatullah *et al.*, 1989). No an equivalent subunit has been identified in any OGDCs or BCOADCs.

1.1.1 Catalytic mechanism

The overall reaction of PDC, catalysed by its three main enzymes, (E1, E2 and E3), results in the decarboxylation of pyruvate with the concomitant production of acetyl-coenzyme A (acetyl CoA), CO_2 and NADH in a series of coordinated reactions involving five coenzymes [thiamine diphosphate (ThDP), lipoic acid (LA), CoA, FAD, and NAD^+] (Figure 1-2). E1, a ThDP-requiring enzyme, catalyses the decarboxylation of pyruvate and reductive acetylation of the lipoyl moieties of E2, (Figure 1-2, reactions 1 and 2). In fact, E1 has an absolute requirement for the cofactor ThDP and Mg^{2+}. Pyruvate forms an adduct with the thiazolium ring of ThDP, 2-(2-hydroxypropionyl)-ThDP (L-ThDP); then the adduct is decarboxylated to produce a 2-(1-hydroxyethylidene)-ThDP intermediate (HE-ThDP). This intermediate undergoes oxidation while the dithiolane ring of the lipoyl moiety on E2 becomes reductively acetylated. This step produces an acetyl-dihydrolipoamide intermediate prior to acetyl group transfer to CoA by E2 leaving the dithiolane ring in the reduced form (Figure 1-2, reactions 3 and 4). E3 reoxidizes the lipoyl moiety using its FAD cofactor (Figure 1-2, reaction 5). Finally, the reduced form of the FAD cofactor is reoxidised by transfer of electrons to NAD^+ as the final electron acceptor (Figure 1-2, reaction 6) (Reed & Hackert 1990; Ciszak *et al.*, 2006).

1.1.2 Complex organisation

Mammalian pyruvate dehydrogenase complex (PDC) is responsible for overall glucose homeostasis controlling the flux of two-carbon units from glycolysis into the citric acid cycle. PDC exists as a stable, highly organised assembly of 9-10 x 10^6 Da comprising multiple copies of its three main catalytic enzymes: pyruvate dehydrogenase (E1, EC 1.2.4.1), dihydrolipoamide acetyltransferase (E2, EC 2.3.1.12) and dihydrolipoamide dehydrogenase E3 (EC 1.8.1.4) as well as an additional lipoyl containing component called E3BP. In addition, there are two regulatory enzymes, pyruvate dehydrogenase kinase (PDK, EC 2.7.1.99) and phosphatase (PDP, EC 3.1.3.43) interacting with the complex.

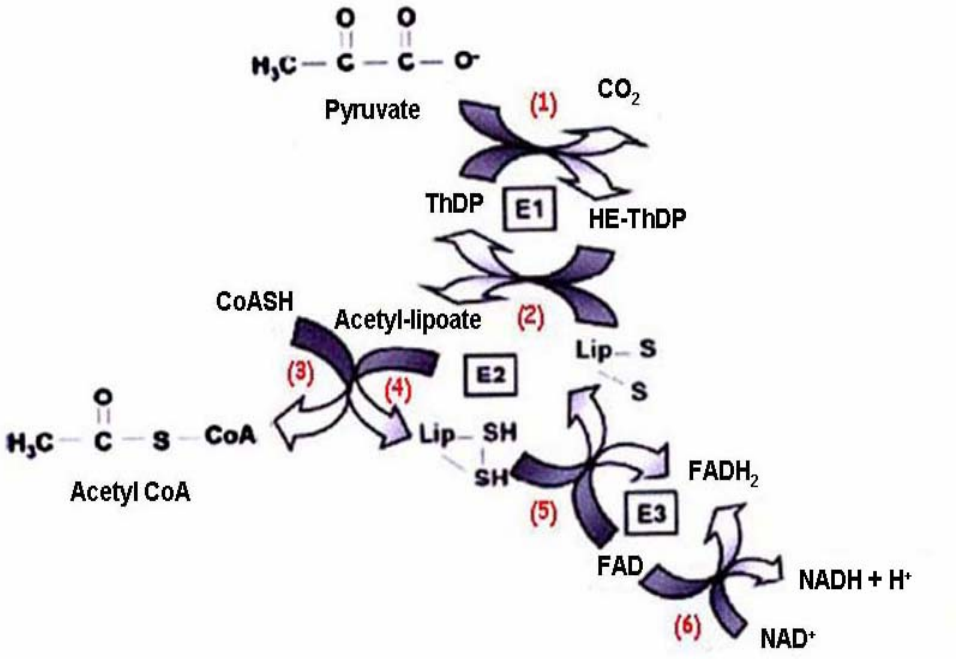

Figure 1-2 Reaction mechanism of pyruvate dehydrogenase complex
E1, pyruvate dehydrogenase; **E2**, dihydrolipoamide acetyltransferase; **E3**, dihydrolipoamide dehydrogenase; **HE-ThDP**, 2-(1-hydroxyethylidene)-ThDP; **ThDP**, thiamine diphosphate; **CoA**, coenzyme A; **NAD^+/NADH + H^+**, the oxidized and reduced forms of nicotinamide adenine dinucleotide; and **FAD/$FADH_2$,** the oxidized and the reduced forms of flavin adenine dinucleotide.

E1 employs ThDP cofactor to carry out the oxidative decarboxylation of pyruvate **(reaction 1)**, forming acetyl-dihydrolipoate that is covalently attached to the E2 component **(reaction 2)**. The E2 component catalyses the transfer of the acetyl group to CoA **(reaction 3)** leaving the dithiolane ring in the reduced form **(reaction 4)**. The resulting dihydrolipoyl group is then reoxidised by E3 forming NADH as the final product **(reactions 5 and 6)**.

They are jointly responsible for the acute regulation of PDC by controlling the reversible phosphorylation of its bound E1 enzymes (De Marcucci & Lindsay, 1985; Jilka *et al.*, 1986; Rahmatullah *et al.*, 1986; Patel & Roche, 1990; Ciszak *et al.*, 2006; Maj *et al.*, 2006).

Central to the assembly of these complexes is the oligomeric E2 'core' around which the other catalytic components are tethered tightly but non-covalently. E2 can exist in two morphologically distinct forms depending on its source. A pentagonal dodecahedral core consisting of 60 E2-PDC polypeptides with icosahedral (532) symmetry is found in complexes from mammalian cells and Gram positive bacteria, eg *Bacillus stearothermophilus* (Reed & Hackert, 1990; Perham, 1991; Milne *et al.*, 2002). However, in PDCs of Gram negative bacteria, eg *A. vinelandii* and in all known OGDCs as well as BCOADCs, the E2 core is present as a 24-meric structure with octahedral (432) symmetry. Figure 1-3 illustrates these two types of central core architecture (Reed & Hackert, 1990; Perham, 2000).

Mammalian PDC can accommodate up to 30 $\alpha_2\beta_2$ E1 heterotetramers bound noncovalently at the 30 edges of the 60-meric E2 core. An E3BP monomer is thought to bind to each of the 12 faces of the E2 core to give a stable association of 6-12 E3 dimers (Sanderson *et al.*, 1996a; Stoops *et al.*, 1997). However, an alternative substitution model has been proposed recently in which 12 subunits E3BP replace an equivalent number of an E2s to form an $E2_{48}$:$E3BP_{12}$ core (Hiromasa *et al.*, 2004). In mammalian OGDC and BCOADC, 12 E1 molecules bind to the edges of the 24-meric cubic E2 structure. Moreover, studies on mammalian OGDC, employing specific proteolysis and N-terminal sequence analysis have identified a 'lipoyl like' region at the N-terminus of the E1 component with significant sequence similarity to E2 and E3BP of mammalian PDC. Removal of this small N-terminal peptide promotes the dissociation of E3 from the E2 core assembly (Rice *et al.*, 1992; McCartney *et al.*, 1998). In addition, in mammalian BCOADC, an estimated 6 E3 dimers are associated with the 6 faces of this complex (Brautigam *et al.*, 2006).

1.1.2.1 Pyruvate dehydrogenase (E1)

E1 (pyruvate dehydrogenase) catalyzes the first and rate-limiting step of the overall PDC reaction as mentioned above using ThDP and Mg^{2+} as cofactors (Cate *et al.*, 1980).

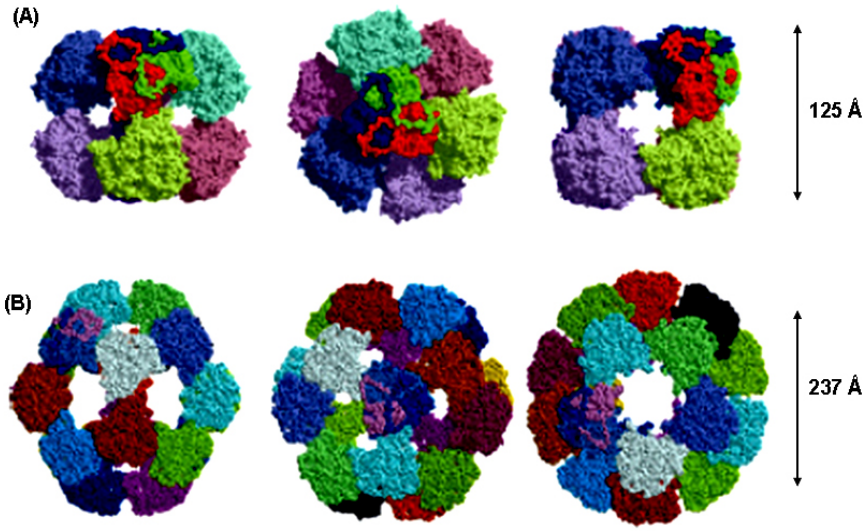

Figure 1-3 Structure of the octahedral and icosahedral E2 inner cores of PDC
Taken from (Perham, 2000)

Panel A The octahedral E2 core from *A. vinelandii* is shown on its two, three and fourfold axes of symmetry.

Panel B The icosahedral E2 core from *B. stearothermophilus* is shown on its two, three, and fivefold axes of symmetry.

The three subunits of a basic trimeric unit are shown in different colours.

$CH_3COCOOH + E1\text{-}ThDP\text{-}Mg^{2+} \longrightarrow CH_3C(OH)=ThDP\text{-}E1\text{-}Mg^{2+} + CO_2$

$CH_3C(OH)=ThDP\text{-}E1\text{-}Mg^{2+} + E2\text{-}[Lip(S)_2] \longrightarrow E1\text{-}ThDP\text{-}Mg^{2+} + E2\text{-}[Lip(SH)SCOCH_3]$

Two types of E1 enzyme are found in nature. In the OGDCs and octahedral PDCs e.g. *E. coli* E1 is a homodimer (α_2) with a subunit mass of approximately 100 kDa where the E1 polypeptide chains are unsplit (Perham, 1991; de Kok *et al.*, 1998). In contrast, in BCOADCs and the icosahedral PDCs, e.g. in *B. stearothermophilus* and eukaryotes, the E1 component consists of a heterotetramer ($\alpha_2\beta_2$), containing two α and two β subunits with subunit masses of approx. 41 kDa and 36 kDa, respectively (Patel & Roche, 1990; Lessard & Perham, 1994).

Crystal structures of several ThDP-dependent E1s have been solved in recent years including the α_2 homodimer from *E. coli* PDC (Arjunan *et al.*, 2002) and its heterotetrameric equivalent from the *Pseudomonas putida* 2-oxoisovalerate dehydrogenase complex (Aevarsson *et al.*, 1999), *Homo sapiens* E1-BCOADC (A *et al.*, 2000) and *Homo sapiens* E1-PDC (Ciszak *et al.*, 2003).

The $\alpha_2\beta_2$ tetramer of human PDC has four lobes each corresponding to one subunit that makes extensive hydrophobic contacts with the other three to form two ThDP-binding pockets at the α/β and the α'/β' interfaces as seen in Figure 1-4 (Ciszak *et al.*, 2003). The N-terminal tails of the α subunits cross over the extended C-terminal domains of the α subunits holding onto the β subunits. In the heterotetrameric form, the *α*-chain is believed to be involved primarily in the binding of ThDP and in catalysis whereas the *β*-chain is involved in the tight non-covalent binding of E1 to the structural core of dihydrolipoamide acyltransferase (Stepp & Reed, 1985; Rahmatullah *et al.*, 1989; Lessard & Perham, 1995; Lessard *et al.*, 1996; Seyda *et al.*, 2000).

The binding location for the ThDP cofactor is found at the two active sites situated in a deep cleft at the α-β interfaces of the heterotetramer such that residues from both subunits mediate non-covalent cofactor binding (Aevarsson *et al.*, 1999; A *et al.*, 2000). The ThDP-binding motif identified by Hawkins and subsequently found in all known ThDP-dependent enzymes is located in the C-terminal domain of the E1α subunit and is responsible for the binding of a metal ion (Mg^{2+}) that anchors ThDP through its phosphate groups (Hawkins *et al.*, 1989). The common sequence motif starts with the highly conserved sequence-GDG- and concludes with the highly conserved sequence -NN-.

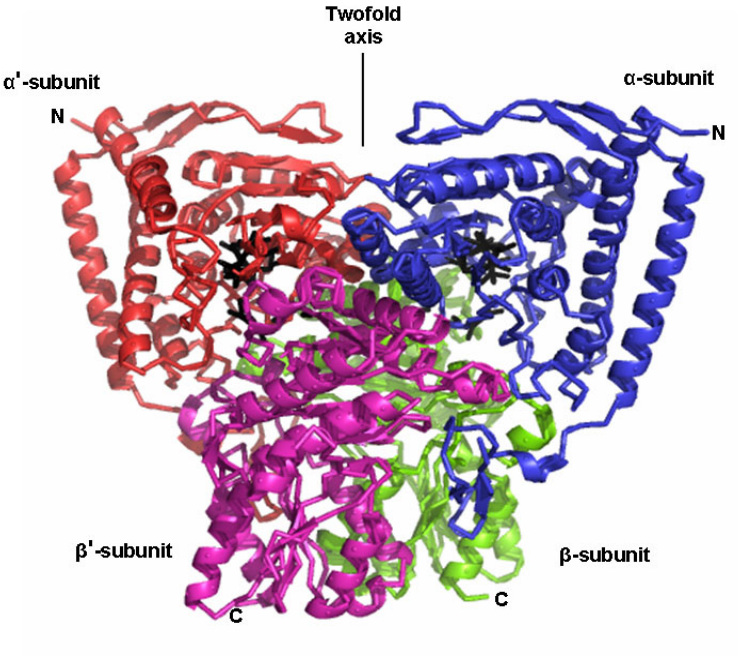

Figure 1-4 Three dimensional structure of E1 from the human pyruvate dehydrogenase complex
The crystal structures of four subunits of human PDC are arranged tetrahedrally as shown in the following colours: α, blue; α', red; β, green; and β', magenta (PDB ID 1NI4). The molecule possesses a two-fold symmetry axis that relates the α- with α'-subunit and β- with β'-subunit. Two cofactor molecules, thiamine diphosphate (ThDP), are shown in black.

In between there are approx 30 residues whose sequence is much less conserved but exhibit several common features (Hawkins *et al.*, 1989; Muller *et al.*, 1993; Hasson *et al.*, 1998).

The E1 component recognises lipoic acid covalently attached to the lipoyl domain of its partner E2 in order to perform an efficient reductive acetylation reaction. Thus it cannot use free lipoic acid, lipoamide or a lipoylated decapeptide with an amino acid sequence identical to that surrounding the lipoyl-lysine residue as substrate (Graham *et al.*, 1989; Berg *et al.*, 1998; Fries *et al.*, 2007). Moreover, the E1 component of *E. coli* OGDC does not interact with the lipoyl domain of E2-PDC as substrate and *vice versa*, implying specific molecular recognition between the lipoyl domain and its cognate E1 (Graham *et al.*, 1989).

1.1.2.2 Dihydrolipoamide acetyltransferase (E2)

The E2 enzyme plays a central role in the structural organisation, integrated function, regulation and assembly of mammalian PDC (Patel & Roche, 1990; Frank *et al.*, 2005). It catalyses the transfer of the acetyl moiety from its lipoamide prosthetic group to CoA to form acetyl CoA leaving the dithiolane ring of the lipoyl moiety in the reduced form.

$$E2\text{-}[Lip(SH)SCOCH_3] + CoA \longrightarrow E2\text{-}[Lip(SH)_2] + CH_3COCoA$$

E2 also forms the core of the multienzyme complex to which other components bind tightly but noncovalently (Rahmatullah *et al.*, 1989; Neagle & Lindsay, 1991; Hiromasa *et al.*, 2004). Generally, each E2 has a distinct domain organisation (Reed & Hackert, 1990; Perham, 1991). It is highly segmented comprising three structurally and functionally distinct regions that are arrayed in tandem and delimited by flexible linker regions (LR) 20-30 residues in length, enriched in Ala and Pro residues (Thekkumkara *et al.*, 1988; Perham & Packman, 1989; Perham, 1991) (Figure 1-5). The catalytic domain (CD) is located at the C-terminus and assembles into a basic trimeric unit in which the subunit interfaces generate the acetyltransferase active sites (Jones *et al.*, 2000a). In addition, the C-terminal domain of E2 mediates further oligomerisation of the E2 chain into the structural core which is either octahedral (24-meric) or icosahedral (60-meric) depending on the organism and the complex as mentioned above. Extending towards from each acetyltransferase domain are two additional domains: the intervening peripheral subunit binding domain (PSBD) and the N-terminal lipoyl domain (LD) (Reed & Hackert, 1990; Perham, 1991; 2000).

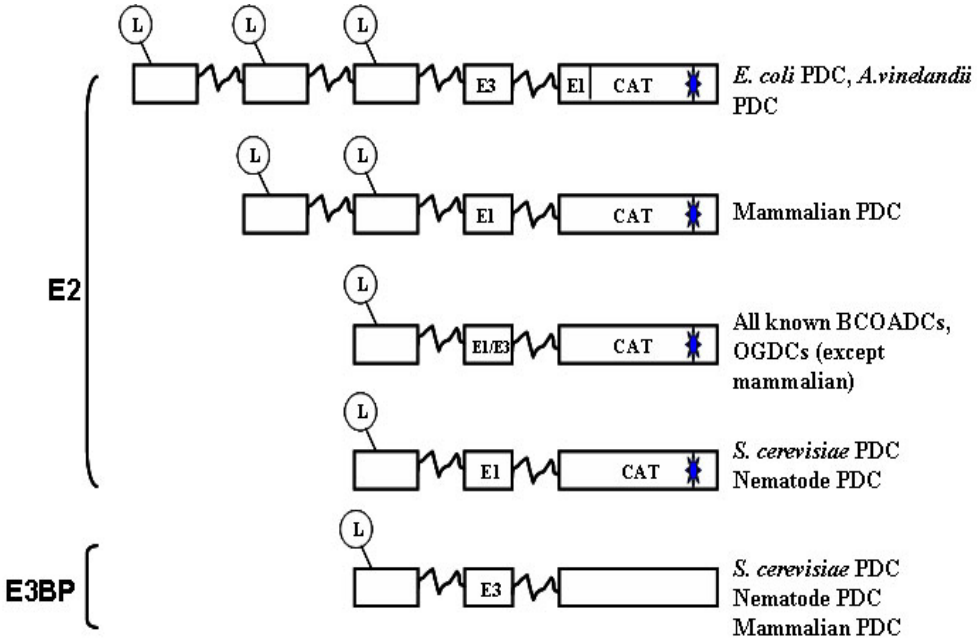

Figure 1-5 Domain organisation of the E2 and E3BP components from the 2-oxoacid dehydrogenase complexes
(L), lipoic acid; **E1**, E1 binding domain; **E3**, E3 binding domain; **E1/E3**, E1 and E3 binding domain; **CAT**, C-terminal acetyltransferase domain; **E2BD**, E2 binding domain; and **E3BP**, E3 binding protein.

The N-terminal lipoyl domain region contains one to three lipoyl domains (LD) (ca 9kDa) depending also on the complex and its source (Reed & Oliver, 1968; Rahmatullah *et al.*, 1989; Dardel *et al.*, 1993) (Figure 1-5). For example, in *E. coli,* E2 contains three lipoyl domains whereas the E2 chains of all OGDCs, BCOADCs and PDCs from Gram-positive bacteria possess only one lipoyl domain. However, in eukaryotic E2-PDCs, there are two lipoyl domains (Reed & Hackert, 1990; Perham, 1991; Jones *et al.*, 2000a). Interestingly, selective removal of the three lipoyl domains of the *E. coli* E2 suggests that the deletion of one or two domains has no detectable effect on overall activity or active-site coupling (Guest *et al.*, 1985). However, PDC activity was abolished when all three lipoyl domains were deleted and also decreased markedly as the number of lipoyl domain was increased from four to nine (Guest *et al.*, 1989; Machado *et al.*, 1992). Further discussion of the lipoyl domain is included in chapter 4.

1.1.2.2.1 The peripheral subunit binding domain (PSBD)

The PSBD (ca 4kD) is one of the smallest known globular domains, located between the LD and CD. It is a compact domain of only about 51 amino acids in *E. coli* 2-OGDC (Robien *et al.*, 1992), 35 amino acids in *B. stearothermophilus* PDC (Mande *et al.*, 1996) and 57 amino acids in *Homo sapiens* PDC (Thekkumkara *et al.*, 1988) that lacks stabilising disulphide bridges, metal ions, ligands or cofactors (Jung *et al.*, 2003).

As its name suggests, the main function of the PSBD is to bind E1 and/or E3 to the E2 core (Packman *et al.*, 1988; Hipps *et al.*, 1994; Lessard & Perham, 1995). In octahedral PDCs, the PSBD provides the binding site for E3 whereas E1 is thought to bind principally to the C-terminal acetyltransferase domain (de Kok *et al.*, 1998; Perham, 2000). In contrast, the PSBD of the icosahedral *B. stearothermophilus* E2-PDC and the octahedral E2-OGDCs as well as BCOADCs is responsible for binding both E1 and E3 in a mutually exclusive fashion (Wynn *et al.*, 1992; Hipps *et al.*, 1994; Lessard & Perham, 1995; Lessard *et al.*, 1996; Jung *et al.*, 2003). However, the situation in the icosahedral PDC of yeast, nematodes and mammals is different owing to the presence of 12 copies of an additional E2-related subunit, termed E3-binding protein (E3BP) (De Marcucci & Lindsay, 1985; Jilka *et al.*, 1986; De Marcucci *et al.*, 1986; Klingbeil *et al.*, 1996).

The three dimensional structure of the PSBD from different organisms has been solved by means of NMR spectroscopy, in particular *E. coli* OGDC (Robien *et al.*, 1992) and *B*

stearothermophilus PDC (Kalia *et al.*, 1993; Mande *et al.*, 1996). Both consist of compact folded structures consisting of two short α-helices (H1 and H2) packed against each other by extensive hydrophobic interactions with a short extended strand. A second hydrophobic core is formed by irregular and more disordered loops (L1 and L2) joining the two α-helix. The second irregular loop forms a finger-like structure consisting of two antiparallel extended regions with a tight turn at the tip of the finger (Robien *et al.*, 1992; Kalia *et al.*, 1993; Mande *et al.*, 1996) (Figure 1-6). Within the loop, glycine residues are conserved in nearly all E2-derived subunit binding domain sequences. *E. coli* E2-OGDC contains Gly37 (Robien *et al.*, 1992) and a series of conserved glycine residues Gly23, Gly25, Gly28 are found in *B. stearothermophilus* E2-PDC (Kalia *et al.*, 1993). It is probable that the presence of a side chain would result in unfavourable steric hindrance preventing the binding of E1 or E3 to the E2 core (Kalia *et al.*, 1993).

Binding studies involving the E2-SBD of *B. stearothermophilus* PDC with the E1 and E3 components of the same complex show that E1 heterotetramer and E3 homodimer bind only one subunit binding domain (Hipps *et al.*, 1994). This 1:1 stiochiometry may be explained by steric hindrance or conformational changes in the E3 dimer or E1 heterotetramer that block occupancy of the second binding site on the enzyme (Hipps *et al.*, 1994; Lessard & Perham, 1995). Further structural evidence for the 1:1 molar ratio was obtained from the crystallization of the *B. stearothermophilus* binding domain with its E3 partner (Mande *et al.*, 1996). The interaction of the SBD-E3 complex is achieved by electrostatic interactions between the negatively charged side chains of Asp and Glu residues derived from one E3 subunit, and positively charged side chains of Arg residues contributed by the PSBD forming an ‘electrostatic zipper’. Most residues of the SBD participating in the interactions are from helix I of the domain while the key residues from E3 are located on both subunits of the E3 dimer. Thus the close proximity of the site of attachment of the SBD to the E3 twofold axis of symmetry precludes the binding of a second molecule (Mande *et al.*, 1996; Jung *et al.*, 2002; Jung *et al.*, 2003).

1.1.2.2.2 The C-terminal domain (CD)

The CD (ca 28 kDa) is the largest domain of the E2 component, consisting of 200-270 amino acid residues. It participates in the self-assembly of the E2 core to form octahedral (24-mer) or icosahedral (60-mer) structures and catalyses the formation of the relevant acyl CoA.

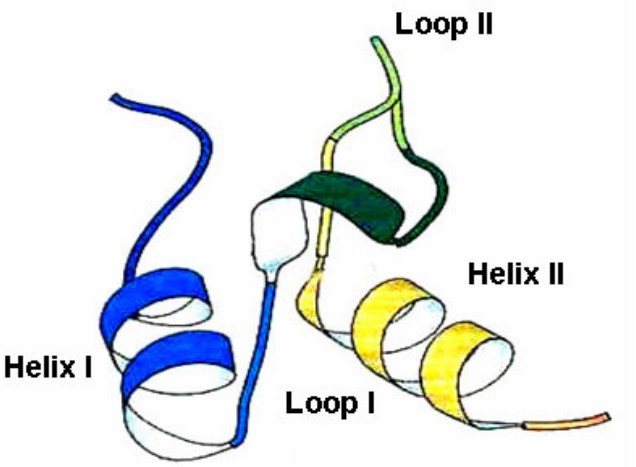

Figure 1-6 Schematic representation of the peripheral subunit binding domain of *B. stearothermophilus* E2-PDC
The solution structure of E2-SBD from *B. stearothermophilus* was solved by NMR (PDB ID 2PDD). The two α-helices (H1 and H2) are joined by loops.

The crystal structures of the octahedral E2p CD of *Azotobacter vinelandii* (Mattevi *et al.*, 1992; Mattevi *et al.*, 1993a), E2o CD of *E. coli* (Knapp *et al.*, 1998), and the icosahedral E2p CD of *B. stearothermophilus* and *E. faecalis* are now available (Izard *et al.*, 1999).

The acetyltransferase site in both octahedral and icosahedral E2 cores is located at the interface of two E2-subunits in a trimer, forming a 30-Å-long channel with two entrances. Lipoamide enters this channel from outside while CoA enters from the inside of the core (Mattevi *et al.*, 1993b; Perham, 2000). There is a formal resemblance between the reaction catalysed by chloramphenicol acetyltransferase (CAT, a trimeric enzyme catalysing the *O*-acetylation of the antibiotic chloramphenicol in Gram-positive and Gram negative antibiotic-resistant bacteria) and the acetyltransferase domain of E2 (Kleanthous *et al.*, 1985; Hendle *et al.*, 1995). From sequence alignment of 13 known E2 sequences with the chloramphenicol acetyltransferase sequence, a conserved sequence motif, DHRXXDG, housing two highly conserved residues, histidine and aspartic acid (underlined), was predicted to be involved in the catalytic reaction. A conserved serine residue located upstream of the conserved sequence motif is also required to help stabilize the tetrahedral intermediate after the attack of the CoA thiol on the S^8-acetyl-dihydrolipoamide thioester (Mattevi *et al.*, 1993b). In fact, E2 and CAT have a long active-site channel with the histidine and serine positioned in the centre of the channel. Substitution of the active site histidine or serine caused a dramatic decrease in catalytic efficiency (Meng & Chuang, 1994; Hendle *et al.*, 1995; Chuang *et al.*, 1997). The histidine acts as a general base catalyst in the proposed mechanism while the serine residue acts as a hydrogen bond donor to stabilise the putative negatively charged tetrahedral transition state. Acetyl group transfer is achieved by rearrangements resulting in the formation of acetyl CoA and dihydrolipoamide, which then dissociate from the active site.

1.1.2.2.3 The linker regions (LR)

Between domains in E2 and E3BP, there are long (20-30 residue) sequences, generally rich in Ala and Pro residues interspersed with charged amino acids (Perham, 1991; 2000). [^{1}H] NMR has shown that they are highly flexible, a property which is important to facilitate movement of the lipoyl domains between the three active sites (Green *et al.*, 1992).The interdomain linker regions occupy segments of poor sequence conservation and high protease susceptibility. Deletion analysis reveals that the linker is considerably

longer than normally required but can limit catalytic activity if shortened excessively (Miles *et al.*, 1988).The importance of Pro and Ala residues was investigated by replacing the natural linker of *E. coli* E2p containing one lipoyl domain by sequences containing: mixtures of Ala and Pro residues; mainly Ala; mainly Pro; and mainly charged residues. It was found that the Ala plus Pro linkers are flexible whereas Ala linkers or Pro linkers displayed limited flexibility and the linkers containing charged residues were completely inflexible (Turner *et al.*, 1993).

1.1.2.3 Dihydrolipoamide dehydrogenase (E3)

Dihydrolipoamide dehydrogenase (E3) is a member of the pyridine nucleotide, FAD-dependent-disulphide oxidoreductase family that includes glutathione reductase, thioredoxin reductase, trypanothione reductase and mercuric reductase (Mande *et al.*, 1996). These enzymes catalyse electron transfer reactions between pyridine nucleotides (NAD^+ or $NADP^+$) and their specific substrates. The electron transfer reactions are mediated by an active-site cysteine pair and the FAD cofactor.

E3 is a dimeric flavoenzyme consisting of two identical subunits (subunit M_r = 55,000). Each monomer is composed of four domains: an N-terminal FAD-binding domain, a NAD-binding domain, a central domain and an interface (C-terminal) domain. Each subunit also contains a non-covalently bound FAD, a redox-active disulphide and an NAD^+-binding site (Schulze *et al.*, 1991; Lindsay *et al.*, 2000). All E3s have two catalytic sites, each of which involves the flavin moiety of FAD and two cysteine residues from one subunit and a histidine residue with its hydrogen binding partner, glutamate from the other subunit. In human E3, the cysteine residues have been identified as Cys-45 and Cys-50 forming the active disulphide centre whereas His-452 has been identified as a possible proton acceptor/donor forming a strong hydrogen bond with Glu-457 (Kim & Patel, 1992; Toyoda *et al.*, 1998).

E3 catalyses the reoxidation of the dihydrolipoyl moiety attached to the lysine residue of E2. Catalysis by E3 is achieved in two half reactions. The first half-reaction involves the transfer of electrons from the dihydrolipoyl moiety of E2 to reactive cysteine disulphide, then to FAD, forming the two electron-reduced enzymes. The second half-reaction is the transfer the electrons from the reduced flavin to NAD^+ as indicated below.

$$E2\text{-}[Lip(SH)_2] + E3\text{-}FAD \longleftrightarrow E2\text{-}[LipS_2] + E3\text{-}FADH_2$$

$$E3\text{-}FADH_2 + NAD^+ \longleftrightarrow E3\text{-}FAD + NADH$$

In mammals, E3 is a common component of the entire family of three 2-oxoacid dehydrogenase complexes (De Marcucci *et al.*, 1985). However, the association of E3 is different depending on the complex and its source; in Gram positive bacteria, E3 competes with E1 for an equivalent binding site on E2 whereas in eukaryotic PDC, another component called E3BP is required to stably integrate E3 into the E2 core. In contrast, in mammalian OGDCs, there is biochemical evidence to suggest that E3 binds to the amino-terminal region of the cognate E1 homodimer (Rice *et al.*, 1992; McCartney *et al.*, 1998).

The structure of human E3 was resolved recently by X-ray crystallography (Ciszak *et al.*, 2006) (Figure 1-7). The FAD-binding domain interacts with the other three domains and comprises nearly two-thirds of the residues. Both FAD- and NAD-binding domains possess the layered β/α/β-type fold characteristic of nucleotide-binding proteins (Ciszak *et al.*, 2006). Two glycine-rich sequence motifs (Gly-x-Gly-x-x-Gly) were found to be located in the FAD- and NAD-binding domains. A cavity between the two domains, which normally hosts the NAD^+ substrate, leads straight to the *re*-side of the isoalloxazine ring of the FAD molecule. When entering the cavity, the NAD^+ moiety is guided by the glycine-rich NAD-binding motif, which facilitates positioning of the nicotinamide planar ring parallel to the FAD planar ring optimizing their interactions (Ciszak *et al.*, 2006). The central domain joins with the interface (C-terminal) domain through an eight-residue loop. Notably, this loop forms contacts with E3BP. The interface domain contains an α/β-type fold consisting of a central five-stranded antiparallel β-sheet surrounded by a single helix on one side and by four helices on the other. Their contacts are secured by the side chains of Glu^{431} at the N-terminal ends of those helices and by Tyr^{348} at the C-terminal ends. The single helix provides the central hydrophobic contacts between two E3 subunits that contribute to a functional dimer (Ciszak *et al.*, 2006).

1.1.2.4 E3-binding protein (E3BP)

E3BP (subunit M_r 50,000, originally termed Protein X), is an accessory polypeptide, tightly but non-covalently associated with the icosahedral core of mammalian and yeast PDC (De Marcucci & Lindsay, 1985; Jilka *et al.*, 1986; Rahmatullah *et al.*, 1989; Behal *et al.*, 1989).

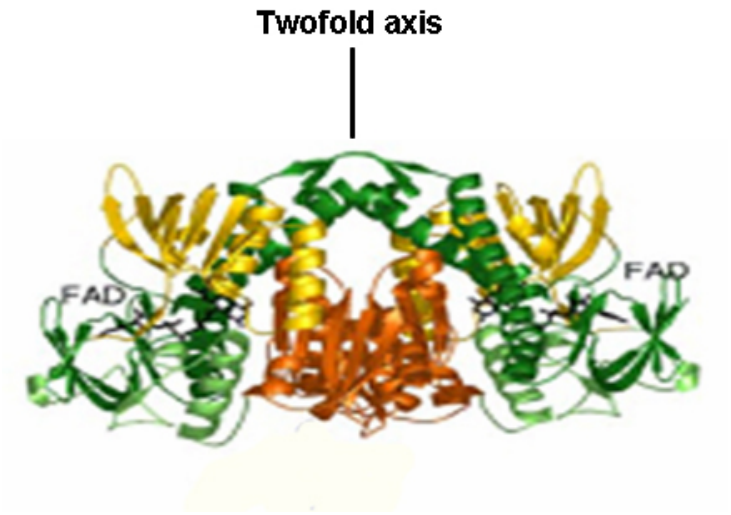

Figure 1-7 Structure of human dihydrolipoamide dehydrogenase (E3)
The structure of human E3 was solved by x-ray crystallography (PDB ID 1ZMC). The two subunits of E3 are arranged dihedrally and the four domains of each monomer of E3 are shown in different colours: green, FAD-binding domain; yellow, NAD-binding domain; light green, interface (C-terminal) domain; and orange, central domain. The FAD cofactors are shown in black sticks representation in each E3 monomer.

It binds via its C-terminal region to the assembly of catalytic domains comprising the inner core of E2 and is now thought to be part of the E2 core of all mammalian, yeast and nematode PDCs (Rahmatullah *et al.*, 1989; Lawson *et al.*, 1991a; b; Klingbeil *et al.*, 1996).

The stiochiometry of E3BP incorporation has been established as 12 copies per E2p (60-mer) core in mammals and yeast (Rahmatullah *et al.*, 1989; Maeng *et al.*, 1996; Sanderson *et al.*, 1996a). E3BP has been shown by selective proteolysis, immunological studies and gene disruption to have a key role in mediating the stable integration of E3 dimers into the complex by means of its PSBD (Lawson *et al.*, 1991a; De Marcucci *et al.*, 1995; Maeng *et al.*, 1996; Sanderson *et al.*, 1996b; Harris *et al.*, 1997). Structural evidence for a subunit molar ratio of 1:1 was obtained from the crystallization of the human E3 dimer with the N-terminal di-domain of E3BP containing the lipoyl and E3-binding domains (E3BPDD) (Ciszak *et al.*, 2006). Two E3 subunits form a single recognition site for the E3-binding domain of E3BP through their hydrophobic interface. Binding is achieved through the insertion of a hydrophobic patch of residues Pro^{133}, Pro^{154} and Ile^{157} in the E3-binding domain of E3BP onto the surface of both E3 polypeptide chains. To stabilize the sub-complex, numerous ionic and hydrogen bonds are present between the residues of the three interacting polypeptide chains in regions adjacent to the central hydrophobic patch (Ciszak *et al.*, 2006). The observed 1:1 stiochiometry between the E3 dimer and E3BP is due to the steric hindrance caused by a loop in E3BP which prevents binding of a second SBD (Ciszak *et al.*, 2006). However, in direct contrast, solution studies suggest the presence of a 2:1 subcomplex between E3BP and E3 employing native gel analysis, analytical ultracentrifugation (AUC), isothermal titration calorimetry (ITC) and small angle x-ray scattering (SAXS) (Smolle *et al.*, 2006).

E3BP consists of three globular domains connected by two linker regions analogous to that of the E2 component although it contains only a single lipoyl domain (Neagle *et al.*, 1989; Harris *et al.*, 1997). Moreover, a novel E3BP lacking an amino-terminal lipoyl domain, p45 has been identified in the PDC of the parasitic nematode, *Ascaris suum* (Klingbeil *et al.*, 1996). The structure-guided alignment of the sequence of E3BP with E2-PDC has revealed that there is considerable similarity between amino acid sequences throughout all domains. However, the conserved catalytic site histidine found in the C-terminal core of all dihydrolipoamide acetyltransferases is replaced by a serine

residue in human E3BP, strongly suggesting that E3BP does not act as an acetyltransferase (Harris *et al.*, 1997).

Biochemical studies have shown different aspects to the three domains of E3BP. Deletion of the lipoyl domain of E3BP in *S. cerevesiae* has little or no effect on overall PDC activity, indicating considerable functional redundancy with respect to the presence of multiple lipoyl domains (Lawson *et al.*, 1991a). However, deletion of the E3BD of E3BP results in loss of high-affinity E3 binding and concomitant loss of overall PDC activity (Rahmatullah *et al.*, 1989; Lawson *et al.*, 1991a). Moreover, removal of E2-linked lipoyl domains by collagenase treatment has revealed that E3BP-linked lipoamide groups can substitute partially for the lipoyl domains of E2 in overall complex catalysis (Rahmatullah *et al.*, 1990; Sanderson *et al.*, 1996a).

1.1.3 Regulation of the pyruvate dehydrogenase complex

Owing to the important role of PDC in the energy-generating pathways of most aerobic tissues, it is of the utmost importance that its activity is tightly regulated. Two separate types of regulatory mechanisms have been identified that are essential to accommodate the complexities of tissue-specific metabolic requirements in which pyruvate dehydrogenase is involved in higher organisms. The first mechanism, which is also the simplest, is end-product inhibition. The second mechanism is specific to PDC and BCOADC and involves covalent modification of the complexes by a phosphorylation/dephosphorylation mechanism. Phosphorylation of PDC and concomitant inactivation of the complex is mediated by a specific tightly bound, pyruvate dehydrogenase kinase (PDK). Dephosphorylation of PDC and concomitant reactivation are catalysed by a specific loosely-associated, pyruvate dehydrogenase phosphatase (PDP) (Behal *et al.*, 1993).

The regulation of pyruvate dehydrogenase by a phosphorylation/dephosphorylation mechanism was first demonstrated by Reed and coworkers (1969) using purified bovine kidney PDC (Linn *et al.*, 1969). The kinase is a hetero/homodimer originally thought to be consist of a catalytic (α) subunit of M_r 48,000 and a regulatory (β) subunit of M_r 45,000 (Stepp *et al.*, 1983). However, current research has shown that PDK exists as a dimer with different isoforms. The phosphatase consists of two subunits, a smaller catalytic subunit (PDPc) and a large regulatory FAD-containing subunit (PDPr). In addition, the catalytic activity of PDP is Mg^{2+} and Ca^{2+} dependent. It is inactive in the

absence of Mg^{2+} and Ca^{2+}, and its catalytic activity is stimulated about 10-fold by Ca^{2+}. Moreover, it has been suggested that the phosphatase contains two Ca^{2+} binding sites, one in PDPc and one that is created when PDP binds to E2 (Teague *et al.*, 1982; Maj *et al.*, 2006). The lipoyl prosthetic group and the inner lipoyl domain of mammalian E2-PDC create the binding site for both PDK and PDP. Indeed the lipoyl-bearing domains of E2 are indispensable in the anchoring of regulatory enzymes to the complex (Liu *et al.*, 1995; Patel & Korotchkina, 2001).

Four tissue-specific PDK isoforms have been identified in mammalian tissues designated as PDK1, PDK2, PDK3, and PDK4 (Popov *et al.*, 1997; Bowker-Kinley *et al.*, 1998) (Bowker-Kinley & Popov, 1999). PDK1 is expressed predominantly in rat heart. PDK2 has been observed in all rat tissues with low levels in spleen and lung whereas PDK3 is predominantly found in rat testis. Expression of PDK4 is mainly in skeletal muscle and heart (Bowker-Kinley *et al.*, 1998). There are, on average, 2-3 kinases bound to the complex. PDK4 is the only kinase that binds to lipoyl domains of E2 and E3BP (Maj *et al.*, 2006). PDK can phosphorylate all E1s by moving around the E2-E3BP core without dissociating from the complex (Liu *et al.*, 1995; Klyuyeva *et al.*, 2005).

Based on substrate specificity, PDKs are strictly serine-specific protein kinase. However, sequence determination of PDK showed that it lacks the motifs usually associated with eukaryotic Ser/Thr-protein kinases. Moreover, considerable sequence similarity exists between these mitochondrial protein kinases and members of the prokaryotic histidine kinase family (Popov *et al.*, 1993; Bowker-Kinley *et al.*, 1998; Steussy *et al.*, 2001).

To date, two PDP isoenzymes, designated PDP1 and PDP2, have been identified in mammalian tissues. The gene encoding PDP2 was identified based on sequence similarity to PDP1. Both isoforms are expressed in heart, brain, spleen, lung, liver and kidney. However, PDP1 is found predominantly in skeletal muscle and testis while PDP2 is expressed mainly in adipose tissue, liver, heart and kidney (Huang *et al.*, 1998; Maj *et al.*, 2006). The major difference between the two isoforms is the presence of a regulatory subunit, PDPr, found only in association with PDP1c which regulates its activity by blocking or distorting the active site (Maj *et al.*, 2006).

Inactivation of mammalian PDC occurs as a result of covalent modification of three serine residues in the α subunit of the heterotetrameric E1 termed site 1, Ser-264; site 2, Ser-271; and site 3, Ser-203 (Yeaman *et al.*, 1978; Dahl *et al.*, 1987). These primary sites are located very close to the active site, next to a conserved histidine that is involved in catalysis. Several recombinant human E1 mutants were generated as single or double mutations at the three phosphorylation sites to study the characteristics of phosphorylation (Korotchkina & Patel, 1995). This study has indicated that (i) the phosphorylation at any one of these three sites results in inactivation of the complex; (ii) the rates of phosphorylation of the three sites are site-specific; site 1 phosphorylation is faster than site 2 and 3; and (iii) phosphorylation is not sequentially ordered. Circular dichroism spectra were used to monitor the effect of phosphorylation on E1 conformation. Phosphorylation of E1 decreases its affinity for ThDP and prevents holo-E1 interaction with pyruvate (Korotchkina *et al.*, 1995). However, the situation with PDPc1 and PDPc2 is different in both isoenzymes can efficiently dephosphorylate all three phosphorylation sites, indicating a random mechanism of dephosphorylation (Korotchkina & Patel, 1995; Karpova *et al.*, 2003)

The PDK/PDP system is acutely regulated on a minute-to-minute basis by a number of effectors as summarized in Figure 1-8. PDK is activated by the end products of the catalytic process, NADH, acetyl CoA and ATP and inhibited by the E1 substrate, pyruvate, NAD^+, CoASH, ADP and products of fatty acid β-oxidation (Sugden & Holness, 2003). The regulation of PDP appears to be less complicated than the regulation of the kinase. The PDP1 reaction requires Mg^{2+} and Ca^{2+} ions. Ca^{2+} stimulates the phosphatase reaction indirectly by facilitating binding of the phosphatase to the transacetylase core, thus enhancing dephosphorylation (Pettit *et al.*, 1972; Huang *et al.*, 1998). In contrast, PDP2 appears to be a calcium-independent enzyme (Linn *et al.*, 1969; Huang *et al.*, 1998). In addition the phosphatase activity is inhibited by NADH and acetyl-CoA and inhibition is reversed by NAD^+ and pyruvate (Behal *et al.*, 1993).

PDC activity is also controlled on a long-term basis by either nutritional or hormonal changes. This kind of PDC regulation is accomplished at transcriptional level by controlling gene expression of PDC constituents and regulatory enzymes (Patel *et al.*, 1995; Patel & Korotchkina, 2006).

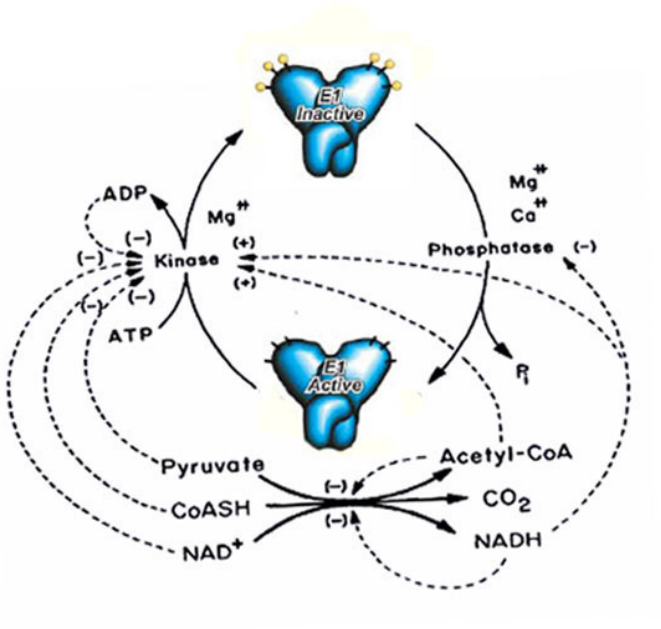

Figure 1-8 Regulatory mechanisms for pyruvate dehydrogenase by feedback inhibition and covalent modification via a protein phosphorylation/dephosphorylation system
E1 is represented in blue and the three serine sites per E1α subunit are shown as black lines

1.1.4 Protein targeting

Mammalian mitochondria contain their own small, circular, double-stranded genome and a complete system for carrying out DNA replication, transcription and protein synthesis. However, only a small number of proteins, 13 polypeptides in total, are encoded by mitochondrial DNA and translated within the organelle. These include specific subunits of the respiratory chain complexes and the ATP synthase. However, the vast majority of mitochondrial proteins are encoded by nuclear genes, translated on cytoplasmic ribosomes as larger precursors and imported into mitochondria post-translationally. The constituent enzymes of PDC, OGDC and BCOADC are nuclear-encoded; therefore, these polypeptides must be targeted to the organelle prior to the assembly of these complexes in the mitochondrial matrix (Maas & Bisswanger, 1990).

Nuclear-encoded polypeptides destined for mitochondria are normally synthesised as larger cytosolic precursors. The majority of imported proteins contain specific N-terminal signal sequences of 20 to 60 amino acids in length that direct their uptake (Pfanner, 2000). Comparison of the mitochondrial targeting signals shows that there is no apparent sequence similarity but they display common physicochemical properties. A common feature of all mitochondrial precursor proteins is that they are enriched in positively charged and hydroxylated amino acids.

There is a virtual absence of acidic residues and usually they can form flexible amphiphilic helices, allowing exchange between helical and extended confirmations. The role of the presequence during targeting of preproteins to the mitochondria is still not completely understood. In addition to directing mitochondrial targeting, the presequence is required for recognition of the nascent precursor polypeptide by cytosolic chaperones or other cytosolic factors that prevent its misfolding, aggregation and degradation. They also maintain it in a loosely folded "translocation-competent state" in order to be efficiently recognised by and imported across mitochondrial membranes (Deshaies *et al.*, 1988; Sheffield *et al.*, 1990; Endo *et al.*, 1996; Roise, 1997; Beddoe & Lithgow, 2002; Pfanner & Wiedemann, 2002).

Several cytoplasmic factors have been proposed to function in the efficient targeting of the precursor proteins. Hsp70 and its co-chaperone Hsp40 are heat shock proteins, found in the cytosol of mammalian cells. They prevent aggregation, misfolding or proteolysis by binding to the precursor protein while it is still being translated on

ribosomes (Beddoe & Lithgow, 2002). Once synthesis is completed, a cytosolic factor termed mitochondrial import stimulation factor (MSF) is required to aid the nascent precursor in its import and can also act on aggregated precursors to restore solubility and import competence (Neupert, 1997). However, if the ribosome encounters a mitochondrion during mitochondrial precursor synthesis, the precursor is translocated in an import-competent state by ribosome-associated factors termed nascent-associated polypeptide complex (NAC) and ribosome-associated complex (RAC) acting in concert (Beddoe & Lithgow, 2002). The binding and release of these factors is regulated by ATP hydrolysis.

Protein import into mitochondria is mediated initially by interaction of the presequence with specific receptor proteins, which are located in the mitochondrial outer membrane and expose their receptor domains to the cytosol. The receptors deliver the precursor proteins to the translocation channel of the TOM complex, (translocase of outer mitochondrial membranes) through which the preproteins traverse the outer membrane (Figure 1-9).

Translocation across the outer membrane is driven by electrostatic interactions between the positively charged presequence and acidic domains of the TOM proteins (Gakh *et al.*, 2002). However, translocation across the inner mitochondrial membrane is achieved by a separate assembly, the TIM complex, (translocase of inner mitochondrial membrane) which requires energy in the form of the proton motive force across the inner membrane, particularly its electrochemical component, the membrane potential ($\Delta\psi$) (Schleyer *et al.*, 1982; Martin *et al.*, 1991). This motor pulls the presequence across both membranes at the expense of ATP hydrolysis (Figure 1-9) (Horst *et al.*, 1997a; Gakh *et al.*, 2002). Once the preprotein arrives in the correct sub-mitochondrial compartment, the targeting signal is no longer necessary and is usually proteolytically removed by the mitochondrial processing peptidase (MPP) leaving the mature protein to participate in folding and assembly events. In fact most leader peptides are proteolytically cleaved in one step by MPP. However, a number of precursors are cleaved in sequential steps by two independent peptidases. These precursors are designed with bipartite presequences consisting of a matrix-targeting signal followed by an intermembrane space-sorting signal that is responsible for relocating precursors to the intermembrane space. Initially MPP is used to cleave a matrix-targeting signal leaving the precursor in an intermediate-sized form; the intermediate is sequentially

cleaved by mitochondrial intermembrane peptidase (MIP) after being re-exported to the intermembrane space of the mitochondrion (Gakh *et al.*, 2002).

Mitochondria contain several members of the major chaperone families that have important functions in maintaining organelle function. Different classes of mitochondrial chaperone proteins have been identified and classified according to their molecular weight. Members of the Hsp70, Hsp60 and Hsp100 families as well as small chaperones (co-chaperones) are all present in mitochondria (Voos & Rottgers, 2002). Hsp70 is the major mitochondrial monomeric chaperone that has sequence homology to the major bacterial Hsp70, DnaK. It mediates protein transport across the inner membrane and initiates protein folding in the matrix. These two reactions are carried out by two different mHsp70 complexes. The ADP-bound form of mHsp70 favours formation of a complex on the inner membrane; this 'import complex' contains mHsp70, its membrane anchor Tim44 and its partner chaperone, the nucleotide exchange factor Mge1 (homologous to bacterial GrpE). The ATP-bound form of mHsp70 favors formation of a complex in the matrix; this 'folding complex' contains mHsp70, its co-chaperones Mge1 and Mdj1 (homologous to bacterial DnaJ). Once a precursor protein enters the matrix, it interacts firstly with the import complex and then with the folding complex (Horst *et al.*, 1997b; Voos & Rottgers, 2002; Stojanovski *et al.*, 2003).

A chaperone of the Hsp60 family is one of the most important components of the protein folding system in the mitochondrial matrix. Hsp60 family forms a homo-oligomer of 14 subunits with seven subunits arranged in a ring, resulting in a characteristic 'double doughnut' structure. The double ring system forms a large cavity that accommodates proteins with a molecular weight of up to 50 kDa. The Hsp60 family consists of Hsp60 and its co-chaperone Hsp10, which are mitochondrial homologues of the bacterial chaperones GroEL and GroES respectively. These chaperones provide a protected environment for the ATP-dependent folding of newly-synthesised proteins (Neupert, 1997; Voos & Rottgers, 2002).

A family of Hsp100 proteins (also named C1p) form large homo-oligomeric protein complexes consisting of rings of six or seven subunits. In contrast to the Hsp70 and Hsp60 chaperone systems which constitute the main machinery required for folding of newly imported proteins, Hsp100 chaperones are important in the re-solubilisation of protein aggregates and in the unfolding of proteins (Voos & Rottgers, 2002).

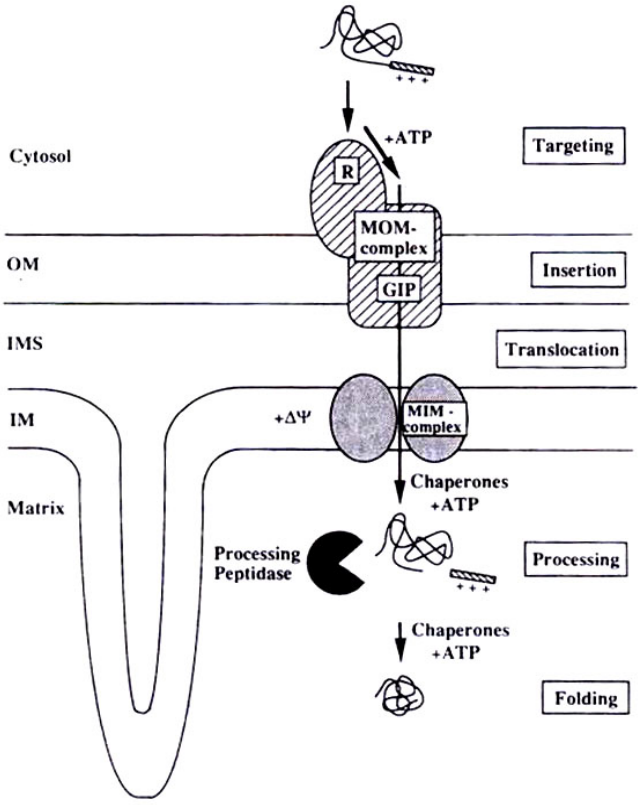

Figure 1-9 Schematic overview of import of preproteins into mitochondria
Precursor proteins are recognised by the mitochondrial import receptors **(R)** and subsequently inserted into the mitochondrial outer membrane **(MOM)** via the general insertion pore **(GIP)**. Then precursors are transported across the intermembrane space **(IMS)** to the translocation complex **(MIM)** of the mitochondrial inner membrane **(MIM)** and enter the matrix.

(Taken from (Kiebler *et al.*, 1993)

1.1.5 Genetic defects in OADCs

PDC deficiency is extremely heterogeneous in its presentation and clinical course. The fact that the brain is the most susceptible tissue to PDC deficiency is due to its dependence on glucose as a primary energy source. Genetic defects in PDC are reported to be the most commonly identified cause of primary congenital lactic acidosis (LA), a frequent manifestation of metabolic disease in young children. The clinical spectrum of PDC deficiency is extremely broad, ranging from intermittent ataxia to a progressive disease with mental retardation and neurological complications or early neonatal presentation with severe lactic acidosis and early death (Cameron *et al.*, 2004).

Studies at both DNA and protein levels have demonstrated that the great majority of PDC deficiencies (>80%) result from mutations in the E1α subunit involving either insertion/deletion or missense/nonsense mutations (Brown *et al.*, 1989; Lissens *et al.*, 1996; 2000; Brivet *et al.*, 2005). In fact, two genes are responsible to E1α production. The *PDHA1* gene codes for the somatic isoform of E1α and resides on the short arm of the X-chromosome whereas the testis-specific isoform of E1α is coded by the *PDHA2* gene located on chromosome 4. Most mutations of E1α are located on the X chromosome (Young *et al.*, 1998).To date, two missense mutations have been reported by Brown and his coworkers (Brown *et al.*, 2004) to be affecting the *PDHB* gene encoding the E1β protein. However, it has been found that primary genetic defects on E1α also affect the level of expression of E1β protein. This is considered to be a secondary phenomenon caused by impaired assembly of the heterotetrameric E1 component (Saijo *et al.*, 1996).

Since the *PDHA1* gene is localised on the X-chromosome, the most typical early presentations of the disease are usually gender specific. Less prominent systemic metabolic problems in female are evident more frequently than in males due to the presence of a mutation in one of two X-chromosomes. Furthermore, the degree of severity in females can vary depending on the variable expression of the mutant and normal genes in different tissues due to random patterns of X-inactivation (Patel & Harris, 1995; Lissens *et al.*, 2000; Cameron *et al.*, 2004).

Mutations in genes for other PDC subunits have all been described. As E3 is a common component in 2-OADCs, errors in this gene simultaneously affect PDC, OGDC and BCOADC manifested by lactic acidaemias, neurological degeneration as well as

elevated levels of plasma branched-chain amino acids and urinary excretion of the respective α-keto and α-hydroxy acids in Maple Syrup Urine Disease (Hengeveld & de Kok, 2002; Odievre *et al.*, 2005). Human E3 mutations have been reported to occur at the homodimer interface and the central domains and are likely to perturb stable dimerisation (Hong *et al.*, 1997; Shany *et al.*, 1999) or at the putative E3/E3BP interaction surface (Odievre *et al.*, 2005). In addition, other deletion mutations have been identified in the FAD binding domain and a single base insertion of an extra adenine in the last codon of the leader peptide sequence causes the premature termination of the E3 precursor polypeptide (Hong *et al.*, 1996; 1997). Nonsense mutations that result in premature termination of translation and deletions in the *PDX1* gene encoding E3BP have also been reported by different laboratories in 12 patients, leading to congenital PDC deficiency manifested by neonatal lactic acidaemia (Marsac *et al.*, 1993; Ling *et al.*, 1998; Hengeveld & de Kok, 2002; Dey *et al.*, 2003; Ramadan *et al.*, 2004). However, patients completely lacking functional E3BP still display 15-20% of normal PDC activity, thus indicating that E2 retains a residual capacity to bind E3 (Marsac *et al.*, 1993; Geoffroy *et al.*, 1996). These findings have been also confirmed *in vitro* where a 100-fold excess of E3 was able to restore PDC activity to 25-30% of wild-type levels (McCartney *et al.*, 1997). To date, only 3 patients with E2 deficiency has been identified (Head *et al.*, 2005). However, all patients with E3BP, E3 and E1β mutations are generally less severely affected than patients with *PDHA1* deficiency (Ramadan *et al.*, 2004; Brown *et al.*, 2006).

Genetic defects in the subunits of BCOADC cause a metabolic block in the oxidative decarboxylation of BCAA, resulting in Maple Syrup Urine Disease (MSUD) or branched-chain ketoaciduria. There is accumulation of BCAA and their derivatives in plasma, leading to severe clinical consequences including fatal acidosis, neurological derangement and/or mental retardation (Patel & Harris, 1995). To date, approximately 100 mutations have been reported in the six genes encoding the BCOADC catalytic machinery, E1αb, E1βb, E2b, E3 and its regulatory complex-specific kinase and phosphatase (Chuang *et al.*, 2006). MSUD patients have been classified in 3 groups according to the position of the mutation in E1b. The first group contains mutations that affect ThDP-binding, the second group comprises mutations affecting the hydrophobic core or structural integrity of E1 whereas the third (largest) group contains mutations that affect subunit association or protein-protein interactions (A *et al.*, 2000). Dihydrolipoamide dehydrogenase-deficient MSUD is caused by a defect in the E3

component of the BCOADC that is shared with PDC and OGDC (Chuang *et al.*, 2006; Homanics *et al.*, 2006).

Although no inborn errors of OGDC have been detected at the molecular level, several reports have been published associating deficiencies in OGDC with specific neurological disorders. These include Alzheimer's disease (AD) where genetic mutations affecting the processing of the amyloid precursor protein (APP) cause overproduction of amyloid β peptide (Gibson *et al.*, 1998). Inhibition of OGDC and complex I of the mitochondrial electron transport chain is induced by exogenous toxins such as 1-methyl-4-phenyl-1,2,3,6-tetrahydropyridine (MPTP) and 1-methyl-4-phenylpyridinium (MPP^+) causing Parkinson's disease (PD)-like symptoms. Similar effects are induced by endogenous neurotoxins such as isoquinoline derivatives, promoting loss of OGDC function in both areas of neurodegeneration and in other brain areas (Nagatsu, 1997; Gibson *et al.*, 2000). Inactivation of OGDC causes impairment of brain energy metabolism and brain function owing to the accumulation of 2-oxoglutarate and glutamate which are neurotoxic at elevated levels (Gibson *et al.*, 1998). Moreover, decline in complex activity in mitochondria leads to reduction of ATP formation and production of oxygen radicals (Nagatsu, 1997).

Alterations in OGDC activity may result from a mixture of causes including non-genetic damage by free radicals, reactive oxygen species (ROS) and 4-hydroxynonenal (HNE), a major lipid peroxidation (Humphries & Szweda, 1998; Humphries *et al.*, 1998) or perhaps due to uncharacterised genetic defects in its component enzymes (Gibson *et al.*, 2000). OGDC is not only a crucial target of ROS but can itself significantly contribute to generation of oxidative stress in the mitochondria. In this regard, it has been demonstrated that OGDC can serve as a source of hydrogen peroxide (H_2O_2) that is inhibited by NAD^+ and accelerated by the presence of NADH (Tretter & Adam-Vizi, 2004; Starkov *et al.*, 2004).

1.2 Immunity and autoimmunity: an overview

The immune system is a complex dynamic network of small molecules, soluble proteins and cellular components including B & T cells designed to respond rapidly and clear the body of foreign substances and organisms. Virus-infected cells, for example, are destroyed by cytotoxic T cells (cellular immune response) whereas soluble antigens are cleared by formation of immune complexes of antibody and antigen (humoral immune

response) that are taken up by cells of the mononuclear phagocytic system such as macrophages and neutrophils (Smith & Germolec, 1999).

The immune system is normally tolerant to self antigens by distinguishing precisely between self and non-self. This discrimination is indispensable to prevent the host from making a destructive self-immune attack. Therefore, tolerance is defined as a phenomenon to protect the body from inappropriate immune responses to self antigens. Tolerance of host molecules is not inherent to the immune system but is acquired during development and actively maintained throughout life (Rao & Richardson, 1999).

A variety of tolerance mechanisms have evolved to differentiate between self and non-self or to silence potentially autoreactive lymphocytes. Most of these mechanisms involve clonal deletion, clonal anergy or suppression. Clonal deletion is a major tolerance mechanism involving the physical elimination of self-reactive B and T lymphocytes that usually occurs at an early stage of development in the central lymphoid tissues, thymus and bone marrow to establish a complete immune repertoire. B and T lymphocytes whose receptors interact weakly with self antigens, or bind self antigens in a particular way, receive a signal that enables them to survive. This type of selection is known as 'positive selection'. On the other hand, lymphocytes whose receptors bind strongly to self antigens are eliminated by a process called 'negative selection'. Deletion is achieved by apoptosis during maturation of lymphocytes (Goodnow, 1996). However, this process alone cannot account for tolerance toward antigens that are not well expressed in the primary lymphoid organs or the presence of mature autoreactive T-cells that escaped clonal deletion and indeed can be found in the peripheral recirculating T-cell pool of many normal individuals. Since the presence of these self-reactive lymphocytes does not inevitably result in autoimmune reactions, their activity must be regulated in some way through peripheral tolerance mechanisms which may include clonal anergy. Clonal anergy is a mechanism that has evolved to eliminate functionally autoreactive B and T-cells present in the peripheral lymphoid organs to conventional antigenic stimulation instead of physically eliminating them via downregulation of responsiveness in the peripheral lymphoid tissues. Thus the anergic lymphocytes are those which survive as functionally inactive cells toward self antigen (Goodnow, 1996; Mondino *et al.*, 1996). Suppression or inhibition of autoreactive lymphocytes is also an active process in which responses to self-antigens are suppressed via interaction with other cell types such as regulatory T lymphocytes or natural killer cells (NK cells) (Rao & Richardson, 1999; Smith & Germolec, 1999).

Autoimmune responses are a natural consequence of the extensive repertoires of both B-cell and T-cell receptors which allow them to recognize any pathogens. Autoimmune diseases are believed to be caused by a failure of the immune system to distinguish between non-self and self for which there exists a state of natural immune tolerance. The failure of tolerance often results in significant immunopathology secondary to abnormalities of both humoral and cell-mediated immune responses. Autoimmune disorders are classified according to their responses into 'organ-specific' in which antibodies and T cells react to self-antigens localized to a specific tissue (e.g. insulin-dependent diabetes mellitus (IDDM), gastric autoimmune disease associated with pernicious anaemia and primary biliary cirrhosis (PBC) or 'non-organ-specific', which are characterized by reactivity against a specific antigen or antigens spread throughout various tissues in the body, e.g. systemic lupus erythematosus (SLE) and rheumatoid arthritis (RA) (Smith & Germolec, 1999; Sakaguchi, 2000).

Development of autoimmune disease is highly dependent on a permissive genetic background but there are other trigger factors such as viral, bacterial or chemical insult (environmental factors) leading to altered self-reactivity. Mechanisms by which environmental or other xenobiotic agents can disrupt tolerance can be divided into three categories. The first of these mechanisms involves inhibition of the process required in establishing tolerance by deletion, permitting release of autoreactive cells into the periphery. The second is alteration of patterns of gene expression in the cells participating in the immune response, permitting lymphocytes to respond to signals normally insufficient to initiate a response or allowing the antigen-presenting cells to abnormally stimulate a response. The third is the modification of self molecules such that they are recognised by the immune system as foreign (Rao & Richardson, 1999).

1.2.1 Primary biliary cirrhosis: an overview

Primary biliary cirrhosis (PBC) is a chronic, progressive cholestatic liver disease of unknown cause. It is characterized by spontaneous inflammatory damage to the biliary epithelial cells lining the small intrahepatic bile ducts followed by fibrosis and subsequently liver failure with the eventual need for liver transplantation (Kaplan, 1996).

The first description of PBC was reported in 1851 (Nishio *et al.*, 2001), and the first comprehensive analysis of the clinical features of PBC published by Ahrens et *al*

(Ahrens *et al.*, 1950). Autoimmune involvement in the pathogenesis of PBC was first suggested by Mackay when high titres of complement-fixing antibodies to tissue homogenates were detected in the sera of patients with PBC (Mackay, 1958). In 1965, Walker *et al* described PBC as the first disease unequivocally recognised as being associated with antimitochondrial antibodies as a serological marker of the disease (Walker *et al.*, 1965). This fact was established by indirect immunofluorescence using sera of patients with PBC on frozen composite rat tissue sections where a distinct mitochondrial staining pattern was apparent. Since the 1960s, it has been shown that most patients with PBC have high titres of antibodies in their serum reactive with non-organ, non-specific mitochondrial antigens, so-called antimitochondrial antibodies (AMA) (Walker *et al.*, 1965). Therefore, the major serologic feature of this disease is the production of AMA that are found in approximately 95% of PBC patients.

PBC is amongst the most female-predominant of all autoimmune diseases. Although, there is a female predominance with a ratio of around 10:1, it is mainly found in middle-aged woman between 40-60 years of age. The basis for the gender and age preferences is unclear (Long *et al.*, 2002). Importantly, however, genes implicated in immunological tolerance are located on the X chromosome. Recently, it has been reported that the frequency of X monosomy in peripheral white blood cells from female PBC patients was significantly higher than in chronic hepatitis C and healthy controls (Ichiki *et al.*, 2004). Furthermore, another study reported that the rate of X monosomy increases with age (Invernizzi *et al.*, 2005). Regardless of the predominance of the disease in women, there is no significant difference in the frequency of occurrence and antigenic specificity of AMAs between men and women (Long *et al.*, 2002).

Similar to other autoimmune diseases, the pathogenesis of PBC should be considered as complex or multifactorial, with multiple genetic and environmental factors playing an important role in disease susceptibility and onset (Risch, 2000; Tanaka *et al.*, 2001). Different surveys have been conducted in various countries, including the USA, England, Italy and Japan to study the prevalence of PBC (Bach & Schaffner, 1994; Brind *et al.*, 1995; Floreani *et al.*, 1997; Tsuji *et al.*, 1999; Jones *et al.*, 1999a). These studies suggest that the incidence of PBC in family members of PBC patients is markedly increased compared to the incidence in the general population. This estimate provides a firm basis for the hypothesis of a genetic, or at least a familial, predisposition to the disease (Selmi *et al.*, 2004). Table 1-1 introduces a summary of the prevalence of PBC in family members from different continents.

PBC presents insidiously with fatigue and pruritus (severe itching); fatigue is found in up to 80% of PBC patients. However, fatigue is relatively non-specific for PBC and is also a common symptom in patients with other chronic liver diseases. Pruritus is the second most common symptom in PBC occurring in 50-60% of patients. Its incidence does not relate to a specific stage of PBC and may disappear during disease progression. It is classically thought to result from the retention of irritant bile salts in the skin. Pruritus and jaundice can occur in the later stages as a result of the obstruction of intrahepatic biliary ductules leading to 'spillover' of biliary constituents. However, the inexorable end stage of the disease is the development of liver cirrhosis (Leung *et al.*, 1996; Selmi *et al.*, 2004). Other less common symptoms may also be present with complications of portal hypertension such as variceal bleeding or ascites as evidence of more-advanced liver disease. Occasionally, PBC patients may have problems from cholestasis, such as severe osteoporosis or fat-soluble vitamin deficiency. Malabsorption may be present with advanced disease (Butler *et al.*, 1995). Elevation of serum alkaline phosphatase, γ-glutamyl transpeptidase and IgM levels are the most characteristic symptoms of abnormal liver chemistries of patients with PBC (Selmi *et al.*, 2004).

The early serological hallmark of PBC is the presence of high titre AMA which are detectable in 95% of patients. Moreover, their presence occurs before clinical symptoms appear and is important in the diagnosis of the disease. Serum IgM AMA levels are frequently increased whereas IgG and IgA levels are usually within normal limits (Gershwin *et al.*, 2000; Nishio *et al.*, 2001).

Histologically, the continuing pathological changes in PBC can be described by classifying into four stages of increasing severity: (I) inflammatory destruction of intrahepatic bile ducts with a dense periportal infiltration of lymphocytes; (II) signs of continued damage with piecemeal necrosis and/or proliferation of the ductules; (III) septal fibrosis and/or bridging necrosis; and (IV) cirrhosis in which virtually all bile ducts have disappeared (Leung *et al.*, 1996). However, there is no clear quantitative immunological difference between these four stages.

Year	Country	No. of patients with PBC	No. of patients with family history of PBC	Prevalence "The percentage of patients with a family history of PBC"
1994	US	405	26	6.4%
1995	England	736	10	1.4%
1997	Italy	156	6	3.8%
1999	Japan	156	8	5.1%
1999	England	157	10	6.4%

Table 1-1Summary of reported prevalence of familial primary biliary cirrhosis
No. = number

(Bach & Schaffner, 1994; Brind *et al.*, 1995; Floreani *et al.*, 1997; Tsuji *et al.*, 1999; Jones *et al.*, 1999a)

1.2.2 Autoantibodies and their autoantigens

In a series of studies Berg and colleagues identified a "family" of AMA directed against various heterogeneous mitochondrial components prepared from beef heart mitochondria termed M1-M9. Some of the nine AMA types react with antigens which are located on the inner (M1, M2 and M7) and some react with antigens located on the outer mitochondrial membranes (M3, M4, M5, M6, M8 and M9) (Berg & Klein, 1989). These antigens can be clearly distinguished by their different physical and chemical properties, and can be related to distinct clinical occurrence.

The antibodies against these antigens can be subdivided into three groups. The first group involves anti-M1, anti-M5 and anti-M7 which are found in non-hepatic disorders. The M1-antibody is directed against cardiolipin and is diagnostic for syphilis. The M5-antibody appears in undefined collagen diseases. The M7-antibody is directed against sarcosine dehydrogenase and is characteristic for acute and chronic cardiac diseases such as cardiomyopathies and myocarditis (De Groote, 1991).

The second category consists of anti-M2, anti-M4, anti-M8 and anti-M9 which appear during the evolution of primary biliary cirrhosis (De Groote, 1991). The M2-antibody is a specific marker for the diagnosis of PBC; 96% of patients with PBC are anti-M2 positive (Berg & Klein, 1986). The M9 antibody is directed against an epitope of the enzyme glycogen phosphorylase (GP), a major enzyme involved in cellular metabolism in particular in hepatocytes and skeletal muscle. The first report of anti-M9 antibodies being present in PBC sera came when reactions were observed against antigenic determinants of 98 kDa and 59 kDa through immunoblotting against a purified antigen fraction derived from rat liver mitochondria that had no apparent M2 contamination (Klein & Berg, 1990; Davis *et al.*, 1992).

Anti-M4 antibodies were preferentially observed with patients who have antibodies to mitochondria and have histological features of both PBC and chronic active hepatitis (CAH), a so-called "mixed form" pathology (Gershwin *et al.*, 1987; Davis *et al.*, 1992; Baum, 1995). The M4-antibody is directed against a trypsin-insensitive antigen, sulphite oxidase (SO), an enzyme of the intermembrane space that co-purifies with outer mitochondrial membranes and microsomes (Klein & Berg, 1991). Anti-M8 antibodies were detected in patients with PBC. Anti-M8 was observed to be associated with anti-M2; however, not all anti-M2-positive patients were anti-M8 positive. The M8 antigen

was isolated from human both liver mitochondria and pig kidney microsomes and could be clearly distinguished from the M4 antigen. In contrast to M4, M8 is trypsin sensitive (Weber *et al.*, 1986).

The third group of antibodies is detected in drug-induced disorders, such as phenopyrazone-induced pseudolupus syndrome (anti-M3) and iproniazid-induced hepatitis (anti-M6) (De Groote, 1991).

1.2.3 Nuclear autoantigens in PBC

In addition to AMA, other non-organ specific autoantibodies are directed at nuclear antigens which are seen with lower frequency, so-called anti-nuclear antigens (ANA). These are present in about a third of PBC patients and occur more commonly in AMA-negative cases (Kaplan & Gershwin, 2005). Two different immunofluorescence staining patterns have been identified. One is the "multiple nuclear dot" pattern in which intranuclear proteins are recognised, and the other is referred to as "nuclear rim" staining in which the antibodies recognise proteins of the nuclear envelope (Jones, 2000b).

Two specific antigens have been identified by multiple nuclear dot immunofluorescence. The first antigen has been cloned and characterised as an acidic phosphorylated nuclear protein termed SP100; the second antigen has been termed PML because it has been shown to be expressed in promyelocytic leukaemia cells and present in the nuclear matrix, co-localising very closely with SP100. Both nuclear antigens show sequence similarity with transcription factors, suggesting a possible role in transcriptional regulation (Jones, 2000b).

Most of the nuclear autoantibodies from patients with PBC that exhibited a nuclear rim staining recognised a nuclear envelope polypeptide with a molecular mass of about 200 kDa. This protein has been identified as the major integral membrane glycoprotein of the nuclear pore, gp210, serving to anchor constituents of the nuclear pore complex to the nuclear membrane (Mackay *et al.*, 2000). Antibodies directed against gp210 are found in about 25% of patients with AMA-positive PBC and up to 50% of those with AMA-negative PBC (Gershwin *et al.*, 2000). Another glycoprotein of the nuclear pore complex, gp62 has been recently identified as an autoantigen in about a third of

patients. The presence of anti-gp210 and anti-gp62 in PBC sera appears to be mutually exclusive (Jones, 2000b).

1.2.4 Identification of the M2 mitochondrial antigens

Immunoblotting techniques were used initially by several groups for detection of distinct antigens in mitochondrial extracts, which have reactivity specifically with PBC sera. Distinct antigens were grouped into M2"a-e" by Berg and Klein according to their reported molecular masses of around 80-68 kDa (M2 "a"), 64-60 kDa (M2 "b"), 56-50 kDa (M2 "c"), 48-43 kDa (M2 "d") and 44-39 kDa (M2 "e") (Table 1-2) (Berg & Klein, 1988). By far the most predominant antigens were shown to be M2 "a" and "c" reacting with over 90% of PBC sera. The other antigen groups "c-e" were recognised by PBC sera at low frequencies.

The specific marker for the serological diagnosis of PBC is the presence of autoantibodies directed against trypsin-sensitive antigen(s) of the inner mitochondrial membrane, termed M2 (Berg *et al.*, 1986). However, the molecular identity of the mitochondrial autoantigens was largely unknown until 1987 when the major mitochondrial autoantigen was cloned from a rat liver cDNA library in λgt11-Amp3 and published as the sequence for the unknown 70-kDa M2 "a" antigen (Gershwin *et al.*, 1987). Immunological evidence was then presented by Yeaman *et al* determining that this 70-kDa M2 "a" autoantigen was, in fact, the E2 component of PDC (Yeaman *et al.*, 1988). This result was confirmed when 95% of PBC patient's sera were shown to react with a purified preparation of bovine E2-PDC (Yeaman *et al.*, 1988). Subsequently, a group of autoantigens associated with E2-PDC constructs and related enzymes were identified by their reactivity with PBC sera.

An additional subunit of PDC, namely E3BP was also identified as the 52-kDa M2 "c" autoantigen by immunoblotting analysis (Yeaman *et al.*, 1988). Moreover, all PBC sera that react with E2-PDC also react with E3BP with the same frequency (Mutimer *et al.*, 1989; Fussey *et al.*, 1991). The co-presence of antibodies to E3BP and E2-PDC was confirmed when a further study reported that E3BP possesses cross-reactive AMA-specific epitopes with E2-PDC. This was discovered by comparing the specificities of PBC sera with E3BP specific rabbit antiserum and by absorbing PBC sera with a recombinant E2-PDC (Surh *et al.*, 1989a). The cross reactivity between E3BP- and E2-PDC results from structural similarities between E2-PDC having two tandemly repeated

amino-terminal lipoyl domains (Coppel *et al.*, 1988) and E3BP with a single lipoyl domain (Rahmatullah *et al.*, 1989; Neagle *et al.*, 1989; Palmer *et al.*, 1999).

E2 enzymes of OGDC and BCOADC, 50 and 52 kDa, were also identified as major M2 "c" autoantigens by immunoblotting the purified proteins with PBC sera (Fussey *et al.*, 1988; Fregeau *et al.*, 1989; Surh *et al.*, 1989b; Fregeau *et al.*, 1990a). However, the frequency of PBC sera cross reactivity with these two enzymes was much less than that for E2-PDC and E3BP (Table 1-2) (Mutimer *et al.*, 1989). 72% of PBC sera reacted against E2-OGDC whereas 53% have cross reactivity with E2-BCOADC (Fussey *et al.*, 1988; Surh *et al.*, 1989b; Mutimer *et al.*, 1989). Moreover, it was found that affinity-purified sera against each E2 enzyme did not react in immunoblotting or ELISA with the other enzyme or with E2-PDC. These data demonstrated that E2-OGDC or E2-BCOADC was recognised by distinct populations of antibodies separate from autoantibodies that recognised E2-PDC. In addition, 10% of PBC patient's sera were observed to react with both E2-OGDC and E2-BCOADC (Fregeau *et al.*, 1989; 1990a).

The M2 "d" and M2 "e" autoantigens were subsequently found to be equivalent to the E1α (40 kDa) and E1β (36 kDa) subunits of PDC respectively. When bovine PDC was probed with individual PBC sera, it was found that bovine E1α cross-reacted with 41% whereas bovine E1β cross reacted with 7% of PBC patients (Fussey *et al.*, 1989a). This finding was confirmed in another study, which showed that PDC activity was inhibited by affinity-purified PBC sera against E1-PDC (Fregeau *et al.*, 1990b).

Antimitochondrial reactivity is usually observed against some, or even all, of the 2-OADCs, but serological cross reactivity is only found between PDC-E2 and E3BP. However, there is a more extensive distribution of B cell autoepitopes within E2-PDC than E3BP. It has been observed that pre-absorption of sera from PBC patients with recombinant E2-PDC or E3BP totally removes antibodies reactive with recombinant E3BP in ELISA but not vice versa, suggesting the presence of distinct autoepitopes in E2-PDC (Fussey *et al.*, 1988; Dubel *et al.*, 1999; Palmer *et al.*, 1999). However, when antibodies reactive with recombinant E2-PDC by immunoblot were eluted and re-blotted against E3BP (and vice versa), full cross-reactivity was observed, suggesting that the co-presence of antibody responses to E2-PDC and E3BP-PDC resulting from antibody cross-reactivity to the two proteins (Surh *et al.*, 1989a; Fussey *et al.*, 1991; Palmer *et al.*, 1999).

Complex	Subunit (M2 designation)	Apparent molecular mass (kDa)	AMA-positive (%)
PDC	E1α (M2 "d")	40	41
PDC	E1β (M2 "e")	36	7
PDC	E2 (M2 "a")	70-74	96
PDC	E3BP(M2 "c")	52	96
OGDC	E2 (M2 "c")	48-50	73
BCOADC	E2 (M2 "c")	50-52	53
OGDC and/or BCOADC	E2 (M2 "c")	48-50 and/or 50-52	10

Table 1-2 Characteristics of mitochondrial antigens in PBC
This illustrates the frequency of occurrence of AMA with the major antigenic components of the inner mitochondrial M2 antigens in PBC as detected by immunoblotting. The table represents an average of various published data.

(Gershwin *et al.*, 1987; Fussey *et al.*, 1988; Yeaman *et al.*, 1988; Fregeau *et al.*, 1989; Surh *et al.*, 1989a; Mutimer *et al.*, 1989; Fussey *et al.*, 1989a; Fregeau *et al.*, 1990a; Palmer *et al.*, 1999)

1.2.4.1 AMA and the 2-oxoacid dehydrogenase complexes

Autoantibodies to mitochondrial antigens are characteristic of the autoimmune liver disease PBC with E2-PDC being established as the major "M2" autoantigen. Several investigations have been performed to identify the main immunogenic region (MIR) recognised by AMA using synthetic peptides (Van de Water *et al.*, 1988a; Tuaillon *et al.*, 1992), recombinant fusion proteins (Fussey *et al.*, 1990; Surh *et al.*, 1990a) and limited tryptic digestion (Fussey *et al.*, 1989b; 1991)

A segment of rat liver cDNA for E2-PDC (603-bp) was subcloned, expressed and identified as the region containing all of the autoreactivity of the original clone (Van de Water *et al.*, 1988a). The MIR was further restricted to a twenty amino acid peptide which corresponded to the lipoylated binding site of the inner lipoyl domain. This was achieved using several synthetic overlapping peptide fragments and testing for cross-reactivity by an inhibition assay using PBC sera indicating that the residues 167-186 of E2-PDC constituted the minimal B cell epitope (Van de Water *et al.*, 1988a). Using fusion proteins expressing various regions of human E2-PDC confirmed the presence of a major epitope in the inner lipoyl domain and identified two other weakly autoreactive determinants (Surh *et al.*, 1990a).

A detailed analysis of the inner lipoyl domain revealed that a minimum of 75 amino acids (residues 146-221) were required for antibody recognition whereas 93 amino acids (residues 128-221) were necessary for characteristic strong antibody reactivity (Surh *et al.*, 1990a). In addition, AMA also react with the outer lipoyl domain (residues 1-90), but at a 100-fold lower dilution and only a minority of PBC sera react weakly with the E1/E3-binding domain. These studies suggested that a conformational autoepitope may be recognised (Surh *et al.*, 1990a).

Experiments performed using limited tryptic digestion of PDC from bacteria (*E. coli*) and yeast (*S. cerevisiae*) confirmed that the MIR lies within the lipoic acid-containing domains of the protein (Fussey *et al.*, 1989b). Further work using wild type or genetically engineered recombinant *E. coli* E2-PDC supported the importance of the lipoyl prosthetic group in antibody reactivity. Moreover, in this study, the epitope was partially mimicked by substituting the lipoyl cofactor with an octanoyl group (Fussey *et al.*, 1990).

Several studies have been performed subsequently to determine the MIR on E3BP, E2-OGDC and E2-BCOADC. The MIR on E3BP was localized within its single lipoyl domain (Fussey *et al.*, 1991). Three fragments were detected after tryptic digestion of bovine E2/E3BP-PDC. Two major proteolytic products were the catalytic core domain of E2 ($E2_c$) and the lipoyl domain of E2 ($E2_{lip}$) and a minor proteolytic product was the lipoyl domain of E3BP ($E3BP_{lip}$). It was found that PBC sera were reactive with both lipoyl domain fragments (Fussey *et al.*, 1991). Further studies, using full length constructs and lipoyl domains of E3BP and E2-PDC, confirmed that the response of PBC sera to E3BP is primarily directed against its lipoylated domain (Dubel *et al.*, 1999; Palmer *et al.*, 1999). In addition, the MIR of E2-OGDC was determined by studying the cross reactivity of PBC sera and a series of expression clones spanning the entire E2-OGDC molecule. A recombinant fusion protein comprising the entire lipoyl domain (residues 67-147) was reactive with all PBC sera previously shown to have autoantibodies to E2-OGDC, suggesting that a conformational autoepitope is recognised by AMA (Moteki *et al.*, 1996). Reactivity of PBC sera to various clones of E2-BCOADC as measured by ELISA also suggested that autoantibodies to E2-BCOADC mapped within peptides spanning amino acid residues 1 to 227 of the mature protein. This suggested that the epitope was dependent on the conformation and included the lipoic acid attachment region. However, only the full length enzyme (amino acid residues 1 to 421) was sufficient to remove all detectable anti-E2-BCOADC antibodies (Leung *et al.*, 1995). The studies of both Leung *etal* and Moteki *etal* did not check the lipoylation status for non-reactive peptides. Therefore, the lack of cross reactivity of PBC sera may be due to the lack of lipoylation and not the absence of the epitope.

Mapping of the MIR of the inner lipoyl domain of E2-PDC has led to interest in the involvement of the covalently attached lipoic acid cofactor. Leung *et al* constructed three mutants to investigate whether lipoic acid is required for Ab recognition (Leung *et al.*, 1990). The mutations were designed to replace the lysine residue in the lipoyl domain with glutamine, a neutral amino acid; histidine, a positively charged amino acid; and tyrosine, an aromatic amino acid. The mutants (non-lipoylated domain) remained fully reactive in ELISA with PBC sera compared to the wild type domain (Leung *et al.*, 1990). In addition, enzymatic delipoylation and relipoylation of porcine E2-PDC and E2-OGDC components did not influence immunoreactivity with PBC sera (Koike *et al.*, 1998). However, work in genetically engineered constructs of *E. coli* E2-PDC with and without lipoic acid determined that the presence of a lipoyl residue within the domain was crucial for effective recognition by AMA (Fussey *et al.*, 1990). Moreover, among

seven synthetic E2-PDC peptides, only the octadecapeptide 167-184 (OVA conjugate) prepared with lipoic acid located on lysine 173 was recognised in ELISA by PBC M2 sera. In contrast, there was no reactivity observed with non-lipoylated peptide (Tuaillon *et al.*, 1992). This study revealed that the presence of the lipoamide cofactor was important in Ab recognition and it formed an integral part of a dominant epitope recognised by PBC sera. Furthermore, Quinn *et al.* using immunoblotting, ELISA inhibition and antibody affinity measurements for analysis of isolated lipoylated and non-lipoylated recombinant domains demonstrated that the presence of the lipoyl moiety was also crucial for Ab recognition and appeared to constitute part of the B-cell epitope (Quinn *et al.*, 1993a). These data clearly showed that AMA were able to bind with lipoylated and non-lipoylated E2-PDC; however, the AMA response to lipoylated recombinant PDC-E2 was of significantly higher titre and affinity than that observed with non-lipoylated antigen (Quinn *et al.*, 1993a; Bruggraber *et al.*, 2003; Mato *et al.*, 2004). In addition, serum antibodies of PBC patients were found to bind both lipoylated and non-lipoylated recombinant E3BP lipoyl domain with significantly higher binding occurring to the lipoylated form (Palmer *et al.*, 1999). The lipoic acid cofactor appeared to constitute part of the dominant B-cell epitope within E2-PDC and E3BP as well as those of E2-OGDC and E2-BCOADC (Fregeau *et al.*, 1989; Leung *et al.*, 1995; Moteki *et al.*, 1996; Koike *et al.*, 1998).

The role of lipoic acid in the B cell autoepitope of E2-PDC has been confirmed in studies of the antigen specificity of human monoclonal antibodies secreted by hybridomas derived from peripheral blood B cells from patients with PBC (Thomson *et al.*, 1998). Two (of five) hybridomas were found to be specific for lipoylated recombinant human ILD-E2-PDC with no binding being observed with non-lipoylated antigen. The other three hybridomas showed greatly reduced binding to non-lipoylated antigen. These observations suggested that the lipoic acid cofactor formed an integral part of the dominant B cell epitope within E2-PDC (Thomson *et al.*, 1998).

1.2.4.2 Enzyme inhibitory properties of antimitochondrial antibodies

AMA have an inhibitory effect on the *in vitro* catalytic function of all 2-OADCs with which they react, namely PDC (Van de Water *et al.*, 1988b; Fregeau *et al.*, 1990b; Surh *et al.*, 1990b), OGDC (Fregeau *et al.*, 1990a) and BCOADC (Fregeau *et al.*, 1989). PDC, OGDC and BCOADC were inhibited by incubation with affinity-purified antibodies against E2-PDC, E2-OGDC and E2-BCOADC respectively. This provided

further evidence that there were distinct populations of antibodies reactive against individual 2-OADCs. Enzymatic inhibition of PDC also occurred by binding affinity-purified antibodies against E1α but not E1β. Moreover, this inhibition was specific for PDC activity but not OGDC or BCOADC (Fregeau *et al.*, 1990b).

A further report has examined the inhibitory effect of AMA against PDC from different sources. PBC sera were found to be highly inhibitory to mammalian PDC activity (99%), moderately inhibitory for yeast PDC activity (70%) and weakly inhibitory for *E. coli* PDC activity (26%) (Teoh *et al.*, 1994).

1.2.4.3 T-cell responses and PBC

The extraordinary specificity of small bile duct destruction, the presence of lymphoid infiltrates, including B cells that produce anti-E2-PDC in the portal tracts, the presence of T cell infiltrates in the portal tracts and the aberrant expression of MHC class II antigen on biliary epithelium in PBC has suggested that intra-hepatic ductular biliary epithelial cells are the target of an immune response (Ishibashi *et al.*, 2003). It has been hypothesized that the destruction of the biliary tract in PBC is mediated by autoreactive liver-infiltrating T-cells through either cytotoxicity or lymphokine production. *In situ* hybridization studies confirmed that cellular immune mechanisms, particularly involving T cells participate in the bile duct damage. mRNAs to the two T-cell subsets, Interferon γ (IFN-γ) as a marker for Th1 cells and interleukin-4 (IL-4) as a marker for Th2 cells were checked in liver sections from 18 patients with PBC, 35 disease controls and normal liver. Mononuclear cells expressing IFN-γ and IL-4 mRNA that accumulated in inflamed portal tracts in PBC livers were rarely present in controls. Moreover, IFN-γ mRNA expression was more commonly detected than IL-4 expression in PBC livers where the levels of its expression were highly correlated with the degree of portal inflammatory activity (Harada *et al.*, 1997a).

Several studies have established the presence of T-cells directed against epitopes within PDC from either peripheral blood or liver infiltrates obtained from PBC patients. Van de Water *et al.* successfully obtained for the first time T cell lines from liver biopsies of patients with PBC. Proliferation studies showed that cloned T cell lines specifically produced IL-2 when stimulated with E2-PDC or E2-BCOADC but not control proteins (Van de Water *et al.*, 1991).

Further research by the same group confirmed the importance of E2 in the T-cell response. It was shown that bovine E2-PDC and its recombinant ILD and/or OLD were able to stimulate peripheral blood mononuclear cells (PBMC) *in vitro* from PBC patients (16/19) but not from control patients (0/12) (Van de Water *et al.*, 1995). Epitope mapping studies indicated that the response was directed to the inner and/or the outer lipoyl domains, although serologic observations suggested that the autoantibody response was directed predominantly to the inner lipoyl domain. However, Van de Water's studies were performed using bovine E2-PDC and its recombinant protein over-expressed in bacteria and although E2-PDC is highly conserved across mammalian species, this investigation did not exclude the possibility that the responses being measured were xenogeneic in nature. Jones *et al.* employing native human E2-PDC, derived from heart muscle, were able to confirm that T cell responses to this antigen were indeed uniquely associated with PBC (Jones *et al.*, 1997).

Shimoda *et al*. isolated six E2-PDC specific CD4+ helper T cell clones from peripheral blood mononuclear cells (PBMC) of four patients with PBC using a panel of overlapping peptides spanning the full-length human E2-PDC. Proliferation assays demonstrated that the precise autoepitopes of these T-cell clones respond positively to amino acid residues 163-176, GDLLAEI**E**T**DK**ATI, within the inner lipoyl domain spanning the lipoic acid-binding residue (Shimoda *et al.*, 1995). All T cell clones specific for human E2-PDC 163-176 were restricted by the same MHC molecule, HLA DRB4 0101. Interestingly, the autoepitope of autoreactive T cells almost overlaps the B cell epitope and includes the lipoyl-lysine residue suggesting that both are responding to the same dominant epitope (Van de Water *et al.*, 1988a; Shimoda *et al.*, 1995). Moreover, E2-PDC 163-176-specific T-cell lines also responded to the sequence 36-49, GDLIAEV**E**T**DK**ATV, which corresponds to the outer lipoyl domain of E2-PDC. These two reactive peptides share a common amino acid motif that includes E, D, and K at positions 170, 172 and 173 (EXDK sequence motif). In addition, these cloned T-cell lines cross react with E2-OGDC peptide 100-113, DEVVCEI**E**T**DK**TSV. However, none of these E2-PDC specific clones cross reacts with the HLA-DR α chain peptide 82-95 or the human glycogen phosphorylase *β* peptide 354-367, both of which display sequence homology with E2-PDC but lack the ExDK sequence motif (Shimoda *et al.*, 1998). Interestingly, limiting dilution analysis (LDA) indicated that the frequency of autoreactive E2-PDC 163-176-specific T-cells is 100- to 150-fold increased in the hilar lymph nodes and liver compared with PBMC from the same patients (Shimoda *et al.*, 1998). Furthermore, the frequency of peripheral T cells responding to peptide 163-176

in the early or moderate stages of PBC was significantly higher than that in the end stage (Shimoda *et al.*, 1998). Moreover, the epitope of the peptide 163-176-specific T cell clones was not a cryptic determinant; it reacted also with purified native E2-PDC. These data provided suggestive evidence for a major role of the E2-PDC 163-176 peptide in the pathogenesis of PBC (Shimoda *et al.*, 1998).

In view of the destruction of BECs in PBC, the major target involved in pathogenesis, characterization of the CD8+ cytotoxic T cell (CTL) response is important. Cytotoxic T lymphocytes (CTLs) are thought to be directly involved in the tissue injury in PBC. The first major histocompatibility complex (MHC) class I, HLA-A2- restricted CD8+ cytotoxic T cells epitope for PDC-E2, namely amino acid 159-167 was characterised by Kita and his coworkers (Kita *et al.*, 2002a). The epitope of these E2-PDC specific clones overlapped to some extent with the epitope recognised by MHC class II restricted CD4+ cells (Shimoda *et al.*, 1995) but not by autoimmune B cells (Van de Water *et al.*, 1988a). Furthermore, it has been found through these studies that the frequency of PDC-$E2_{159-167}$ specific CTLs is 10-fold increased in liver as compared with the blood of patients with PBC (Kita *et al.*, 2002b). The precursor frequency of CTLs in blood was significantly higher in early stage than middle and end stage for the same patients with PBC (Kita *et al.*, 2002b). These data for the first time, documented the abundance of autoantigen-specific CD8+ T cells in PBC liver, suggesting that CD8+ T cells played an important role in the immunopathogenesis of PBC.

1.2.4.4 Biliary epithelial cells and PBC

The key pathological process in PBC is damage to, and apoptotic loss of, the biliary epithelial cells lining the small intrahepatic bile ducts (Harada *et al.*, 1997b). The recent demonstration of enrichment of self-specific cytotoxic CD8+ T cells (CTL) within the livers of PBC patients in early phases of the disease suggests that these CTLs participate in the immunopathogenesis (Kita *et al.*, 2002a; b; Jones, 2003). As the immune responses of PBC are directed against intracellular mitochondrial antigens, it is still unclear how the majority of the autoimmune damage appears to be confined to the small intrahepatic biliary epithelial cells despite the ubiquitous distribution of mitochondrial antigens in all nucleated cells. Additionally, in the normal situation these putative nuclear encoded autoantigens are hidden from the host immune system by double membrane barriers, being located on the inner membrane of the mitochondria.

Several early investigators reported that AMA from PBC patients may react with the surface of isolated hepatocytes or biliary epithelium suggesting for the first time that autoantigens may be aberrantly expressed (Ghadiminejad & Baum, 1987a; b). However, contamination with inner mitochondrial membrane in these experiments was a major criticism of this work (Gerken *et al.*, 1988). A further immunoblotting study revealed that PBC sera were reactive with 67 and 50 kDa components from isolated rat hepatocellular membranes which corresponded to the M2 antigens (Sundin & Sundqvist, 1991).

Subsequent immunohistochemistry studies have shown that there is increased expression of either E2-PDC or a related cross-reactive antigen, on the luminal surface of BECs from PBC patients using polyclonal and monoclonal reagents to E2-PDC. With rabbit polyclonal anti-bovine E2-PDC sera, it has been demonstrated that immunohistochemical staining of liver sections reveals a more intense staining of the BECs in PBC samples compared to controls. In contrast, antibodies raised against bovine E1 and E3 exhibit a uniform mitochondrial staining pattern in PBC and control samples (Joplin *et al.*, 1991). This observation is compatible with the previous work in which it was demonstrated that AMA recognise hepatocyte plasma membranes (Ghadiminejad & Baum, 1987b). Further analysis was performed by Van de Water *et al* using the monoclonal antibody (mAb), C355.1 which reacts exclusively with E2-PDC, binding to its inner lipoyl domain and inhibiting the activity of PDC *in vitro* (Surh *et al.*, 1990b). This study revealed a specific, high intensity staining with the bile ducts of PBC patients but not those from patients with chronic liver disease or normal controls (Van de Water *et al.*, 1991) confirming the observations of Joplin and colleagues described above (Joplin *et al.*, 1991).

A major advance in this area came following the development of methods to isolate intrahepatic BECs from wedges of liver removed at the time of transplantation (Joplin *et al.*, 1989; 1990). Cells were separated from the mix after collagenase digestion by immunogenic separation using magnetic beads (Dynabeads) coupled to a monoclonal antibody (HEA125), specific for a 34 kDa epithelial glycoprotein (egp34) which is present only on the surface of human biliary epithelial cells. Cells could be maintained in culture for up to 4 weeks with limited cellular proliferation and without loss of normal biliary epithelial cell markers (Joplin *et al.*, 1990).

Using these viable preparations of BECs, it was shown that 3 day cultured cells derived from livers of PBC patients but not controls have E2-PDC or an E2 cross-reacting antigen on the cell surface (Joplin *et al.*, 1992). Moreover, it was found that the pattern of E2 staining with polyclonal rabbit anti-E2-PDC was similar to the membrane marker, HEA125. In contrast, cultured BECs from normal liver showed membrane staining only with HEA125. This result suggested the possibility of the presence of an E2 or cross-reacting antigen on the surface of BECs in PBC and supported the idea of a pathogenic association between AMA and bile duct damage (Joplin *et al.*, 1992). This work was verified using human antibodies from PBC patients where the same pattern of staining was observed as in the previous study (Joplin *et al.*, 1995).

Eight murine monoclonal antibodies were mapped to four different regions of E2-PDC when studied by ELISA with overlapping recombinant fragments (Surh *et al.*, 1990b). In addition to the murine mAbs, six antibodies were developed from a PBC lymph node human Fab combinatorial library and mapped to the inner lipoyl domain of E2-PDC (Cha *et al.*, 1993). One combinatorial antibody termed LC5 also reacted with E2-PDC and weakly with E3BP but not with other E2 or E1 antigens by immunoblotting (Cha *et al.*, 1993). Employing these eight murine mAbs and the combinatorial Ab (LC5) in indirect immunofluorescence and confocal microscopy revealed that all antibodies exhibited typical mitochondrial staining patterns on incubation with liver sections from PBC, primary sclerosing cholangitis (PSC) and control livers. However, only murine mAb (C355.1) recognising an epitope lying between residues 160-221 of E2-PDC and the human combinatorial antibody (LC5) showed a distinct, intense staining of the luminal (apical) aspect of the bile duct epithelium in a PBC restricted manner. There was significant overlap of the epitopes recognized by C355.1 and LC5 as demonstrated by the inhibitory effect of LC5 on C335.1 staining of bile duct epithelium. This suggested that the increased staining was not caused by a molecule immunologically identical to the E2-PDC present in mitochondria and may be a truncated or altered form of the enzyme, or indeed an unrelated cross-reactive molecule that shares an epitope with E2-PDC (Van de Water *et al.*, 1993).

A possible explanation for the apparent high level of E2-PDC or cross-reactive antigen on the surface of BECs from PBC patients could simply be increased numbers of mitochondria in these cells. This possibility was studied by a double-antibody staining technique using polyclonal rabbit anti-E2-PDC and a control mAb directed against an inner mitochondrial membrane antigen termed MCA151A. Confocal microscopy

revealed that there was an increase in the biliary epithelial cell expression of E2-PDC in liver sections from PBC patients in the absence of increased MCA151A (Joplin *et al.*, 1994), suggesting that the high intensity of E2-PDC or cross-reactive antigen on bile ducts was not accounted by an increase in mitochondria. Further analysis by the same group has suggested that the antigen on biliary epithelial cells could be E3BP of PDC (Joplin *et al.*, 1997). 50 and 70 kDa antigens corresponding to E2-PDC and E3BP were detected in the plasma membrane enriched fractions of BECs. Importantly, no difference was observed between E2-PDC in BECs from PBC and controls when immunoblotted with affinity-purified anti-PDC whereas a 50 kDa of E3BP was detected in PBC patients but not controls. This result raised the possibility that E3BP or a similar cross-reactive 50 kDa antigen expressed aberrantly in BECs of PBC patients (Joplin *et al.*, 1997).

Several lines of evidence have now indicated that an autoantigen recognised by antibodies to E2-PDC or a cross-reactive molecule was present on the luminal surface of BECs of PBC patients (Joplin *et al.*, 1991; Van de Water *et al.*, 1993). In addition, the presence of E3BP or a cross reactive 50-kDa antigen in BECs by patient autoantibodies in PBC was also reported by Joplin *et al.* (Joplin *et al.*, 1997). A further study was conducted to investigate if autoantigen expression is increased in BECs of PBC patients. However, *in situ* hybridization staining for E2-PDC or E3BP mRNA failed to demonstrate an increase in their transcription in the interlobular bile ducts of PBC. It has also been suggested that an increase in E2-PDC and E3BP was caused by exogenous imported or cross-reactive molecules since by immunohistochemical staining with C355.1, the interlobular bile ducts showed typical aberrant apical staining in all PBC cases but not in liver controls (Harada *et al.*, 1997c; 1999).

A previous investigation has also reported that apical staining was also evident employing mAbs against the BCOADC and OGDC that did not cross-react with E2-PDC (Migliaccio *et al.*, 1998). This analysis was performed by immunising BALB/c mice with recombinant 'tri-hybrid' protein containing the lipoyl domains of E2-PDC, -OGDC and –BCOADC and producing mAbs specific for one or more of the mitochondrial autoantigens (Migliaccio *et al.*, 1998). Seven mAbs produced intense staining in the apical region of bile duct cells exclusively in PBC patients (Migliaccio *et al.*, 1998). It was observed by ELISA and immunoblotting that three of these mAbs reacted with OGDC, one with PDC and two with BCOADC while one reacts with all three complexes (Migliaccio *et al.*, 1998). This work was extended to fully characterize

the disease-specific E2-PDC mAbs and define the epitopes recognised by 4 anti-E2-PDC mAbs (3 mouse and 1 human) (C355.1, 2H4, 4C8, and PD2). All these mAbs were shown to be disease specific as evidenced by their ability to stain BECs from PBC tissue but not controls in an apical pattern. In particular, by using a combination of recombinant antigens, competitive inhibition assays, and a unique peptide-on-bead-ELISA assay, these mAbs have been found to recognise 3 or 4 distinct epitopes on E2-PDC. More importantly, this study suggested that the entire inner lipoyl domain of E2-PDC could be found on the apical region of BECs in PBC tissue (Migliaccio *et al.*, 2001).

1.2.4.5 Selective targeting of bile ducts in PBC

Emerging data have suggested that the specific staining in the biliary epithelial cells of PBC was due to the abnormal presence of large fragments of E2-PDC or E3BP, if not full-length polypeptides, as the disease-specific mAbs recognise distinct regions of ILD-E2-PDC (Migliaccio *et al.*, 2001). However, several reports have supported the hypothesis that mAb recognition of the apical region of BECs may be caused by the presence of E2-related antigens and not by E2-PDC itself. Thus not all monoclonal antibodies specific for E2-PDC stain the apical surface of BECs (Van de Water *et al.*, 1993) and E2-OGDC and E2-BCOADC-specific mAbs can also display a similar pattern of staining (Migliaccio *et al.*, 1998).

Three main theories have been proposed to account for the selective targeting and destruction of BECs by the immune system in PBC. Firstly, aberrant import of E2-PDC could be a result of mutations in its mitochondrial matrix-targeting sequence, leading to cytoplasmic accumulation of E2-PDC in these cells. It is known that biliary ducts are one of the routes by which toxic metabolites are removed from the body, so it is possible that toxic substances accumulated within the biliary epithelium could potentially modify the accumulated E2-PDC, leading to generation of abnormal variants of E2-PDC (Gershwin *et al.*, 2000). Secondly, errors in transcription of the E2-PDC gene could produce altered E2-PDC mRNA. For example, aberrant splicing during transcription of the E2-PDC gene could substitute an endoplasmic reticulum targeting signal for a mitochondrial targeting signal in E2-PDC. Thus, E2-PDC may potentially transfer to the endoplasmic reticulum and Golgi apparatus via a secretory route to be expressed on the cell surface of biliary ducts (Kiebler *et al.*, 1993; Kaplan, 1996).

Thirdly, the autoantigen-specific IgA antibody of E2-PDC might play an important role in the pathogenesis of PBC. IgA is the predominant antibody of the mucosal immune system, which acts as a first line of defence against many microbial pathogens, protecting the expansive epithelial cell surface area of the body including biliary epithelium (Gershwin *et al.*, 2000). IgA synthesis takes place in plasma cells of mucosal tissue located in the *lamina propria* (Kerr *et al.*, 1990). In addition to its ability to clear the body of microorganisms or toxins on mucosal membranes, secretory IgA binds to a poly-Ig receptor that is present only on the basolateral surfaces of BECs and transported actively through the cells. Following internalization with the receptor, IgA is transported through the cytoplasm in a transport vesicle as part of the normal physiological process (transcytosis) and secreted into the bile ducts at the apical surface. If antimitochondrial IgA autoantibodies are responsible for the presence of E2-PDC or E3BP on the BECs, it is possible that IgA anti-PDC, while undergoing transcytosis, binds to nascent PDC components forming antigen-antibody complexes that are trapped in the bile duct. Several reports have proven that IgA can bind intracellular material, such as newly-synthesised viral proteins, during transcytosis, via the IgA receptor on the surface of epithelial cells, and neutralize the virus (Mazanec *et al.*, 1992; Mazanec *et al.*, 1995; Bomsel *et al.*, 1998). All these three models would, if correct, cause depletion of this crucial mitochondrial complex resulting in chronic metabolic damage to the cell (Van de Water *et al.*, 1993; Tsuneyama *et al.*, 1995; Nishio *et al.*, 1997; Gershwin *et al.*, 2000; Jones, 2000b).

Several studies have supported the idea that IgA may have a pathogenic role in PBC. By using indirect immunofluorescence and confocal microscopy and an ant-isotype-specific reagent for human IgA, it has been reported previously that IgA from PBC patients reacted with molecules present on the surface of BECs in the livers of PBC patients but not normal liver tissues or in liver tissues from patients with other liver diseases (Van de Water *et al.*, 1993). In addition, the ability of serum IgA purified from six patients with PBC and a recombinant monoclonal anti-E2-PDC IgA derived from patients with PBC to penetrate human Madine-Darby canine kidney (MDCK) cells transfected with polymeric IgA receptors (MDCK-pIgR) was studied by immunohistochemistry (Malmborg *et al.*, 1998; Fukushima *et al.*, 2002). Serum and monoclonal IgA from all PBC patients penetrated epithelial cells in the human MDCK-pIgR and interacted with E2-PDC in the cytoplasm of these cells. In addition, co-localization of AMA-IgA and E2-PDC or a mimicking molecule was demonstrated on the apical surface and in the cytoplasm of PBC-BECs using dual staining with anti-

human IgA and a mouse monoclonal antibody directed to E2-PDC, C355.1. However, no co-localisation was observed with controls, primary sclerosis cholangitis PSC-BEC (Malmborg *et al.*, 1998; Fukushima *et al.*, 2002).

The direct pathogenicity of AMA-IgA to BECs was studied by Matsumura *et al.* (Matsumura *et al.*, 2004) by incubating highly purified AMA-IgAs from PBC sera with MDCK cells transfected with the human pIgR. It was reported that IgA from AMA induces caspase activation in MDCK-pIgR cells whereas no increase in caspase activity was observed when IgA from the control sera or IgG from PBC patients were used. In addition, the caspase induction was seen with anti-E2-PDC IgA only and did not correlate with autoantibodies to E2-OGDC or E2-BCOADC (Matsumura *et al.*, 2004). These data supported the idea that both the aberrant polar expression of E2-PDC and the trafficking of IgA in BECs were a possible mechanism for selective damage of BECs.

Further studies were performed to establish whether cell surface expression of PDC components, of the type observed in patients with PBC, could occur as a consequence of the induction of apoptosis. This hypothesis was supported by the work of Macdonald *et al.* who induced apoptosis of one murine and two human cell lines by treatment with stauroporine (Macdonald *et al.*, 2004). Different approaches were used to examine the apoptotic process including measurement of the release of cytochrome c from mitochondrial intermembrane space and demonstration of the activation of caspases 9, 3, and 8. PBC patient-derived anti-PDC Abs were used to detect extra-mitochondrial PDC in order to investigate the potential of aberrantly expressed complex to play a role in the pathogenesis of this disease (Macdonald *et al.*, 2004). Interestingly, healthy cells showed no significant expression of immunoreactive PDC in their cytoplasm or on the plasma membrane. However, the induction of apoptosis caused the release of this antigen into these two sites but not cytochrome c oxidase subunit 4 (COX 4) which was also present on the inner surface of the inner mitochondrial membrane (Macdonald *et al.*, 2004). One explanation for this apparent specificity is that PDC is only loosely associated with the membrane while COX 4 is intrinsic and its release would require more complete disruption of the inner membrane. This study highlighted the possible role of apoptosis in PBC which may involve the export of autoantigenic PDC from the inner mitochondrial compartment, where it is concealed from the immune system by 3 membranes from the external surface. However, it is still unclear at present how this apoptotic process could lead to abnormal presentation of E2 or an E2-related antigen on the cell surface of BECs (Macdonald *et al.*, 2004).

1.2.4.6 Molecular mimicry and PBC

Molecular mimicry is defined as a sharing of epitopes between host autoantigens and unrelated (but structurally similar) exogenous microbial (viral or bacterial) antigens. It is one of the hypotheses developed to explain that similar epitopes present in infectious agents prime autoaggressive immune responses against self epitopes, known as 'a breakage of tolerance. These autoimmune responses spread progressively to incorporate other intrinsic (self) antigens as their targets of attack; the agitating exogenous (mimicking) antigens derived from the infectious agent may or may not be detectable at the time of clinical presentation of the autoimmune disease (Farris *et al.*, 2000; Davies, 2000).

Different autoimmune diseases have been reported to support the hypothesis of molecular mimicry. Rheumatic fever involves autoimmune-mediated microbial pathology that can arise following respiratory infection with group A *Streptococcus* (*S. pyogenes*). At the molecular level, streptococcal surface M proteins share amino acid sequence with cardiac myosin. Therefore, serum and monoclonal antibodies from patients with acute rheumatic fever against streptococcal M protein cross-react with cardiac muscle myosin leading to rheumatic carditis (Liang & Mamula, 2000). Another example of molecular mimicry has been reported; herpes simplex virus (HSV)-type1 mediates the induction of keratitis, a leading cause of blindness of humans. This autoimmune disease is characterized by the presence of T cells that respond to both coat protein of HSV-type 1 and corneal self antigen (Liang & Mamula, 2000).

The possibility of molecular mimicry accounting for the development of PBC has been investigated in the SJL/J murine model by Jones *et al* who were able to induce a humoral and cellular autoimmune response by co-immunizing mice with both self and non-self (bovine) E2-PDC (Jones *et al.*, 1999b; 2002).

Several lines of evidence support a role for infectious agents, especially bacteria (at least at the B-cell level) in the pathogenesis of PBC. Since anti-mitochondrial autoantibodies and granulomatous portal lesions are characteristic in PBC and granuloma may be induced by *Mycobacteria*, it has been tempting to implicate these organisms as infectious agents capable of initiating autoimmunity. Vilagut *et al.* showed that the sera from patients with PBC but not controls (with other chronic liver disease and healthy subjects) cross-reacted with the cellular extracts from *Mycobacterium*

gordonae, recognizing two membrane polypeptides of 70 and 55 kDa (Vilagut *et al.*, 1994). When the eluted immunoglobulins reacting with 70 and 55 kDa polypeptides from *M. gordonae* were tested against mitochondrial proteins, it was observed that these eluted immunoglobulins bound to E2-PDC and E2-BCOADC M2 autoantigens. This result suggested that *M. gordanae* may play a potential pathogenic role in PBC (Vilagut *et al.*, 1994). Additional support for a role for *Mycobacteria* came when it was observed that 12 out of 28 sera (43%) from patients with active mycobacterial infection (pulmonary tuberculosis) recognised E2-PDC. On the other hand only sera from two of 82 patients (2.5%) with other bacterial and viral infections reacted with E2-PDC (Klein *et al.*, 1993).

One source of infection proposed to contribute to PBC is the presence of recurrent urinary tract infection (UTI). In fact, it has been observed that patients with PBC have a higher incidence of UTI than other chronic liver disease patients (Butler *et al.*, 1993). Furthermore, Butler *et al.* have reported that a high proportion (69%) of subjects with UTI with normal liver function has low titre AMA reactivity predominantly against E2-PDC (Butler *et al.*, 1993). However, a much lower proportion of AMA was registered in controls; 15.6% chronic liver disease patients and 8% normals (Butler *et al.*, 1993). Further studies by the same group were performed to confirm the previous result using purified M2 antigens and ELISA (Butler *et al.*, 1995). These results suggested that M2 antibodies may be induced by urinary organisms, in cases of recurrent bacteriuria, especially in females (Butler *et al.*, 1993; 1995).

Although much research has suggested the potential involvement of microbial agents in the pathogenesis of PBC, several pieces of evidence indicate that E2-PDC specific responses are mounted against self PDC and not PDC of microbial origin which would argue against the proposed mechanism of molecular mimicry. Although PBC sera contain antibodies capable of binding to both mammalian and bacterial E2 proteins, antibody titres against mammalian E2 are approximately 100-fold higher than against bacterial E2 (Fussey *et al.*, 1991). Moreover, pre-absorption of PBC sera with purified mammalian PDC complex did not remove reactivity against the *E. coli* antigen (Surh *et al.*, 1990a). These observation indicate the presence of distinct antibodies against these homologous prokaryotic and eukaryotic antigens (Surh *et al.*, 1990a; Fussey *et al.*, 1991).Supporting data for the presence of distinct antibody populations was seen in the inability of AMA to inhibit the catalytic function of PDC of bacterial origin as opposed to eukaryotic PDC (Teoh *et al.*, 1994).

T-cell-mediated immune responses specific for the autoantigen are necessary to initiate the immune response by providing appropriate helper T-cell function for B cells to produce antibody response. Thus, cross-reactivity at T-cell level is required to beak self-tolerance. Shimoda *et al*. have demonstrated the presence of molecular mimicry at T cell clonal level between human and *E. coli* E2-PDC (Shimoda *et al.*, 1995). One T cell clone, specific to the lipoyl domain of human E2-PDC (GDLLAEI**E**T**DK**ATI), PDC-$E2_{163-176}$-specific CD4+ T cells derived from different PBC patients cross-reacts with the exogenous peptide derived from the lipoyl domain of *E. coli* E2-PDC (EQSLITV**E**G**DK**ASM) containing the EXDK motif. However, it is important to note that while the T cell clone was cross reactive with E2-PDC from *E. coli*, none of the T cell clones cross-reacted with E2-PDC purified from *P. putida* which not only has the EXDK motif, but also has sequence greater similarity to human E2-PDC than *E. coli* E2-PDC (Shimoda *et al.*, 1995). Shimoda *et al.* further evaluated the role of molecular mimicry by analysing 30 kinds of mimicry peptide with EXDK-sequences and identified seven active mimicry peptides derived from microbial proteins (Shimoda *et al.*, 2000). Various patterns and degrees of activation by mimicry peptides were shown in each T cell clone, indicating a diverse spectrum of autoreactive T cells reacting to a single epitope of the human E2-PDC. In addition, since 2 of 7 mimicry peptides were from *E. coli*; this result may support the hypothesis that PBC has a bacterial aetiology at the T-cell level (Shimoda *et al.*, 2000).

Molecular mimicry in PBC has also been analyzed at the CD8+ T cell level. Kita *et al*. used alignment algorithms to search for amino acid homologies between PDC-$E2_{159-167}$, MHC class I restricted epitope, and microbial proteins. PDC-$E2_{159-167}$-specific CTLs cross react with a partially homologous peptide derived from *Pseudomonas aeruginosa* (Kita *et al.*, 2002c). This result supported the hypothesis that molecular mimicry may be implicated in the initiation of the autoreactive CD8 T-cell responses.

Overall these studies supported the hypothesis that PBC may have a bacterial or other microbial origin. In response to an infection, the T cells first recognize the lipoyl domain of bacterial E2-PDC or other microorganisms containing a homologous sequence or corresponding peptide for human E2-PDC. These T-cells stimulate a conventional immune response to the infecting immunogens. As a result of molecular mimicry and epitope spreading, the autoimmune responses spread progressively to incorporate other intrinsic (self) antigens as their targets of attack. Molecular mimicry subsequently occurs when these T-cells recognise self-peptides presented on aberrantly

expressed Class II HLA on BECs. It is possible that high levels of antigen expression could lead to an association with Class I HLA and Class II HLA. Finally, this would initiate the autoimmune cascade leading to the destruction of the bile ducts in which AMA and/or autoreactive T cells specific for mitochondrial antigens may play a pathogenic role. At this stage the autoimmune process would take place in the absence of the exogenous antigens, such as bacterial E2-PDC that may have been the trigger for the immune response. (Van de Water *et al.*, 2001).

1.3 Aims of this thesis

Approximately 95% of patients with primary biliary cirrhosis have AMA against the E2-PDC and E3BP polypeptides although the precise molecular basis for this is unclear at present. Immunodominant sites on both autoantigens have been localised to the LD and, in particular, to the region that serves as an attachment site for the essential prosthetic group, lipoic acid. Herein, the epitope recognised by two patient-derived mAbs, PD1 and PD2, was determined since this was of interest in terms of gaining a more precise understanding of the aetiology of the disease (chapter3).

As the lipoamide moiety is considered to constitute an integral part of the epitope recognised by these mAbs, the second part of the thesis focused on the importance of dithiolane ring of the lipoate cofactor of the ILD-PDC and the extent to which the lipoamide dithiols contributed to antibody recognition (chapter 4).

The mechanisms responsible for the development of human autoimmune disease remain enigmatic but have been the subject of intensive theoretical, empirical and epidemiologic investigations in recent years. One recent hypothesis, an extension of the original concept of molecular mimicry, is that xenobiotics have the capacity to modify self-antigens, thereby initiating an autoimmune response and subsequent immunopathology by generating autoreactive lymphocytes that simultaneously recognise cross-reactive determinants from both the original immunogen and the host. In this context, bacterial LplA ligase was employed to incorporate different lengths of fatty acids and related compounds into the human non-lipoylated ILD-PDC mimicking production of an aberrantly-modified lipoyl domain (chapter 4). Two aspects were examined in this study: the efficiency of bacterial LplA ligase to employ different fatty acids/xenobiotics as substrate rather than lipoic acid and the ability of these aberrantly-

modified LDs to elicit a response with mAbs PD1 and PD2 with a view to establishing possible routes that could potentially trigger an autoimmune response.

As a corollary to the main aims of the thesis, the purpose of this study was to investigate the effects of elongated N-terminal presequences on the expression, solubility and folding of pre-E2, its N-terminal truncated form and pre-E3BP *in vivo* by comparing them with their mature equivalents and with a precursor housing a standard length of presequence, pre-E3 (chapter 5). Previous research has shown that the cytosolic E2 and E3BP precursors of 2-OADCs have extended signal sequences (53-86 amino acids in length) whereas the other constituent polypeptides have standard length presequences (24-50 amino acids). In order to achieve this objective it was first necessary to devise a strategy for the successful cloning of both types of precursors. This was followed by analyses of the effect of these presequences on their expression and solubility as compared to their respective mature forms. In addition, the folding of these constructs was examined by assessing their susceptibility to degradation and extent of lipoylation since this post-translational modification requires the presence of mature, folded apodomain.

Chapter 2

Materials and Methods

2.1 Molecular biology materials

2.1.1 Chemicals

All standard laboratory chemicals used were of the highest grade available commercially. Duchefa (Haarlem, the Netherlands) supplied the chemicals for the bacterial media. Roche Diagnostics Ltd., East Sussex, UK, supplied agarose and Complete EDTA-free Protease Inhibitor Cocktailts. Isopropyl β -thiogalactopyranoside (IPTG) was obtained from Melford Laboratories Ltd. Specialised chemicals like ampicillin, chloramphenicol and lipoic acid were all from Sigma. The PCR nucleotide mix was purchased from Promega, Southampton, UK.

2.1.2 Enzymes

DNA restriction enzymes, DNA T4 ligase, Pfu DNA polymerase and Calf intestinal alkaline phosphatase were supplied by Promega, Southampton, UK. Expand high Fidelity Enzyme was supplied by Roche. VentR ® DNA polymerase was purchased from New England Biolabs, UK.

2.1.3 Synthetic oligonucleotides

Primers for gene amplification by PCR were designed in the laboratory and synthesized on the 0.01μmole scale by MWG-Biotech AG, London, UK. Mutagenic primers were also designed in the laboratory and synthesized on the 0.05 μmole scale including a PAGE purification step by Sigma-Genosys Ltd.

2.1.3.1 Oligonucleotides for precursor cloning of human PDC

2.1.3.1.1 Oligonucleotides used for subcloning pre-E2, N-terminal pre-E2 truncate and its mature form

NdeI and BamHI restriction endonuclease recognition sites are underlined. Start and stop codons are indicated in red.

Pre-E2 forward primer with NdeI restriction endonuclease site

5'- CGC CGC CAT ATG ATG TGG CGC GTC TGT GCG CGA CGG-3'

E2 forward primer with NdeI restriction endonuclease site

5'- CGC CGC CAT ATG AGT CTT CCC CCG CAT CAG AAG G-3'

E2 reverse primer with BamHI restriction endonuclease site

5'-CGC CGC GGA TCC TTA CAA CAA CAT AGT GAT AGG-3'

N-terminal E2 truncate reverse primer with BamHI restriction endonuclease site

5'-CGC CGC GGA TCC TCA GGG AGG CAC AAC AGC TGC-3'

2.1.3.1.2 Oligonucleotides for pre-E3 cloning

BamHI restriction endonuclease recognition sites are underlined. Start and stop codons are indicated in red.

Pre-E3 forward primer with BamHI restriction endonuclease site

5'- CGC CGC GGA TCC AAT GCA GAG CTG GAG TCG TGT G-3'

E3 reverse primer with BamHI restriction endonuclease site

5'- CGC CGC GGA TCC TCA AAA GTT GAT TGA TTT GCC -3'

2.1.3.1.3 Oligonucleotides for pre-E3BP cloning

BamHI restriction endonuclease recognition sites are underlined. Start and stop codons are indicated in red.

Pre-E3BP forward primer with BamHI restriction endonuclease site

5'-CGC CGC GGA TCC GAT GGC GGC CTC CTG G-3'

E3BP reverse primer with BamHI restriction endonuclease site

5'-CGC CGC GGA TCC CTA GGC AAG TCG GAT AGG -3'

2.1.3.1.4 Oligonucleotides for pE2-E3 cloning

BamHI and SacI restriction endonuclease recognition sites are underlined. Start codons are indicated in red.

Pre-E2 forward primer with BamHI restriction endonuclease site

5'-CGC CGC GGA TCC AAT GTG GCG CGT CTG TGC GCG ACG -3'

E2 presequence reverse primer with SacI restriction endonuclease site

5'- CGC CGC GAG CTC TGA GTA ATA GCG GCG GCC GGG C -3'

E3 forward primer with SacI restriction endonuclease site

5'- CGC CGC GAG CTC GCA GAT CAG CCG ATT GAT GC -3'

E3 reverse primer with BamHI restriction endonuclease site

5'- CGC CGC GGA TCC TCA AAA GTT GAT TGA TTT GCC -3'

2.1.3.1.5 Oligonucleotides for pE3-E2 cloning

BamHI and SacI restriction endonuclease recognition sites are underlined. Start codons are indicated in red.

Pre-E3 forward primer with BamHI restriction endonuclease site

5'- CGC CGC GGA TCC AAT GCA GAG CTG GAG TCG TGT G-3'

E3 presequence reverse primer with SacI restriction endonuclease site

5'-CGC CGC GAG CTC TGA GTA AGT TCT CAG AGG CAC TGC-3'

E2 forward primer with SacI restriction endonuclease site

CGC CGC GAG CTC AGT CTT CCC CCG CAT CAG AAG -3'

E2 reverse primer with BamHI restriction endonuclease site

5'-CGC CGC GGA TCC TTA CAA CAA CAT AGT GAT AGG-3'

2.1.3.2 Oligonucleotides for cloning the lipoyl domains of *Arabidopsis thaliana (A. thaliana)*

2.1.3.2.1 Oligonucleotides used for cloning the lipoyl domain of A. thaliana plastic E2-PDC

Primers were designed to the 5' region upstream of the respective start codon and 3' region downstream of the lipoyl domain of the *A. thaliana* E2-PDC gene. BamHI and EcoRI restriction endonuclease recognition sites are underlined. Start and stop codons are indicated in red.

Forward primer with BamHI restriction endonuclease site

5'-CCG GAC GGA TCC ATG CCG GCG TTA TCA TCA ACC-3'

Reverse primer with EcoRI restriction endonuclease site

5'-CCG GAC GAA TTC TCA AGC GGC TTT ACT CTT AGC-3'

2.1.3.2.2 Oligonucleotides used for cloning the inner lipoyl domain of A. thaliana mitochondrial E2-PDC

Primers were designed to the 5' and 3' regions adjacent to mitochondrial ILD of the *A. thaliana* E2-PDC gene. BamHI and EcoRI restriction endonuclease recognition sites are underlined. Start and stop codons are indicated in red.

Forward primer with BamHI restriction endonuclease site

5'-CCG GAC GGA TCC GAT CTT CCC CCA CAT GTC GTC-3'

Reverse primer with EcoRI restriction endonuclease site

5'-CCG GAC GAA TTC TCA TTC AAT ACT TTC AGC ATC-3'

2.1.3.3 Oligonucleotide primers for site-directed mutagenesis

Both primers were designed with the desired mutation and complementary to each other. The mutated bases are indicated in blue

2.1.3.3.1 Oligonucleotides for human ILD-E2 mutations

Single mutations

E168V Primers

5' Primer: 5'-GGA GAC TTA CTG GCA GTG ATA GAA ACT GAC AAA GCC-3'
3' Primer: 5'-GGC TTT GTC AGT TTC TAT CAC TAC CAG TAA GTC TCC-3'

T171S Primers

5' Primer:
5'-C TTA CTG GCA GAG ATA GAA TCT GAC AAA GCC ACT ATA GG-3'
3' Primer:
5'-CC TAT AGT GGC TTT GTC AGA TTC TATCTCTGC CAG TAA G-3'

T175D Primers

5' Primer:
5'-GAG ATA GAA ACT GAC AAA GCC GAT ATA GGT TTT GAA GTA CAG-3'
3' Primer:
5'-CTG TAC TTC AAA ACC TAT ATC GGC TTT GTC AGT TTC TAT CTC-3'

Double mutations

E168V:T171S Primers

5’ Primer:
5’-GAA GGA GAC TTA CTG GCA GTG ATA GAA TCT GAC AAA GCC-3’
3’ Primer:
5’-GGC TTT GTC AGA TTC TAT CAC TGC CAG TAA GTC TCC TTC-3’

T171S:T175D Primers

5’ Primer:
5’-GCA GAG ATA GAA TCT GAC AAA GCC GAT ATA TAG GTT TTG-3’
3’ Primer:
5’-CAA AAC CTA TAT ATC GGC TTT GTC AGA TTC TAT CTC TGC-3’

E168V:T175D Primers

E168V and T175D primers were used to create E168V:T175D mutant of ILD-PDC.

Triple mutation

E168V:T171S:T175D Primers

5’Primer:
5’-C TTA CTG GCA GTG ATA GAA TCT GAC AAA GCC GAT ATA GG-3’
3’Primer:
5’-CC TAT ATC GGC TTT GTC AGA TTC TAT CAC TGC CAG TAA G-3’

2.1.3.3.2 Oligonucleotides for human LD-OGDC mutations

T44A Primers

5’ Primer: 5’-GT GAG ATT GAA ACT GAC AAG GCA TCT GTG CAG GTT CC-3’
3’ Primer: 5’-GG AAC CTG CAC AGA TGC CTT GTC AGT TTC AAT CTC AC-3’

S45T Primers

5’ Primer: 5’-GAA ACT GAC AAG ACA ACT GTG CAG GTT CCA TCA CC-3’
3’ Primer: 5’-GG TGA TGG AAC CTG CAC AGT TGT CTT GTC AGT TTC-3’

T44A:S45T Primers

5’Primer:
5’GAG ATT GAA ACT GAC AAG GCA ACT GTG CAG GTT CCA TCA CC-3’
3’Primer:
5’-GG TGA TGG AAC CTG CAC AGT TGC CTT GTCAGT TTC AAT CTC-3’

D33G Primers

5’ Primer:
5’-GGA GAC ACA GTT GCA GAA GGT GAA GTG GTT TGT GAG ATT G-3’
3’Primer:
5’-C AAT CTC ACA AAC CAC TTC ACC TTC TGC AAC TGT GTC TCC-3’

P49E Primers

5'Primer:
5'-GAA ACT GAC AAG ACA TCT GTG CAG GTT GAA TCA CCA GCA AATG-3'
3' Primer:
5'-CATT TGC TGG TGA TTC AAC CTG CAC AGA TGT CTT GTC AGT TTC-3'

P49E* Primers (for S45T:P49E and T44A:S45T:P49E production)

5' Primer: 5'-CT GTG CAG GTT GAA TCA CCA GCA AAT GGC GTG-3'
3' Primer: 5'-CAC GCC ATT TGC TGG TGA TTC AAC CTGCAC AG-3'

T44A:S45T:Q47G:P49E Primers

5' Primer: 5'-GAC AAG GCA ACT GTG GGG GTT GAA TCA CCA GCA AAT G-3'
3' Primer: 5'-C ATT TGC TGG TGA TTC AAC CCC CAC AGT TGC CTT GTC-3'

T44A:S45T:Q47G:V48F:P49E Primers

5' Primer: 5'-GAC AAG GCA ACT GTG GGG TTT GAA TCA CCA GCA AAT G-3'
3' Primer: 5'-C ATT TGC TGG TGA TTC AAA CCC CAC AGT TGC CTT GTC -3'

2.1.4 Bacterial strains

2.1.4.1 For molecular biology techniques

Escherichia coli DH5α: (Stratagene)-a recombination deficient strain for the general propagation of plasmid vectors. This is a high transformation efficiency strain producing good yields of plasmid.

XL10-Gold ultra competent cells: (Stratagene)-a recombination deficient strain for transformation of large DNA molecules with high efficiency.

XL1blue supercompetent cells: (Stratagene)-this strain was used for transformation of QuickChange PCR products.

2.1.4.2 For protein expression

***Escherichia coli* BL21 (DE3)**: (Stratagene)-used for non-toxic proteins, encodes T7 RNA polymerase under the control of the lacUV5 promoter.

***Escherichia coli* BL21 (DE3) pLysS**: (Stratagene)-employed for toxic and non-toxic proteins with high level expression of genes cloned into expression vectors under the control of the bacteriophage T7 promoter. The pLysS plasmid expresses T7 lysozyme, a

natural inhibitor of T7 RNA polymerase, allowing for improved transcriptional control and reduction of "leaky" expression.

***Escherichia coli* BL21 (DE3) Codon^{+}:** (Stratagene)-derived from Stratagene's high-performance Epicurian Coli® BL21-Gold competent cells. These cells are designed with extra copies of rare *E. coli* tRNA genes to allow high-level expression of heterologous proteins which are difficult to express in *E. coli*.

2.1.5 Plasmid vectors

pGEX-2T: (4.9Kb) for the expression of glutathione S-transferase recombinant fusion proteins; the GST-fusion protein is added to the N-terminal end of the cloned protein (ampicillin resistant). (Pharmacia, Appendix 1.).

pET-14b: (4.671Kb) for the expression of His-tagged recombinant fusion proteins; the six histidine residues are present at the N-terminus of the cloned protein (ampicillin resistant). (Novagen, Appendix 2.).

pCR®2.1 TOPO®: (3.9Kb): is used to facilitate the cloning of PCR products into the reporter plasmid. It is supplied linearized with single 3'-thymidine (T) overhangs for TA Cloning with topoisomerase I covalently bound to the vector (Invitrogen, Appendix 3).

2.1.6 Molecular biology kits

Wizard® *Plus* Mini Preps purification system was purchased from Promega. The QIAquick Gel Extraction kit for DNA purification was purchased from QIAGEN Ltd. The QuikChange™ Site-Directed Mutagenesis Kit containing *E. coli* XL-1 Blue chemically competent cells was obtained from Stratagene. TOPO TA Cloning Kit containing TOP10 cells was used to facilitate the cloning of the gene into the reporter plasmid (pET-14b) and supplied by Invitrogen.

2.1.7 Gel documentation

Photographs were taken by a Polaroid DS34 direct screen-imaging camera and recorded on MITSUBISHI K56HM$_{CE}$ glossy thermal paper supplied by Amersham Pharmacia Biotech.

2.1.8 Nucleotide accession numbers

All sequences of the genes and their proteins which were used in this work were supplied by the Entrez Nucleotide Database (http://www.ncbi.nlm.nih.gov/entrez). Accession number of human E3BP is AF001437, human E3 is NM 000108, human E2-OGDC is NM 001933, the chloroplastic E2-PDC of *A. thaliana* is AF066079 and the mitochondrial E2-PDC of *A. thaliana* is Z46230. See chapter 5 for details of the human E2 precursor.

2.2 Molecular biology methods

2.2.1 Bacterial media

All strains of *E. coli* were grown in Luria Broth (10g Bacto-tryptone, 5g Bacto yeast extract and 10g NaCl per litre, pH 7.0). LB plates were made by adding 1.5% Bacto Agar (equivalent to 15g/l). All media were autoclaved to sterilize before use.

SOB medium, prepared immediately before use, was used in all transformation reactions. **SOC medium** was filter-sterilized following the addition of 0.02% (w/v) glucose to sterile SOB media (2% (w/v) bactro-tryptone, 0.5% (w/v) yeast extract, 0.5% (w/v) NaCl, 10mM $MgCl_2$, and 10mM $MgSO_4$, pH 7.0).

Selective media

Selective media were prepared with addition of antibiotics, either immediately before inoculation in the case of liquid media, or before pouring plates in the case of solid media. Filter sterilized appropriate antibiotics (ampicillin at 50µg/ml in distilled H_2O, chloramphenicol at 34µg/ml in ethanol) were added as required.

2.2.2 Bacterial cell storage

Cells could be stored for 1-3 weeks on LB plates at 4°C. Cells in LB Broth could be stored for longer periods of several months at -80°C. The longer period of storage was achieved by mixing cells with 15% (v/v) glycerol.

2.2.3 Initiating bacterial growth

A small volume of frozen culture was used to inoculate LB Broth or plate media. The inoculation was carried out by using a sterile loop or tip. Growth was achieved by incubating the media at 37°C overnight (16h maximum).

2.2.4 Preparation of chemically competent E. coli cells

Competent cells were made using the rubidium chloride method. The appropriate bacterial *E. coli* strain was streaked out on a minimal LB plate and grown overnight at 37°C (section 2.2.3). A single colony was used to inoculate 5ml LB liquid medium overnight at 37°C. This culture was inoculated into 100ml LB and grown at 37°C with shaking until the optical density at 550nm was 0.48. The culture was then chilled on ice for 5min and spun at 3,000 rpm for 10 min at 4°C in a 50ml sterile Falcon tube. After pouring off the supernatant, the pellet was resuspended by gently pipetting up and down in 40ml filtered sterilized cold buffer I (30mM potassium acetate, 100mM $RbCl_2$, 10mM $CaCl_2$, 50mM $MnCl_2$ and 15% (v/v) glycerol, pH 5.8) and spun as before. The pellet was finally resuspended in 4ml of filtered sterilized cold buffer II (10mM 3-[N-Morpholino] propanesulphonate (MOPS), 10mM $RbCl_2$ and 15% (v/v) glycerol, pH 6.8) as before and chilled on ice for a further 15min. The cells were stored in 220µl aliquots at -80°C.

2.2.5 Transformation of chemically competent E. coli by heat shock

E. coli DH5α, XL-1 Blue and TOP10 cells were routinely used for the propagation and harvesting of recombinant plasmid DNA while *E. coli* BL21 DE3, BL21 DE3 pLysS and BL21 (DE3) Codon$^+$ cells were used for the expression of the desired recombinant proteins (see section 2.1.4). These bacterial strains were made competent and were transformed following the same method.

2.2.5.1 Transformation of competent *E. coli* with plasmid DNA

Competent cells were thawed on ice immediately before use. Cells (50µl) were used for a single transformation. DNA plasmid (1µl) was added to the cells and incubated on ice for 15min. Cells were heat shocked for 90 seconds (sec) at 42°C, then returned to the ice for a further 2min. SOC medium (450µl) was added to the cells and incubated with shaking at 37°C for 45min. This mix (200µl) was plated out onto an appropriate antibiotic plate and incubated at 37°C overnight (16h).

2.2.5.2 Transformation of competent *E. coli* with ligated plasmid

Transformation of competent bacteria with ligated plasmid followed the same method as above (section 2.2.5.1) but with one exception in that only 20µl of the entire ligation mix was used per transformation.

2.2.5.3 Transformation of *E. coli* XL-1 Blue chemically competent cells

E. coli XL-1 Blue chemically competent cells were used for transformation of mutated plasmid produced by site-directed mutagenesis. Transformation of competent cells with the mutated plasmid followed the same method as above (section 2.2.5.1) but with small variations in that 30 min on ice and 45sec heat shock were required for transformation. In addition, 500µl of LB medium was added to the heat shocked cells and incubated for 1h at 37°C.

2.2.5.4 Transformation of one shot TOP10 competent cells with ligated plasmid

The same method as above (section 2.2.5.1) was used for transformation of one shot TOP10 competent cells with ligated plasmid with small variations according to the manufacturers's instructions; 2µl of the entire ligation mix was added to 50µl competent cells, 30min on ice incubation time and 30sec as heat shock were used for transformation. Moreover, 250µl of SOC medium was added to the cells.

2.3 DNA techniques

2.3.1 Agarose gel electrophoresis

Depending on the size of plasmid DNA and PCR products, an appropriate amount of agarose (0.8%-3%) (w/v) was added to 1x Tris-acetate-EDTA (TAE) buffer (50x, 2M Tris-HCl, pH 7.6, 50mM EDTA and 5.7% (v/v) acetic acid) and heated in a microwave oven until completely dissolved. DNA was diluted in 6x loading buffer (0.25% (w/v) Bromophenol Blue, 0.25% (w/v) Xylene Cyanol FF and 15% (w/v) Ficoll). Gels were run at 100 volts as described by Sambrook *et al.* (1989). Agarose gels were stained for 30min with ethidium bromide (EtBr), DNA samples were viewed under UV light and photographed with E. A. S. Y imaging software using K65HM-CE glossy thermal film (section 0).

2.3.2 Polymerase chain reaction (PCR)

Human full length pre-E2 and pre-E3BP, N-terminal pre-E2 truncate and its mature form, human full length pre-E3, and hybrid pE2-E3 and pE3-E2 were subcloned using PCR. In addition, the chloroplastic lipoyl domain (LD) and the mitochondrial inner lipoyl domain (ILD) of *Arabidopsis thaliana* were subcloned using PCR. PCR reactions were carried out in a total volume of 50µl containing 50ng of template DNA, 5µl reaction buffer (10X), 1µl dNTP mix (0.25mM each of dATP, dCTP, dGTP, and dTTP), 1µl specific forward and reverse primers and 1µl specific DNA polymerase (3.5U/µl), prepared to a total volume of 50µl with sterile dH_2O. Amplification was carried out in a PTC-100^{TM} programmable thermocycler (MJ Research Inc.).

To minimise errors in base incorporation, the Expand High Fidelity enzyme and Vent$_R$ $^{®}$ DNA polymerases were used in the PCR reactions. Expand High Fidelity PCR System is composed of a unique enzyme mix containing thermostable hybrid *Taq* DNA Polymerase and Tgo DNA Polymerase with proofreading activity. Therefore the fidelity of DNA synthesis with Expand High Fidelity PCR System (error rate approx. 4.8×10^{-6}) shows a 3-fold improvement compared to *Taq* DNA polymerase (error rate approx. 1.6×10^{-5}). Moreover, Vent$_R$$^{®}$ DNA Polymerase has a 5-15-fold lower rate of base misincorporation than *Taq* DNA Polymerase due to its intrinsic 3'-5' exonuclease proofreading activity.

The reaction cycle comprising six steps is shown below:

- PCR programme using Expand High Fidelity DNA Polymerase

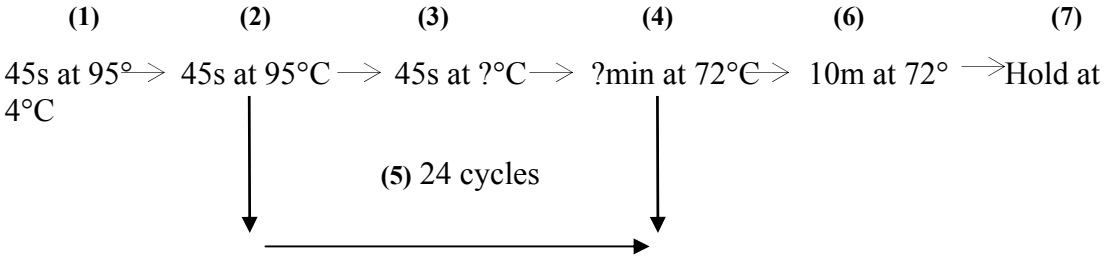

- PCR programme using Vent$_R$® DNA Polymerase

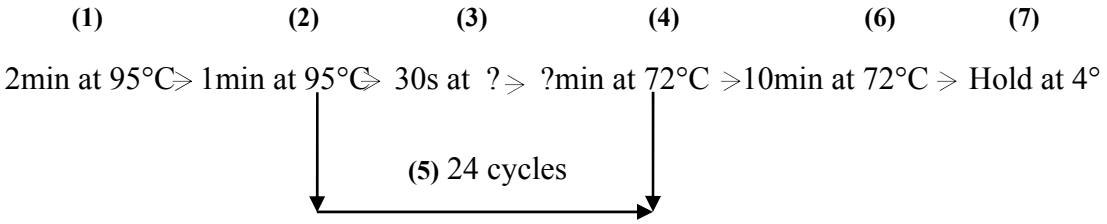

Annealing temperature depends on the melting temperature (Tm) of the primers whereas elongation time depends on the length of the fragment.

Successful amplification was determined by agarose gel electrophoresis (section 2.3.1)

2.3.2.1 Amplification of E2, E3, E3BP precursors, N-terminal pre-E2 truncate and its mature form

Full length E2 precursor, previously cloned in the laboratory into pET-28b, was used as a template for the PCR reaction of pre-E2 and its N-terminal truncated form with NdeI and BamHI restriction sites. The reaction was catalysed by Expand High Fidelity DNA Polymerase. An annealing temperature of 50°C was used for both PCR reactions whereas 4min and 2.7min elongation times were chosen to produce precursor full length and its N-terminal truncated form respectively.

E2, previously cloned into pET-14b in the lab and kindly provided by Dr. Audrey Brown, was used as a template for the PCR reaction of the N-terminal E2 truncate with NdeI and BamHI restriction sites. The reaction was catalysed with Expand High

Fidelity DNA Polymerase. An annealing temperature of 55°C and 2min elongation time was used to produce this length of fragment.

A clone from MRC Geneservice, Babraham, Cambridge was used as the template for the PCR reaction of pre-E3 with BamHI restriction sites, catalysed by Expand High Fidelity DNA Polymerase. An annealing temperature of 55°C and 2.5min elongation time was used to produce the full length E3 precursor.

Full length pre-E2 (previously cloned in this project into pET-14b) was used as the template for the PCR reactions to produce the presequence of E2 with BamHI and SacI restriction sites for the hybrid pE2-E3 cloning and mature E2 with SacI and BamHI restriction sites for pE3-E2 cloning. An annealing temperature of 55°C and 1min elongation time was used to produce the E2 presequence whereas an annealing temperature of 58°C and 2min elongation time was used to produce E2. Both PCR reactions were catalysed with Expand High Fidelity DNA Polymerase.

Full length pre-E3 (previously cloned in this project into pET-14b) was used as the template for the PCR reactions to produce the presequence of E3 with BamHI and SacI restriction sites for the hybrid pE3-E2 cloning and mature E3 with SacI and BamHI restriction sites for pE2-E3 cloning. An annealing temperature of 58°C and 1min elongation time was used to produce the presequence of E3 whereas an annealing temperature of 55°C and 2.5min elongation time was used to produce E3. Both PCR reactions were catalysed with Expand High Fidelity DNA Polymerase.

A clone from MRC Geneservice, Babraham, Cambridge was used as the template for the PCR reaction of pre-E3BP with BamHI restriction sites, catalysed with $Vent_R$ ® DNA Polymerase. An annealing temperature of 50°C and 3min elongation time was used for the E3BP precursor.

2.3.2.2 Amplification of LD and ILD of *A thaliana* chloroplastic and mitochondrial E2-PDC

An N-terminal truncated construct of *A. thaliana* chloroplastic E2-PDC (lipoyl and subunit binding domains) previously cloned into PGEX-2T and kindly provided by Dr. Donna McGow was used as the template for the PCR reaction catalysed by Expand High Fidelity DNA Polymerase. An annealing temperature of 45°C and 1min

elongation time was chosen to produce the chloroplastic lipoyl domain (LD) of *A. thaliana* PDC (Atpt LD-PDC).

An N-terminal truncated construct of *A. thaliana* mitochondrial E2-PDC (outer, inner lipoyl and subunit binding domains) previously cloned into PGEX-2T and also kindly provided by Dr. Donna McGow was used as the template for the PCR reaction catalysed with Expand High Fidelity DNA Polymerase. An annealing temperature of 58°C and 1min elongation time was chosen to produce the mitochondrial inner lipoyl domain (ILD) of *A. thaliana* PDC (Atmt ILD-PDC).

2.3.3 TOPO TA vector cloning

The TOPO TA cloning vector system (Invitrogen) was used to facilitate the cloning of PCR products into the reporter vector, pET-14b. The TOPO cloning vector, pCR®2.1-TOPO® is supplied with 3' deoxythymidine (T) overhangs which is important for ligation with PCR products contained overhanging 3' deoxyadenosine (A). Expand High Fidelity Enzyme has the ability to provide A tails to the PCR products, However, $Vent_R$ ® DNA Polymerase does not have this ability. Therefore, fresh PCR products produced by Vent DNA Polymerase should be incubated with a non template-dependent terminal transferase enzyme such as *Taq* Polymerase.

The TOPO vector cloning system was used according to the manufacturer's instructions. Briefly, the reaction was performed in a total volume of 6µl containing 2µl of the freshly purified PCR product, 1µl of the TOPO vector (approx. 5ng), 2µl of salt solution and 1µl of sterile H_2O. Routinely, the ligation mix was incubated at RT for 5min, followed by transformation into one shot chemically competent cells (TOP10) supplied in the kit; 1µl of the reaction mix was added to 50µl competent cells (see section 2.2.5.4). Colonies containing the ligated constructs were selected according to their ampicillin resistance. Ligated construct was purified from a 5ml LB/Amp overnight culture using a Wizard® *Plus* Mini preps kit (section 2.3.9). The TOPO cloning vector system was used in the cloning of E2, E3 and E3BP precursors as well as N-terminal pre-E2 truncate and its mature form. However, pE2-E3 and pE3-E2 as well as LDs of *A. thaliana* plastid and mitochondria were cloned directly into pET-14b and pGEX-2T respectively.

2.3.4 Restriction digestion

DNA plasmids and PCR fragments were digested using restriction endonucleases (Promega) according to the manufacturer's protocol.

2.3.4.1 Restriction digestion of plasmids

Plasmid DNA (20µl) was digested in a total volume of 40µl with 4µl of appropriate enzymes (10U/µl) and 4µl of the 10x buffer as provided by the manufacturer. The volume of the reaction was made up to 40µl using sterile dH_2O. Digestion was performed at 37°C for 3h. For single digestions, to prevent self-ligation of the digested vector during the ligation step, the 5' protruding termini were dephosphorylated immediately following the incubation. This was achieved by adding 2U of calf intestinal alkaline phosphatase to the total volume, and then incubating at 37°C for a further 30min. The digested plasmid was purified from agarose gels as described in section 2.3.6.

2.3.4.2 Restriction digestion of PCR Products

PCR products (30µl) were digested in a total volume of 60µl with appropriate enzymes for 3h at 37°C. The digested PCR products were purified as described in section 2.3.6.

2.3.4.2.1 Restriction endonuclease digestion of E2, E3, E3BP precursors, N-terminal pre-E2 and E2 truncates as well as presequences of E2 and E3

Following TOPO TA cloning, different restriction endonucleases were used to generate sticky end products. TOPO TA cloning vector with the desired insert was digested with *Nde*I and *Bam*HI for pre-E2, N-terminal pre-E2 truncate and its mature form (see section 2.1.3.1.1). However, only *Bam*HI was used to digest TA cloning plasmids of pre-E3 and pre-E3BP (see sections 2.1.3.1.2 and 2.1.3.1.3). The purified inserts containing the desired sticky ends were then ligated into appropriately digested pET-14b (section 2.3.8).

PCR products of E2 and E3 presequences and mature E2 and E3 were directly digested using *Sac*I and *Bam*HI (see sections 2.1.3.1.4 and 2.1.3.1.5). The PCR fragments

containing the desired sticky ends were then ligated into BamHI digested pET-14b vector in a one step ligation (section 2.3.8).

E. coli DH5α cells were transformed with the resultant plasmid and grown on plates containing LB medium supplemented with ampicillin. Colonies were picked and grown overnight in 5ml aliquots of ampicillin-supplemented LB. Wizard® *Plus* Mini preps kit was used as described in section 2.3.9 to obtain plasmid DNA

2.3.4.2.2 Restriction endonuclease digestion of A. thaliana chloroplastic LD- and mitochondrial ILD-PDC and pGEX-2T vector

Following PCR amplification of LD and ILD of *A. thaliana* chloroplastic and mitochondrial E2 clones, these were digested using *Bam*HI and *Eco*RI restriction endonucleases (see sections 2.1.3.2). PCR fragments contained the desired sticky ends were ligated directly into appropriately digested pGEX-2T (section 2.3.8). The resultant plasmid was transformed into *E. coli* DH5α cells and grown on plates containing LB medium supplemented with ampicillin. Colonies were picked and grown overnight in 5ml aliquots of ampicillin-supplemented LB. Minipreps were carried out to obtain plasmid DNA as described in section 2.3.9.

2.3.5 PCR Based mutagenesis of ILD-PDC and LD-OGDC

A QuickChange ™ Site Directed Mutagenesis Kit (Stratagene) was used to make a variety of mutations in the lipoyl domains of human PDC and OGDC. Two strands of the plasmid template were separated by thermal denaturation, enabling the mutagenic primers to anneal to their complementary regions. Specific oligonucleotide primers (see section 2.1.3.3), each complementary to opposite strands of the recombinant ILD-E2-PDC and LD-OGDC/pGEX-2T plasmid, were extended during temperature cycling in a PTC-100™ programmable thermocycler before the duplex DNA was religated by DNA ligase using *Pfu Turbo* ™ DNA Polymerase.

Pfu Turbo ™ DNA Polymerase is a mix of cloned *Pfu* DNA Polymerase and a novel thermostable factor which enhances PCR product yields without compromising DNA replication fidelity. *Pfu* DNA Polymerases generally have lower error rates (1.3×10^{-6}) than other enzymes such as *Taq* DNA Polymerase. The reaction mix contained 20ng template (ILD-PDC or LD-OGDC in pGEX-2T), 125ng each primer, 1µl dNTP mix (0.25mM each of dATP, dTTP, dCTP and dGTP), 5µl reaction buffer (10x), and 1µl

Pfu turbo DNA Polymerase (3U/µl), prepared in a total volume of 50µl with sterile dH_2O. The cycling parameters for the mutagenesis reaction were as follows:

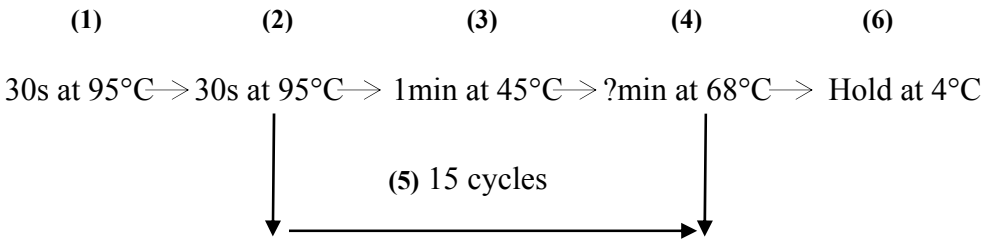

The elongation time (step 4) was 10min for ILD-E2-PDC and 12min for LD-E2-OGDC mutagenesis. Following temperature cycling, the reaction mix was cooled on ice for 2min. To determine whether amplification was successful, 10µl PCR product was analysed by agarose gel electrophoresis (section 2.3.1).

Amplification of the mutant constructs yields two products: one new non-methylated (mutated) strand and one parental methylated (non-mutated) strand. The parental (non-mutated) DNA template was digested prior to the amplification using the enzyme *Dpn*I which is specific for methylated and hemimethylated DNA, leaving behind the non-methylated, mutated strand. As DNA isolated from *E. coli* is generally methylated, it is a suitable substrate for *Dpn* I. Digestion of the parental plasmid was carried out by adding 1µl *Dpn*I (10U/µl) and incubating for 1h at 37°C after spinning the mix at RT for 1min.

The mutant constructs produced contain nicks in their circular DNA which are repaired following transformation into *E. coli* XL-1 Blue chemically competent cells. Reaction mix (1µl) was added to 50µl competent cells (section 2.2.5.3). Colonies containing mutant constructs were selected according to their ampicillin resistance. Mutated plasmid DNA was purified from a 5ml LB/Amp overnight culture using Wizard® *Plus* Mini Preps Kit (section 2.3.9). Successful mutagenesis was determined by sequencing the mutated constructs at the Molecular Biology Sequencing Unit (MBSU), University of Glasgow or MWG Biotech, London, UK.

2.3.6 DNA isolation and purification from agarose

PCR products and digested plasmid DNA were subjected to electrophoresis as above (section 2.3.1), then the band of interest was excised from an agarose gel under UV

light, using a sterile scalpel and purified from the agarose gel using the QIAquick Gel Extraction Kit (QIAGEN Ltd) as in the manufacturer's protocol. Digested PCR products were purified from the reaction mixture using this kit but without gel electrophoresis. The purity and yield of DNA (5µl) was then viewed by agarose gel electrophoresis (section 2.3.1).

2.3.7 Determination of DNA size

A 1Kb ladder DNA marker (Promega) consisting of 13 DNA fragments ranging from 250 to 10,000 base pairs, was used to check the size of linear double stranded DNA and DNA plasmid whereas, a 50bp ladder DNA (Promega) consisting of 16 DNA fragments ranging from 50bp to 800bp, was used to check the size of small PCR products. The determination was achieved by running the ladder DNA marker in parallel to the unknown sample on an agarose gel.

2.3.8 Ligation of Digested Plasmids and PCR products

Usually purified digested plasmid DNA was ligated with purified digested PCR product DNA at various ratios of vector to insert (1:3, 1:6 and 1:9). In addition, one reaction involving only the plasmid was used as a control. The reaction was performed in a total volume of 20µl containing 2µl reaction buffer (10x) and 1.5µl T_4 DNA ligase (3U/µl) (Promega). The volume was made up to 20µl using sterile H_2O. Routinely ligation reactions were incubated at room temperature (approx. 20°C) overnight. Ligation protocols were adapted from Sambrook *et al.* (1989). Next day, 20µl ligation mix was transformed directly into *E. coli* DH5α (section 2.2.5.2).

Purified digested pE2-E3 and pE3-E2 ligation into appropriate pET-14b plasmid was also performed by the same routine ligation protocol. However, the ligation was conducted at various ratios of vector to inserts (presequence and mature E2 and E3 DNA fragments (1:2:2, 1:4:6 and 1:6:8) in a total volume of 20µl.

2.3.9 Plasmid Propagation and Purification

Following transformation of a plasmid into chemically competent *E. coli* DH5α cells (section 2.2.5), single colonies were grown overnight in 5µl LB with the appropriate antibiotic (16h) with constant shaking at 37°C. The cells were harvested by

centrifugation at 3,000rpm for 10min at 4°C in a Beckman AllegraTM 6R centrifuge and the LB was discarded. Plasmid DNA was then prepared using the Wizard® Plus SV Minipreps DNA Purification System (Promega) as instructed by the manufacturer. The quality and yield of isolated DNA (5µl) was viewed by agarose gel electrophoresis (section 2.3.1).

2.3.10 DNA preparation for sequencing

The successful mutation of plasmids (ILD-PDC or LD-OGDC) produced by QuickChange ™ Site Directed Mutagenesis was determined by sending the sample either to MWG-Biotech or The Molecular Biology Sequencing Unit (MBSU), University of Glasgow after purification of the plasmids using the Wizard® Plus *SV* Minipreps DNA Purification System (section 2.3.9). However, only the sample for MWG-Biotech was precipitated using an ethanol precipitation protocol. Briefly, 50µl of 3M cold sterilized CH_3COONa, pH 5.2-5.6 was added to 100µl plasmid then 300µl of 100% ethanol was used to precipitate the plasmid by incubation for 30min to overnight at -20°C. The precipitated DNA was spun for 15min at 14000xg at RT and the supernatant was decanted. The resulting pellet was resuspended in 250µl of 70% ethanol for washing. The resuspended solution was centrifuged for 10min at 14000xg in a bench top microfuge at RT and then the pellet of DNA was ready to be sent for sequencing.

2.3.11 Protein overexpression

2.3.11.1 Small scale over-expression of precursor and mature proteins of various constructs of human PDC as well as N-terminal E2-PDC truncate and its LD form of *A. thaliana* plastid

All precursors and mature constructs (cloned in pET-14b) involving mature and pre-E2, their N-terminal truncated forms, mature and pre-E3, hybrid pE2-E3 and pE3-E2 and mature plus pre-E3BP were expressed in *E. coli* BL21 (DE3) pLysS. Briefly, single colonies of transformed cells were grown overnight in 5ml LB, supplemented with the appropriate antibiotics, ampicillin (50µg/ml) and chloramphenicol (34µg/ml). LB (50ml) plus appropriate antibiotic (ampicillin) was inoculated with 1ml of the overnight culture and grown at 37°C until an A_{600} of 0.5 was obtained. For overexpression of the precursor and mature constructs of human E2- and E3BP-PDC, the LB was

supplemented with lipoic acid (final concentration 0.1mM) at the time of IPTG (1mM) induction. *E. coli* cells were induced either for 3h at 37°C, 4h at 30°C or 6h at 22°C with vigorous shaking. Samples were taken before and after the induction period and harvested by centrifugation in a bench top microfuge at 13,000 xg for 10min to pellet the cells. Pellets were resuspended in Laemmli sample buffer, (10% (w/v) sucrose, 2% (w/v) SDS, 62.5mM Tris-HCl, pH 6.8 and a small amount of Pyronin Y dye using 10µl buffer per 0.1 A_{600} unit of the sample. Successful overexpression was determined by SDS-PAGE (section 2.5.4.1). Cells were harvested by centrifugation using a Beckman Allegra^{TM} 6R centrifuge at 3000rpm for 15min. The pellet was then resuspended in 3ml of filter-sterilized 1x PBS (170mM NaCl, 3mM KCl, 10mM Na_2HPO_4, and 1mM KH_2PO_4, pH 7.4) supplemented with Complete EDTA-free Protease Inhibitor Cocktailts before being stored at -20°C.

N-terminal didomain of E2-PDC of *A. thaliana* plastid and its LD form (cloned in pGEX-2T) were expressed in the same strain of *E. coli* at 30°C for 4h. In addition, the inoculated LB was supplemented with lipoic acid during the induction time with IPTG. As before, samples before and after induction were taken to check the efficiency of the expression of these proteins by SDS-PAGE.

2.3.11.2 Large scale over-expression of E3, *LplA*, and lipoyl domain constructs of E2-PDC and E2-OGDC as well as LDS of human E3BP, Atpt LD-PDC and Atmt lLD-PDC

Wild type (wt) and mutant human lipoyl domains of PDC and OGDC as well as human LD-E3BP cloned in pGEX-2T were expressed in *E. coli* BL21 (DE3) at 37°C for 3h. In addition, the mitochondrial and chloroplastic lipoyl domains of *A. thaliana* E2 cloned also in pGEX-2T were grown in *E. coli* BL21 (DE3) pLysS at 30°C for 4h. Briefly, a single colony of these plasmids was used to inoculate 20ml of LB, supplemented either with ampicillin (50µg/µl) in the case of *E. coli* BL21 (DE3) or with ampicillin and chloramphenicol (34µg/µl) in the case of *E. coli* BL21 (DE3) pLysS and grown at 37°C overnight with shaking. LB (500ml) supplemented with ampicillin was inoculated with the 10ml overnight culture and grown at 37°C or 30°C with constant shaking until an A_{600} of 0.5 was reached. The cultures were induced by the addition of IPTG (1mM). Cultures of E2s and E3BP were expressed in the presence of lipoic acid (0.1mM) and then cultures were incubated for the desired time and temperature with constant vigorous shaking. Again 1ml samples before and after expression were taken for A_{600}

determination. All samples were centrifuged at 13,000 xg for 10min to pellet the cells which were then resuspended in Laemmli sample buffer using 10µl buffer per 0.1 A_{600} unit of the sample. Protein expression was visualized by SDS-PAGE (section 2.5.4.1). Bacterial cultures were harvested by centrifugation at 10,000rpm for 20min in the JA14 rotor of a Beckman J2-21 centrifuge. The supernatants were discarded and the pellets of E2s and E3BP cultures were resuspended in 20ml filter-sterilized 1xPBS, pH 7.4, supplemented with Complete EDTA-free Protease Inhibitor Cocktailts before being stored at -20°C.

E3 constructs in pET-14b were overexpressed in a large scale culture of LB at 30°C for 4h in *E. coli* BL21 (DE3) pLysS cells as above. A single colony of recombinant plasmid transformed into *E. coli* BL21 (DE3) pLysS was used to inoculate 20ml LB supplemented with ampicillin (50µg/ml) and chloramphenicol (34µg/ml). E3 was overexpressed in a 500ml culture as described above. However, the harvested bacterial pellet was resuspended in 20ml 50mM KH_2PO_4 buffer, pH 8.0 supplemented with Complete EDTA-free Protease Inhibitor Cocktailts before being stored at -20°C

The plasmid TM202 housing the *E. coli* lipoate-protein ligase gene (*lplA*) (Morris *et al.*, 1994) (a kind donation from Prof Ben Luisi, University of Cambridge) was transformed into *E. coli* BL21 (DE3) cells and expressed in 500ml LB supplemented with ampicillin (50µg/ml) at 30°C for 6h. The cells were then harvested by centrifugation at 10,000rpm for 20min in the JA-14 rotor of a Beckman J2-21 centrifuge and resuspended in 20ml of filtered-sterilised 50mM Tris-HCl buffer, pH 7.5, containing 1mM PMSF, 1mM EDTA and 10% glycerol (v/v) (Reche *et al.*, 1998). The cells were harvested again by the same buffer. The pellet was resuspended in the same buffer supplemented with Complete EDTA-free Protease Inhibitor Cocktailts and stored at -20°C.

2.3.12 Bacterial cell disruption

Prior to the purification, the bacterial extract was passed three times through a French Pressure Cell (AMINCO) at 950Psi or 750Psi for 500ml and 50ml cultures respectively. Insoluble and soluble fractions of 500ml cultures were prepared by centrifugation at 10,000rpm for 20 min in a JA-17 rotor in Beckman J2-MC centrifuge whereas fractions of 50ml cultures were prepared by centrifugation at 3,000rpm for 15min using a Beckman Allegra™ 6R centrifuge. The clarified supernatant was kept for protein purification or for checking the solubility of protein.

2.4 Protein Materials

2.4.1 Chemicals

2.4.1.1 Chemicals for modification of the lipoamide cofactor of ILD-PDC

4-hydroxynonenal (HNE), a major aldehydic product formed by peroxidation of ω-6-unsaturated fatty acids, was obtained from Calbiochem UK. Methoxy poly (ethylene glycol) maleimide (mPEG-maleimide), M_r 5,000 Da was purchased from NEKTAR^{TM} Transforming Therapeutics. Iodoacetamide and N-ethylmaleimide (NEM) were supplied by Sigma-Aldrich.

2.4.1.2 Chemicals for modification of the lipoyl-lysine residue of ILD-PDC

Different lengths of saturated fatty acids and related compounds were used to modify the lipoyl-lysine residue *in vitro* through an ATP-dependent reaction catalyzed by *E. coli* lipoate-protein ligase A. Sigma-Aldrich was the supplier of these fatty acids: acetic acid (C2), malonic acid (C3), butyric acid (C4), hexanoic acid (C6), octanoic acid (C8), lipoic acid (C8), decanoic acid (C10), dodecanoic acid (C12), tetradecanoic acid (C14) and valproic acid as sodium salts. ABCR GmbH, Germany supplied trans-2-nonenoic acid.

2.4.1.3 General chemicals

The following chemicals were purchased from Sigma-Aldrich: β-nicotinamide adenine dinucleotide (oxidized form β-NAD^+) and the reduced form (β-NADH) (sodium salts), glutathione (reduced form), pyruvic acid (sodium salt), thiamine diphosphate (ThDP), and 3,3',5,5'Tetramethylbenzamidine (TMB), super sensitive form for ELISA. Glutathione Sepharose 4B was supplied by Amersham Pharmacia Biotech. Imidazole and $ZnCl_2$ were purchased from MERCK, BDH. Dithiothreitol (DTT) was obtained from Melford Laboratories Ltd, Suffolk. Bradford protein assay reagent was purchased from BIO-RAD. Pre-made 29:1 (v/v) acrylamide:bisacrylamide solution was supplied by Severn Biotech, Ltd.

2.4.2 Enzymes

Thrombin protease was bought from Amersham Pharmacia Biotech Ltd and Sigma-Aldrich.

2.4.3 Antibodies

QIA*express*® Anti-His HRP Conjugate Kit for detection of 6xHis-tagged proteins was supplied by QIAGEN. Abcam Ltd, Cambridge, UK was a supplier for goat polyclonal serum to human IgG conjugated to Horse Radish Peroxidase (HRP). Patient-derived hybridomas (IgG/λ) secreting hypermutated monoclonal antibodies PD1 and PD2 directed against the lipoylated forms of E2 and E3BP were a kind donation from Prof. Freda K. Stevenson, University of Southampton.

PD1 and PD2 were produced by immortalising B lymphocytes from two female patients with the autoimmune disease, primary biliary cirrhosis (PBC). Blood lymphocytes were isolated from venous blood (60ml) and immortalised by exposing to Epstein Barr Virus (EBV). Following incubation of the EBV-transformed B cells at 37°C in Roswell Park Memorial Institute (RPMI) supplemented with 10% 'myclone' fetal calf serum, pyruvate, glutamine, non-essential amino acids, penicillin, streptomycin, and amphotericin, the cells were hybridised with mouse myeloma cells. Once the hybridomas were visible, each clone was screened for reactivity with E2-PDC (the major autoantigen in PBC) and Ig class and light chain type. Positive clones were selected and cloned until stable monoclonal populations were obtained (Thomson *et al.*, 1998).

2.4.4 Biological tissues

Bovine hearts for isolation of PDC (bPDC) were obtained from Paisley Abattoir, Sandyford Road, Paisley, UK. Hearts were maintained and transported on ice following removal before storage at -80°C in aliquots of 300g. Tissue was thawed overnight at 4°C prior to use. Bovine PDC (bPDC) was purified as described by (Stanley & Perham, 1980) with minor modifications.

2.4.5 Equipments

The BioCAD® SPRINT ™ and BioCAD 700 Series Perfusion Chromatography® Workstations as well as POROS 20 Metal Chelate Affinity and POROS 20 HQ anion exchange packing materials were purchased from PerSeptive Biosystems, Framingham, MA, U.S.A.

A pre-packed HiPrep (16mm x 600mm) Sephacryl S-300 High Resolution column was purchased from Pharmacia with a bed volume of 120ml and fractionation range of 1 x 10^4 – 2 x 10^6 M_r . The column was run using a BioCAD® 700E perfusion Chromatography® Workstation.

Chelating Sepharose® Fast Flow gel matrix, glutathione Sepharose 4B Fast Flow prepacked columns (1ml and 5ml bed-volumes), Hybond ECL Nitrocellulose Membrane and Hyperfilm™ ECL™ detection kit were purchased from Amersham Pharmacia Biotech.

ELISA plates were supplied by Castar, USA.

2.4.6 Spectrophotometric equipment

All spectrophotometric measurements for enzyme assays and protein concentration determination were recorded using a UV-2101 PC scanning spectrophotometer (SHIMADZU). UV quartz cuvettes (0.5ml and 1ml, Jencons) with 10mm light path length were routinely used. In addition, an Ultraspec 4300 pro UV/visible spectrophotometer was used to measure the growth of cells, as well as the concentration of protein. Disposable plastic cuvettes were used mainly for measuring the growth of cells.

2.4.7 Dialysis, buffer exchange and protein concentration

Dialysis was performed at 4°C using either Pierce Slide-A-Lyser dialysis cassettes or dialysis tubing with an appropriate molecular mass cut off for the target protein; both were supplied by Pierce or Dialysis Medical International Ltd, Liverpool, UK.

Proteins were concentrated using Millipore Ultra-Free concentrators with appropriate molecular mass cut off. The concentrator was centrifuged at 3500 rpm in a Beckman Allegra™ 6R centrifuge with a swing out rotor. The concentrated protein was collected by centrifuging it at 1000rpm for 2min.

Dialysis tubing was prepared by boiling the desired length in distilled water with 2% (w/v) Na_2CO_3 and 1mM EDTA. When cool, the tubing was repeatedly rinsed with distilled water before being stored in 20% (v/v) ethanol. Before use the tubing was rinsed thoroughly with distilled water. Routine dialysis of protein samples was performed at 4°C with continual stirring on a magnetic stirrer in 50x buffer volume with several changes of the buffer over the period of time.

Two different capacities of dialysis cassettes were used in this project, 0.1-0.5ml and 0.5-3ml. In addition, two sizes of membranes were used with 3,500 and 10,000 molecular weight cut offs (MWCO). Dialysis cassettes were immersed in dialysis buffer for 30min before use.

2.5 Protein methods

2.5.1 Solubilisation of expressed fusion proteins

Cell pellets from 50ml cultures resuspended in 3ml PBS, pH 7.5 and disrupted using French Press treatment (section 2.3.12) were used to check the protein solubility. Briefly, disrupted cells were centrifuged at 3,000rpm in a Beckman Allegra™ 6R centrifuge for 15min at 4°C and the supernatant retained. An aliquot (100µl) of the original disrupted cell extract was resuspended in an equal volume (100µl) of Laemmli sample buffer and labelled as a cell extract sample (E). Similarly, a further 100µl aliquot of cell extract was centrifuged in a bench top microfuge at 13,000 xg for 10min and the supernatant (90µl) resuspended in an equal volume (90µl) of Laemmli sample buffer and labelled as a supernatant sample (S/N). The pellet from the last spin was washed to remove any traces of supernatant by resuspending in the original volume of 1x PBS buffer and centrifuged as before. This step was repeated two times; each time the supernatant was discarded and replaced with fresh 1x PBS buffer. Finally, the washed pellet was resuspended in an equal volume of Laemmli sample buffer (100µl) and labelled as a pellet sample (P). An equal volume of the three samples (10µl) was

loaded on SDS-PAGE to view the solubility of the recombinant proteins (section 2.5.4.1).

2.5.2 Protein purification

2.5.2.1 Purification of GST-fusion proteins

Clarified supernatant of glutathione S-transferase (GST) tagged protein produced after disruption cell (section 2.3.12) was applied to prepacked GSTrap^{TM} FF columns (1ml and 5ml HiTrap^{TM}). Two 5ml injection steps were incorporated into the BioCAD elution protocol to load the 10ml sample onto the glutathione Sepharose affinity column after equilibrating the column with ice-cold filtered sterilized 1x PBS over 5 column vol. To minimise non-specific binding, the column was washed with 1x PBS over 10 column vol. The bound fusion protein was eluted by washing the column with 4 column vol using glutathione elution buffer (10mM reduced glutathione in 50mM Tris-HCl, pH 8.0) and fractions (1ml) were collected. The purification of the GST-fusion protein was visualised by SDS-PAGE and staining with Coomassie Brilliant Blue.

2.5.2.2 Cleavage of GST-tag

The serine protease thrombin, supplied as a lyophilized powder, was used to cleave recombinant fusion proteins containing a GST-tag. Cleavage of the GST-tag of wild type and mutated ILDs was achieved during the purification of GST-fusion proteins. A glutathione Sepharose 4B column with a bed volume of 2ml was used to purify the protein from the clarified supernatant produced after disrupting bacterial cells (section 2.3.12). The column was pre-washed with 60 bed volumes (120ml) of ice cold PBS before the supernatant was loaded; then the prepacked column was incubated with the clarified supernatant on an ORBITRON ROTATOR II at RT for 1h to let the GST-fusion protein bind to the column; then the column was washed with 60 bed volumes to remove any bacterial protein. Most cleavage of ILDs-PDC was achieved after 4h incubation at RT on the ORBITRON ROTATOR II and complete cleavage was achieved by overnight incubation of the GST-fusion protein bound to glutathione Sepharose 4B with thrombin at 4°C (10U cleaves approx 1mg protein) in 3ml PBS. The cleaved protein was eluted and the column was washed with 3ml PBS to remove any trace of the cleaved protein. The quality of cleaved protein was determined by SDS-PAGE analysis (2.5.4.1).

Thrombin cleavage of wt and mutant LDs-OGDC was achieved by 6h incubation at 37°C and RT with purified GST-fusion proteins previously purified on a glutathione Sepharose 4B Fast Flow prepacked column with 5ml bed-volume (section 2.5.2.1).

2.5.2.3 Metal chelate chromatography

2.5.2.3.1 Preparation for metal chelate chromatography

Metal chelate chromatography used to purify His-tagged proteins was carried out using a BioCAD® SPRINT™ Chromatography® Workstation. A column (10mm x 100mm) with a bed volume of 8.5ml was packed in the laboratory with Self-Pack POROS 20 Metal Chelate Affinity Packing media according to the manufacturer's instructions. The POROS® MC media is designed for immobilized metal chelate chromatography. It consists of cross linked poly (styrene-divinylbenzene) particles which are surface coated with a cross linked polyhydroxylated polymer functionalized with imidodiacetate groups. These groups bind Zn^{2+} ions which in turn interact with the histidine residues of His-tagged proteins. All buffers and dH_2O used in BioCAD® SPRINT™ or 700 Series Workstations were filtered and kept at 4°C until required. The preparation of the metal affinity column was achieved by loading zinc ions (Zn^{2+}) onto the matrix; 20 column vol of 0.1M $ZnCl_2$, pH 4.5-5.0 was passed through the column. The low pH was used to minimize precipitation of metal hydroxide complexes. To remove excess zinc ions, the column was washed with 5 column vol of filtered dH_2O followed by 5 column vol of 0.5M NaCl to remove non-specifically bound metal ions. The column was saturated with elution buffer (0.5M imidazole, 1.0M NaCl and 50mM KH_2PO_4, pH 6), to improve selectively and recovery of His-tagged proteins followed by a 5 column vol wash with filtered dH_2O. The metal chelate column was primed with 5 column vol of starting buffer (0.5mM imidazole, 1.0M NaCl and 50mM KH_2PO_4 buffer, pH 8.0) prior to protein loading.

2.5.2.3.2 His-Tag purification of human E3

Cooled, filtered starting and elution buffers containing 50mM KH_2PO_4 (section 2.5.2.3.1) were used to purify human E3. Clarified material produced after disrupting the cells (20ml) (section 2.3.12) was applied to a metal chelate column. Briefly, four 5ml injection steps were incorporated into the BioCAD elution protocol to load the 20ml sample onto the metal chelate affinity column. An increasing imidazole gradient, from 0.5mM - 0.5M over 5 column vol was carried out, eluting the His-tagged protein

in 2ml fractions. Column regeneration was achieved by stripping with 1.0M NaCl containing 50mM EDTA, or alternatively using 1.0M NaOH for more tightly bound proteins followed by an extended wash with dH_2O. The column was stored in filtered dH_2O or 20% (v/v) ethanol for longer time periods. Fractions were stored at 4°C.

2.5.2.4 Anion exchange chromatography

Anion exchange chromatography was performed to purify bacterial LplA ligase protein from crude bacterial extract using an anionic POROS® HQ column connected to the BIOCAD® SPRINT™, Perfusion Chromatography® System (PE Biosystems) (Reche *et al.*, 1998). The BIOCAD® SPRINT™ SYSTEM automatically mixes the correct quantities of stock buffers to yield the desired concentrations.

Buffers

Washing buffer 20mM NaCl in 100mM Tris/HCl, pH 7.0

Elution buffer 2M NaCl in 100mM Tris/HCl, pH 7.0

All buffers and dH_2O were filtered through a 0.2μm vacuum filter (Millipore) and stored at 4°C.

An initial column wash was performed with 1M NaCl to remove any bound proteins followed by equilibration with 100mM Tris-HCl, pH 7.0, 20mM NaCl for 15 CV. A bacterial pellet (250ml culture) was routinely resuspended in 20ml of starting buffer (section 2.3.11.2) and disrupted using a French Pressure Cell (section 2.3.12). 2ml injection steps were incorporated into the BioCAD elution protocol to load 10ml clarified supernatant (section 2.3.12) in equilibration buffer. Elution of bound proteins was achieved by an increasing (20mM to 1M) NaCl gradient over 20 CV. Fractions of the eluted material (2ml) were collected throughout the gradient. Finally a wash with 1M NaCl buffer was used to clean the column. The purity of the protein was judged by SDS-PAGE (section 2.5.4.1) and Coomassie Brilliant Blue staining.

2.5.2.5 Gel filtration

Bacterial LplA ligase purified by the anion exchange chromatography (section 2.5.2.4) was further purified using gel filtration chromatography (GFC). GFC was performed at

room temperature using a prepacked HiPrep 16/60 Sephacryl S-300 High Resolution column connected to a BIOCAD® 700E Perfusion Chromatography® Workstation. Partially-purified ligase, typically 1ml (recommended < 2% of the bed volume) was loaded onto the pre-equilibrated column and the absorbance at 280nm monitored at a flow rate of 1ml/min. Fractions (2ml) were collected. The column was prepared routinely by equilibrating with 2CV of the appropriate buffer (50mM Tris-HCl buffer, pH 7.5 containing 1mM PMSF, 1mM EDTA, and 10% (v/v) glycerol) at a flow rate of 0.5ml/min (Reche *et al.*, 1998), washing with 2 CV of filtered dH_2O between runs and storing in 20% ethanol for longer periods.

2.5.3 Enzyme assays

All enzyme assays were performed on a Shimadzu UV-2101 PC uv-vis scanning spectrophotometer. Activities were expressed as U/ml, where one unit (U) of enzyme catalyses the conversion of 1μmol of substrate to product per minute under the specified conditions.

2.5.3.1 Dihydrolipoamide dehydrogenase (E3) activity

E3 activity was measured by the formation of NADH which is coupled to the oxidation of dihydrolipoamide at 30°C. The E3 protein was added to a cuvette containing 670μl solution A (3mM NAD^+ and 2mM $MgCl_2$ dissolved in 1M potassium phosphate, pH 7.5) and 20μl (2mM) dihydrolipoamide (DHL). E3 activity is determined from the increase in the absorbance at 340nm. The molecular extinction coefficient of NADH was taken to be 6220 $M^{-1}cm^{-1}$.

Dihydrolipoamide (DHL) was prepared in the laboratory by dissolving 60mg of DL-lipoamide in 1.2ml of 1M potassium phosphate, pH 8.0, 50% (v/v) ethanol. Addition of 2.4ml of freshly prepared 5% (w/v) sodium borohydride in 10mM NaOH resulted in the reduction of DL-lipoamide to DHL. The reaction was terminated after 10min by addition of 1.2ml of 3M HCl which neutralises the reaction and destroys any excess reducing agent. The DHL was then extracted into toluene (3x3ml) and after solvent evaporation under nitrogen, it was stored at -20°C as a white solid.

2.5.3.2 PDC activity

PDC activity was measured by monitoring the formation NADH at 340nm after oxidative decarboxylation of pyruvate to acetyl CoA. All assays were carried out at 30°C. Purified PDC (10µl) was added to the mixture, containing 670µl solution A (3mM NAD^+, 2mM $MgCl_2$ and 0.2mM ThDP) and 14µl solution B (0.13M cysteine-HCl and 6.8mM CoASH) in a quartz cuvette. The reaction was initiated by addition of 14µl of solution C (100mM pyruvate) and mixed rapidly.

2.5.4 Protein analysis

2.5.4.1 SDS-Polyacrylamide Gel Electrophoresis (SDS-PAGE)

2.5.4.1.1 SDS-PAGE Buffers

Resolving gel: 8-15% (w/v) acrylamide,

0.5M Tris-HCl buffer, pH 8.8,

0.1% (w/v) sodium dodecyl sulphate (SDS),

0.1% (w/v) ammonium persulphate,

0.1% (v/v) N, N, N^1, N^1- tetramethylethylene diamine (TEMED)

Stacking gel: 5.4% (w/v) acrylamide,

0.06M Tris-HCl buffer, pH 6.8,

0.1% (w/v) SDS,

0.1% (w/v) ammonium persulphate,

0.1% (w/v) TEMED,

10x SDS buffer:	0.49M Tris-HCl buffer, pH 8.3,
	0.2M glycine,
	1% (w/v) SDS
1x Laemmli sample buffer	62.5mM Tris-HCl buffer, pH 6.8,
	2% (w/v) SDS,
	10% (w/v) sucrose,
	Trace of pyronin Y,
1M DTT	final concentration 150mM

2.5.4.1.2 SDS-PAGE

Proteins were resolved under denaturating conditions using the method of Laemmli (1970). Each gel comprised a 3% stacking gel and an 8-15% resolving gel depending on the molecular weight of the protein of interest. Samples were resuspended in Laemmli buffer to which 1M DTT is added to a final concentration of 150mM, and boiled for 10min before loading onto the gel. Typically, 10-20µl sample was loaded per well. Electrophoresis was carried out at a constant voltage (400V) and 50mA/gel in 1x SDS running buffer. Protein bands were stained with Coomassie Brilliant Blue G250 in 50% (v/v) methanol and 10% (v/v) glacial acetic acid with shaking for 30min at room temperature. The gel was immersed in an appropriate volume of destain (10% (v/v) methanol and 10% (v/v) glacial acetic acid) to remove excess stain and enable clear band visualization.

For superior resolution when necessary, samples were analysed on precast 4-12% NUPPAGE® Novex Bis-Tris gels (Invitrogen) held within a XCell *surelock*™ Mini-Cell. The preparation of protein samples for electrophoresis was the same as for SDS-PAGE. Electrophoresis was carried out in 1x NUPAGE™ MES SDS Running buffer (1M 2-(N-morpholino) ethane sulfonic acid, 1M Tris-base, 69.3mM SDS and 20.5mM EDTA) at constant voltage (200V) and 125mA/gel. The staining and destaining procedures were as for standard polyacrylamide gels.

2.5.4.2 Discontinuous non-denaturing gel electrophoresis

Working buffers

4x separating buffer: 1.5M Tris-HCl, pH 8.8

4x stacking buffer: 0.5M Tris-HCl, pH 6.8

10% (w/v) ammonium persulphate

5x Sample Buffer: 312.5mM Tris-HCl, pH 6.8

50% (v/v) glycerol

0.05% (w/v) bromophenol blue

10x Electrophoresis buffer 25mM Tris-HCl, pH 8.8

192mM glycine

Non-denaturing gel electrophoresis, also called native gel electrophoresis, separates proteins based on their size and charge properties. Native gels are commonly run with high pH buffers (pH 8.8). At this pH, most proteins are negatively charged and migrate towards the anode. Typically samples were resuspended in 5x sample buffer and loaded on the gel. Each gel comprised a 5% stacking gel and 5-15% resolving gel depending on the protein of interest. Electrophoresis was carried out vertically at constant voltage (200V) and 50mA/gel in 1x electrophoresis buffer. Protein bands were visualized by staining the gel using Coomassie Brilliant Blue with shaking for 30min at room temperature. The gel was immersed in an appropriate volume of destain to remove excess stain and enable clear band visualization.

Long term storage of these gels (SDS-PAGE and non-denaturing) was achieved by soaking for 2h in 35% (v/v) ethanol and 2% (v/v) glycerol before being dried between two sheets of cellophane (Pharmacia) in an Easy Breeze apparatus (Hoefer Scientific Instruments, USA).

2.5.5 Estimation of protein concentration

Protein concentration was determined by the method of (Bradford, 1976). The dye Coomassie Brilliant Blue G-250 is converted from red to blue upon protein binding followed by an increase in absorption at 595nm. The absorbance value for known protein concentrations can be used to produce a standard curve of absorbance versus concentration. Thereafter the absorbance of unknown protein samples can be determined from the standard curve. Routinely bovine IgG was used to construct a standard curve at 595nm on a Shimadzu UV-2101 PC UV-VIS scanning spectrophotometer.

Alternatively, protein concentration was determined according to the absorbance at 280nm using buffer as the reference. The protein was analysed in the far UV spectrum over 240-400nm, then the concentration (mg/ml) was calculated using the extension coefficient and the molecular mass for each construct. The extinction coefficient was calculated using the following equation:

$$\frac{\text{No. of tryptophan residues} \times 5690 + \text{No. of tyrosine residues} \times 1280}{\text{Monomeric molecular weight of protein}}$$

2.5.6 Immunoblotting

2.5.6.1 Enhanced chemiluminescence (ECL™) for detection of specific antigens (Western Blot)

Western blotting is a light emitting, non-radioactive method for detecting immobilised specific antigen. The Western blotting procedure was adapted from Sambrook *et al*. (1989).

Following separation by SDS-PAGE or native gel analysis, proteins were electrophoretically transferred onto HybondTM ECLTM nitrocellulose membrane using a BioRad Trans-BlotTM cell at 40mA overnight or 425mA for 45min. Transfer buffer was prepared as a 10x stock (30.3g Tris-HCl, pH 8.3, 144g glycine and 2g SDS, prepared to 2.5L) and used at 1x dilution containing 20% (v/v) methanol. The immunoblotting apparatus was assembled with the nitrocellulose membrane facing the anode and the gel facing the cathode.

Successful transfer was established following staining with Ponceau Red stain. Non-specific binding sites were blocked by immersing the nitrocellulose for 1-2h with agitation in blocking solution (20mM Tris-HCl buffer, pH 7.2, 15mM NaCl, 5% (w/v) non fat milk, 0.2% (v/v) Tween 20) at room temperature or overnight at 4°C. The membrane was subsequently incubated with shaking for 1h at room temperature or overnight at 4°C with the primary antibody solution. Excess primary antibody was removed by three 15min large volume washes with washing solution (20mM Tris-HCl buffer, pH 7.2 and 15mM NaCl, 1% (w/v) non fat milk). The membrane was then incubated for a further 1h at room temperature with the secondary antibody conjugated with horseradish peroxidase. After secondary antibody incubation, the membrane was washed twice for 15min to remove excess secondary antibody. Finally, a 30min incubation was carried out in high salt solution (20mM Tris-HCl buffer, pH 7.2 and 150mM NaCl). Protein blots were developed according to the maker's instructions using the HyperfilmTM ECLTM detection kit. Exposure times were typically 10s to 5min. The primary antibodies used were mAb PD1 or PD2 at 1 in 4000 dilution and at 1 in 500 dilution respectively in 20mM Tris-HCl buffer, pH 7.2, 1% (w/v) non fat milk and 0.1% (v/v) Tween 20. Monoclonal Abs were detected by goat polyclonal serum to human IgG conjugated HRP as secondary antibodies at 1 in 2000 dilution in 20mM Tris-HCl buffer, pH 7.2, 150mM NaCl and 1% (w/v) non fat milk.

2.5.6.2 Immunodetection with Anti-His antibodies or Anti-HisHRP conjugates (chemiluminescent method)

Immunodetection using Anti-His HRP conjugates was applied according to the manufacturer's protocol.

Blocking solution 3% (w/v) (bovine serum albumin) BSA in (Tris-Buffered Saline) TBS buffer and 0.1% (v/v) Tween 20

TBS buffer: 10mM Tris-HCl, pH 7.5, 150mM NaCl

TBS-Tween/Triton: 20mM Tris-HCl, pH 7.5, 500mM NaCl and 0.05% (v/v) Tween 20

0.2% (v/v) Triton X-100

Antibody 1:1000-2000 dilution in blocking buffer

After transferring the protein onto the Hybond^{TM} ECL^{TM} nitrocellulose membrane, the membrane was washed twice with TBS buffer for 10min at RT before incubation with blocking buffer for 1h at RT. The incubation step was followed by washing the membrane twice with TBS-Tween-20/Triton X-100 buffer for 10min at RT and a single wash with TBS buffer. At RT, the membrane was incubated in a 1:2000 dilution of a penta.His Antibody conjugated to HRP (Qiagen) for 1h at RT. Excess antibody was removed by a series of large volume washes as described previously. The detection step was carried out as described in the Amersham Protocol for ECL detection. Exposure times were typically 10s to 1min.

2.5.6.3 Stripping and preparing the membrane

The membrane can be re-blotted again after stripping the previous antibody. Each membrane was stripped by incubation in 100ml stripping buffer (62.5mM Tris-HCl, pH 6.7 and 2% SDS) containing 700µl 2-mercaptoethanol added prior to stripping for 30min at 50°C. At this stage the membrane was washed with washing buffer for 2x 10min to prepare the membrane for the next blot.

2.5.7 Measurement of antibody titre against different lipoyl domain constructs by enzyme-linked immunoabsorbent assay (ELISA)

Quantitation of PD1 and PD2 binding to different constructs of lipoyl domains was determined using a well-established, in-house ELISA assay. To determine optimal antigen concentrations, all proteins were diluted in coating buffer (100mM $NaHCO_3$, pH 8.2-9.0) to obtain 2µg/100µl of each protein. Briefly, wells of a microtitre plate were coated with 100µl protein solution in 100mM $NaHCO_3$ and allowed to adsorb to wells by incubating overnight at 4°C (each row was coated with the same protein). Non-specific sites were blocked by incubation with PBS containing 1% (w/v) Bovine Serum Albumin (BSA) for 2h. Blocking buffer was followed by two wash steps with 0.05% (v/v) Tween 20/PBS; then each row was coated with different concentrations of mAbs PD1 (1 in 1000-64000 dilution) or PD2 (1 in 50-6400 dilution) in 1x PBS and incubated for 2h at RT. Following 4x washes with 0.05% (v/v) Tween/PBS, bound Ab-Ag complexes were detected with goat polyclonal serum to human IgG (HRP) antibodies diluted to 1:2000 in blocking buffer. Following 4 washes, bound peroxidase activity was determined using a peroxidase substrate, 3, 3', 5, 5'

tetramethylbenzamidine (TMB). The plate was incubated in the dark for 30min after adding the reagent. The reagent produces a soluble end product ranging from dark to pale blue in colour according to the amount of immune complex present and can be read spectrophotometrically at 630nm.

2.5.8 Modification of the lipoamide cofactor

mPEG maleimide (M_r 5000) was used to study the extent of lipoylation of wt and mutant ILDs-PDC and LDs-OGDC. In addition, mPEG, HNE (C8), NEM (C6) and iodoacetamide (C2) were used to investigate the effect of chemical modification of the lipoamide prosthetic group on mAb PD1 and PD2 cross reactivity.

Chemical modification of the recombinant ILD and E2/E3BP-bPDC were performed by covalent attachment to the free reduced form of the sulphydryl groups of the dithiolane ring of the lipoic acid using the series of reagents of different sizes and structures listed above.

2.5.8.1 mPEG maleimide, N-ethylmaleimide (NEM) and iodoacetamide modification

Chemical modification was performed in a 50µl reaction volume with 20µg ILD protein, 5µg of human E3 and NADH or NAD^+ (0.1mM) in 50mM Tris-HCl, pH7.5 and incubated for 10 min at RT. The reaction was started after adding mPEG (0.5mM), NEM (0.5, 1 and 2mM), or iodoacetamide (1, 2, 5, 10, 25 and 100mM), incubated for 30min at 25°C and then excess chemical was scavenged by adding DTT (100mM). Chemical modification was assessed by 15% native gel electrophoresis (section 2.5.4.2). Western blot analysis was performed to study the effect of chemical modification of the lipoamide prosthetic group on PD1 and PD2 recognition (section 2.5.6.1).

Chemical modification was also performed on E2 and E3BP-bPDC using mPEG or NEM. The reaction was carried out in a 100µl reaction volume with 1mg/ml bPDC and NAD^+ or NADH (0.1mM) in 50mM Tris-HCl pH 7.5 and incubated for 10min at RT. Then the reaction was started by adding 0.5mM mPEG or 0.5-1mM NEM and incubated at 25°C for 30min. Excess chemical reagent was scavenged by adding DTT (100mM). PDC activity was measured to confirm the complete modification achieved as described

in section 2.5.3.2. At the same time, modified bPDC (15µg) was assessed by running SDS-PAGE and blotting with PD1 and PD2 to check the cross reactivity of the modified bPDCs.

The extent of lipoylation for the various mutated domains of ILD-PDC and LD-OGDC was estimated as above using mPEG maleimide. However, the reaction was performed either with the LD or LD-GST fusion proteins of PDC and OGDC. Modification was visualised by gel shift assay using either SDS-PAGE (section 2.5.4.1) or non-denaturing gel analysis (section 2.5.4.2).

2.5.8.2 HNE modification

HNE modification of ILD was carried out in a 50µl reaction volume with 20µg ILD, 5µg human E3 and 0.1mM NADH or NAD^+ in 50mM KPi (KH_2PO_4/K_2HPO_4), pH 7.4 and incubated for 10min at RT. The reactions were started by adding different concentrations of HNE (0.05, 0.1, 0.25 and 0.5mM) and incubated for 1h at 30°C. The reactions were stopped by adding native gel sample buffer. The success of HNE modification was determined by performing 15% native gel electrophoresis. Western blot analysis of PD1 and PD2 was used to study the effect of HNE modification on Ab recognition.

HNE modification of purified bPDC was also performed in 50mM KPi, pH 7.4. Bovine PDC (1mg/ml) was incubated with 0.1mM NADH or NAD^+ for 10min at RT. The reaction was initiated by adding different concentrations of HNE (0.05, 0.1, 0.25 and 0.5mM) and incubated for 1h at 30°C. After incubation, the activity of bPDC was measured to ensure complete modification (section 2.5.3.2). In addition, 5µg of modified protein from each reaction (0.05 and 0.1mM) was blotted with PD1 and PD2 (section 2.5.6.1).

2.5.9 Modification of the lipoyl-lysine residue

The apo-form of the ILD was modified *in vitro* by incubation with *E. coli* Lp1A in the presence of different fatty acids of varying chain length and related compounds. A reaction mixture (50µl) containing 1.2mM ATP, 1.2mM $MgCl_2$, 0.5mM fatty acids or related compounds plus 0.1, 0.3 or 0.7mg/ml Lp1A and 0.4mg/ml of the lipoyl domain in 20mM Tris-HCl, pH 7.5 was incubated at 25°C for 3h. Since the lipoyl ligase protein

was contaminated with a small amount of endogenous substrate, a control reaction was included in each case. Reactions were stopped by the addition of sample buffer.

The incorporation of the fatty acids was assessed by non-denaturing (native) gel electrophoresis (section 2.5.4.2). To study the effect of the incorporation of these fatty acids on PD1 and PD2 responses, immunoblotting was performed for each modification. (section 2.5.6.1).

2.5.10 Quadrupole-time of flight (Q-TOF) Mass spectrometry

Mass spectrometry is a valuable tool employed routinely in different areas of biochemical research. It is an analytical technique used to measure the mass-to-charge ratio of ions. It gives accurate molecular weight measurements which helps to confirm the nature of the sample, to determine the purity of the samples, to verify amino acid substitutions, to detect post-translational modifications and to calculate the number of disulphide bridges. This technique is also used to monitor enzyme reactions, chemical modification and protein digestion. In addition it is an accurate instrument for peptide and oligonucleotide sequencing.

Generally, the mass spectrometer is divided into three fundamental parts, namely the ionisation source, analyser and detector (Figure 2-1). Mass spectrometers can measure the mass of charged particles in a gas (analyte); therefore, the sample of interest has to be introduced into the ionisation source of the instrument. The two ionisation methods most commonly used for mass spectrometric analysis in the majority of biochemical applications are Electrospray Ionisation (ESI) and Matrix Assisted Laser Desorption Ionisation (MALDI). After ionisation, the sample ions are extracted into the analyser region of the mass spectrometer where they are separated according to their mass (m)-to-charge (z) ratios (m/z) (Lane, 2005). Again, there are a number of mass analysers currently available, quadrupole (Q), time-of-flight (TOF), magnetic sectors, and both Fourier transform and quadrupole ion traps. The TOF analyser measures the time for an ionised molecule to travel a set distance with the time taken directly related to the mass/charge (m/z) ratio. The separated ions are monitored and amplified by the detector which converts the ion energy into electrical signals that are then transmitted to a computer. Different types of detectors are supplied to suit the type of analyser; the more common ones are the photomultiplier, the electron multiplier and micro-channel plate (MCP) detectors. The signal is then transmitted to the data system where it is recorded

in the form of mass spectra. The three regions of the mass spectrometer are maintained under high vacuum to give the ions a reasonable chance of the travelling from one end of the instrument to the other without any hindrance from air molecules (Morris *et al.*, 1997; Chernushevich *et al.*, 2001).

Tandem (MS/MS) mass spectrometers are the main instruments used for structural and sequencing studies. These instruments are connected to two, three or four analysers and they do not necessarily have to be of the same type. Most popular tandem mass spectrometers include those of the quadrupole-quadrupole, magnetic sector-quadrupole and quadrupole-time of flight geometries. The Q analyser can be used either as a lens under MS mode analysis to focus the ion beam into the second analyser or as an analyser under MS/MS mode analysis to transmit solely the ions of interest into the collision cell housing inert gas such as argon or helium where the sample ions are bombarded in this area and fragmented. The fragment ions are then analysed by the second (TOF) analyser (Morris *et al.*, 1997).

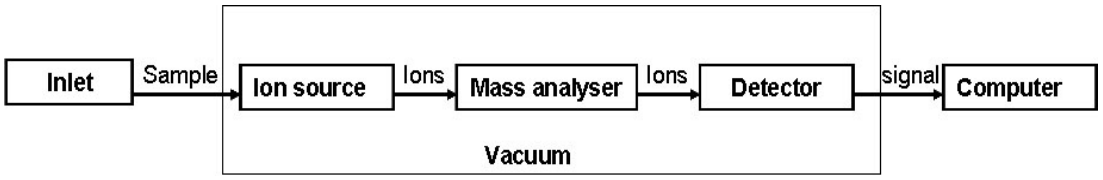

Figure 2-1 Basic diagram for a mass spectrometer

2.5.10.1 Electrospray ionisation (ESI) mass spectrometry

Q-TOF mass spectrometer analysis uses the ESI ionisation source, one of the Atmospheric Pressure Ionisation (API) techniques used to generate gaseous ionized molecules directly from a liquid solution. Briefly, as shown in Figure 2-2, the sample is dissolved in a polar, volatile solvent and pumped through a narrow, stainless steel capillary at a flow rate of between 1µl/min and 1ml/min. An electric field with a high voltage of 3 or 4 kV is applied to the tip of a capillary which is situated within the ionisation source of the mass spectrometer. As a consequence of this strong field, the sample emerging from the tip is dispersed into an aerosol of highly charged droplets, a process that is aided by a co-axially introduced nebulising gas flowing around the outside of the capillary. The nitrogen gas usually helps to direct the spray emerging from the capillary tip towards the mass spectrometer (Figure 2-2, panel A).

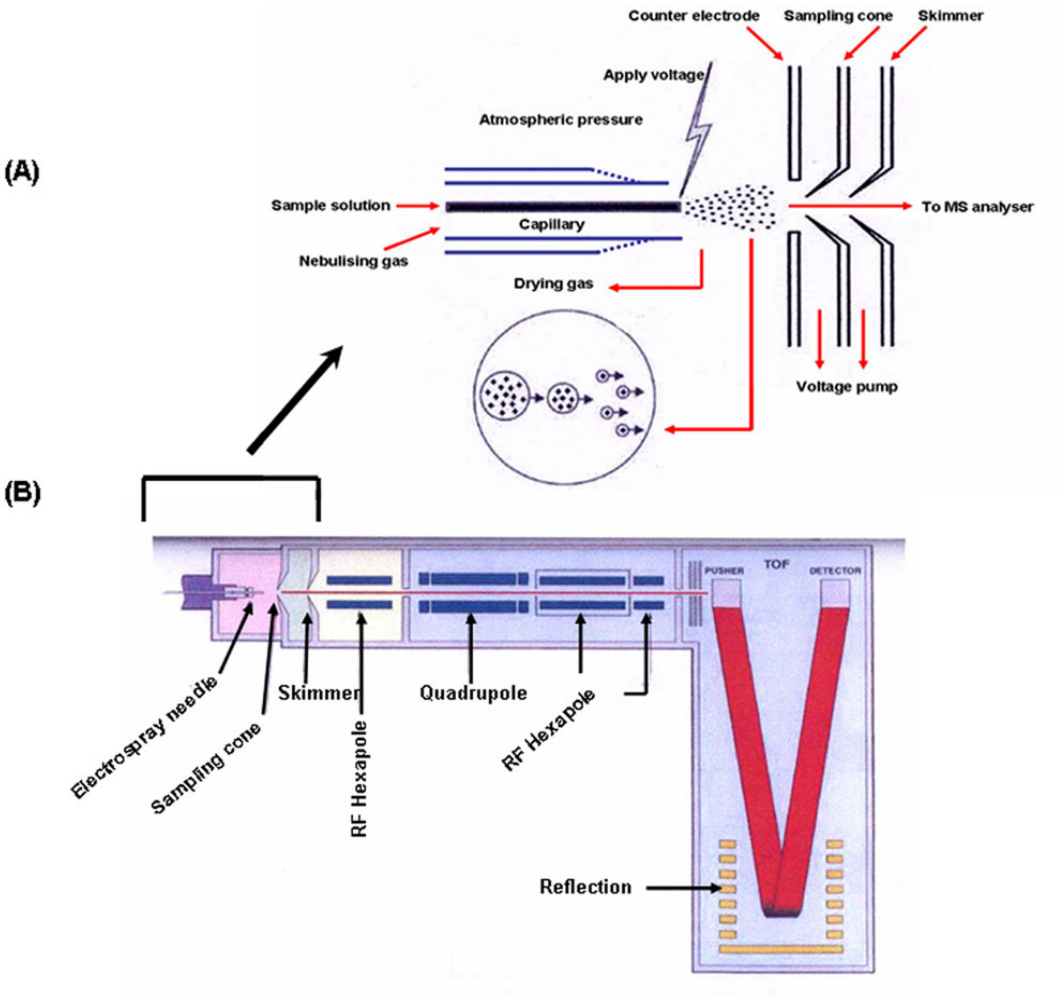

Figure 2-2 Q-TOF mass spectrometry in MS mode
Panel (A) Schematic diagram of an ESI interface and the ESI process

Panel (B) Schematic diagram of Q-TOF mass spectrometer

The charged droplets diminish in size by solvent evaporation, assisted by a warm flow of nitrogen known as the drying gas, which passes across the front of the ionisation source. Eventually charged sample ions, free from solvent, are released from the droplets, some of which pass through a sampling cone or orifice into the skimmer region and from there through a small aperture into the analyser of the mass spectrometer which is held under high vacuum (Figure 2-2, panel B) (Morris *et al.*, 1997; Chernushevich *et al.*, 2001).

2.5.10.2 Sample preparation

GST cleaved proteins of ILDs-PDC produced in the presence and absence of exogenous lipoic acid plus non-lipoylatable mutant domain (K173Q) were dialysed in 20mM ammonium acetate pH 7.5, dissolved at concentration 10 pmol/µl in 1:1 1% (v/v) aqueous formic acid:methanol and then subjected to nanospray ionisation. This technique is a low flow adaptation of the electrospray technique to generate positive ions in the presence of nitrogen as the API gas. Positive ions, free from solvent pass through the sampling cone at a voltage of 40V and then the skimmer lenses, radio frequency (RF) hexapole focusing system and the first Q analyser in turn to focus the ion beam into the second TOF analyser. The TOF analyser separates the ions according to their mass-to-charge ratio. Separated ions are detected by MCP at 2700V. Data are acquired over the appropriate m/z range and transmitted as mass spectra in continuum mode, plotting the m/z ratio against intensity (indication of the abundance of each component in the sample). An external calibration was made using horse heart myoglobin (MW 16,951.5 Da). Data were processed using the MassLynx suite of software programs supplied with the mass spectrometer. Mass spectra were recorded in collaboration with Dr. A. E. Ashcroft, Astbury Centre for Structural Molecular Biology, University of Leeds.

2.5.10.3 Identification of the lipoyl domain substituent

Previous studies using mass spectrometry have shown that overexpression of the human lipoyl domain in a wild-type host in the absence of added lipoate generates two types of products representing lipoylated and non-lipoylated domains (Quinn *et al.*, 1993b). In contrast, two types of domains, identified as octanoylated and non-modified domains were detected when the *E. coli* lipoyl domain was expressed in a lipoyl deficient strain of *E. coli* under lipoate deficient conditions (Ali *et al.*, 1990). In our study, the minor

putative lipoylated band of ILD-PDC produced in the wild-type host in the absence of exogenous lipoic acid was not amenable to mPEG maleimide modification (chapter 3). This evidence suggested that this minor band may be the octanoylated domain which lacks the dithiol groups required for reaction with mPEG maleimide. In order to confirm the octanoylation status of this band, the technique of mass spectrometry was employed with the aim of detecting a change in mass corresponding to the presence of the octanoic acid prosthetic group (126 Da) using ILD-PDC housing the lipoic acid prosthetic group (188 Da) and ILD-PDC (K173Q) as positive and negative controls.

As shown in Figure 2-3 (peak A), the mass spectrum of the ILD-PDC generated with exogenous lipoate illustrates the presence of a major peak with a M_r of 11,838.5 Da. The measured mass is consistent with the predicted M_r 11,838 Da for lipoylated ILD-PDC. Moreover, the mass spectrum of the K173Q mutant lacking the lipoic acid prosthetic group is 11,649.9 Da which is also consistent with its predicted value of M_r 11,650 Da for lysine mutated ILD-PDC (Figure 2-4, peak A). Interestingly, a major peak corresponding to the major band of the ILD-PDC produced in the absence of the exogenous lipoate yielded an estimated mass of 11, 650.4 Da which is consistent with the predicted M_r value of 11,650 for the non-lipoylated ILD-PDC (Figure 2-5, peak A). However, the mass of the minor peak produced in this case is 11,774.5 Da which is closely to the predicted molecular mass for ILD-PDC housing the octanoate prosthetic group, M_r 11,776 Da (Figure 2-5, peak C). Current data are in agreement with previous studies suggesting that octanoylated and non-modified domains are generated under lipoate shortage. However, in our case, the production of these domains occurred in wt host and not in a lipoate deficient strain as reported by Ali *et al.* (Ali *et al.*, 1990)

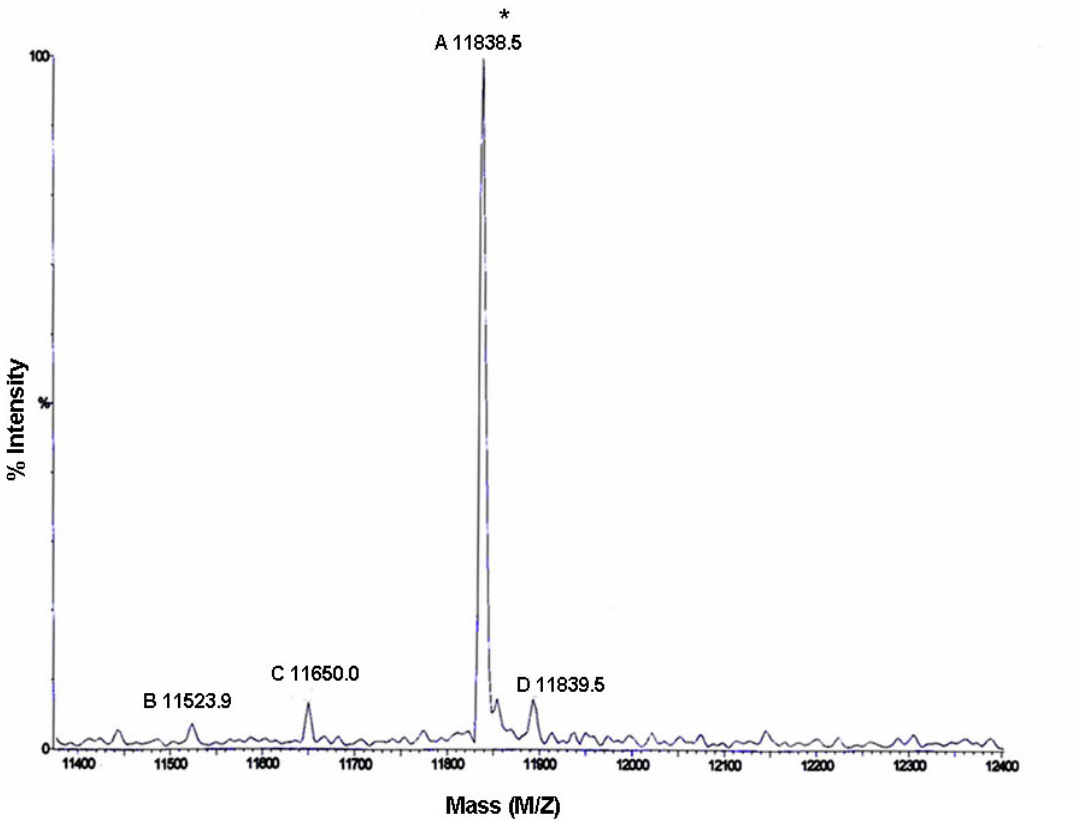

Figure 2-3 Mass spectra of ILD-PDC plus lipoate
Measured in quadrupole-time of flight mass spectrometer with Electrospray ionisation source, calibrated with myoglobin

Peak A corresponds to the lipoylated ILD.

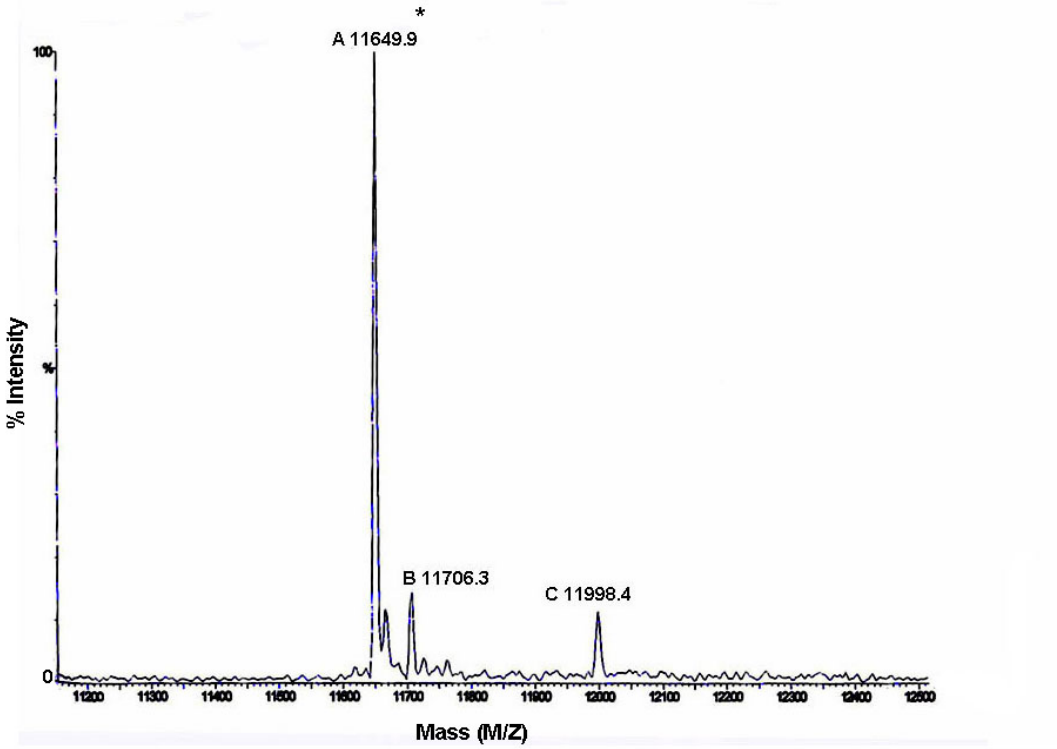

Figure 2-4 Mass spectra of ILD-PDC K173Q
Measured in Q-TOF mass spectrometer with Electrospray ionisation source, calibrated with myoglobin

Peak A corresponds to non-lipoylated ILD.

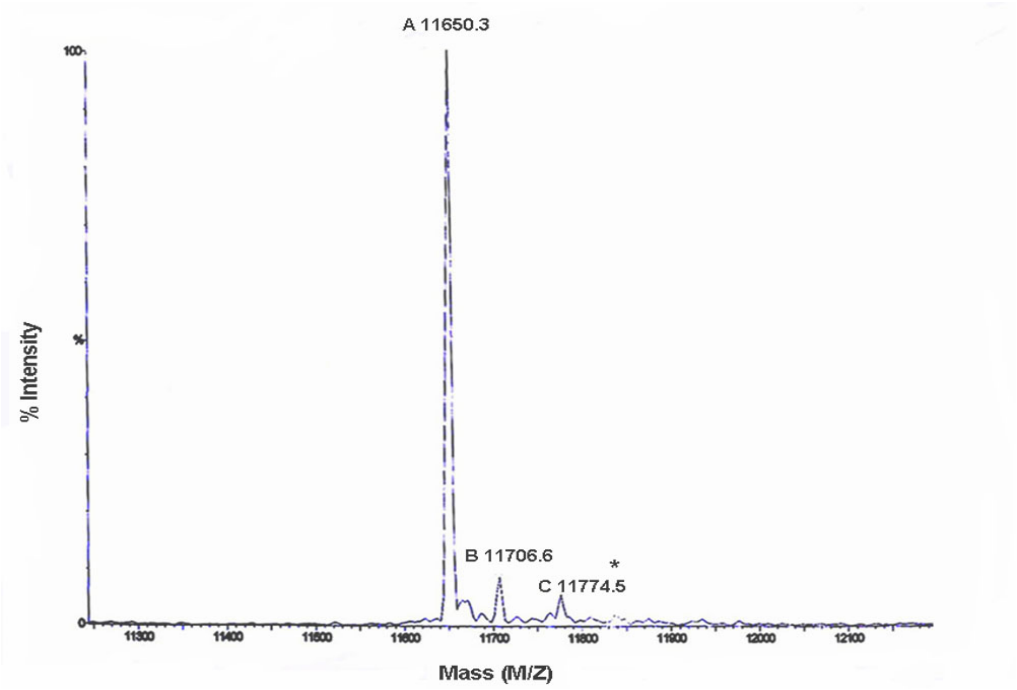

Figure 2-5 Mass spectra of ILD-PDC minus lipoate
Measured in Q-TOF mass spectrometer with Electrospray ionisation source, calibrated with myoglobin

Peak A corresponds to the non-modified ILD whereas **peak C** corresponds to octanoylated domain.

Chapter 3

Investigation of the molecular basis of patient derived monoclonal antibody interactions with E2 and E3BP lipoyl domains of the human pyruvate dehydrogenase complex

3.1 Section 1

Primary biliary cirrhosis (PBC) is a chronic inflammatory autoimmune liver disease characterised by destruction of biliary epithelial cells (BECs) lining the small intra-hepatic bile ducts, which interferes with bile secretion, causing fibrosis and eventually cirrhosis of the liver. In this autoimmune disease, the sera, bile and saliva of the majority of patients (95%) contain high levels of anti-mitochondrial antibodies (AMA) directed mainly against the family of 2-oxoacid dehydrogenase complexes (Gershwin *et al.*, 1987; Coppel *et al.*, 1988; Fussey *et al.*, 1988; Surh *et al.*, 1989a; Fregeau *et al.*, 1990a; Leung *et al.*, 1996; Nishio *et al.*, 2001). Numerous studies have been performed by different laboratories using polyclonal and monoclonal antibodies derived from PBC patients where it has been found that the predominant autoimmune response is directed against E2 and/or E3BP of PDC. Therefore, E2-PDC is considered to be the major target for the AMA response with its lipoic prosthetic group exerting a major influence on antibody recognition (Van de Water *et al.*, 1988a; Surh *et al.*, 1990a; Matsui *et al.*, 1993; Quinn *et al.*, 1993a). However, neither lipoic acid itself nor lipoamide were found to be antigenic (Flannery *et al.*, 1989). In addition, the conserved primary sequence around the lipoate attachment site of E2-PDC and E3BP is important for Ab recognition (Fussey *et al.*, 1989b).

Five hybridoma-derived mAbs have been generated by Thomson *et al.* from peripheral blood lymphocytes of two patients with PBC by immortalising B lymphocytes (Thomson *et al.*, 1998). Two are IgG2λ (PD2, DWZ) isotypes, two are IgG3λ (PD1, PD5) isotypes and one is an IgMλ (PD3) isotype. All clones have reactivity against the major autoantigen, E2-PDC; however, three clones (PD3, PD5, and DWZ) also recognise the non-lipoylated form to a lesser extent which a common feature of the PBC-specific polyclonal antibody population as a whole. mAbs PD1 and PD2 show exclusive specificity for lipoylated E2-PDC. Therefore, determination of the precise epitope recognised by these mAbs is of interest in terms of gaining a more precise understanding of the aetiology of the disease.

It is apparent from previous studies (Thomson *et al.*, 1998; Potter *et al.*, 2001) that mAbs PD1 and PD2 interact with a common lipoylation-dependent epitope that is present on both human E2 and E3BP lipoyl domains. However, although these mAbs recognise the lipoylated form of human E2- and E3BP-PDC, the presence of the attached cofactor alone is not in itself sufficient for mAb recognition. Thus negligible

holodomain reactivity is detected with E2-OGDC, E2-BCOADC and *E. coli* E2-PDC (Thomson *et al.*, 1998); (Richards, S.D, PhD thesis, University of Glasgow, 2000). In addition, it has been observed from previous work in our laboratory that there is no cross reactivity between mAb PD2 and the lipoylated chloroplastic E2-PDC from *Arabidopsis thaliana* (Atpt E2-PDC) whereas the mitochondrial E2-PDC (Atmt E2-PDC) equivalent displayed a strong cross-reaction (McGow, D, PhD thesis, University of Glasgow, 2002).

As a result of the previous observation, this study was initiated by screening purified recombinant lipoyl domains from a variety of sources with mAb PD2. These were as follows: the wt inner lipoyl domain (ILD) and its non-lipoylatable control domain (K173Q) of human E2-PDC cloned into the pGEX-2T vector (Quinn *et al.*, 1993b); the outer lipoyl domain of human E2-PDC (OLD-PDC); the lipoyl domain of human OGDC (LD-OGDC); the lipoyl domain of human E3BP-PDC (LD-E3BP) cloned previously into pGEX-2T as well as the chloroplastic lipoyl domain of (Atpt LD-PDC) and mitochondrial inner lipoyl domain (Atmt ILD-PDC) of *A. thaliana* cloned into the pGEX-2T vector during this work. All the LDs were blotted with mAbs PD1 and PD2.

3.1.1 Aims of this section

- To describe the strategy used to clone mitochondrial and chloroplastic LDs of *A. thaliana* E2-PDC.

- To compare the reactivities of lipoyl domains from different sources with mAb PD2.

- To confirm that the presence of the attached cofactor alone is not in itself sufficient for mAb recognition.

3.1.2 RESULTS

3.1.2.1 PCR amplification of lipoyl domains of *A. thaliana* E2-PDCs

Recombinant plasmids encoding the N-terminal chloroplastic E2-PDC didomain, (lipoyl and subunit binding domains) and mitochondrial E2-PDC tridomain, (outer and inner lipoyl, and subunit binding domains) from *A. thaliana* served as templates to amplify

the chloroplastic lipoyl domain and the mitochondrial inner lipoyl domain respectively as described in Materials and Methods, section 2.3.2.2. The two plasmids were previously cloned and kindly provided by Dr. Donna McGow. Specific primers were designed to the appropriate 5' and 3' regions adjacent to downstream of the chloroplastic lipoyl domain and the mitochondrial inner lipoyl domain of the *A. thaliana* E2-PDC genes as shown in Materials and Methods, section 2.1.3.2.

PCR products were gel-purified and analysed on 1% (w/v) agarose gels alongside a 1kb DNA ladder (Materials and Methods, section 2.3.1). Bands of approx. 250 bps were observed, corresponding to the chloroplastic and mitochondrial LDs (Figure 3-1, panels A and B).

3.1.2.2 Cloning of LDs of *Arabidopsis thaliana* E2-PDCs

PCR products (LDs) and pGEX-2T vector were treated with *Bam*HI and *Eco*RI to generate sticky ends (Materials and Methods, section 2.3.4). After digestion, both vector and PCR product were purified using the QIAquick gel extraction kit (Qiagen) and DNA was eluted in 30µl elution buffer. Samples (5µl) of each were run on a 1% (w/v) TAE agarose gel to check the quantity and quality of DNA produced (data not shown).

For ligation, purified digested insert was ligated into pGEX-2T at a range of vector to insert ratios (1:3, 1:6 and 1:9) as described previously in Materials and Methods, section 2.3.8. After amplification in *E. coli* DH5α cells, colonies were checked at all three ratios.

Seven and five colonies of the chloroplastic LD and mitochondrial ILD respectively were selected. The plasmid DNA, purified from 5ml overnight cultures as described in Materials and Methods, section 2.3.9, was analysed on a 1% agarose gel (data not shown).

Plasmids were then digested with *Eco*RI and *Bam*HI to confirm the presence of an insert of the correct size (Figure 3-2) as described in Materials and Methods, section 2.3.4.1. For Atpt LD-PDC, out of six colonies examined five contain the insert (Figure 3-2, panel A) whereas five colonies of Atmt ILD-PDC digested successfully with the restriction enzymes (Figure 3-2, panel B).

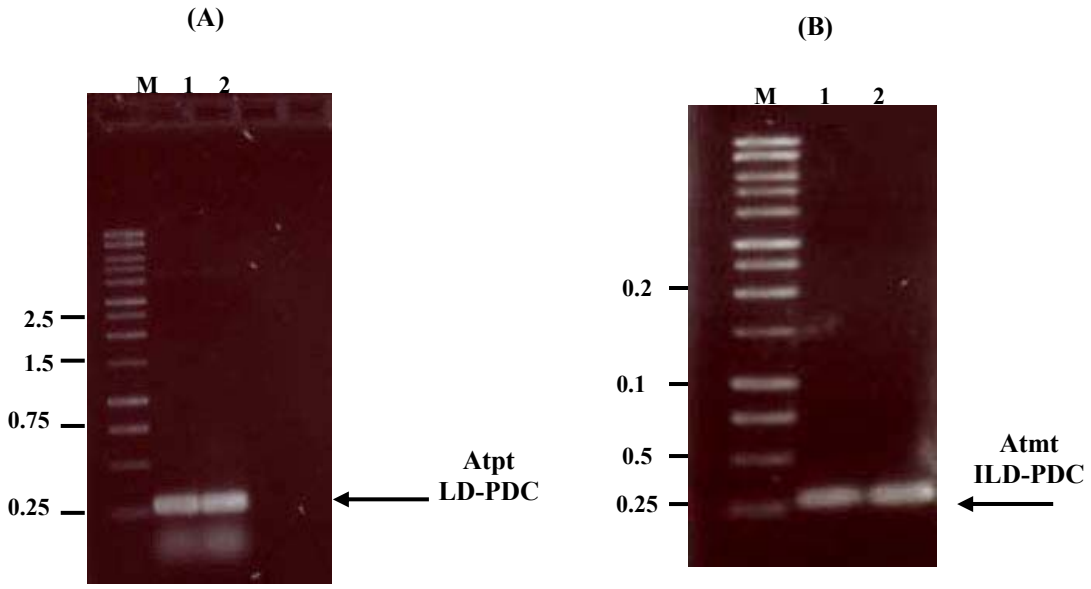

Figure 3-1 Amplification products of chloroplastic and mitochondrial lipoyl domains of *A. thaliana* E2-PDC
PCR mixtures (5µl) were resolved on 1% agarose gels and the DNA viewed under UV light after staining with ethidium bromide.

Panel A: The lipoyl domain was amplified from a clone of the N-terminal chloroplastic E2-PDC didomain in pGEX-2T. A positive result was seen by the presence of a single band of expected size ~250 bps.

Panel B: The inner lipoyl domain was amplified from a clone of the N-terminal mitochondrial E2-PDC tridomain in pGEX-2T. A positive result was seen by the presence of a single band of expected size ~250 bps.

M: 1 kb DNA ladder markers.

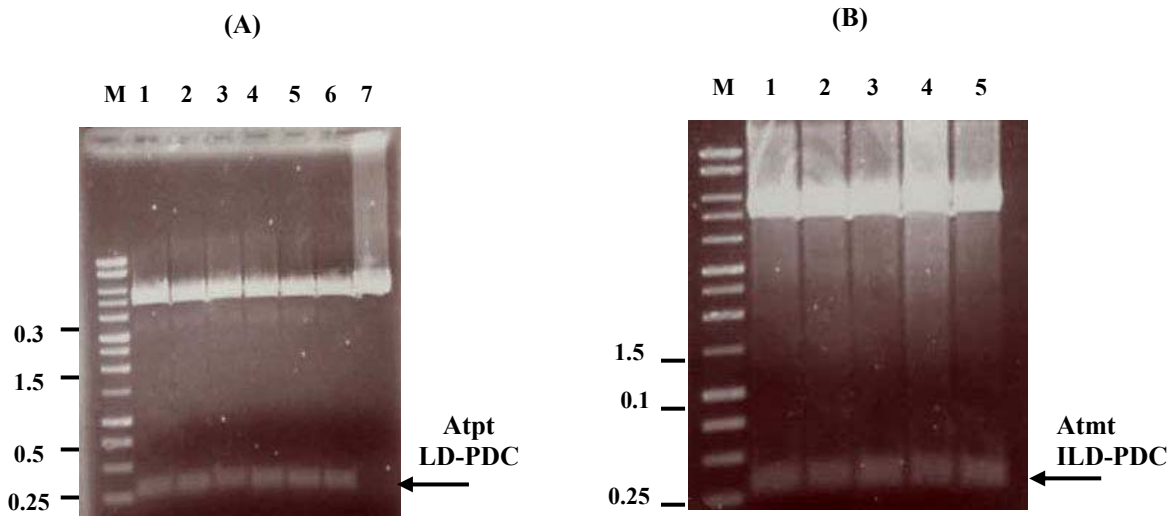

Figure 3-2 Restriction digestion of putative positive colonies showing the presence of inserts of the expected sizes
Samples were resolved on 1% (w/v) agarose gels and then stained with ethidium bromide and viewed under a UV transilluminator.

Panel A: six positive directional clones from seven putative clones encoding the lipoyl domain of chloroplast E2-PDC (250 bps) present in lanes 1-6 were confirmed by BamHI and EcoRI digestion

Panel B: five positive directional clones encoding the inner lipoyl domain of mitochondrial E2-PDC (250 bps) present in lanes 1-5 were confirmed by BamHI and EcoRI digestion.

M: 1 kb DNA ladder markers.

3.1.2.3 Protein expression

The heterologous expression of the chloroplastic and mitochondrial LDs (derived from *A. thaliana* E2-PDCs) were carried out in *E. coli* BL21 (DE3) cells at 37°C for a 3h induction period as described in Materials and Methods, section 2.3.11.2. Following reducing SDS-PAGE (Material and Methods, section 2.5.4.1), bands at 38-40kDa were observed corresponding to the predicted M_r values of the chloroplastic LD and mitochondrial ILD expressed as GST fusion proteins (Figure 3-3). At the same time, similar expression of other previously cloned human lipoyl domains, ILD-PDC, OLD-PDC, LD-E3BP, LD-OGDC and ILD-PDC K173Q was performed in *E. coli* BL21 (DE3) at 37°C for 3h (data not shown). The solubilities of *A. thaliana* and human LDs were assessed and it was found that all LDs were soluble after IPTG induction at 37°C. Figure 3-4 shows the solubilities of *A. thaliana* LDs.

3.1.2.4 GST-tag purification of LDs from various sources

LDs from *A. thaliana* and mammalian species were routinely purified from large-scale (250ml) bacterial cultures by affinity chromatography on glutathione Sepharose 4B prepacked columns (5ml) employing either a BioCAD® SPRINT ™ or BioCAD 700 Chromatography® Workstation (Materials and Methods, section 2.5.2.1). This system was extremely efficient in producing high yields of pure LDs. Insignificant levels of contaminating *E. coli* proteins were detected; therefore no other purification steps were deemed necessary. A typical SDS-PAGE gel analysis of purified LD-GST fusion proteins of *A. thaliana* chloroplastic LD-PDC and mitochondrial ILD-PDC, human ILD-PDC, mutated human ILD K173Q, human OLD-PDC, human LD-E3BP and human LD-OGDC is illustrated in Figure 3-5, panel (A) as examples of the quality of GST-tag purifications.

3.1.2.5 Investigation into the reactivity of different wild type LDs with mAb PD2

Purified LD-GST fusion proteins (1µg) were separated on a 12% SDS-gel, transferred to Hybond™ ECL™ nitrocellulose membrane and blotted with mAb PD2 (Figure 3-5, panel B). In addition, samples were also blotted with PD1 (data not shown). Western blot analysis was performed to study the cross reactivity between the wild type LDs

from various species and mAb PD2 and carried out as described in Materials and Methods, section 2.5.6.1.

At the same time, purified LD-GST fusion proteins (5µg) were resolved on a 12% SDS gel and stained with Coomassie Brilliant Blue (Figure 3-5, panel A) to confirm their purity and equality of loading prior to immunoblotting.

It is clear from Figure 3-5, panel B that mAb PD2 displays strong cross reactivity with some LDs such as human ILD- and OLD-PDC. Moreover, the strength of PD2 interaction with the OLD is similar or perhaps slightly enhanced relative to the ILD. ILD-PDC-Atmt displays significant cross reactivity but to a lower extent than the ILD and OLD-PDC. All these LDs were subsequently shown to be fully lipoylated (see Figure 3-6 for details).

There is no cross reactivity between mAb PD2 and LDs of OGDC and Atpt LD-PDC. In addition, PD2 displays a reduced reactivity with LD-E3BP, although this domain was subsequently shown to be extensively lipoylated (see Figure 3-6 for details).

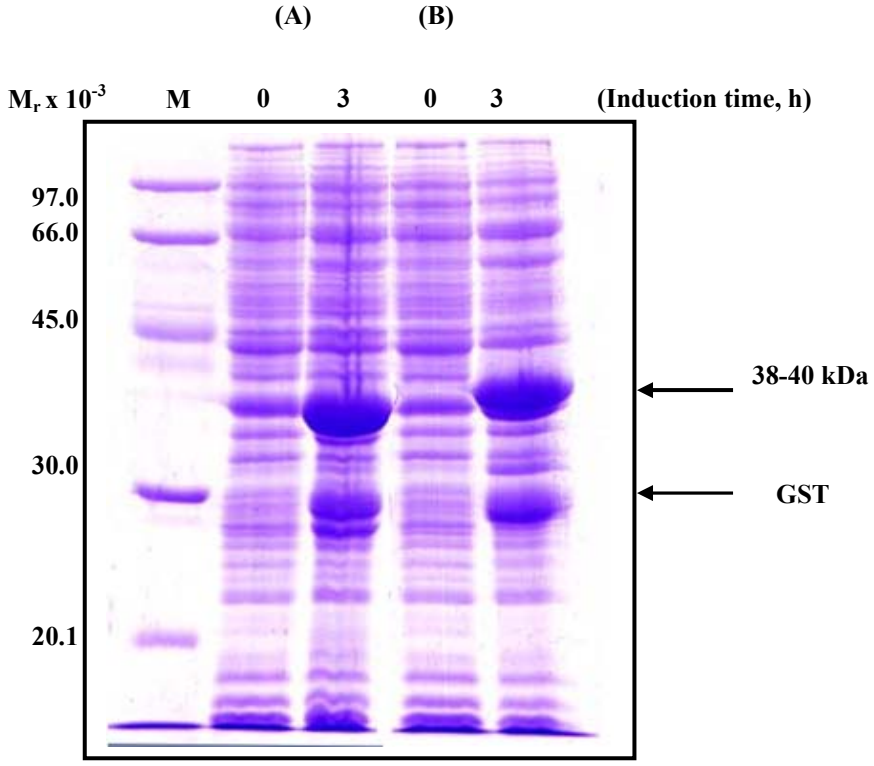

Figure 3-3 Overexpression of ILD and LD of mitochondrial and chloroplastic E2-PDC from *A. thaliana* expressed as GST fusion proteins
Two clones of LDs were expressed over 3h at 37°C in *E. coli* BL21 (DE3) cells. Samples were denatured in the presence of DTT (150mM) at 100°C for 5-10min prior to analysis on a 12% SDS/polyacrylamide gel. Protein bands were stained with Coomassie Brilliant Blue. Molecular weight markers (M) are shown to the left of the gel. The arrow on the right of the gel denotes overexpressed recombinant proteins.

Sample (A): Expression of ILD of *A. thaliana* mitochondrial E2-PDC before (T0) and after induction (T3).

Sample (B): Expression of LD of *A. thaliana* chloroplastic E2-PDC before (T0) and after induction (T3).

M: relative molecular mass

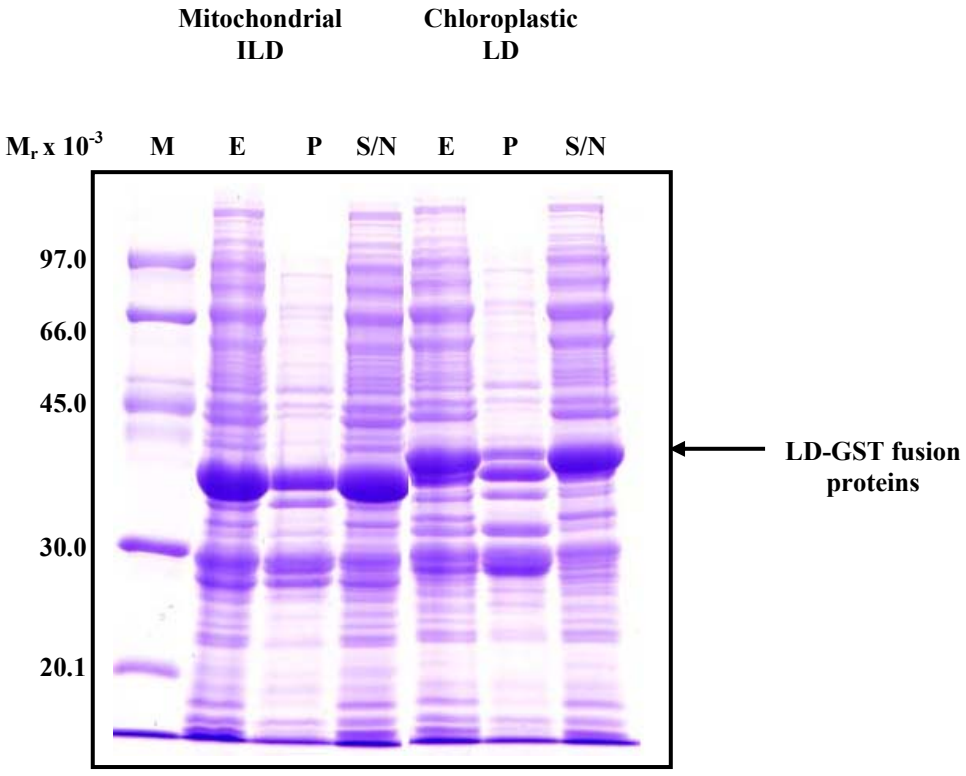

Figure 3-4 Solubilities of LDs of plant mitochondrial and chloroplastic E2-PDC expressed as GST fusion proteins
Following protein overexpression of the LDs at 37°C for 3h, the bacterial culture (50ml) was centrifuged and the pellet resuspended in 3ml 1 x PBS buffer pH 7.5. Cells were lysed by passing cells three times through a French Press at 750Psi. The cell extract (E) was separated into its soluble (S/N) and insoluble (P) fractions by centrifugation at 3000 rpm. Samples were prepared in Laemmli sample buffer and denatured for 5-10min at 100°C in the presence of DTT (150mM), prior to loading on a 12% SDS/polyacrylamide gel. Bands were stained with Coomassie Brilliant Blue.

The arrow indicates the LD-GST fusion proteins.

M: Molecular weight markers are shown to the left of the gel.

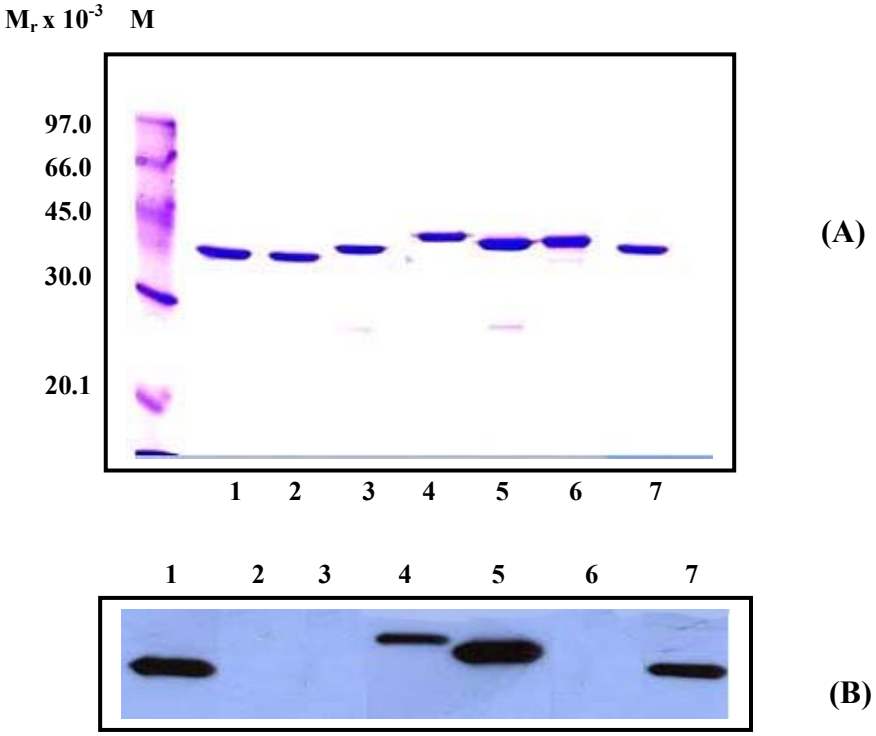

Figure 3-5 The reactivities of various wild type lipoyl domains (LDs) with mAb PD2
Panel (A) 12% SDS-PAGE analysis of purified LD-GST fusion proteins (5µg) stained with Coomassie Brilliant Blue.

Panel (B) Western blot analysis of LD-GST fusion proteins (1µg) with mAb PD2

Lane 1, human ILD-PDC; *lane 2*, human ILD-PDC K173Q; *lane 3*, Atpt LD-PDC; *lane 4*, LD-E3BP; *lane 5*, human OLD-PDC; *lane 6*, LD-OGDC; and *lane 7*, Atmt ILD-PDC.

M: Molecular weight markers are shown to the left of the gel.

3.1.2.6 Checking the lipoylation of LD-GST fusion proteins by methoxy poly (ethylene glycol) maleimide (mPEG maleimide) modification

There are two possible explanations for lack of cross reactivity with PD2. This may be due to lack of lipoylation *per se* or relate to the requirement for a specific sequence around the lysine residue of the lipoamide cofactor which is important for Ab recognition. To distinguish between these two possibilities LDs as GST fusion proteins were subjected to modification using mPEG maleimide, a thiol group reagent (M_r 5000) as described in Materials and Methods, section 2.5.8.1.

LDs containing the reduced lipoamide prosthetic group (in the presence of NADH and human E3) were treated with 0.5mM mPEG maleimide for 30min at 25°C. Reactions with NAD^+ were carried out as negative controls. Modification was visualised by gel shift assay in which the affected LD domain exhibited a markedly decreased rate of migration. Modification of LDs is specific to the reduced thiol groups of the dithiolane ring of the lipoic acid cofactor as seen below, since no shift is observed in the presence of NAD^+. These data also confirm that the GST segment of the fusion protein contains no accessible cysteines. In contrast, E3 is also susceptible to mPEG maleimide modification in its reduced state. This is presumably because the active-site cysteine pair is amenable to modification when reduced in the presence of NADH. Modified LD samples were subjected to 12% SDS-PAGE (gel shift analysis) (Figure 3-6).

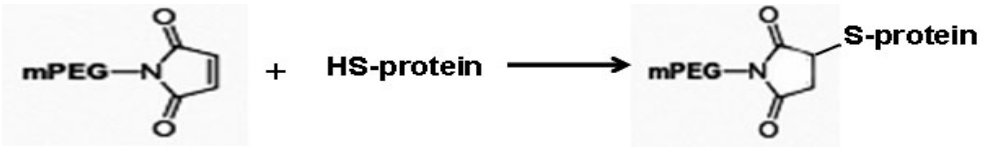

mPEG maleimide modification showed that ILD- and OLD-PDC, LD-E3BP and Atmt ILD-PDC were extensively lipoylated whereas LD-OGDC was lipoylated only to a very limited extent. However, subsequently it was shown that approx. 70% of LD-OGDC could be lipoylated and modified completely with mPEG maleimide (see Figure 3-22 for more details). In addition, lack of mPEG maleimide modification suggests that LD-PDC-Atpt was not lipoylated. This observation contradicted a previous result in our group demonstrating that the equivalent Atpt N-terminal E2-PDC didomain was indeed lipoylated. Thus this conflicting evidence prompted us to conduct further checks into the lipoylation status of the chloroplastic LD. The negative result for ILD-PDC K173Q was expected as it has a key lipoylatable lysine replaced by glutamine.

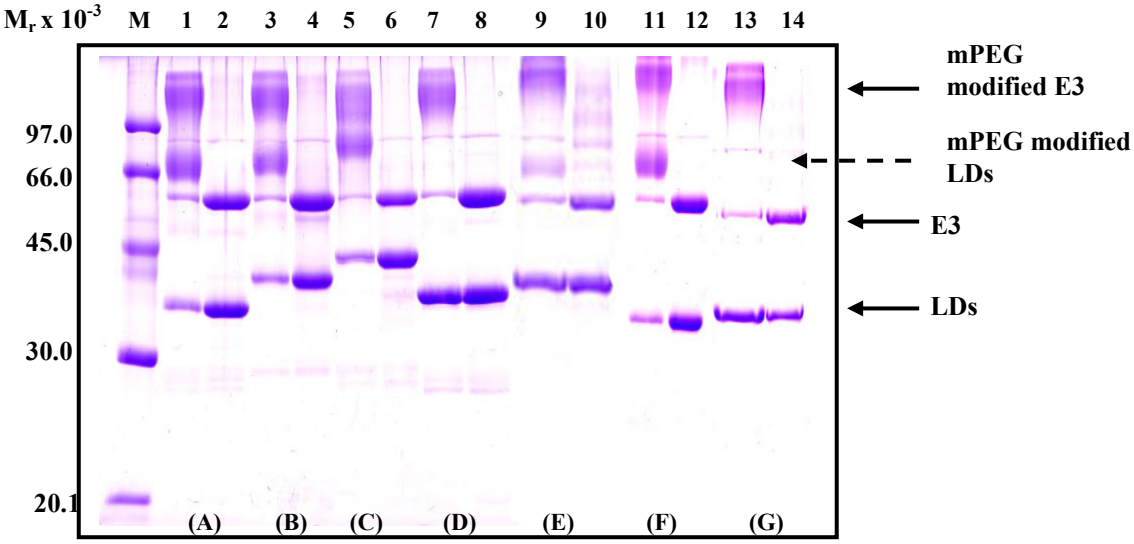

Figure 3-6 mPEG-maleimide modification (gel shift assay) of different lipoyl domain GST fusion constructs
LD-GST fusions (20µg) were treated with 0.5mM mPEG maleimide in the presence of NADH and NAD^+ respectively to check the extent of lipoylation after resolution by 12% SDS-PAGE

Sample A, ILD-PDC; **sample B**, OLD-PDC; **sample C**, LD-E3BP; **sample D**, ILD-PDC K173Q; **sample E**, LD-OGDC; **sample F**, Atmt ILD-PDC; and **sample G**, Atpt LD-PDC.

Lanes 1, 3, 5, 7, 9, 11, and *13:* modification of LDs in the presence of NADH

Lanes 2, 4, 6, 8, 10, 12, and *14*: modification of LDs in the presence of NAD^+

M: Molecular weight markers are shown to the left of the gel.

3.1.2.7 Checking the lipoylation of the chloroplastic *A. thaliana* E2-PDC didomain

A) Expression of the chloroplastic N-terminal didomain of *A. thaliana* E2-PDC

The expression of the recombinant plasmid for the chloroplastic N-terminal didomain of *A. thaliana* E2-PDC was carried out in *E. coli* BL21 (DE3) pLysS cells at 30°C for a 4h induction period. Small scale over-expression was carried out as described in Materials and Methods, section 2.3.11.1.

B) Western blot analysis of the chloroplastic N-terminal didomain of *Arabidopsis thaliana* E2-PDC using mAb PD2

Western blot analysis was carried out to check the cross reactivity between the chloroplastic N-terminal didomain of *A. thaliana* E2-PDC and mAb PD2 as described in Materials and Methods, section 2.5.6.1. *E. coli* extracts of various LD-GST constructs prepared before and after induction were run on two 12% SDS/polyacrylamide gels. One gel was stained with Coomassie Brilliant Blue (Figure 3-7, panel A) and the other was electrophoretically transferred onto Hybond^{TM} ECL^{TM} nitrocellulose membrane (Figure 3-7, panel B). Wild type ILD and its K173Q mutant were used as positive and negative controls. Following blotting with mAb PD2, it was found that there is cross reactivity between PD2 and the ILD-PDC (a positive control); however, no cross reactivity was observed with either the N-terminal didomain or lipoyl-domain-GST constructs of chloroplastic E2-PDC (Figure 3-7 , panel B).

C) Checking the lipoylation of the N-terminal truncate of *A. thaliana* using mPEG maleimide modification

The lipoylation status of the chloroplastic E2-PDC didomain was checked by chemical modification using mPEG maleimide as previously. It was observed in previous mPEG modifications on GST fusion proteins that the reaction was variable and incomplete, perhaps due to the presence of the GST-Tag (M_r 2.7 kDa) causing a degree of steric hindrance. Therefore, mPEG maleimide treatment was performed on purified thrombin-cleaved protein dialysed in 50mM Tris-HCl buffer, pH 7.5 as described in Materials and Methods, section 2.5.8.1. Apart from the LD-Atpt, all proteins were quite stable under these conditions.

Modification was visualised by gel shift assay in which the modified protein exhibited a markedly decrease rate of migration. The reaction was carried out in the presence of NADH or NAD^+. A native PAGE gel (15%) was run to check the mPEG modification (Figure 3-8). It was found that the chloroplastic N-terminal didomain was fully lipoylated whereas the LD alone is non-lipoylated and also appears to be susceptible to degradation as seen by the presence of multiple bands. No further work was carried out on Atpt LD-PDC as it was apparent that the fully lipoylated didomain was not recognised by mAb PD2.

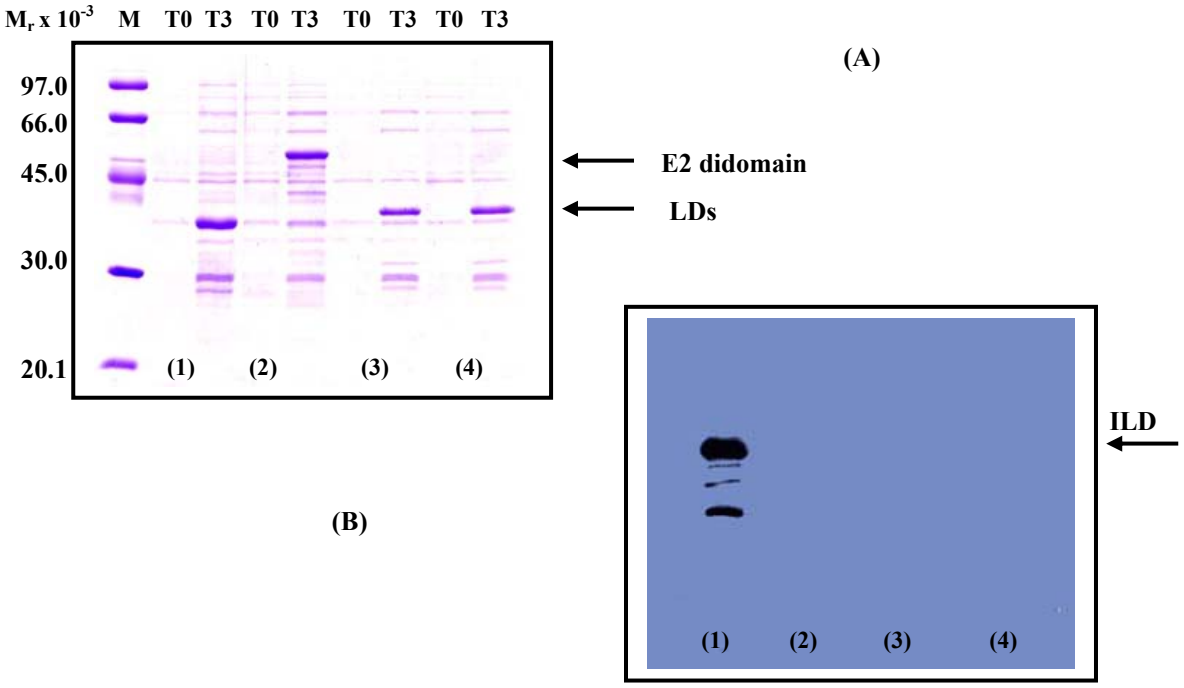

Figure 3-7 Cross reactivities of different wild type LDs with mAb PD2
Panel (A): 12% SDS-PAGE analysis of bacterial extracts (1 in 20 dilution) taken at 0h (T0) and 3h (T3) overexpression of GST fusion proteins. *Sample 1*: ILD-PDC, *Sample 2*: N-terminal Atpt of E2-PDC didomain, *sample 3*: Atpt LD-PDC, and *sample 4*: K173Q.

Panel (B): Western blot analysis of bacterial extracts (1 in 20 dilution) taken at 0 (T0) and 3h (T3) overexpression of GST fusion proteins with 1 in 500 dilution of mAb PD2. . *Sample 1*: ILD-PDC, *Sample 2*: N-terminal Atpt of E2-PDC didomain, *sample 3*: Atpt LD-PDC, and *sample 4*: K173Q.

M: low molecular mass markers are shown to the left of the gel

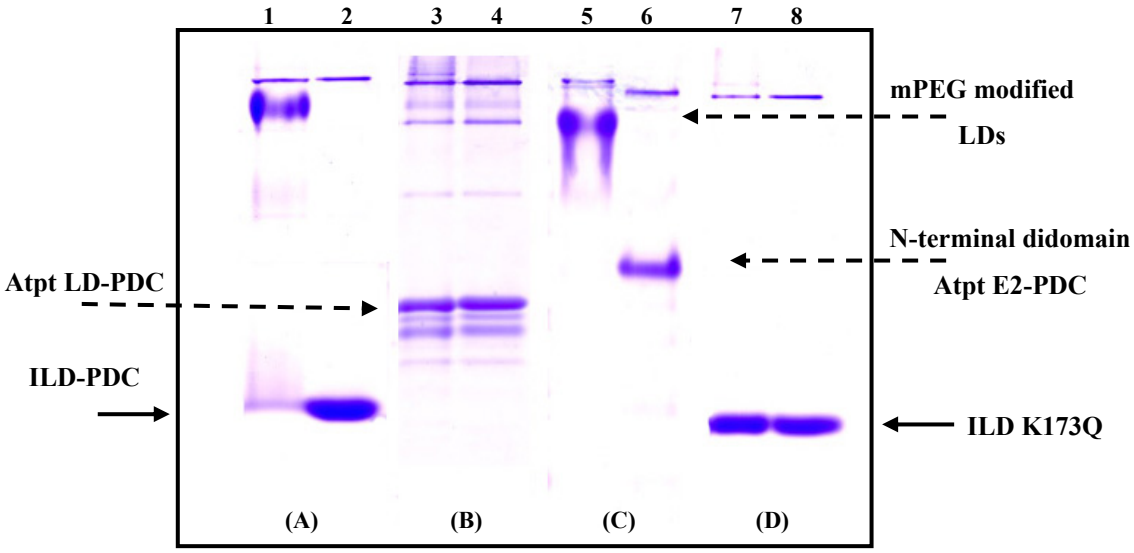

Figure 3-8 mPEG-maleimide modification (gel shift assay) of different thrombin cleaved LDs
Following modification of LDs with 500mM PEG-maleimide in the presence of NADH and NAD^+, 6µg from each modified sample was run on 15% native gel. Two gels were joined; the first gel invoves samples A, B, and D whereas the second gel involves a sample C.

Sample A, ILD-PDC; **sample B**, Atpt LD-PDC; **sample C**, N-terminal Atpt E2-PDC didomain; and **sample D**, ILD-PDC (K173Q)

Lanes 1, 3, 5, and *7*: modification of LDs in the presence of NADH

Lanes 2, 4, 6, and *8*: modification of LDs in the presence of NAD^+

3.2 Section 2

In the previous section it was confirmed that the presence of the attached cofactor alone is not in itself sufficient for mAb recognition. This result permitted us to focus on several conserved key amino acids around the lipoyl lysine group that could be integral to immune recognition. In order to identify key candidate residues, LD sequences from various enzymes and species were aligned to allow their direct comparison (Table 3-1).

Initial inspection of the different LD sequences showed that there is a highly-conserved block of 8 amino acid residues (Table 3-1, highlighted in yellow), immediately adjacent to the lipoyl lysine residue. Three conserved amino acids around the lipoylatable lysine of human ILD-PDC are distinct from the non-reactive Atpt LD-PDC (Table 3-1). Site-directed mutagenesis enables us to examine the importance of these residues, Glu-168, Thr-171 and Thr-175 of ILD-PDC in Ab recognition. Human ILD-PDC was mutated in these three amino acids as single, E168V, T171S and T175D; double, E168V:T171S, E168V:T175D and T171S:T175D; and triple mutations E168V:T171S:T175D to the equivalent residues found in the non-reactive lipoyl domain of Atpt E2-PDC. Single, double, and triple mutations were incorporated into the wild type plasmid pGlip2T.

3.2.1 Aims of this section

- To generate single, double and triple mutants of human ILD-PDC.
- To investigate the effect of these mutations on the lipoylation of human ILD-PDC.
- To investigate the effect of these mutations on Ab recognition.

H.s E3BP.....	E	G	E	A	V	S	A	G	D	A	L	C	**E**	**I**	**E**	**T**	**D**	**K**	**A**	V	V	T	L	D	A	S	D	D	G	I	L	A
H.s Inner…….	V	G	E	K	L	S	E	G	D	L	L	A	**E** * 168	**I**	**E**	**T** * 171	**D**	**K**	**A**	**T** * 175	I	G	F	E	V	Q	E	E	G	Y	L	A
H.s Outer…….	E	G	D	K	I	N	E	G	D	L	I	A	**E**	V	**E**	**T**	**D**	**K**	**A**	**T**	V	G	F	E	S	L	E	E	C	Y	M	A
A.t Inner…….	E	G	D	K	I	E	V	G	D	V	I	G	**E**	**I**	**E**	**T**	**D**	**K**	**A**	**T**	L	E	F	E	S	L	E	E	G	Y	L	A
A.t Outer……	E	G	D	K	V	E	V	G	D	V	L	C	**E**	**I**	**E**	**T**	**D**	**K**	**A**	**T**	V	E	F	E	S	Q	E	E	G	F	L	A
A.t Pt…….	E	G	E	K	L	A	K	G	E	S	V	V	V *	V	**E**	S *	**D**	**K**	**A**	D *	M	D	V	E	T	F	Y	D	G	Y	L	A
H.s OGDCLD	V	G	D	T	V	A	E	D	E	V	V	C	**E**	**I**	**E**	**T**	**D**	**K**	T	S	V	Q	V	P	S	P	A	N	G	V	I	E

Table 3-1 Alignment of E2 and E3BP lipoyl domains from various species
Boxes highlighted in yellow show regions of sequence identity in lipoyl domain sequences.

H. s: Homo sapiens, E3 binding protein lipoyl domain (LD-E3BP).

H. s: Homo sapiens, where outer and inner refer to the human E2 lipoyl domains of PDC (OLD-PDC) (ILD-PDC).

A.t: Arabidopsis thaliana, where outer and inner refer to the mitochondrial E2-PDC lipoyl domains of Atmt (Atmt ILD-PDC and Atmt OLD-PDC).

A.t: Arabidopsis thaliana plastid E2-PDC lipoyl domain contains a single lipoyl domain of Atpt (Atpt LD-PDC).

H. s: Homo sapiens lipoyl domain of human E2-OGDC (LD-OGDC).

Starred residues (in black) of ILD-PDC (situated at 168, 171, and 175) in the region of high sequence identity were mutated to be equivalent to the starred residues (in blue) of the LD-Atpt.

3.2.2 RESULTS

3.2.2.1 Generation of the ILD-PDC mutants

Human ILD-PDC/pGEX2T recombinant plasmid was used as the starting template for the mutagenic PCR reaction to produce the single, double and triple mutants of human ILD-PDC using appropriate primers as described in Materials and Methods, section 2.3.5.

Several colonies were selected, and the mutant plasmid DNA was isolated from 5ml overnight cultures as described in Materials and Methods, section 2.3.9 and analysed on a 1% (w/v) agarose gel (results not shown). Successful mutagenesis of the single, double and triple mutations was confirmed by DNA sequencing (see Materials and Methods, section 2.3.10).

3.2.2.2 Expression and purification of the mutant constructs

Each of the mutant constructs was transformed into competent *E. coli* BL21 (DE3) cells for heterologous expression. The expression of all mutant constructs was carried out successfully out at 37°C for a 3h induction period. Figure 3-9 shows the level of expression of E168V, T171S:T175D and E168V:T171S:T175D mutant constructs as examples of the expression of single, double and triple mutants, respectively. Cell extracts from a 50ml bacterial culture were prepared to check the solubility of the mutant constructs. Different temeratures were tried to produce these mutated proteins in a soluble form. Analysis by SDS-PAGE on a 12% polyacrylamide gel showed that 37°C induction is the optimum temperature to obtain completely soluble protein in all cases. Figure 3-10 shows the solubility of three mutated constructs, ILD-PDC E168V, T171S:T175D and E168V:T171S:T175D as examples of the solubility of single, double and triple mutants respectively.

The mutant ILDs (250ml) cultures were purified as for wt ILD-PDC using a GSTrap™ FF column (5ml) connected to either a BIOCAD® SPRINT or 700 Perfusion® Chromatography Workstation (Materials and Methods, section 2.5.2.1). Peak fractions were collected and samples (10µl) analysed on a 12% SDS gel as described previously (result not shown). The purified mutant GST fusion proteins were then pooled and dialysed into the required buffer.

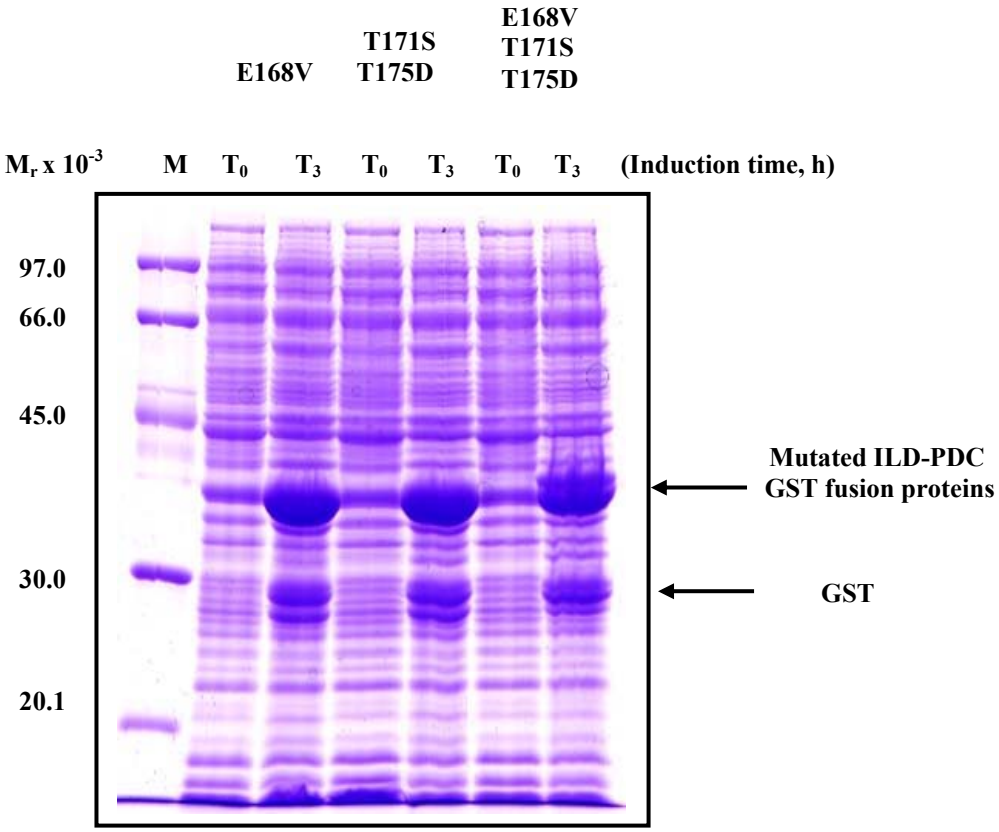

Figure 3-9 Overexpression of single (E168V), double (T171S:T175D), and triple (E168V:T171S:T175D) ILD mutants
Mutated proteins were expressed for 3h at 37°C in *E. coli* (DE3) cells. Samples were denatured in the presence of DTT (150mM) at 100°C for 5-10min prior to analysis on a 12% SDS/polyacrylamide gel. Protein bands were stained with Coomassie Brilliant Blue.

The arrow on the right of the gel denotes overexpressed recombinant proteins.

Note: This figure shows the overexpression of ILD-PDC **E168V, T171S:T175D** and **E168V:T171S:T175D** mutants as examples of single, double and triple mutants respectively.

T_0 and T_3 represent samples taken just before and 3h after induction with 1mM IPTG.

M: low molecular mass markers are shown to the left of the gel.

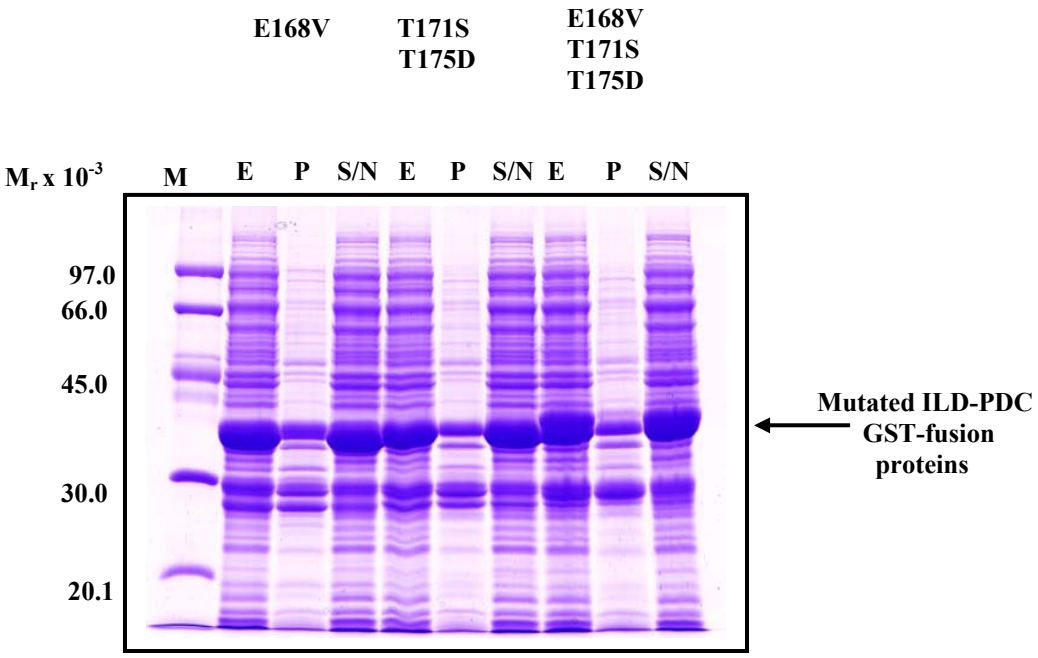

Figure 3-10 Solubility assessment of single (E168V), double (T171S:T175D) and triple (E168V:T171S:T175D) mutants of human ILD-PDC-GST-fusion proteins
Following overexpression of mutant ILDs at 37°C for 3h, the bacterial culture was centrifuged and the pellet resuspended in 3ml 1 x PBS buffer pH 7.5. Cells were lysed by passing cells three times through a French Press at 750Psi. The cell extract *(E)* was separated into its soluble *(S/N)* and insoluble *(P)* fractions by centrifugation at 3000 rpm. Samples were prepared in Laemmli sample buffer and denatured for 5-10min at 100°C in the presence of DTT (150mM), prior to loading on a 12% SDS/polyacrylamide gel. Bands were stained with Coomassie Brilliant Blue.

The arrow indicates ILD-GST fusion.

Note: This figure shows the solubilities of human ILD-PDC **E168V**, **T171S:T175D** and **E168V:T171S:T175D** as representative examples of the solubility of the single, double and triple mutants of ILD respectively.

M: low molecular mass markers are shown to the left of the gel

3.2.2.3 Checking the cross reactivity of ILD-PDC mutants with mAbs PD1 and PD2

To pinpoint the residues that participate in mAb recognition, single, double and triple mutants of human ILD-PDC-GST fusion proteins were subjected to Western blot analysis as described in Materials and Methods, section 2.5.6.1. Following the separation of mutant ILD-GST fusion proteins (1µg) on 12% SDS/polyacrylamide gels, they were electrophoretically transferred onto Hybond^{TM} ECL^{TM} nitrocellulose membrane. Protein was blotted with PD2 (Figure 3-11, panel B) and PD1 (results not shown). At the same time, 5µg of each protein was run and stained with Coomassie Brilliant Blue to confirm their purity and equality of loading (Figure 3-11, panel A).

Western blot analysis following SDS-PAGE shows that the single mutants ILD-PDC E168V and T171S and the double mutant ILD-PDC E168V:T171S show no obvious decrease in cross reactivity with mAb PD2 compared to wt ILD. However, the cross reactivity of PD2 decreased markedly with the single T175D mutant and is even more pronounced with T171S:T175D whereas it disappeared completely with the double mutant E168V:T175D and the triple mutant E168V:T171S:T175D. This observation has two possible interpretations as introduction of these mutations may cause inhibition of lipoylation *per se* or may suggest that specific residues such as Thr-175 play a key part in Ab recognition.

3.2.2.4 Checking the lipoylation of ILD mutants

The lipoylation status of mutant ILDs was checked using two techniques-native gel analysis and mPEG maleimide modification.

(A) Native gel analysis

The separation of lipoylated domains (holo-form) from non-lipoylated domains (apo-form) was achieved by running thrombin-cleaved ILD-PDC constructs (wt and mutants) on a 15% native gel. The serine protease thrombin was used to cleave GST from wt ILD-PDC and its mutants during the manual purification of proteins on a glutathione Sepharose 4B column as described in Materials and Methods, section 2.5.2.2

Release of the GST-tag was achieved in all cases by incubation of wt ILD-PDC and its mutants with thrombin for 2-4h at RT followed by overnight at 4°C to obtain complete

release of the GST-tag. All LDs were quite stable under these conditions and also after thrombin cleavage. Purified wt ILD-PDC expressed in the presence and absence of exogenous lipoic acid; mutant ILD-PDC K173Q; and single, double and triple ILD mutants were run on a native gel (15%). Wt ILD-PDC and its non-lipoylatable mutant K173Q were used as positive and negative controls.

Figure 3-12, panel (A) depicts the separation between lipoylated and non-lipoylated domains. Native gel analysis showed that single mutations E168V, T175D and double mutations E168V:T171S and T171S:T175D all partially affected lipoylation as seen in lanes 4, 6, 7 and 9 respectively. This was indicated by the presence of 2 distinct bands with the lower band representing the lipoylated form. A similar conclusion is also evident from comparison of a native gel of wt ILD-PDC expressed in the presence and absence of exogenous lipoate. It was observed that the expression of wt ILD-PDC in the absence of the exogenous lipoic acid produces 80-90% non-lipoylated protein (upper band) and 10-20% putative lipoylated protein (lower band) (lane 1). Human ILD-PDC expressed in the presence of added lipoate was completely lipoylated whereas ILD-PDC K173Q was completely non-lipoylated whether grown with or without lipoate (lanes 2 and 3). Single, double and triple mutations T171S, E168V:T175D and E168V:T171S:T175D respectively produced a single band which could potentially represent either fully lipoylated or totally non-lipoylated domains of the protein (lanes 5, 8 and 10).

Mutated ILD-PDC constructs (5µg) were analysed by immunoblotting after resolution on a 15% native gel mAb PD2 (Figure 3-12, panel B). Significant reactivity was displayed with the lipoylated domain of the single mutant ILD-PDC E168V but to a lesser extent than wt ILD-PDC due to the partial lipoylation of this domain (lane 4). In addition PD2 displayed reactivity with the single band of ILD-PDC T171S. However, reactivity was also decreased in this case (lane 5) even though this mutant was subsequently shown to be fully lipoylated (see Figure 3-13 for details). Moreover, the reactivity disappeared completely with the T175D mutant (lane 6) despite it retaining approx. 50% lipoylation (Figure 3-12, panel A, lane 6).

There was a clear cumulative effect with double and triple mutations on LD reactivity with PD2 (Figure 3-12, panel B). Thus the reactivity of PD2 decreased with the double mutant ILD-PDC E168V:T171S (lane 7) compared to the single mutants, ILD-PDC E168V and T171S, probably because the T171S mutation affected only reactivity with

PD2 whereas the E168V mutation affected only the degree of lipoylation. Since there was no reactivity with the single band of ILD-PDC E168V:T175D and T168V:T171S:T175D mutants, it might suggest that these domains were non-lipoylated (lanes 8 and 10). However, reactivity also disappeared with the double mutant ILD-PDC T171S:T175D (lane 9) to a similar extent as the single mutant ILD-PDC T175D although the domain remained partially lipoylated (Figure 3-12, panel A, lane 9). Thus, a more definitive study on native gels has revealed that the ILD-PDC E168V, T171S and E168V:T171S mutants did in fact display reduced cross reactivity compared to the wt ILD-PDC although this was not obvious in the original SDS-PAGE analysis (Figure 3-11). This variation could be interpreted as a result of the different techniques employed (SDS and native PAGE analysis) and the difficulties in detecting small changes in cross-reactivity by this approach. As a result of this observation, the cross reactivity of mAb with these mutants were checked quantitatively using ELISA.

ILD-PDC and K173Q were used as positive and negative controls respectively (Figure 3-12, panel B, lanes 2 and 3). In addition, a minor band (10-20%) corresponding to the putative lipoylated form of ILD-PDC expressed in the absence of the exogenous lipoic acid expression also displayed strong cross reactivity with PD2 (Figure 3-12, panel B, lane 1).

The rate of migration of individual lipoyl domains on native polyacrylamide gels is primarily dependent on their net charge (Figure 3-12, panel A). Mutations that involve neutral replacements have little or no effect on mobility such as ILD T171S (lane 5). In contrast, mutations that remove negatively charged amino acids promote decreased mobility such as ILD-PDC E168V (lane 4) whereas mutations that replace a positively charged amino acid result in increased migration such as ILD-PDC K173Q (lane 3).

To confirm the extent of lipoylation of the various mutant domains and the identities of the putative lipoylated and non-lipoylated species, mPEG maleimide modification was performed to achieve this goal.

(B) mPEG maleimide modification

Modification with mPEG maleimide was performed on thrombin cleaved LDs produced as described in Materials and Methods, section 2.5.2.2. Thrombin-cleaved ILD mutants created in this work, wild-type ILD produced in the presence and absence of exogenous

lipoate, and ILD (K173Q) dialysed into 50mM Tris/HCl pH 7.5 were incubated with mPEG maleimide at 25°C for 30min in the presence of E3 and NADH or NAD^+ as described in Materials and Methods, section 2.5.8.1.

Figure 3-13 shows native gel analysis (15%) of the mobility shift of mPEG maleimide modified mutant ILD-PDC constructs, as well as ILD-PDC expressed in the presence and absence of added lipoate and ILD-PDC K173Q.

Modification was visualised by gel shift assay in which the modified proteins exhibited a markedly decreased rate of migration in the presence of NADH owing to the incorporation of mPEG maleimide. Modification of LDs was specific to the reduced thiols of the dithiolane ring of the lipoamide prosthetic group since no shift was observed in the presence of NAD^+. Apart from T175D and T171S:T175D, all constructs displayed the same pattern of mPEG maleimide modification occurring only in the presence of NADH.

ILD-PDC expressed in the presence of exogenous lipoic acid ie the fully lipoylated domain was totally shifted by mPEG maleimide in the presence of NADH whereas ILD K173Q which is non-lipoylatable domain was unaffected (samples 2 and 10).

Interestingly, the minor band, presumed to correspond to the lipoylated form of the ILD expressed in the absence of exogenous lipoate, exhibits no apparent shift despite displaying strong cross reactivity with PD2 (sample 1). As a result of this observation, the nature of the modification was explored subsequently by Q-TOF mass spectrometry (see chapter 2, section 2.5.10.3 for more details).

All mutant constructs of ILD-PDC that were partially lipoylated exhibit complete mPEG maleimide modification of their putative lipoylated domains (lower bands), ILD-PDC E168V, T175D, E168V:T171S and T171S:T175D (samples 3, 5, 6 and 8 respectively). In addition, the T171S mutant is totally shifted confirming the full lipoylation of this domain (sample 4) despite exhibiting a weaker reactivity with PD2 compared to the wt ILD-PDC (see Figure 3-12, panel B, lanes 2 and 5 for details). As expected with the double and triple mutants, E168V:T175D and E168V:T171S:T175D respectively, there was no apparent shift (samples 7 and 9) consistent with their lack of lipoylation (see Figure 3-12, panel A, lanes 8 and 10 for more details).

Since there are three thiol groups in ILD-PDC, two in the dithiolane ring of the lipoic acid (in the reduced state) and one from a single cysteine residue in the domain, three sites of mPEG maleimide modification are potentially available. However, apart from ILD-PDC T175D and T171S:T175D, all ILD-PDC mutants displayed mostly a single modified higher M_r species. This was seen clearly after running the mPEG maleimide modified thrombin cleaved ILD-PDC mutants on 12% SDS/polyacrylamide gels (Figure 3-14).

In order to estimate the apparent M_r shift achieved on modification of a single thiol group by mPEG maleimide (M_r 5000 Da), calibration experiments were performed using the enzyme peroxiredoxin III, a thioredoxin-dependent peroxide reductase as a protein containing two accessible thiol groups (C47 and C168) and its C168S mutant as a protein with a single thiol group. It was found that single mPEG maleimide modification of C168S induced a mobility shift corresponding to approx. 15 kDa whereas the wt enzyme shifted approx. 30 kDa (data not shown).

Our studies indicated that all lipoylated domains of ILD-PDC mutants were doubly modified with mPEG maleimide (approx. 30 KDa shift) as was the wild-type ILD-PDC produced in the presence of the exogenous lipoic acid. Since this double modification occurred in the presence of NADH, it was apparent that both thiol groups of the dithiolane ring were involved in the reaction. Moreover, these findings indicated that the single cysteine thiol was not accessible to this thiol group reagent (samples B, lane 3; C, lane 5; D, lane 7; and F, lane 11).

However, an unusual modification pattern was observed with the T175D and T171S:T175D mutants. In these mutants, M_r shifts corresponding to single, double and triple mPEG maleimide modifications were achieved in the presence of NADH (samples E, lane 9; and H, lane 15). The single modification suggested availability of the cysteine residue of the domain, since it also occurred in the presence of NAD^+ (samples E, lane 10; and H, lane 16).

3.2.2.5 Comparison of the cross reactivity between mAbs PD1 and PD2 and mutated constructs of ILD-PDC by ELISA

The cross reactivities of monoclonal antibodies PD1 and PD2 to the thrombin cleaved wt ILD and its mutant constructs were measured quantitatively using ELISA as

described in Materials and Methods, section 2.5.7. Eight different dilutions of PD1 ranging from 1 in 1000 to 1 in 64000 plus eight different dilutions of PD2 ranging from 1 in 50 to 1 in 6400 were prepared to determine quantitatively the cross reactivity of ILD mutants with PD1 (data not shown) and with PD2 (Figure 3-15).

Wt ILD expressed with and without exogenous lipoate and the K173Q mutant were used as positive and negative controls respectively. ELISA confirmed the immunoblotting results after separation on native gels (Figure 3-12, panel B). mAb PD2 gave a negative result with E168V:T175D and E168V:T171S:T175D due to lack of lipoylation (Figure 3-13, sample 7 and 9) and showed reduced cross reactivity with E168V and T171S as expected since the E168V mutant construct is not fully lipoylated (Figure 3-12, panel A, lane 4) and the T171S mutation directly affected cross reactivity with PD2 (Figure 3-12, panel A and B, lanes 5). There was a cumulative effect in the E168V:T171S mutant involving a further decrease of cross reactivity compared to the single mutants, E168V and T171S although there was improved lipoylation in this mutant construct (Figure 3-12, panel A, lane 7). mAb PD2 also gave a negative result with T175D and T171S:T175D as expected even though there was approx. 50% lipoylation of these domains (Figure 3-12, panel A, lanes 6 and 9).

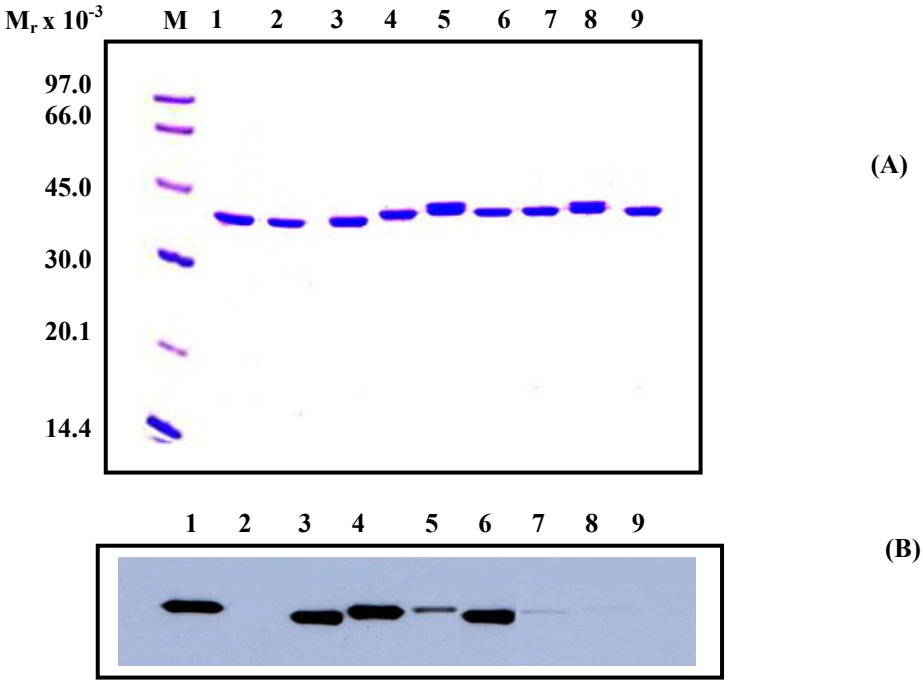

Figure 3-11 Immunoblotting of the recombinant ILD-PDC mutants with mAb PD2
Panel (A): Purified mutated ILD-GST fusion proteins (5µg) were separated by 12% SDS/polyacrylamide gel electrophoresis and stained with Coomassie Brilliant Blue.

Panel (B): Purified mutated ILD-GST fusion proteins (1µg) probed with mAb PD2 (1 in 500 dilution).

Lanes 1 and *2*: ILD-PDC and its K173Q mutant as positive and negative controls respectively; *lanes 3, 4* and *5*: single mutations, E168V, T171S and T175D respectively; *lanes 6, 7* and *8*: double mutations, E168V:T171S, E168V:T175D and T171S:T175D respectively; *lane 9*: the triple mutation, E168V:T171S:T175D.

M: low molecular mass markers are shown to the left

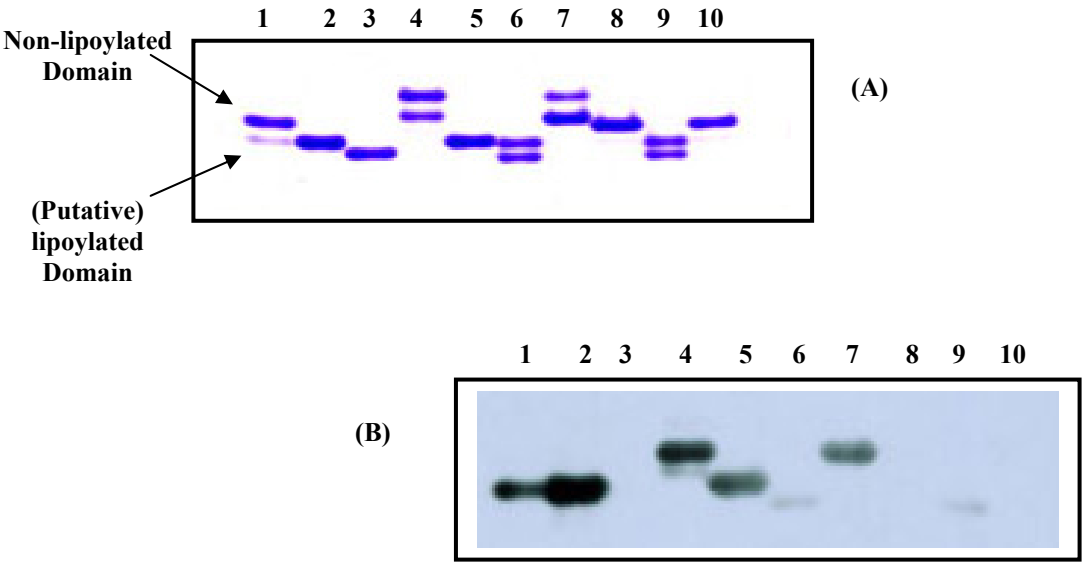

Figure 3-12 Checking the lipoylation of ILD-PDC mutants using non-denaturing PAGE analysis
Panel (A): Thrombin cleaved ILD proteins (5µg) were separated on a 15% native gel before staining with Coomassie Brilliant Blue

Panel (B): Thrombin cleaved ILD proteins (1µg) were separated on a 15% native gel, blotted and probed with mAb PD2.

Lanes 1 and *2*: ILD produced in the absence and presence of lipoic acid expression (0.1mM) respectively; *lanes 3*: ILD K173Q; *lanes 4, 5* and *6*: single mutants, E168V, T171S and T175D respectively; *lanes 7, 8* and *9*: double mutants, E168V:T171S, E168V:T175D and T171S:T175D respectively; *lane 10*: the triple mutant, ILD-PDC E168V:T171S:T175D.

In all lanes, the upper band represents the apo-form of the domain.

Lanes 2 and *3* were used as positive and negative controls.

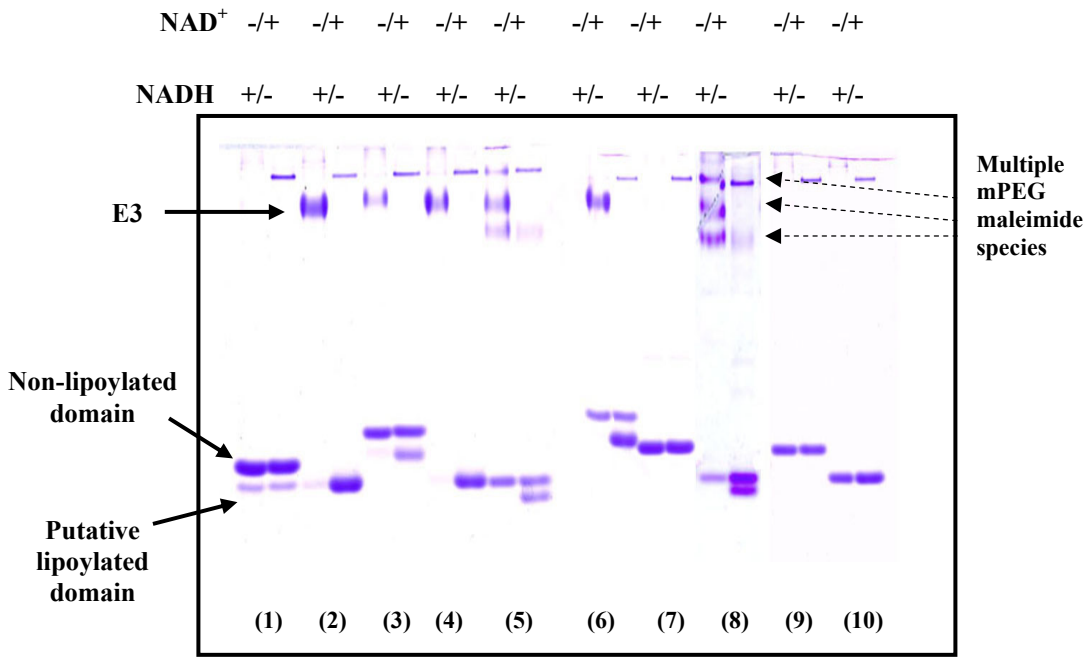

Figure 3-13 Checking the lipoylation of mutant ILD constructs of PDC by native PAGE
Purified thrombin cleaved wild-type and mutant ILDs (6µg) were modified with mPEG maleimide and analysed on a 15% native gel. Protein bands were stained with Coomassie Brilliant Blue. Two gels were joined; the first gel involves samples 1, 2, 3, 4, and 5 whereas the second gel involves samples 6, 7, 8, 9, and 10.

Samples 1 and 2, modification of wild type of ILD produced in the absence and in the presence of the lipoic acid respectively; **samples 3, 4 and 5**, modification of the single mutants, E168V, T171S and T175V respectively; **samples 6, 7 and 8**, modification of the double mutants, E168V:T171S, E168V:T175V and T171S:T175V respectively; **sample 9**, modification of the triple mutant, E168V:T171S:T175V; **sample 10**, modification of ILD K173Q. mPEG modification was carried out in the presence of NADH or NAD^+. Modification of wild type ILD and ILD K173Q were used as positive and negative controls respectively.

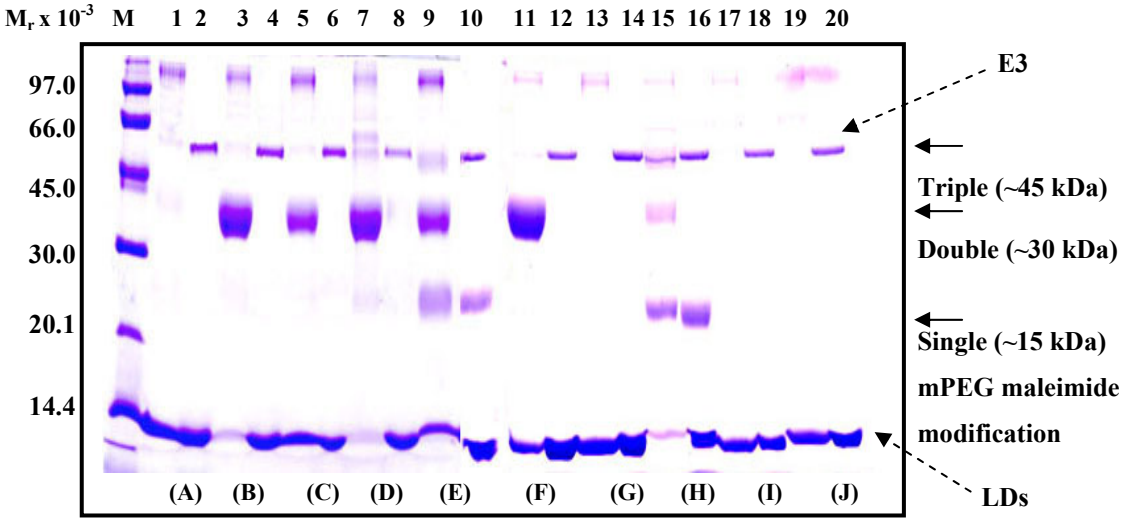

Figure 3-14 mPEG maleimide modified ILD-PDC mutants on SDS-PAGE analysis
mPEG maleimide modified thrombin cleaved proteins of wild type and mutant ILDs (6µg) were analysed on a 12% SDS/polyacrylamide gel. Protein bands were stained with Coomassie Brilliant Blue. Two gels were joined; the first gel involves samples A, B, C, D, and E whereas the second gel involves samples F, G, H, I, and J.

Sample A, ILD-PDC (-lipoic acid expression); **sample B**, ILD-PDC (+lipoic acid expression) as a positive control; **sample C**, E168V; **sample D**, T171S; **sample E**, T175D; **sample F**, E168V:T171S; **sample G**, E168V:T175D; **sample H**, T171S:T175D; **sample I**, E168V:T171S:T175D; and **sample J**, K173Q as a negative control

Lanes 1, 3, 5, 7, 9, 11, 13, 15, 17 and *19* represent the modification in the presence of NADH

Lanes 2, 4, 6, 8, 10, 12, 14, 16, 18, and *20* represent the modification in the presence of NAD^+

M: low molecular mass markers are shown to the left of the gel.

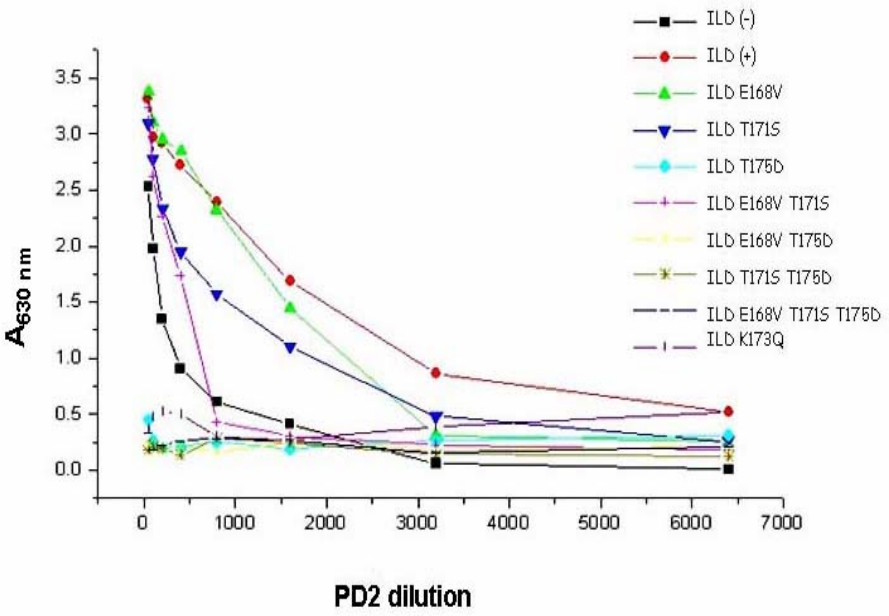

Figure 3-15 Binding of mAb PD2 to mutant ILD-PDC constructs detected by ELISA
mAb PD2 at various dilutions as indicated was incubated on a plate coated with thrombin cleaved proteins of the mutant ILD constructs. The amount of antibody bound to the solid phase was detected with goat anti-human IgG conjugated to horseradish peroxidase (HRP), 3,3`,5,5` Tetramethylbenzidine (TMB) was used as a substrate to detect immune complex, forming a coloured product absorbing at 630nm.

3.3 Section 3

In the previous sections it was established that lipoylation of the inner lipoyl domain of human PDC is necessary for Ab recognition; however, it is not sufficient in itself as, although human ILD-PDC T175D and T171S:T175D mutants are partially lipoylated LDs, they display little or no cross reactivity with PD1 and PD2. This indicates that these two residues (Thr-171 and Thr-175) located in the highly conserved block of 8 amino acid residues immediately adjacent to the lipoyl lysine residue of human ILD-PDC are important for Ab recognition (Table 3-2). Moreover, our earlier studies have shown that the fully lipoylated domain LD-E3BP exhibits reduced cross reactivity with PD1/PD2 compared to the ILD-PDC (see Figure 3-5, panel B, lanes 1 and 4 for more details). Sequence comparison of the highly-conserved block of 8 amino acid residues, immediately adjacent to the lipoyl lysine residue in LD-E3BP and ILD-PDC, showed that a valine residue was present in LD-E3BP replacing the corresponding residue Thr-175 in the ILD-PDC at the C-terminal end of the central core. Furthermore, the non-reactive LD-OGDC (see Figure 3-5, panel B, lane 6 for more details) displays two altered amino acid residues, threonine and serine also situated at the C-terminal end of this block. These observations prompted us to employ further site-directed mutagenesis to the non-reactive domain LD-OGDC to try to recover its cross reactivity with mAbs PD1 and PD2.

Thus, human LD-OGDC was mutated systematically at several amino acid residues to the equivalent residues found in the reactive lipoyl domains of E2-PDC.

3.3.1 Aims of this section

- To restore the reactivity of human LD-OGDC by systematically creating mutations in this domain to mimic equivalent residues in ILD-PDC.

- To investigate the effect of these mutations on the lipoylation of human LD-OGDC.

- To investigate the effect of these mutations on Ab recognition.

H.s E3BP.....	E	G	E	A	V	S	A	G	D	A	L	C	**E**	**I**	**E**	**T**	**D**	**K**	**A**	V	V	T	L	D	A	S	D	D	G	I	L	A
H.s Inner…….	V	G	E	K	L	S	E	G	D	L	L	A	**E**	**I**	**E**	**T**	**D**	**K**	**A**	**T**	I	G	F	E	V	Q	E	E	G	Y	L	A
H.s Outer…….	E	G	D	K	I	N	E	G	D	L	I	A	**E**	V	**E**	**T**	**D**	**K**	**A**	**T**	V	G	F	E	S	L	E	E	C	Y	M	A
A.t Inner…….	E	G	D	K	I	E	V	G	D	V	I	G	**E**	**I**	**E**	**T**	**D**	**K**	**A**	**T**	L	E	F	E	S	L	E	E	G	Y	L	A
A.t Outer……	E	G	D	K	V	E	V	G	D	V	L	C	**E**	**I**	**E**	**T**	**D**	**K**	**A**	**T**	V	E	F	E	S	Q	E	E	G	F	L	A
A.t Pt……...	E	G	E	K	L	A	K	G	E	S	V	V	V	V	**E**	S	**D**	**K**	**A**	D	M	D	V	E	T	F	Y	D	G	Y	L	A
H.s OGDCLD	V	G	D	T	V	A	E	D 33	E	V	V	C	**E**	**I**	**E**	**T**	**D**	**K**	T 44	S 45	V	Q 47	V 48	P 49	S	P	A	N	G	V	I	E

Table 3-2 Alignment of E2 and E3BP lipoyl domains from various species
Boxes highlighted in yellow show regions of sequence identity in lipoyl domain sequences.

H. s: Homo sapiens, E3 binding protein lipoyl domain (LD-E3BP).

H. s: Homo sapiens, where outer and inner refer to the human E2 lipoyl domains of PDC (ILD-PDC) (OLD-PDC).

A. t: Arabidopsis thaliana, where outer and inner refer to the mitochondrial E2 lipoyl domains of Atmt (Atmt ILD-PDC and Atmt OLD-PDC).

A. t: Arabidopsis thaliana plastid E2-PDC lipoyl domain contains a single lipoyl domain of Atpt (Atpt LD-PDC).

H. s: Homo sapiens, lipoyl domain of human E2-OGDC (LD-OGDC).

Red numbered amino acid residues of the non reactive LD-OGDC were mutated to the equivalent residues of the fully reactive ILD-PDC reactive lipoyl domain.

3.3.2 RESULTS

3.3.2.1 Generation of LD-OGDC mutant constructs and checking the cross reactivities of these mutants with mAbs PD1 and PD2

3.3.2.1.1 Mutation of the two residues differing in LD-OGDC in the highly conserved central block

Initially, the work focused on the highly-conserved block of 8 amino acid residues immediately adjacent to the lipoyl-lysine residue since Abs can accommodate approx 10-12 amino acids in their binding sites. Therefore, LD-OGDC was mutated in the two non-conserved amino acids (Thr-44 and Ser-45) to the equivalent residues found in the cross reactive lipoyl domain, ILD-PDC. Mutations were performed as described in Materials and Methods, section 2.3.5 to produce the single mutants T44A, S45T and the double mutant T44A:S45T of LD-OGDC using the wt LD-OGDC construct as a template. Each of the mutant constructs was transformed into competent BL21 (DE3) cells for heterologous expression. The expression of all mutant constructs was carried out successfully at 37°C for a 3h induction period (Figure 3-16). Cell extracts from a 50ml bacterial culture were prepared to check the solubility of these constructs. Analysis on 12% SDS/polyacrylamide gels showed that a 37°C induction temperature yielded soluble protein. Figure 3-17 shows the solubility of T44A:S45T as an example of the solubility of the mutant constructs of LD-OGDC.

Mutant LD-OGDCs, T44A, S45T and T44A:S45T were purified as for wild type OGDC-LD-pGEX-2T using a GSTrap™ FF column (5ml) connected to either a BIOCAD® SPRINT or 700 Perfusion® Chromatography Workstation (Materials and Methods, section 2.5.2.1). Peak fractions were collected and analysed by 12% SDS-PAGE (Figure 3-18, panel A, lanes 3-5). To check the cross reactivity of these mutants, purified mutant LD-OGDC-GST constructs (5µg) as well as, wt ILD-PDC (0.5µg) were probed with PD1 (data not shown) and PD2 (Figure 3-18, panel B, lanes 3-5). Only minimal cross reactivity was restored in the S45T mutant with PD2 (lane 3) compared to ILD-PDC (lane 1) whereas no cross reactivity was noticed with T44A and T44A:S45T, although these domains were subsequently shown to be lipoylated to the same extent as wt OGDC in the case of T44A and T44A:S45T and fully lipoylated in the case of LD-OGDC S45T (see Figure 3-21 for more details).

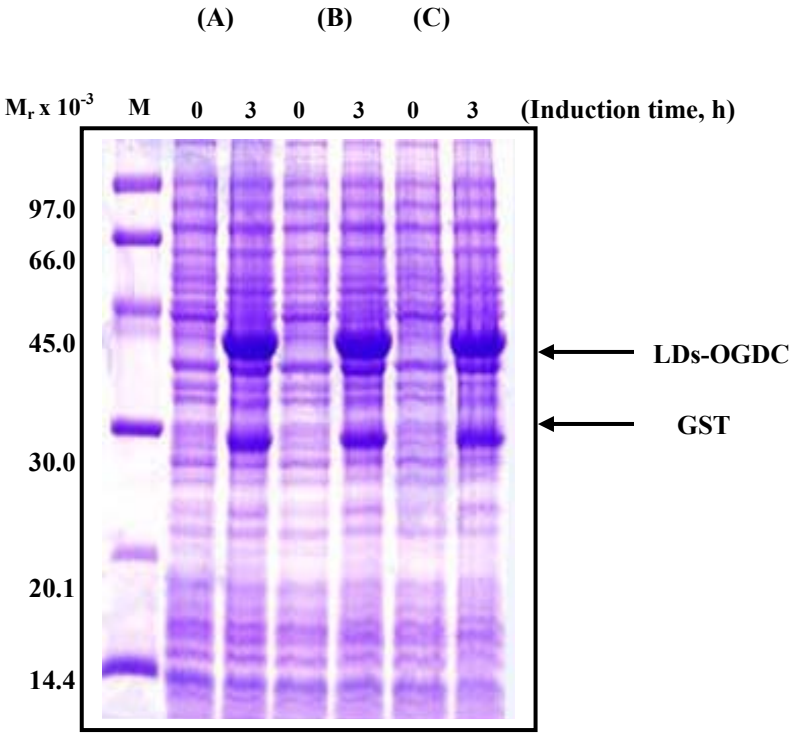

Figure 3-16 Overexpression of T44A, S45T and T44A:S45T mutants of LD-OGDC
Mutated LDs of OGDC were expressed over 3h at 37°C in *E. coli* BL21 (DE3) cells. Samples were denatured in the presence of DTT (150mM) at 100°C for 5min prior to analysis on a 12% SDS/polyacrylamide gel. Protein bands were stained with Coomassie Brilliant Blue.

Sample A, T44A; **sample B**, S45T and **sample C**, T44A:S45T expressed as GST-fusion proteins.

The arrow on the right of the gel indicates LD-GST fusion proteins.

M: low molecular mass markers are shown to the left of the gel.

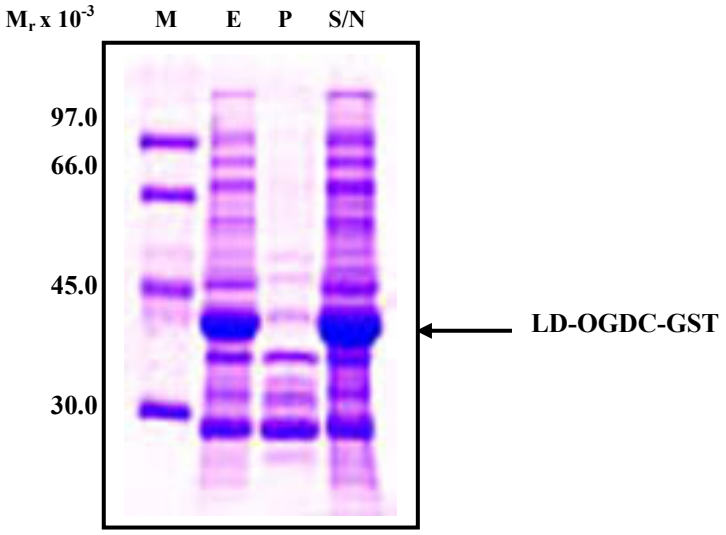

Figure 3-17 Solubility assessment of LD-OGDC T44A:S45T expressed as a GST-fusion protein

Following protein overexpression of LD-OGDC T44A:S45T at 37°C for 3h, the bacterial culture was centrifuged and the pellet resuspended in 3ml 1 x PBS buffer pH 7.5. Cells were lysed by passing cells three times through a French Press at 750Psi. The cell extract *(E)* was separated into its soluble *(S/N)* and insoluble *(P)* fractions by centrifugation. Samples were prepared in Laemmli sample buffer and denatured for 5-10min at 100°C in the presence of DTT (150mM), prior to loading on a 12% SDS/polyacrylamide gel. Bands were stained with Coomassie Brilliant Blue.

Note: This figure shows the solubility of T44A:S45T LD-OGDC as a representative example of the solubility of LD-OGDC mutants in general.

The arrow on the right of the gel indicates the mutant LD-OGDC GST-fusion protein

M: low molecular mass markers are shown to the left of the gel.

3.3.2.1.2 Mutation of single conserved N- and C-terminal residues located outside the central block differing in LD-OGDC

Previous data indicated for the first time that the major epitope recognized by PD1 and PD2 did not solely involve the highly-conserved block of 8 amino acid residues immediately adjacent to the lipoyl-lysine. Therefore, our search was extended outwith this block to focus on additional conserved residues within 10 amino acid residues of the lipoylation sites which could potentially be accommodated within the Ab binding site. Two additional amino acids were identified on the N- and C-terminal sites of the central block (Asp-33 and Pro-49) to be non-conserved residues with respect to the residues in the reactive lipoyl domains, ILD/OLD-PDC and ILD-Atmt-PDC. Therefore, Asp-33 and Pro-49 were mutated to the equivalent amino acids of the reactive lipoyl domains; glycine and glutamate respectively as described in Materials and Methods, section 2.3.5. Wt LD-OGDC plasmid was employed as a template to produce single mutants D33G, and P49E whereas the double mutant D33G:P49E was produced using the D33G LD-OGDC construct as a template. Expression and solubility of these mutants were achieved successfully at 37°C for 3h induction period (data not shown). In addition, the purification of these mutants was carried out using GSTrap^{TM} FF column (5ml) as for previous mutants (data not shown). Western blot analysis was applied again to study the cross reactivity of these mutants with PD1 (data not shown) and PD2 (Figure 3-18, panel B, lanes 6-8). In parallel, the same amount of each protein was run and stained with Coomassie Brilliant Blue to confirm their purity and equality of loading (Figure 3-18, panel A, lanes 6-8). Interestingly, a low level of cross reactivity was restored with P49E and D33G:P49E (less than 5%) (lanes 6 and 8) compared to the ILD-PDC (lane 1) but no significant cross reactivity was restored with the D33G mutant (lane 7). It was subsequently shown that the extent of the lipoylation of D33G decreased slightly compared to that of wild-type LD-OGDC as a result of this mutation whereas P49E and G33D:P49E mutants were fully lipoylated (see Figure 3-21 for more details).

3.3.2.1.3 Multiple mutations involving residues inside and outside of the central core

This encouraging result prompted us to create a series of double, triple and quadruple mutations involving these four amino acids (Thr-44, Ser-45, Asp-33 and Pro-49) to determine if there was a cumulative effect of multiple mutations; S45T:P49E was created using LD-OGDC S45T as a template; D33G:T44A:S45T was created using LD-OGDC T44A:S45T as a template; T44A:S45T:P49E was created using LD-OGDC as a

template; and D33G:T44A:S45T:P49E was produced using LD-OGDC T44A:S45T:P49E as a template. Appropriate primers were used to create these mutant constructs (see Materials and Methods, section 2.1.3.3.2 for more details). All mutants were expressed and purified successfully as described for previous mutants (data not shown). Figure 3-19, panels A and B, lanes 2-5 display the SDS/polyacrylamide gels of purified GST-fusion proteins of LD-OGDC mutants stained with Coomassie Brilliant Blue gel and probed with PD2. Approx. 10% cross reactivity with PD2 was restored with LD-OGDC S45T:P49E, T44A:S45T:P49E and D33G:T44A:S45T:P49E (lanes 2, 3 and 5) compared to the ILD-PDC (lane 1) but no significant cross reactivity was restored with LD-OGDC D33G:T44A:S45T (lanes 5). It was again shown that the extent of its lipoylation decreased slightly compared to the wild-type domain (see Figure 3-21 for more details). This result permitted us to focus on several key residues on the C-terminal side of the lipoyl lysine of LD-OGDC that could be integral to immune recognition, since the LD-OGDC D33G and D33G:T44A:S45T constructs exhibited no reactivity with PD2.

3.3.2.1.4 Additional mutations of LD-OGDC in the C-terminal region adjacent to the central block

Two additional amino acids were identified as highly-conserved residues in the reactive lipoyl domains in the extended C-terminal region ILD-PDC, Gln-47 and Val-48. Quadruple and quintuple mutants, T44A:S45T:Q47G:P49E and T44A:S45T:Q47G:V48F:P49E respectively were produced using LD-OGDC T44A:S45T:P49E and T44A:S45T:Q47G:P49E respectively as templates. Again the expression and solubility of these mutants were checked successfully at 37°C expression (data not shown). Purified GST fusions of these mutants were probed with PD2 (Figure 3-20, lanes 13 and 14) in addition to blotting the entire range of LD-OGDC mutants produced previously (Figure 3-20, lanes 3-12). As before, the same amount of each protein was run and stained with Coomassie Brilliant Blue to confirm their purity and equality of loading. Significant cross reactivity was restored with PD2 in LD-OGDC T44A:S45T:Q47G:P49E (approx 30-40%) (lane 13) and completely with LD-OGDC T44A:S45T:Q47G:V48F:P49E compared to the ILD-PDC (lane 14) whereas low or insignificant cross reactivities were detected with all other LD-OGDC mutants (lanes 3-12). To check if these effects could be attributed partially to variations in the extent of lipoylation, native gel analysis combined with mPEG maleimide modification was employed to achieve this goal as described previously.

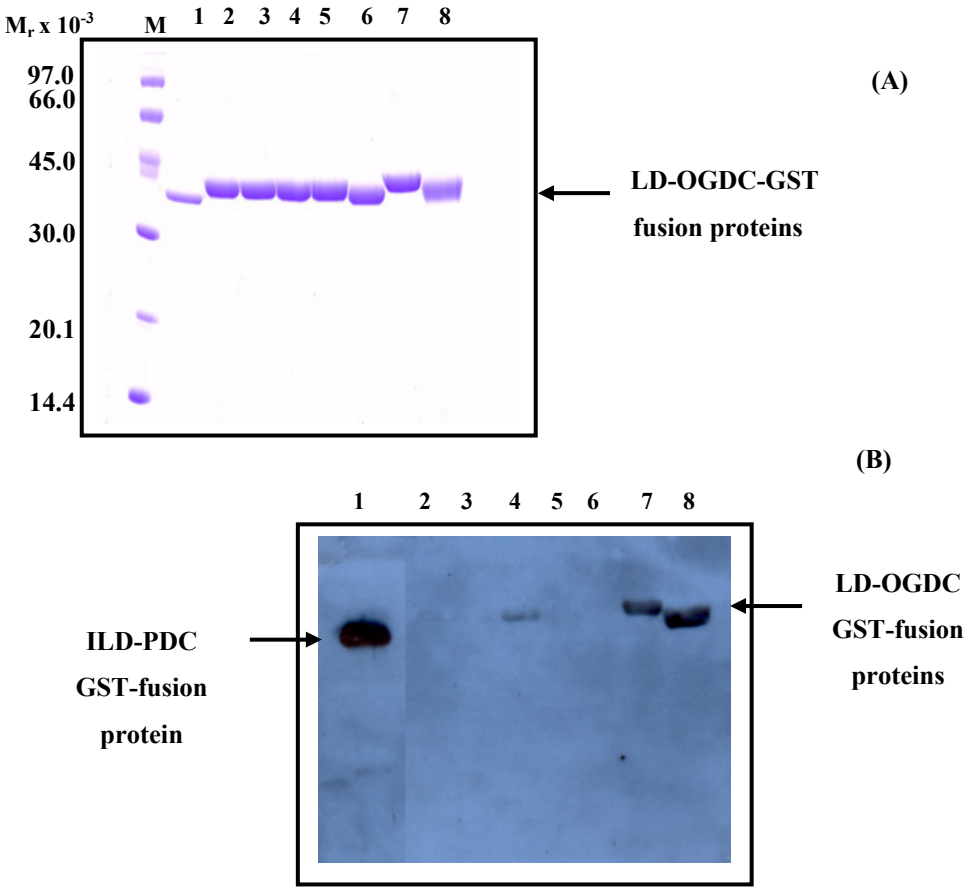

Figure 3-18 Immunoblotting of recombinant LDs-OGDC T44A, S45T, T44A:S45T, D33G, P49E and D33G:P49E constructs with mAb PD2
Panel (A): Purified mutated LD-OGDC GST fusion proteins (5µg) were separated on a 12% SDS/polyacrylamide gel and stained with Coomassie Brilliant Blue. ILD-PDC (0.5µg) was used as a positive control.

Panel (B): Purified mutated LD-OGDCs GST fusion proteins (5µg) were probed with mAb PD2. ILD-PDC (0.5µg) was also used as a positive control

Lane 1, wt ILD-PDC as a positive control; *lanes 2*, wild type LD-OGDC as a negative control; *lanes 3, 4* and *5*, T44A, S45T and T44A:S45T respectively; *lanes 6, 7* and *8*, D33G, P49E and D33G:P49E respectively.

M: low molecular mass markers are shown to the left of the gel.

NB. Wild-type ILD-PDC was loaded at 10% of the level of mutant domains

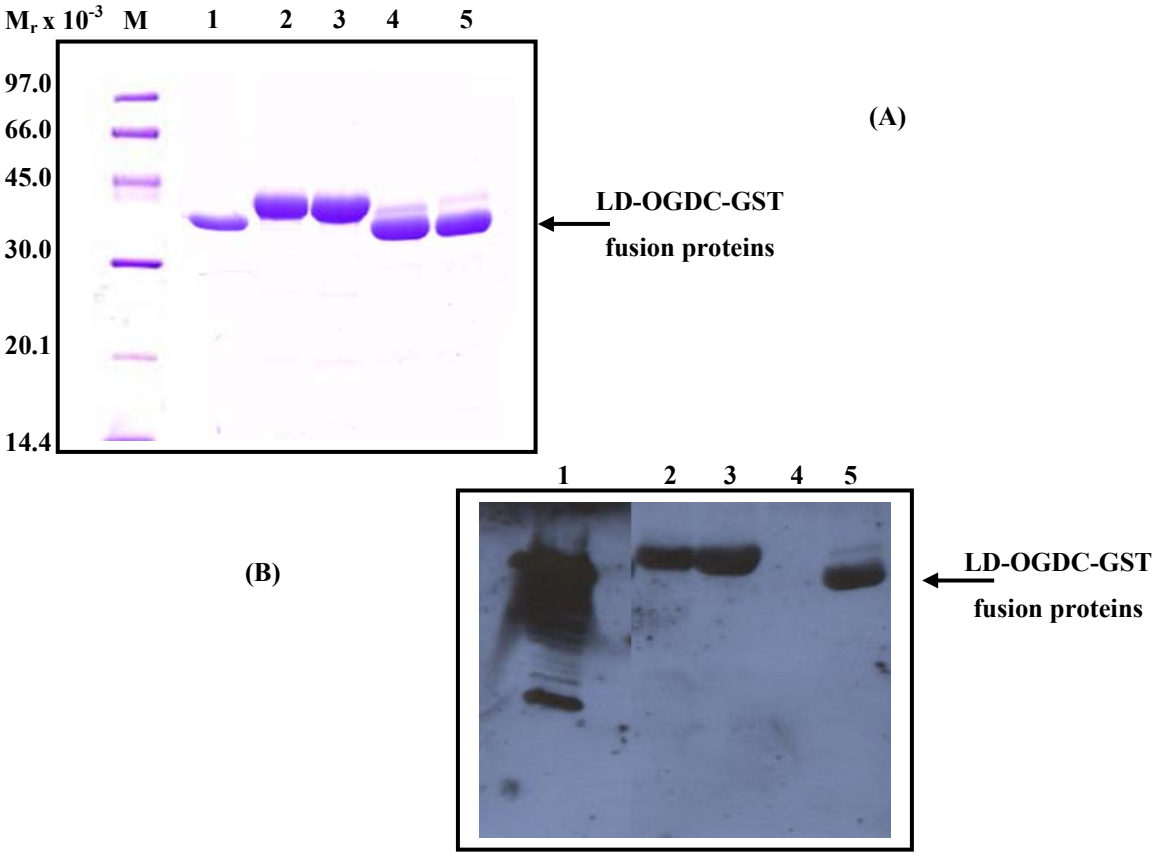

Figure 3-19 Immunoblotting of the recombinant S45T:P49E, T44A:S45T:P49E, D33G:T44A:S45T and D33G:T44A:S45T:P49E LD-OGDC constructs with mAb PD2
Panel (A): Purified mutated LD-OGDC GST fusion proteins (5µg) were separated on a 12% SDS/polyacrylamide gel and stained with Coomassie Brilliant Blue. ILD-PDC (1µg) was used as a positive control.

Panel (B): Purified mutated LD-OGDC-GST fusion proteins (5µg) were probed with mAb PD2. ILD-PDC (1µg) was also used as a positive control

Lane 1, wt ILD-PDC as a positive control; *lane 2*, S45T:P49E; *lanes 3*, T44A:S45T:P49E; *lanes 4*, D33G:T44A:S45T and *lane 5*, D33G:T44A:S45T:P49E.

M: low molecular mass markers are shown to the left of the gel

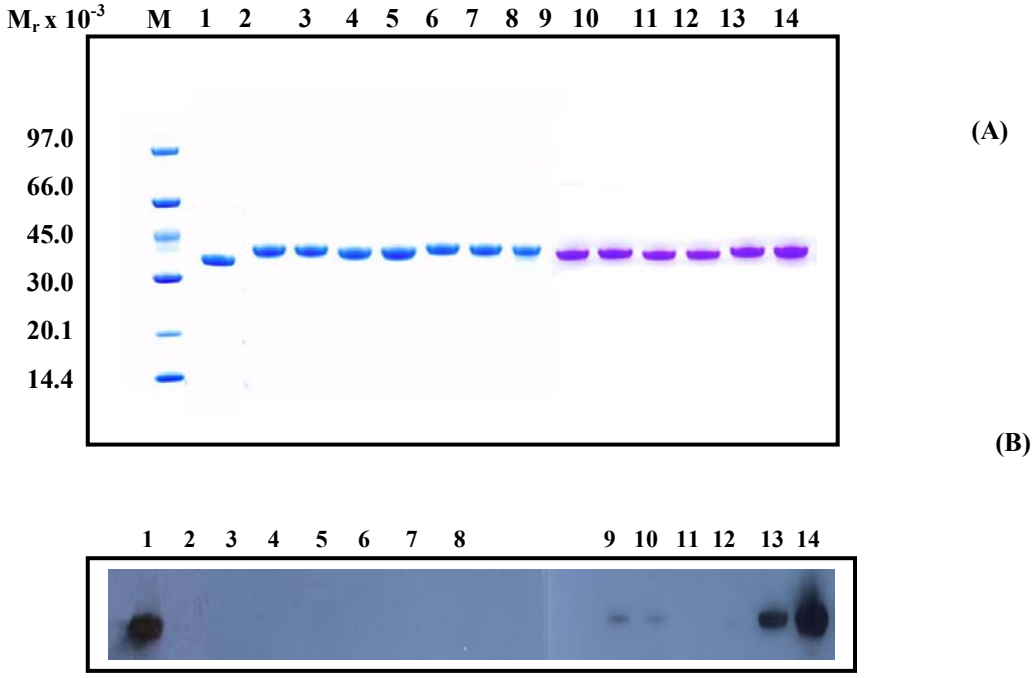

Figure 3-20 Immunoblotting of the recombinant LD-OGDC mutant constructs with mAb PD2

Panel (A): Purified mutated LD-OGDC GST fusion proteins (5µg) were separated by 12% SDS/polyacrylamide gel electrophoresis and stained with Coomassie Brilliant Blue. In addition, ILD-PDC (5µg) was used as a positive control.

Panel (B): Purified mutated LD-OGDC-GST fusion proteins (1µg) were probed with mAb PD2.

Lane 1,wild type ILD-PDC as a positive control; *lane 2*, wild type LD-OGDC; *lanes 3, 4* and *5*, T44A, S45T and T44A:S45T respectively; *lanes 6, 7* and *8*, D33G, P49E and D33G:P45E respectively; *lane 9, 10, 11* and *12*, S45T:P49E, T44A:S45T:P49E, D33G:T44A:S45T and D33G:T44A:S45T:P49E respectively; *lanes 13* and *14*, T44A:S45T:Q47G:P49E and T44A:S45T:Q47G:V48F:P49E.

M: low molecular mass markers are shown to the left of the gel

Two gels are joined; the first gel involves lanes 1-8 whereas the second gel involves 9-14.

3.3.2.2 Checking the lipoylation of LD-OGDC mutants

(A) Native gel analysis

The separation of lipoylated domain (holo-form) from non-lipoylated domain (apo-form) of LD-OGDC constructs was achieved by resolving thrombin cleaved LDs on a native gel. The serine protease thrombin was used to digest the GST-tag from purified LD-OGDC GST-fusion constructs at 37°C and RT in Tris-HCl buffer pH 7.5 for 6h as described in Materials and Methods, section 2.5.2.2. All mutated LDs-OGDC were digested successfully and loaded onto a 15% native gel (Figure 3-21).

Native gel analysis showed that when wt LD-OGDC was expressed in the absence of exogenous lipoate, the protein was completely non-lipoylated. However, approx. 70% lipoylation of LD-OGDC was achieved when the protein was expressed in the presence of added lipoate (lanes 1 and 2).

For the mutated LD-OGDC constructs, it can be seen that the mutation of LD-OGDC has variable effects on the extent of lipoylation depending on the type of mutant. Some mutations have no effect on lipoylation; such as T44A and T44A:S45T showing approx. 70% lipoylation equivalent to the wt domain, lane 3 and 5. However, most mutations have a positive effect on lipoylation; constructs that became fully lipoylated are as follows: S45T, lane 4; P49E, lane 7; D33G:P49E, lane 8; S45T:P49E, lane 9; T44A:S45T:P49E, lane 10; D33G:T44A:S45T:P49E, lane 12; T44A:S45T:Q47G:P49E, lane 13; and T44A:S45T:Q47G:V48F:P49E, lane 14. In addition, two mutations have a minor negative effect on the extent of lipoylation, namely D33G, lane 6 and T44A:S45T:D33G, lane 11 compared to wt LD-OGDC.

Interestingly, LD-OGDC T44A:S45T:Q47G:V48F:P49E exhibits a markedly decreased rate of migration on native gels compared to the other constructs. Samples of this mutant with and without DTT were subsequently displayed on native gels. It was observed that this band of lower mobility was observed only in the absence of DTT (data not shown). This indicates that this mutation (V48F) affects the folding of the domain to the extent that the hidden cysteine is accessible and capable of forming a disulphide bond adventitiously with another lipoyl domain.

(B) mPEG maleimide modification.

Modification of wt and mutated LD-OGDC constructs expressed in the presence and absence of the lipoate was carried out on LDs released by thrombin cleavage as described in Materials and Methods section 2.5.2.2. Thrombin-cleaved LD-OGDC mutant constructs were incubated with mPEG maleimide as described in Materials and Methods, section 2.5.8.1 mPEG maleimide modified domains (6µg) in the presence of NADH or NAD^+ were resolved on a 15% native gel (Figure 3-22). It was clearly seen that the lower (lipoylated) band of each partially lipoylated construct (samples 2, 3, 5, 6 and 11) and the single bands of the fully lipoylated constructs (samples 4, 7, 8, 9, 10, 12 and 13) exhibited a markedly decreased rate of migration in the presence of NADH, owing to incorporation of mPEG maleimide. Wt LD-OGDC expressed with and without exogenous lipoate were used as positive and negative controls respectively.

As the LD-OGDC T44A:S45T:Q47G:V48F:P49E mutant proved to be relatively unstable and susceptible to degradation during attempts to cleave GST, mPEG modification was carried out using the GST-fusion protein as substrates for mPEG maleimide. mPEG maleimide modified proteins (6µg) were resolved on a 12% SDS/polyacrylamide gel for each modified protein (Figure 3-23). LD-OGDC T44A:S45T:Q47G:P49E was used as a positive control (sample 1). NAD^+ reactions were performed in each sample as negative controls (sample 1 and 2, lanes b). SDS-PAGE shows that LD-OGDC T44A:S45T:Q47G:V48F:P49E was modified with mPEG maleimide exhibiting a markedly decrease rate of migration (sample 2, lane a). However, the migration of this construct was higher than that exhibited by the positive control T44A:S45T:Q47G:P49E. This observation suggests the additional modification of a cysteine thiol in the domain that is only available in the reduced state.

3.3.2.3 Determining the cross reactivity between mAbs PD1 and PD2 and mutated constructs of LD-OGDC by ELISA

mAbs PD1 and PD2 reactivity to the wt LD-OGDC and its mutant constructs fused into GST-tag was measured quantitatively by ELISA. Eight different dilutions ranging from 1 in 1000 to 1 in 64000 of PD1 (data not shown) as well as eight different dilutions of PD2 ranging from 1 in 50 to 1 in 6400 were used (Figure 3-24) with 2µg/well of the LD-OGDC fusion proteins dialysed in 100mM $NaHCO_3$. Figure 3-24 shows the extent of cross reactivity between mAb PD2 and the LD-OGDC mutant constructs. Mutated and wt constructs gave similar results to those observed by immunoblotting.

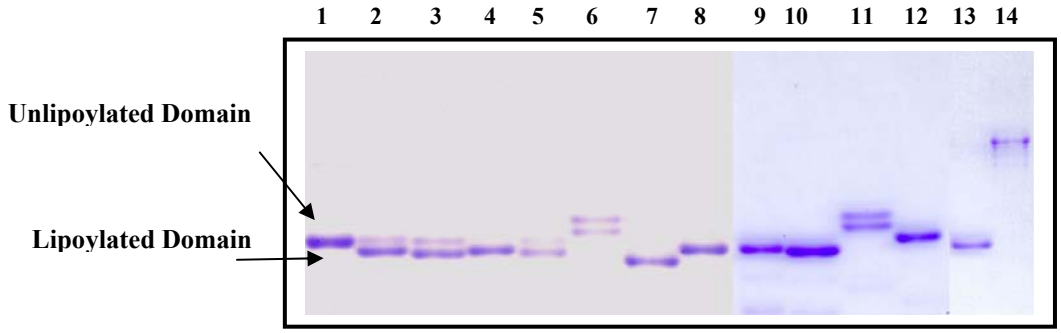

Figure 3-21 Checking the lipoylation of LD-OGDC mutants using native PAGE analysis
Thrombin cleaved ILDs proteins (5µg) were separated on a 15% native gel. The gel was stained with Coomassie Brilliant Blue Two gels were joined; the first gel involves lanes 1-8 whereas the second gel involves lanes 9-14.

Lanes 1 and **2,** wild type LDs-OGDC produced in the absence and presence of the exogenous lipoate (0.1mM) respectively; **lanes 3, 4** and **5,** T44A, S45T and T44A:S45T respectively; **lanes 6, 7** and **8,** D33G, P49E and D33G:P49E respectively; **lanes 9, 10, 11** and **12,** S45T:P49E, T44A:S45T:P49E, D33G:T44A:S45T and D33G:T44A:S45T:P49E respectively; **lanes 13** and **14,** LD-OGDC T44A:S45T:Q47G:P49E and T44A:S45T:Q47G:V48F:P49E, respectively.

In each lane, the upper band represents the apo-form of the domain. *Lanes 1* and *2* were used as a positive and a negative control respectively.

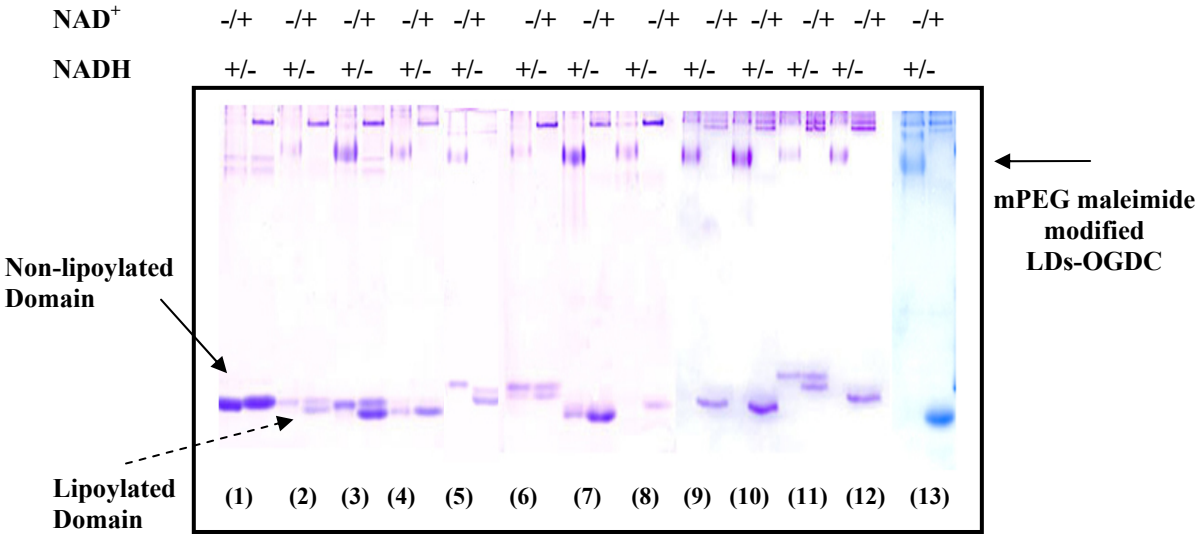

Figure 3-22 Checking the lipoylation of LD-OGDC mutants using mPEG maleimide modification
mPEG modified thrombin cleaved proteins of wild type and mutant LDs-OGDC (6µg) were analysed on a 15% native gel. Protein bands were stained with Coomassie Brilliant Blue.

Samples 1 and ***2*****,** wild type of LD-OGDC produced in the absence and in the presence of the lipoic acid respectively; **samples 3, 4** and **5,** T44A, S45T and T44A:S45T respectively; **samples 6, 7** and **8,** D33G, P49E and D33G:P49E respectively; **samples 9, 10, 11** and **12,** S45T:P49E, T44A:S45T:P49E, D33G:T44A:S45T and D33G:T44A:S45T:P49E respectively; **Sample 13,** T44A:S45T:Q47G:P49E.

mPEG modification was carried out in the presence of NADH or NAD^+.

Three gels were joined; the first gel involves samples 1-8, the second gel involves samples 9-12, and the third gel involves a sample 13.

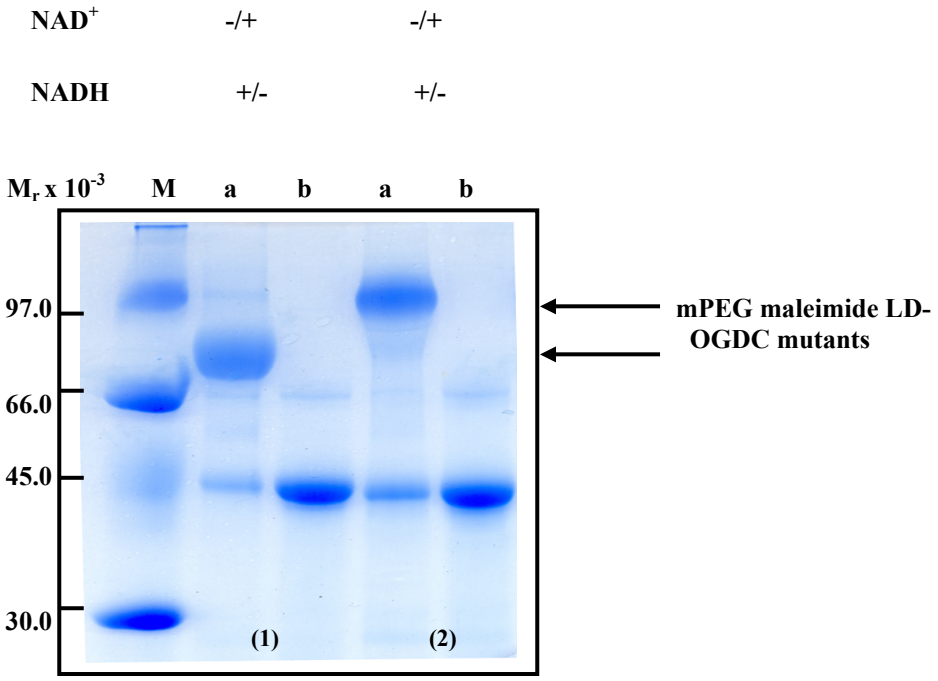

Figure 3-23 Checking the lipoylation of LD-OGDC-GST mutants using mPEG maleimide modification
mPEG modified GST-fusion proteins of LD-OGDC T44A:S45T:Q47G:P49E, **sample 1** and T44A:S45T:Q47G:V48F:P49E, **sample 2** mutants (6µg) were analysed on a 12% SDS/ polyacrylamide gel. Protein bands were stained with Coomassie Brilliant Blue.

Lanes a: LD-OGDC mutants modified in the presence of NADH.

Lanes b: LD-OGDC mutants modified in the presence of NAD^+.

M: low molecular mass markers are shown to the left of the gel.

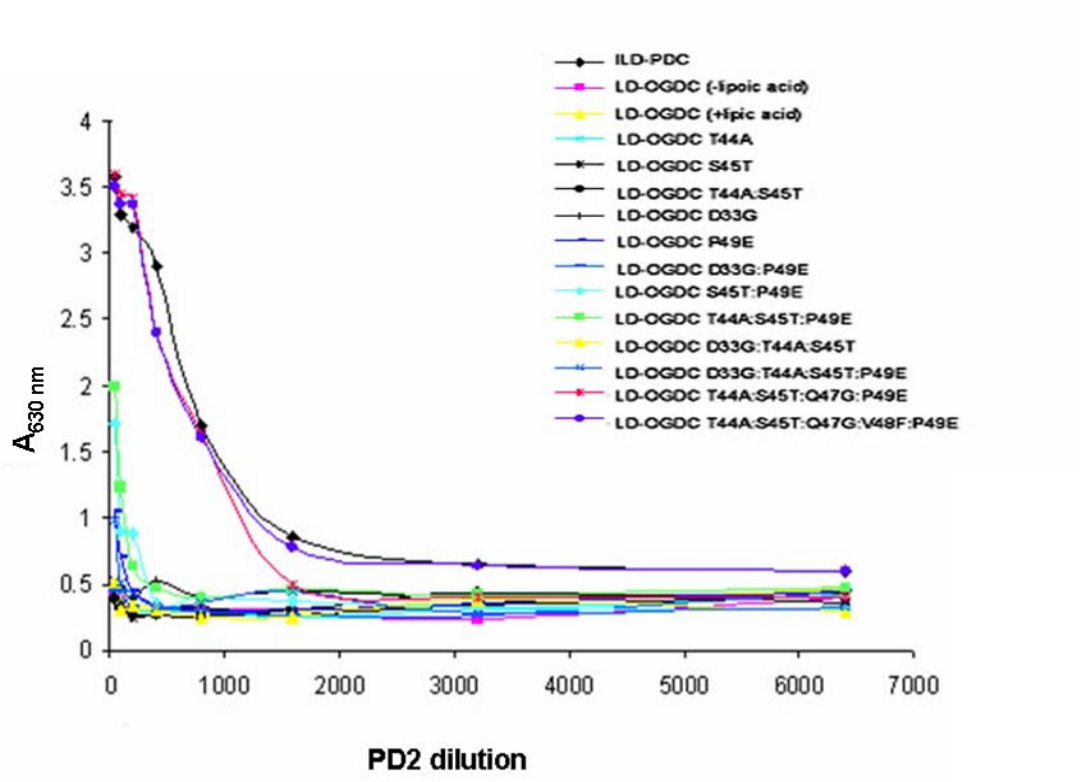

Figure 3-24 Binding of mAb PD2 to mutant constructs of LD-OGDC detected by ELISA
mAb PD2 at different dilutions was incubated on a plate coated with mutant OGDC-LD-GST fusion proteins. The amount of antibody bound to the solid phase was detected with goat anti-human IgG linked to specific horseradish peroxidase (HRP) conjugate, 3,3`,5,5` Tetramethylbenzidine (TMB) was used as a substrate forming a coloured product absorbing at 630nm.

3.4 Discussion

In this chapter our investigations were targeted at determining the precise molecular basis for recognition of E2 and E3BP lipoyl domains of human PDC by mAbs PD1 and PD2. Initially, it was confirmed that the presence of the covalently-linked lipoate prosthetic group was necessary but not sufficient to induce a positive immune response. Thus, Western blot analyses showed that not all lipoylated LDs exhibited cross reactivity with mAbs PD1 and PD2. This finding agreed with various studies that have been made to determine the dominant B-cell epitope within E2-PDC which have suggested that the lipoamide prosthetic group linked to E2 itself appeared to constitute an important part of the epitope but it was not the sole equivalent to give a signal with AMA (Fussey *et al.*, 1989b; Surh *et al.*, 1990a). Therefore, no cross reactivity was observed on testing chicken liver H-protein (a component of the mitochondrial glycine cleavage system) with PBC sera, even though it contained covalently-bound lipoic acid (Fussey *et al.*, 1989b). Indeed, the AMA response to lipoylated recombinant E2-PDC was always of significantly higher titre and affinity than that found with non-lipoylated antigen (Quinn *et al.*, 1993a). In addition, it has been reported that the lipoic acid prosthetic group appeared to constitute part of the dominant B-cell epitope within E3BP (Palmer *et al.*, 1999) as well as those of E2-BCOADC and E2-OGDC (Leung *et al.*, 1995; Moteki *et al.*, 1996).

PD1 and PD2 were able to recognise ILD-E2 constructs analysed on SDS-PAGE. Therefore, the denaturing conditions did not affect the specificity or inhibit the cross reactivity of the antibody, despite the fact that many monoclonal antibodies are only active against native proteins since they are produced against non-contiguous epitopes. Moreover, it was demonstrated that PD1 and PD2 displayed a strong cross reactivity with ILD-, OLD-human E2 and also ILD-Atmt to a lesser extent. In contrast, there was no detectable cross reactivity with human LD-OGDC and Atpt E2-PDC didomain even though both were lipoylated. In addition, fully lipoylated LD-E3BP-PDC displayed cross reactivity with PD1 and PD2 but at a reduced level compared to ILD-PDC whereas the response to the OLD-E2 was similar, if not slightly increased, relative to ILD-PDC. This result was at variance with a previous report by Surh *et al* who found that polyclonal AMA react with human OLD-E2 but at 100-fold lower dilution than that with human ILD-E2 (Surh *et al.*, 1990a).

LD-E3BP	E	I	E	T	D	K*	A	V
ILD-PDC	E	I	E	T	D	K*	A	T
OLD-PDC	E	V	E	T	D	K*	A	T
ILD-Atmt	E	I	E	T	D	K*	A	T
LD-Atpt	V	V	E	S	D	K*	A	D
LD-OGDC	E	I	E	T	D	K*	T	S

Sequence comparison of the various LDs (reactive and non-reactive) around the lipoyl-lysine attachment site indicated that a central block of 8 highly-conserved amino acids is a common feature of all cross-reacting domains. Interestingly, there is a valine substitution at the C-terminal end of this central core in the weakly cross-reacting lipoyl domain, LD-E3BP. In addition, two non-conserved residues (threonine and serine) lie at the C-terminal end of this block in the non-reactive lipoyl domain, LD-OGDC. Three altered residues were observed in the non cross-reacting lipoyl domain of *A. thaliana* plastid E2-PDC, a valine residue situated at the N-terminus of this block, a serine situated two residues to the N-terminal side of the lipoylation site and an aspartic acid situated at the C-terminal end of this central core. A second valine residue near the N-terminus of this block in Atpt LD-PDC was excluded from the comparison, since the same residue occurs in the reactive lipoyl domain OLD-PDC. These differences highlighted the potential involvement of these residues as important parts of the antigenic determinant recognised by PD1 and PD2.

3.4.1 Cross reactivity and lipoylation states of wt ILD-PDC and its mutant K173Q in the presence and absence of exogenous lipoate

As these mAbs have been shown previously to exhibit exclusive specificity for the lipoylated form of E2-PDC (Thomson *et al.*, 1998), Western blot analysis of SDS-PAGE and native gels as well as ELISA confirmed that wt, fully lipoylated ILD-PDC exhibited strong cross reactivity with these mAbs whereas as expected its non-lipoylated ILD K173Q mutant elicited no reaction. However, previous works have shown that the effect of lipoylation of K173 of mammalian E2-PDC on reactivity with PBC sera has remained controversial (Quinn *et al.*, 1993a; Koike *et al.*, 1998). This would be consistent with a probable heterogeneity of the antibody response to E2-PDC in PBC as suggested by (Migliaccio *et al.*, 2001). In our case, using native gels, it was possible to separate the minor putative lipoylated form of the wt ILD-E2 expressed in

the absence of exogenous lipoic acid which displayed strong cross reactivity with PD1 and PD2.

Covalent incorporation of mPEG maleimide, a thiol group reagent was used to confirm the lipoylation status of the domain. Interestingly, it was realised that the minor species, thought to be the lipoylated form of ILD-PDC, was not amenable to mPEG maleimide modification. Our evidence now suggests that this band represents the octanoylated domain which lacks the dithiol groups required for reaction with mPEG maleimide. Our observation contrasts with a report by Quinn *et al.* who showed that two forms the human ILD-PDC were produced in *E. coli*, corresponding to the lipoylated and non-lipoylated species (Quinn *et al.*, 1993b). However, it is consistent with a report by Ali *et al.* (Ali *et al.*, 1990) who showed that octanoylation of *E. coli* lipoyl domains occurred in a lipoic acid-deficient mutant of *E. coli* growing under lipoate-deficient conditions. The octanoylated nature of the domain was subsequently confirmed by (Q-TOF) mass spectrophotometry. As the octanoylated species displays strong cross reactivity with mAbs PD1 and PD2, this indicates that the dithiol groups of the dithiolane ring of lipoic acid are not an integral part of the epitope. The current observation is similar to an observation by Fussey *et al.* who reported that octanoylated *E. coli* E2-PDC and octanoylated ILD-PDC produced by a mutant deficient in lipoate biosynthesis is recognised by AMA, but not as efficiently as their lipoylated counterparts (Fussey *et al.*, 1990). In our case, the strength of cross reactivity of mAb PD2 with lipoylated and octanoylated ILD is very similar if not identical (more details in chapter 2, section 2.5.10.3 and chapter 4).

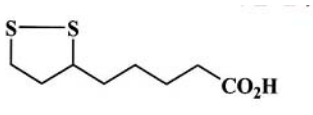

Lipoic acid

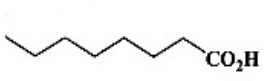

Octanoic acid

3.4.2 Cross reactivity and lipoylation states of ILD-PDC mutants

Site-directed mutagenesis was employed to convert the reactive lipoyl domain of human ILD-PDC to be equivalent to the sequence of the non-reactive lipoyl domain of *A. thaliana* plastid LD-PDC around the lipoyl-lysine residue as single, ILD-PDC **E168V**, **T171S**, and **T175D**; double **E168V:T171S**, **E168V:T175D** and **T171S:T175D**; and triple **E168V:T171S:T175D** mutants.

Using Western blotting following SDS-PAGE or native gel analysis as well as ELISA, it was possible to investigate which amino acid residues in the central region around the lipoyl-lysine play an integral part in the epitope recognised by PD1 and PD2. In addition, native gel studies facilitated separation of the lipoylated and non-lipoylated domains. mPEG maleimide modification was then employed to confirm the identity of the putative lipoylated species. It was realised that mutation of these residues can affect antibody responses in two different ways: (a) either by altering the degree of lipoylation or (b) by influencing antibody recognition directly by replacement of a key residue in the antigenic determinant.

Although inspection of lipoyl domains from different sources has shown that the amino acid residues on either side of the lipoyl lysine are highly conserved in the DKA motif (Russell & Guest, 1991; Dardel *et al.*, 1993), site directed mutagenesis has indicated that neither the aspartic acid nor the alanine residue is essential for recognition by the lipoylating enzyme (Wallis & Perham, 1994; Reche *et al.*, 1998). However, changing the position of the target lysine in the β-turn has a crucial effect on lipoylation (Wallis & Perham, 1994). It appears that the correct positioning of the lysine at the tip of a type I β-turn is essential for efficient post-translational modification (Morris *et al.*, 1994). It is therefore a precise structural cue that is a prerequisite for recognition by the lipoylating enzyme(s) and not the adjacent amino acid sequence *per se.*

The threonine residue situated one residue from the C-terminal end of the central core of ILD-PDC (Thr-175) plays a major role in Ab recognition. Thus although the **T175D** mutant was approx. 50% lipoylated there was a dramatic loss of cross reactivity with mAbs PD1 and PD2. A second threonine situated two residues to the N-terminal side of the lipoylation site also has a significant effect on the extent of Ab recognition. Thus antibody cross reactivity decreased markedly with this **T171S** mutant even though it remained fully lipoylated. In contrast, mutation of a glutamic acid (E168) situated at the start of 8-residue central block partially affects lipoylation but has no direct effect on the extent of Ab recognition.

The apparent lipoylation of the **E168V** mutant is interesting in view of a report by Fujiwara *et al.* who conducted *in vitro* studies on mutant lipoyl domains of mammalian PDC, OGDC and BCOADC (Fujiwara *et al.*, 1996). This group showed that when an adjacent conserved glutamic acid (Glu-170) residue in E2-PDC and its equivalent in E2-OGDC, situated 3 residues to the N-terminal side of the lipoylation site, was replaced by glutamine, the rate of lipoylation decreased more than 100-fold. In agreement with this finding, when the equivalent residue (glutamine in the case of E2-BCOADC) was mutated to glutamate, the rate of lipoylation increased about 100-fold and became comparable to that of E2-PDC and E2-OGDC. In our case, the second glutamic acid residue (Glu-168) situated 5 residues upstream of the lipoyl-lysine of human ILD-PDC also has a positive influence on lipoylation.

As expected a cumulative effect on Ab recognition was produced as a result of the double Thr-171 and Thr-175 mutations. Thus, the cross reactivity of the **T171S:T175D** mutant was totally abolished although the lipoyl domain was still partially lipoylated as the thr-171 replacement has no effect on cofactor insertion. In addition, a cumulative effect was also observed on the extent of lipoylation with **E168V:T175D** and **E168V:T171S:T175D** mutants since both residues, Glu-168 and Thr-175 are necessary for optimal lipoylation. Therefore, these mutants are mostly non-lipoylated as confirmed by mPEG maleimide modification. Some recovery of lipoylation was observed when the threonine residue (Thr-171) in the mostly non-lipoylated mutant construct, ILD-PDC E168V was replaced by serine to generate the double mutant, E168V:T171S. Therefore, it appears that the mutated domain **E168V:T171S** serves as a more suitable substrate for the lipoyl ligase *in vivo* than E168V alone (Morris *et al.*, 1994). Despite the increased level of lipoylation, this construct induces a weaker response with PD2 confirming the importance of Thr-171 for Ab recognition.

The mPEG maleimide-induced mobility shift was calibrated using peroxiredoxin III and its mutants (see section 3.2.2.4 for more details). SDS-PAGE analysis of mPEG maleimide-modified wt and mutant ILD-PDC constructs indicated that, apart from T175D and T171S:T175D, all lipoylated domains were modified to a similar extent displaying mobility shifts in the order of 30 kDa. These data suggest that both thiol groups of the dithiolane ring are accessible to reaction with mPEG maleimide. However, the ILD-PDC T175D and T171S T175D mutants display more complex patterns of mobility shift (15, 30, and 45 kDa) in the presence of NADH and a single modification (15 kDa) in the presence of $NAD^{+\cdot}$. It is proposed that this redox-

independent shift is due to the modification of the single cysteine residue in the ILD suggesting that the T175D mutation affects folding or stability of the domain accounting for the unexpected accessibility of the single cysteine.

The effects of the various mutations of the ILD-PDC on lipoylation and mAb recognition are summarised in this following:-

Constructs	mAb recognition	Lipoylation
ILD-PDC	+++	+++
K173Q	-	-
E168V	+++	++
T171S	++	+++
T175D	+	++
E168V:T171S	++	++
E168V: T175D	-	-
T171S:T175D	+	++
E168V: T171S:T175D	-	-

+++ full lipoylation and Ab recognition equivalent to wild type ILD-PDC

++ strong lipoylation or Ab recognition

+ weak lipoylation or Ab recognition

- no lipoylation or Ab recognition

3.4.3 Cross reactivity and lipoylation states of LD-OGDC mutant constructs

In a parallel study, the non-reactive domain, LD-OGDC was mutated in a stepwise fashion in attempts to restore the level of Ab recognition to that of ILD-PDC. A series of 12 mutant domains were produced systematically in LD-OGDC using site-directed mutagenesis to determine their involvement in the mAb PD1 and PD2 response. Western blot analysis and ELISA were used to assay the cross reactivity between LD-OGDC mutant constructs and mAbs.

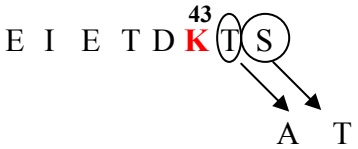

Initially, in order to verify the importance of the central block of 8 amino acids immediately adjacent to the lipoyl-lysine residue in Ab recognition, the two distinctive C-terminal amino acids in the non-reactive LD-OGDC central region were replaced by the corresponding residues in the reactive lipoyl domain, ILD-PDC as single and double mutations. However, it was found that only negligible cross activity was restored in **S45T** even though it was fully lipoylated whereas no cross reactivity appeared with **T44A** and **T44A:S45T** although their lipoylation status was similar to wt LD-OGDC (70%). Thus it was realised for the first time that the major epitope recognised by mAbs PD1 and PD2 did not solely involve this highly-conserved block of 8 amino acids.

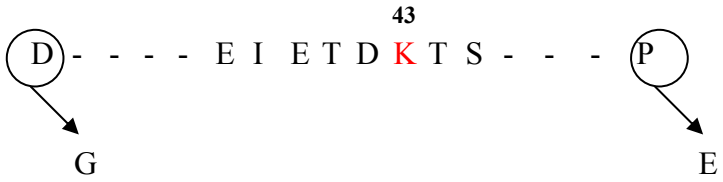

Following this result, our search was extended outside this block to focus on additional conserved residues within 10 amino acid residues of the lipoylation site which could potentially be accommodated within the Ab binding site. It was noted that two additional highly conserved residues located on the N- and C-terminal sides of the reactive lipoyl domain ILD-PDC were altered in LD-OGDC, namely Asp-33 and Pro-49. These two residues were replaced by the equivalent residues in the reactive lipoyl domains as single and double mutations. It was found that slight cross reactivity (< 5%) was restored with **P45E** and **D33G:P49E** mutants even though they were fully lipoylated. There was no detectable cross reactivity with the single **D33G** mutant.

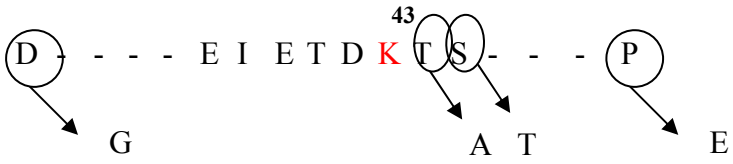

This encouraging result prompted us to study the cumulative effect of these four mutations around the lipoyl-lysine residue on Ab recognition. A series of double, **S45T:P45E**; triple, **T44A:S45T:P49E** and **D33G:T44A:S45T**; and quadruple, **D33G:T44A:S45T:P59E** mutations were produced. It was observed that approx. 10% reactivity was restored with the fully lipoylated **S45T:P45E**, **T44A:S45T:P49E** and **D33G:T44A:S45T:P59E** constructs. However, no detectable reactivity was apparent with the **D33G:T44A:S45T** mutant.

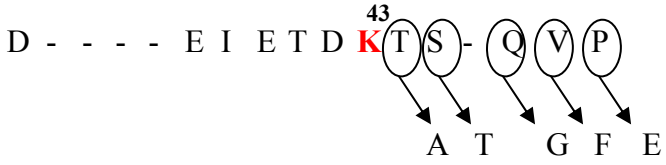

These findings directed our attention to the C-terminal side of the lipoylation site of LD-OGDC since the replacement of Asp-33 by Gly alone or in combination with the two residues in the central block had no detectable effect on reactivity with PD2. Two further residues were identified to be highly conserved in the reactive human ILD- and OLD-E2 located four and five residues to the C-terminal side of the lipoylation site. Accordingly, T44A:S45T:Q47G:P49E and T44A:S45T:Q47G:V48F:P49E were produced. It was found that partial recognition (approx 40%) was restored with **T44A:S45T:Q47G:P49E** and 100% with **T44A:S45T:Q47G:V48F:P49E** compared to wt ILD-E2. Complete recovery of cross reactivity in LD-OGDC was associated with the replacement of Gln-47 and Val-48 residues to the equivalent residues in ILD-E2.

Native gel analysis and mPEG maleimide modification were used to check the lipoylation status of all LD-OGDC mutant constructs. The GST-tag was released by thrombin treatment to facilitate separation of the purified apo-and holodomain proteins on native gels. In contrast to ILD-PDC, removal of the GST-tag from LD-OGDC and its mutants proved to be extremely difficult; incubation at 37°C and RT were used for thrombin digestion and the LDs were susceptible to degradation after digestion.

Wt LD-OGDC was found to be completely non-lipoylated when expressed in the absence of the exogenous lipoic acid and only approx. 70% lipoylated in its presence. This result indicated that the human LD-OGDC was a relatively poor substrate for the *E. coli* lipoylating enzyme (Morris *et al.*, 1994).

As with the ILD-PDC, there was no single mutation that caused complete abolition of lipoylation of the domain although certain multiple mutants were non-lipoylated. For OGDC, however, most mutations on the 70% lipoylated wt LD-OGDC promoted complete recovery of lipoylation. In addition, some amino acid replacements had a minor negative effect while other had no appreciable effect on the extent of lipoylation.

LD-OGDC became completely lipoylated when the serine residue situated 2 residues to the C-terminal side of the lipoylation site (Ser-45) was replaced by threonine and when

the proline residue situated 6 residues to the C-terminal side of the lipoylation site (Pro-49) was replaced by glutamate as single and double mutations in LD-OGDC **S45T, P49E,** and **S45T:P49E**. Therefore, these threonine and glutamate residues play an important role in the lipoylation reaction possibly functioning as a recognition signal for *E. coli* ligase (Wallis & Perham, 1994; Morris *et al.*, 1994). However, the lipoylation of LD-OGDC declined slightly when Asp-33 was mutated to glycine to form the D33G construct. In addition, the extent of lipoylation was similar to the native domain in the T44A construct.

Both S45T and P49E mutations have a positive effect on lipoylation with the P49E substitution having the major influence. Thus, when Pro-49 of the partially lipoylated LD-OGDC D33G mutant was changed to glutamate, **D33G:P49E**, the domain became fully lipoylated. In contrast, LD-OGDC T44A displays equivalent levels of partial lipoylation when Ser-45 was replaced by threonine to form **T44A:S45T** mutant. Moreover, when the P49E mutant was incorporated into the partially lipoylated T44A:S45T construct to form the **T44A:S45T:P49E** mutant**,** the domain once again became fully lipoylated whereas the partial lipoylation of this domain in the T44A:S45T construct declined further when the D33G mutation was introduced to form **D33G:T44A:S45T**. Furthermore, the partially lipoylated D33G:T44A:S45T domain became fully lipoylated when the Pro-49 replacement was added to form the quadruple mutant **D33G:T44A:S45T:P49E.**

Although, LD-OGDC **S45T**, **P49E**, **D33G**:**P49E**, **S45T:P49E**, **T44A:S45T:P49E** and **D33G:T44A:S45T:P49E** mutants were fully lipoylated, their degree of cross reactivity with mAb PD2 was extremely minor. This again confirmed that the primary sequence adjacent to the lipoylation site in LD-OGDC is important for Ab recognition in addition to their lipoylation status.

There was no change in the lipoylation state of the fully lipoylated T44A:S45T:P49E construct when the Q47G and V48F substitutions were incorporated into the domain to yield quadruple and quintuple mutants. Thus the replacement of these two residues did not alter the ability of these domains to serve as substrates for the *E. coli* lipoyl ligase.

3.4.4 Concluding remarks

Both mAbs display a strong signal with OLD-PDC reacting to a similar or slightly greater extent than with the ILD-PDC. Comparison of the sequences comprising the putative epitope shows that there are only two amino acid differences in this region with isoleucine and valine in the ILD sequence replaced by valine and serine respectively in the OLD. The hydrophobic amino acid change was excluded from the comparison since this difference involved a conservative replacement and it was unlikely to have a major effect on Ab binding. However, the serine may have a positive influence on Ab recognition as the OLD-PDC has a tendency to elicit a slightly stronger signal than ILD.

Human ILD-PDC	T 171	D	K	A	T	I	G	F	E	V 180
Human OLD-PDC	T 44	D	K	A	T	V	G	F	E	S 53

ILD-Atmt also displays significant cross reactivity but to a lower extent compared to the ILD and OLD-PDC. Once again there are two amino acid (leucine and glutamate) changes in the region relative to ILD and OLD-PDC. Again the hydrophobic substitution was excluded as it is a conservative change. Interestingly it was noted that there is glutamate in Atmt-ILD instead of glycine representing a significant change in the epitope. Therefore, glycine was considered to constitute an important part of the antigenic determinant. It seems probable that the presence of an amino acid side chain would result in unfavourable steric hindrance disturbing the binding of mAb.

Human ILD-PDC	T 171	D	K	A	T	I	G	F	E	V 180
Human OLD-PDC	T 44	D	K	A	T	V	G	F	E	S 53
Atmt ILD-PDC	T	D	K	A	T	L	E	F	E	S

LD-E3BP was also able to react with PD1 and PD2 but to a lesser extent than OLD/ILD-PDC. Inspection of this domain showed that there were four amino acid changes compared to OLD/ILD-PDC that may play an integral part in the epitope. The Glu to Asp replacement was excluded as it a conservative change. There is a valine in LD-E3BP instead of threonine which was shown previously to constitute part of the epitope in ILD-PDC (see section 2 for more details). Furthermore, there are Thr, Leu and Ala replacements instead of Gly, Phe and Val or Ser respectively. Therefore, the

changes in these residues in LD-E3BP may induce a weaker signal with LD-E3BP than ILD/OLD-PDC as a result of their cumulative effect.

Human ILD-PDC	T	D	K	A	T	I	G	F	E	V
	171									**180**
Human OLD-PDC	T	D	K	A	T	V	G	F	E	S
	44									**53**
Human E3BP-PDC	T	D	K	A	V	V	T	L	D	A

The non-reactive lipoyl domain, LD-OGDC has five different amino acids compared to ILD/OLD-PDC. The replacement of these residues in LD-OGDC to be equivalent to the sequence of the OLD/ILD-PDC is sufficient to recover the full cross reactivity of this domain with mAbs PD1 and PD2

Human ILD-PDC	T	D	K	A	T	I	G	F	E	V
	171									**180**
Human OLD-PDC	T	D	K	A	T	V	G	F	E	S
Human LD-OGDC	T	D	K	T	S	V	Q	V	P	S

This work was able to establish a consensus epitope recognised by both PD1 and PD2. In addition, a degree of variability can be tolerated, as there is no particular amino acid, apart from the key lipoyl lysine residue that could be considered as essential to Ab recognition. However, a cumulative effect with gradual restoration was observed with the non-reactive domain, LD-OGDC.

T	D	K	A	T	**Hydrophobic amino acids I/V/L**	G	F	E/D	V/S

All available evidence suggests that mAbs PD1 and PD2 bind to a contiguous (linear) epitope accessible on the surface of the LD since these mAbs are able to recognise their antigens under both denaturing and non-denaturing conditions. In addition, the sequence motif that forms the antigenic determinant can be presented in a variety of lipoyl domain backgrounds indicating that other parts of the domain are not important for Ab recognition.

Octanoylated ILD-PDC produced in the absence of the exogenous lipoic acid expression elicits a strong signal with these mAbs to a similar extent as ILD-PDC.

Therefore, although the lipoic acid prosthetic group attached to the ILD-PDC is an important element in mAb PD1 and PD2 recognition, the thiol groups of the dithiolane ring of the lipoate prosthetic group are not an integral part of the antigenic determinant.

The major epitope recognised by mAbs PD1 and PD2 lies on the C-terminal of the ILD-PDC rather than in the centrally-located block of 8 amino acid residues. From our site-directed mutagenesis studies on ILD-PDC and LD-OGDC, the consensus motif recognised for these Ab on ILD-PDC is located between Thr-171 and Val-180. The postulated epitope is a part of the previously described linear epitope comprising amino acids 167-183 (Van de Water *et al.*, 1988a). This result is supported by two previous studies reported by Long *et al*. (2001) and Amano *et al*. (2005). The first group used different lengths of synthetic lipoylated ILD peptides to analyse PBC patient sera affinity purified against full-length rE2-PDC. They found that only the 12- amino acid peptide, 172-183 (D**K**ATIGFEVQEE) of ILD-PDC bound tightly to affinity purified AMA (Long *et al.*, 2001). The second group found that a 15-meric 169-183 (IETD**K**ATIGEFEVQEE) lipoylated peptide ILD-PDC gave a strong signal with PBC sera (Amano *et al.*, 2005). Although these studies employed affinity purified AMA instead of mAbs, they confirmed that the major immune response was directed to a linear epitope located on the C-terminal side of the lipoylation site. However, Shimoda *et al.* suggested that there is a single dominant T-cell auto-epitope from 6 peripheral blood-derived CD4+ T-cell clones within E2-PDC which is entirely within the 14 amino acid peptide lying to the N-terminal side of the lipoylation site, GDLLAEIETD**K**ATI (Shimoda *et al.*, 1995). Moreover, Kita *et al.* identified the epitope of an HLA-A2-restricted CTL reactive with self E2-PDC which spans the residues 159-167 of E2-PDC excluding the lipoyl-lysine residue (Kita *et al.*, 2002a).

This work has also confirmed that there is no specific motif for lipoylation. Apart from the lipoyl-lysine residue, single mutations generally have a minor effect on the extent of lipoylation presumably by produced small structural changes in the lipoyl domain. Moreover, despite significant alterations in sequence around the lipoyl-lysine in LD-E3BP compared to ILD/OLD-PDC, this domain is still fully lipoylated. This is not surprising as the lipoylation system must retain the capacity to efficiently utilise a relatively broad range of native lipoyl domain substrates. In addition it is able to carry out post-translational modification of a number of heterologous recombinant substrates including human E2-OADCs and E3BP-PDC, and the H-protein of the glycine cleavage system.

Chapter 4

Investigation of the effect of chemical modification of the lipoic acid prosthetic group and the lipoyl lysine residue on mAbs recognition

4.1 Section 1

Although mAbs PD1 and PD2 recognise the lipoylated forms of the ILD/OLD-PDC and the related lipoyl domain of E3BP, the presence of the attached cofactor is not the sole prerequisite for antibody recognition. Thus no or negligible cross-reactivity is detected with human E2-OGDC, E2-BCOADC and *E. coli* E2-PDC. More detailed mapping of the antigenic determinant within E2-PDC via several studies using oligopeptides or recombinant truncated forms of ILD-E2 have shown that the major AMA epitope is localised to a linear sequence within the inner lipoyl domain (Surh *et al.*, 1990b). Moreover, a homologous lipoyl domain has been identified as containing the immuno-dominant epitope in a second auto-antigenic PDC component, E3BP-PDC (Palmer *et al.*, 1999). Lipoic acid itself, in the case of both E2-PDC and E3BP, appears to constitute an important part of the B-cell epitope, as autoantibodies derived from PBC patients show higher affinity for lipoylated than for non-lipoylated domains (Quinn *et al.*, 1993a; Palmer *et al.*, 1999). More recently, the lipoylation site in the inner lipoyl domain of E2 has been demonstrated to lie at the heart of immuno-dominant class II restricted T-cell and B-cell autoepitopes (Van de Water *et al.*, 1988a; Shimoda *et al.*, 1995). Taken together, these studies suggest that lipoic acid plays a key role in the auto-immunogenicity of PDC.

Most proteins (50-90%) in the human body are post-translationally modified. In most cases, the modification of these proteins is necessary for their biological function. However, one postulated mechanism for the breakdown of immune self tolerance is through aberrant modification of self antigens during post-translational modification, creating neoantigens to which the immune system has never been exposed previously and to which a state of central tolerance has never been established. Exposure to altered forms of self antigen with the resulting immune response spreading to the native antigen has now been suggested to contribute to the pathogenesis of a number of human and animal autoimmune diseases (Doyle & Mamula, 2001).

Component enzymes of the 2-OADCs are nuclear encoded proteins and their post-translational modification occurs following active uptake into the mitochondrion. Lipoylation, therefore, represents a very specific form of post-translation modification to which only a select group of proteins are subjected (Brookfield *et al.*, 1991). Several studies have shown that there are no autoreactive B-cell and T-cell responses to PDC in normal individuals (Jones *et al.*, 1995; 1997), In addition, B-cells and T-cells fail to

stimulate after sensitization of SJL/J mice with self-PDC (Jones *et al.*, 2002). Moreover, lipoylated complexes are normally present through immune system development and maturation. Therefore, it is unlikely that lipoylation *per se* renders self-proteins immunogenic.

4.1.1 Chemical compounds and PBC

Exposure to drugs and environmental chemicals has been speculated to be a possible initiation factor for autoimmune disease by creating neoantigens to which the immune system has not been exposed previously. Xenobiotics are defined as foreign compounds that may either complex to specific self-proteins or may induce changes in the molecular structure of native self-proteins sufficient to alter their recognition by the immune system. Such immune responses may be not able to distinguish between modified and non-modified native proteins (Medzhitov & Janeway, 2000; Rose, 2000). They are present in the environment in the form of industrial chemicals, drugs and even food additives. Xenobiotics may exhibit direct toxicity to vital cellular targets, and thus are usually eliminated either in the urine or in the bile. Why are only bile ducts affected in PBC despite the fact that mitochondrial antigens are ubiquitous? One of the reasons may be that the liver is a unique organ for metabolism and degradation of xenobiotics (Bustamante *et al.*, 1998). A large number of chemicals, including halogenated compounds, are metabolized, degraded and detoxified in the liver and secreted in the bile through biliary epithelial cells. Therefore, exposure of the liver to these xenobiotics could potentially modify self antigens triggering an autoimmune response (Furst *et al.*, 1997; Bustamante *et al.*, 1998).

Several drugs or chemicals have been reported to induce hepatitis with autoimmune involvement, e.g., tienilic acid, dihydralazine, and halothane (Obermayer-Straub *et al.*, 2000). Halothane (2-bromo-2-chloro-1,1,1-trifluoroethane) is an anaesthetic transformed by bio-oxidation via the cytochrome P450 system into trifluoroacetyl chloride (CF_3COCl), a very reactive intermediate that may bind to cellular proteins, to form trifluoroacetylated (TFA) proteins (Eliasson *et al.*, 1998). Halothane hepatitis occurs when susceptible patients mount an immune response to TFA-protein antigens. Exposure to trifluoroacetyl (TFA)-conjugated self proteins, both in humans and experimental animals, has led to antibody responses against such TFA-self proteins (Eliasson *et al.*, 1998). There is evidence based on *in vivo* studies in guinea pigs exposed to halothane that Kupffer cells, resident macrophages of the liver carry (TFA)-

protein adducts (Furst *et al.*, 1997). Moreover, these protein adducts are not found in other organs, including spleen, lung and hilar lymph nodes, suggesting that the generation of autoreactivity to this protein adduct is likely to be caused by a local liver response (Furst *et al.*, 1997). In fact a liver autoimmune disease similar to PBC can be observed in some patients exposed to chlorofluorohydrocarbon anaesthetics. Previous research has documented that exposure to halothane can induce the formation of antibodies that cross-react with not only the haptenated trifluoroacetylated protein (TFA) immunogen, but also to lipoylated E2-PDC whereas there is no cross-reaction with its non-lipoylated counterpart (Sasaki *et al.*, 2000) (Christen *et al.*, 1994). Similar observations were reported for the other E2 subunits of 2-OADCs (Frey *et al.*, 1995). Immunochemical and molecular modelling analysis has shown that the lipoic acid prosthetic group is a perfect structural mimic of N^6-trifluoroacetyl-L-lysine (CF_3CO-Lys), the major haptenic group in CF_3CO modified-proteins (Gut *et al.*, 1995; Frey *et al.*, 1995). Thus trifluoroacetylated lysine, racemic (6RS)-lipoic acid and lipoylated peptide (EIDKATIG) of the ILD-E2-PDC specifically inhibit the recognition of E2-PDC by anti-TFA antibodies generated to trifluoroacetylated rabbit serum albumin and human liver TFA proteins (Christen *et al.*, 1994).

The lipoic acid attachment site itself has also been hypothesized to serve as a xenobiotic target which becomes immunogenic after aberrant modification of the lipoyl-lysine residue cause a breakdown of tolerance. Long *et al.* synthesized ILD of E2-PDC, replacing the lipoic acid moiety with synthetic structures, and quantitated the reactivity of these structures with sera from PBC patients (Long *et al.*, 2001). Results showed that AMA from all patients reacted against 3 of the 18 modified organic autoepitopes significantly better than the native domain. As many chemicals, including pharmaceuticals and household detergents, have the potential to form such halogenated derivatives as metabolites, they may serve as mimeotopes for autoantigens (Long *et al.*, 2001). Structural analysis of reactive compounds revealed that features correlating with autoantibody binding include componds with a halide or methyl halide in the meta- or peta- position containing no strong hydrogen bond accepting groups on the phenyl ring (Long *et al.*, 2001). Amano and his coworkers were able to couple the lipoyl-lysine residue of a 15 amino acid peptide of the E2-PDC inner lipoyl domain with 107 potential xenobiotic mimics and spotted them on microarray slides with antisera from 47 PBC patients and 20 healthy volunteers. It was observed that 33 xenobiotics had a significantly higher IgG reactivity with PBC sera compared to controls. Moreover, 9 of 33 compounds were more reactive than the native lipoylated peptide. In addition, PBC

sera demonstrated high Ig reactivity against 2-octynoic acid-modified E2-PDC peptide, a chemical widely found in the environment including perfumes, lipstick and many common food flavourings (Amano *et al.*, 2005).

It has also been suggested that *in vivo* the lipoic acid group of E2-PDC may be a target for xenobiotics via its reactive thiol groups leading to a breakdown of tolerance and induction of a self-reactive response that is target specific (Long *et al.*, 2001). This theory was tested *in vitro* by modifying reduced lipoic acid linked to the 12 amino acid peptide of ILD-PDC with trifluoroacetaldehyde to yield R/S-5-(2-trifluoromethyl-[1,3]dithian-4-yl) pentanoic acid. This group found that AMA (affinity purified PBC sera to recombinant E2-PDC) had a greater cross reactivity to the halogenated lipoamide ILD peptide than the native domain (Long *et al.*, 2001). Thus modification of the inner lipoyl domain, either on the lipoylatable lysine via the attached lipoyl cofactor or on the lysine itself, may lead to loss of tolerance and hence generation of an anti-mitochondrial response.

Further work has demonstrated that immunization of rabbits with one of these organic compounds (6-bromohexanoate), coupled to a protein backbone unrelated to E2-PDC (BSA), resulted in a specific immunological response with AMA production. This evidence suggests that lipoic acid is important for the induction of AMA and those environmental xenobiotic agents such as 6-bromohexanoate that mimic lipoic acid are able to break self-tolerance *in vivo* and can be a risk factor for the induction of PBC (Leung *et al.*, 2003). However, a further study showed that although 6-bromohexanoate-BSA-immunized rabbit sera were cross-reactive with the lipoylated E2-PDC peptide, they did not show concomitant histological or biochemical evidence of liver/bile duct damage during the period of this study. Thus, while exposure and sensitization to xenobiotics results in autoantibodies to E2-PDC, there are additional factors required to generate immunopathology (Amano *et al.*, 2004).

It is apparent that anti-PDC antibody responses can be inducing by exposure to organic xenobiotics; however, there is no direct evidence to suggest that these specific compounds are actually present *in vivo* (Jones *et al.*, 1999b). SJL/J mice sensitized with covalently modified biotinylated PDC produced high titre, high affinity responses reactive with non-modified self-PDC (Palmer *et al.*, 2004). It was postulated, based on these observations, that the initial B-cell response was induced in response to biotin-self-PDC through biotin-containing epitopes with subsequent epitope spreading to non-

modified, wholly self epitopes (Mamula, 1998). In addition, the induction of antibody responses, reactive with self-antigen after sensitization with modified self was accompanied by production of major histocompatibility complex II-cell restricted T-cell responses to native PDC which was present in all animals treated with biotinylated self-PDC at 6 weeks after sensitization (Palmer *et al.*, 2004). However, both the rabbit and the SJL/J mice models do not show any evidence of bile duct injury, cholestasis or fibrosis that is characteristic of PBC livers. Therefore, it is likely that other factors such as architecture of the biliary system, inflammatory signals, and detoxification pathways are important in the development of PBC.

Leung *et al* have recently found an animal model of PBC. It was provided serologic and immunhistochemical evidence that immunization of guinea pigs with 6-bromohexanoate conjugated to BSA.was able not only develop antimitochondrial autoantibody responses similar to human PBC, but also develop autoimmune cholangitis after 18 months (Leung *et al*; 2007).

4.1.2 Aims of this chapter

In this chapter, possible routes by which ILD-E2 may elicit an autoimmune response were investigated. The specific aims of this chapter were as follows.

- To determine the extent to which the dithiolane ring of the lipoate cofactor of the ILD-PDC constitutes an important part of the antibody recognition site.

- To overexpress and purify bacterial *E. coli* lipoyl ligase A.

- To analyse the specificity of bacterial lipoyl ligase by modification of the lipoyl-lysine residue of the ILD-PDC *in vitro* using fatty acids of varying chain length and related compounds

- To characterise the effects of various modifications of the lipoyl-lysine residue on antibody recognition.

4.1.3 RESULTS

4.1.3.1 Determination of the extent to which the dithiolane ring of the lipoate cofactor of the ILD-PDC constitutes an important part of the antibody recognition site

In the normal catalytic cycle, the lipoyl group is converted between its oxidised, reduced and acetylated states and can be trapped in each of these particular states. In bovine PDC, reduced lipoamide can be chemically modified with a variety of thiol group reagents of varying sizes and structures namely mPEG maleimide (M_r 5000), 4-hydroxy-2-nonenal (C9) (HNE), and N-ethylmaleimide (C6) (NEM). In parallel, recombinant human ILD was also modified with iodoacetamide as the smallest reagent (C2) to investigate their influence on mAb response.

4.1.3.1.1 Methoxy poly (ethylene glycol) maleimide (mPEG maleimide) modification

4.1.3.1.1.1 Modification of bPDC with mPEG maleimide

Bovine heart PDC (bPDC) was treated with mPEG maleimide (M_r 5000 Da) (0.5mM) as described in Materials and Methods, section 2.5.8.1. The reaction was performed in the presence of 0.1mM NADH or NAD^+ at 25°C for 30min. After incubation, excess mPEG maleimide was scavenged by adding DTT

Initially, PDC activity was measured to test the effect of mPEG maleimide incorporation (Figure 4-1) as described in Materials & Methods (section 2.5.3.2). It was observed that overall PDC activity declined to 5% after treatment with mPEG maleimide in the presence of NADH. Moreover, this loss is NADH dependent although there is also a slight decrease in activity in the presence of NAD^+.

mPEG maleimide-bPDC produced using 0.5mM mPEG maleimide in the presence of NADH and NAD^+ was blotted with PD2 (Figure 4-2, panel B). In parallel, SDS-PAGE of modified samples was performed and stained with Coomassie Brilliant Blue to confirm equality of loading and also the specific modification of E2 and E3BP as judged by a dramatic decrease in their migration rate after mPEG maleimide modification (Figure 4-2, panel A). Immunoblotting analysis showed that the loss of

complex activity is accompanied by loss of the cross reactivity of these subunits with PD2 in an NADH-dependent manner.

4.1.3.1.1.2 Modification of recombinant ILD with mPEG maleimide

To confirm the previous result, the free reduced lipoamide thiols of ILD-PDC (using NADH and E3) were chemically modified with mPEG maleimide (0.5mM) at 25°C for 30min. Samples were taken after 1, 5, 10, 15, 20, and 30min incubation prior to removal of excess mPEG maleimide by adding DTT.

A time course was conducted to determine if intermediate state(s) of modification of the dithiolane ring could be observed. However, even after 1min both lipoamide thiols of the ILD appeared to be fully modified. The modified products were analysed and visualised by means of gel shift assay. Non-denaturating PAGE (15% gels) were performed in which the modified ILDs exhibited a markedly decreased rate of migration after staining with Coomassie Brilliant Blue (Figure 4-3, panel A). In parallel, non-denaturating PAGE of mPEG maleimide-ILD was blotted with PD2 to check the cross reactivity of the modified domain (Figure 4-3, panel B). It is apparent from the immunoblotting analysis that the disappearance of the ILD cross-reactivity with PD2 was also accompanied by modification of the thiol groups of the dithiolane ring.

4.1.3.1.2 4-hydroxy-2-nonenal (HNE) modification

4.1.3.1.2.1 Modification of bPDC with HNE

Bovine heart PDC was treated with HNE (C9) as described in Materials and Methods, section 2.5.8.2. The reaction was performed with increasing concentrations of HNE (0, 0.05, 0.1, 0.25, and 0.5mM) in the presence of 0.1mM NADH and NAD^+ at 30°C for 1h. The reaction was terminated by adding sample buffer.

Incubation of purified bovine PDC with HNE resulted in the selective inactivation of complex activity. As shown in Figure 4-4, overall PDC activity declined to 25% and 5% with 0.05 and 0.1mM HNE, respectively in the presence of NADH. Reduced lipoic acid is a strong nucleophile at physiological pH and is located on the surface of the E2 subunit of PDC. Model studies reveal that thiol group (s) on the lipoic acid react with the double bond (C3) of HNE to form a Michael addition product. Although, this modification is NADH dependent, there is also a slight decrease in activity in the presence of NAD^+. However, at higher HNE concentrations (0.25 and 0.5mM), PDC

activity decreased with both NADH and NAD^+ due to non-specific HNE modification. This result suggests that at low concentrations of HNE the modification is more specific to the thiol groups of the dithiolane ring of the lipoamide residues of E2- and E3BP-PDC.

HNE-bPDC incubated with 0.05mM and 0.1mM HNE in the presence of NADH and NAD^+ was blotted with PD2 (Figure 4-5, panel B). In parallel, SDS-PAGE of modified samples was performed and stained with Coomassie Brilliant Blue to confirm their equality of loading (Figure 4-5, panel A). Immunoblotting analysis again revealed that loss of complex activity was accompanied by the loss of cross reactivity with PD2. In addition, HNE modification was NADH-dependent. No E3BP-bPDC was detected in this case due to the lower level of exposure and the weak cross reactivity of E3BP with PD2.

4.1.3.1.2.2 Modification of recombinant ILD-E2 with NHE

To confirm the previous result, free sulphydryl groups of the ILD-E2 in the reduced form using NADH were chemically modified with increasing concentrations of HNE (0, 0.05, 0.1, 0.25 and 0.5mM). Chemical modification was performed also in the presence of NAD^+ as a negative control under conditions described in Materials and Methods, section 2.5.8.2. Products of modification were analysed and visualised by means of the gel shift assay, on non-denaturating PAGE (15% gels) in which the modified protein exhibited a markedly decrease rate of migration after staining with Coomassie Brilliant Blue (Figure 4-6, panel A). In parallel, non-denaturating PAGE of HNE-ILD-E2 was blotted with PD2 to check the cross reactivity with the modified protein (Figure 4-6, panel B). Immunoblotting analysis again demonstrated that abolition of the cross reactivity of PD2 with ILD occurred on the modification of the dithiolane ring dithiols. In addition, HNE modification is NADH dependent at low concentrations although, some non-specific HNE modification was observed (in the presence of NAD^+) at higher levels HNE (0.25 and 0.5mM).

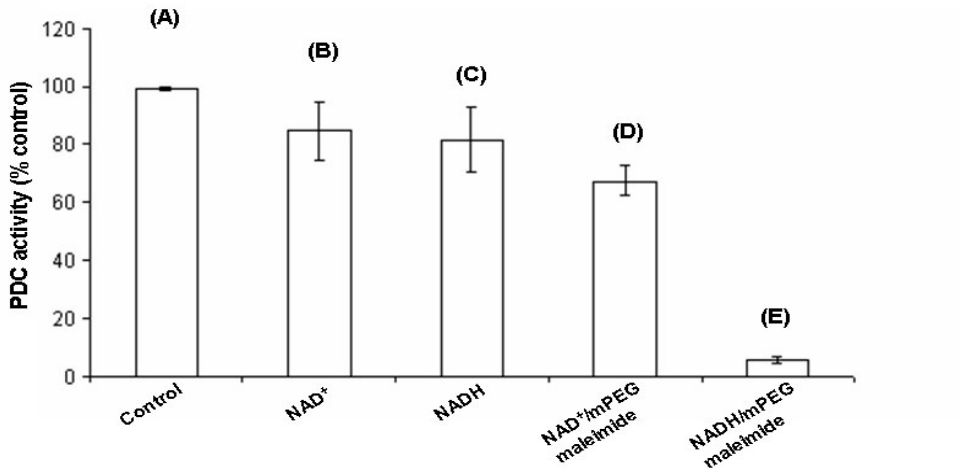

Figure 4-1 Activity of bovine PDC after modification with mPEG maleimide
Purified bovine PDC was modified with 0.5mM mPEG maleimide in the presence of NAD^+ or NADH. After mPEG maleimide modification, the activity of modified bovine PDC was measured at 340nm.

Column (A), bovine PDC as a control; **column (B)**, bovine PDC plus NAD^+; **column (C)**, bovine PDC plus NADH; **column (D)**, as column B plus 0.5mM mPEG maleimide, and **column (E)**, as column C plus 0.5mM mPEG maleimide.

Error bars show the extent of variation of duplicate readings.

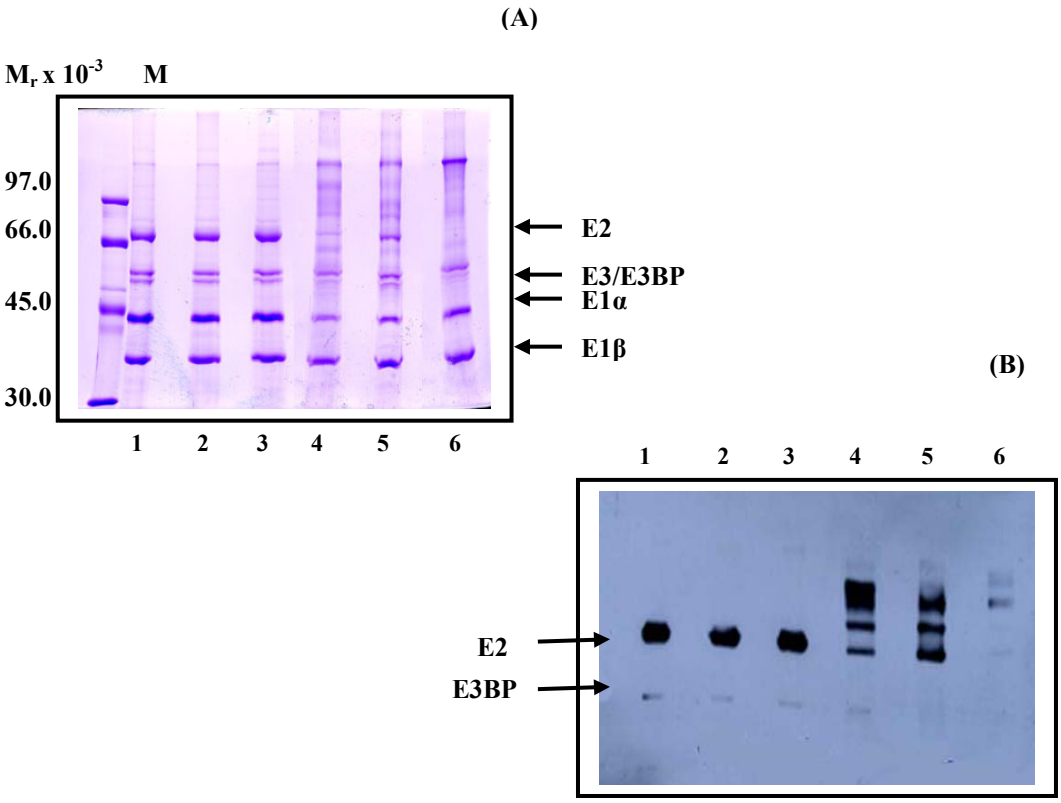

Figure 4-2 Modification of bovine PDC with mPEG maleimide: effect on enzyme recognition by PD2

Bovine PDC (1mg/ml) was modified chemically with mPEG maleimide (0.5mM) at 25°C for 30min after incubation with NAD^+ or NADH in 50mM Tris-HCl buffer, pH 7.5 and separated by (8%) SDS-PAGE (15µg of modified proteins) and stained with Coomassie Brilliant Blue (A) or immunoblotted with PD2 antibody (B).

Lane 1, bovine PDC; **lane 2**, bovine PDC plus NAD^+; **lane 3**, bovine PDC plus NADH; **lane 4**, 0.5mM mPEG maleimide-modified bovine PDC; **lane 5**, 0.5mM mPEG maleimide-modified bovine PDC in the presence of NAD^+; and **lane 6**, 0.5mM mPEG maleimide-modified bovine PDC in the presence of NADH.

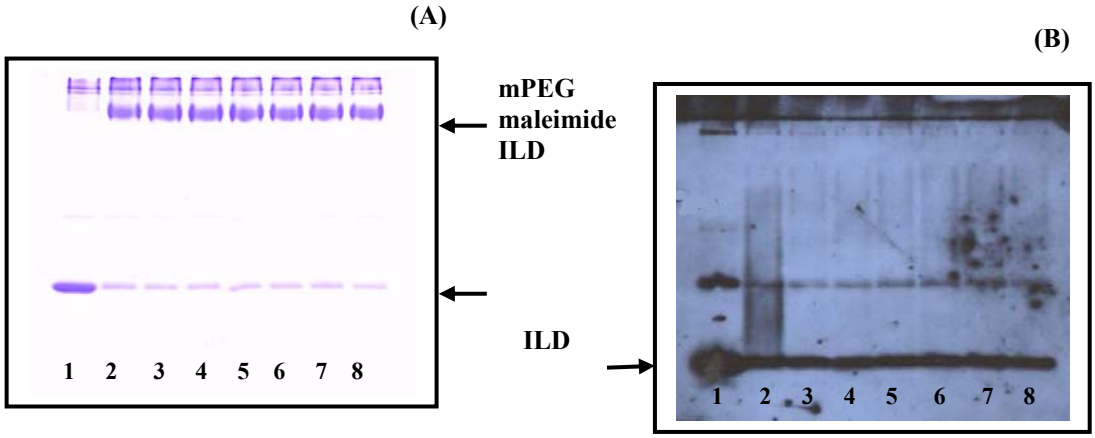

Figure 4-3 Modification of human ILD-E2 with mPEG maleimide: effect on recognition by PD2

ILD-E2 (20µg) was modified chemically with mPEG maleimide (0.5mM) at 25°C for 30min in the presence of NADH and E3 in 50mM Tris-HCl buffer pH 7.5. Modified samples (6µg or 3µg) were taken after 1, 5, 10, 15, 20, 25, 30min incubation and separated on a 15% native gel, stained with Coomassie Brilliant Blue (A) or immunoblotted with PD2 antibody (B).

Lane 1, ILD-E2 as a control; **lane 2**, mPEG maleimide-ILD-E2 after 1min incubation; **lane 3**, 5min incubation; **lane 4**, 10min incubation; **lane 5**, 15min incubation; **lane 6**, 20min incubation; **lane 7**, 25min incubation; and **lane 8**, 30min incubation.

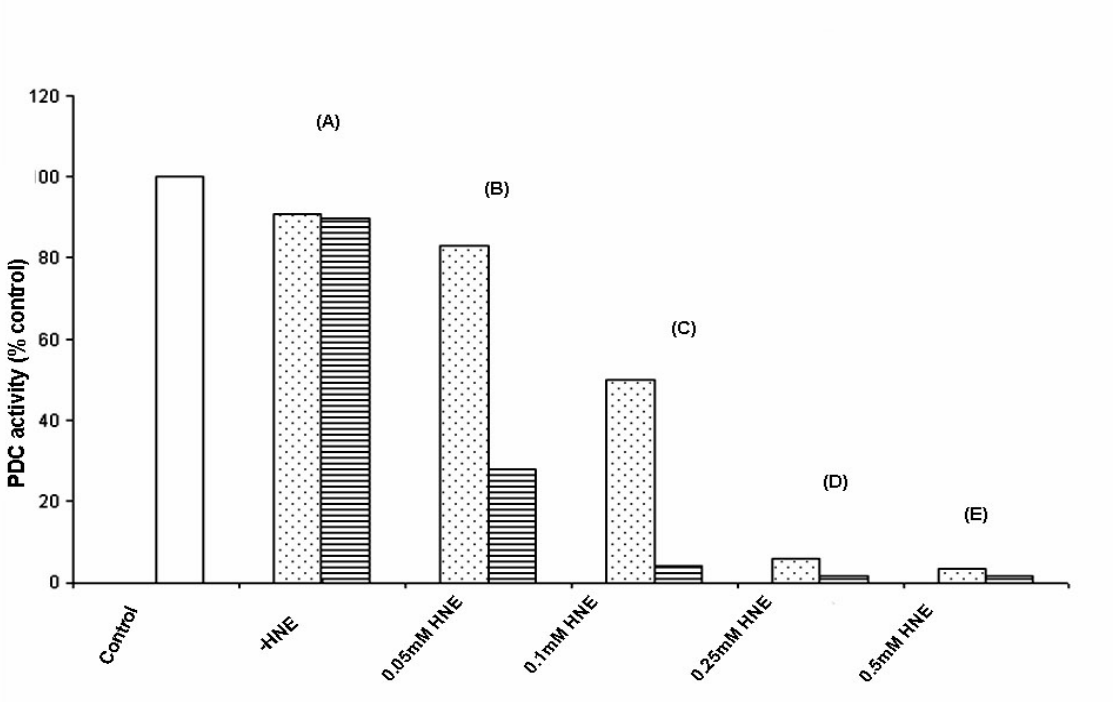

Figure 4-4 Activity of bovine PDC after modification with increasing concentrations of HNE
Purified bovine PDC was modified with increasing concentrations of HNE in the presence of NAD^+ or NADH. After HNE modification, the activity of HNE modified bovine PDC was assayed at 340nm (at 30°C) as described in Materials & Methods.

First column, bovine PDC as a control; **track (A)**, bovine PDC without HNE modification; **track (B)**, 0.05mM HNE-bPDC; **track (C)**, 0.1mM bPDC; **track (D)**, 0.25mM HNE-bPDC; and **track (F)**, 0.5mM HNE.

Note spotted and striped columns represent the HNE modification in the presence of NAD^+ and NADH respectively.

Bars represent the average different of duplicate readings differing by less than 5%

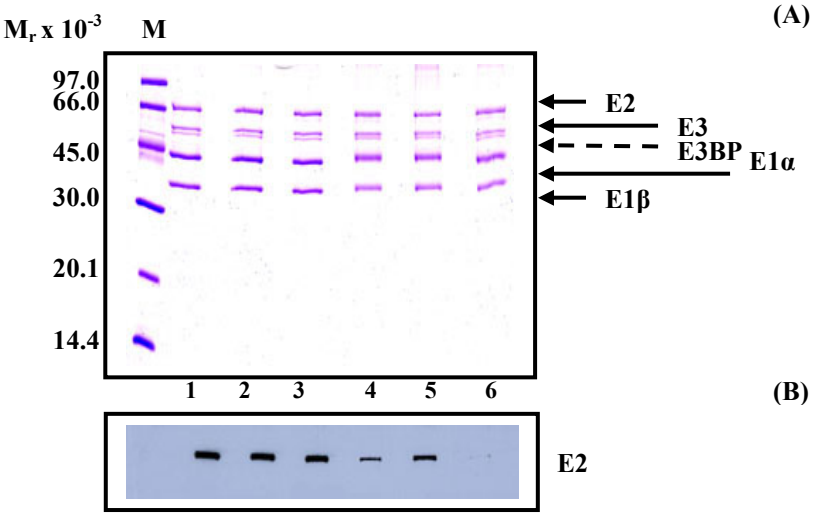

Figure 4-5 Modification of bovine PDC with HNE: effect on autoantibody recognition
Bovine heart PDC (2mg/ml) was modified chemically with HNE at 30°C for 1h after incubation with 0.1mM NAD^+ or NADH, separated by reducing SDS-PAGE (5µg of modified proteins), stained with Coomassie Brilliant Blue (A) and immunoblotted with PD2 antibody (B).

Lane 1, bovine heart PDC plus NAD^+; **lane 2**, bovine PDC plus NADH; **lane 3**, as lane 1 with 0.05mM HNE; **lane 4**, as lane 2 with 0.05mM HNE; **lane 5**, as lane 1 with 0.1mM HNE; and **lane 6**, as lane 2 with 0.1mM HNE.

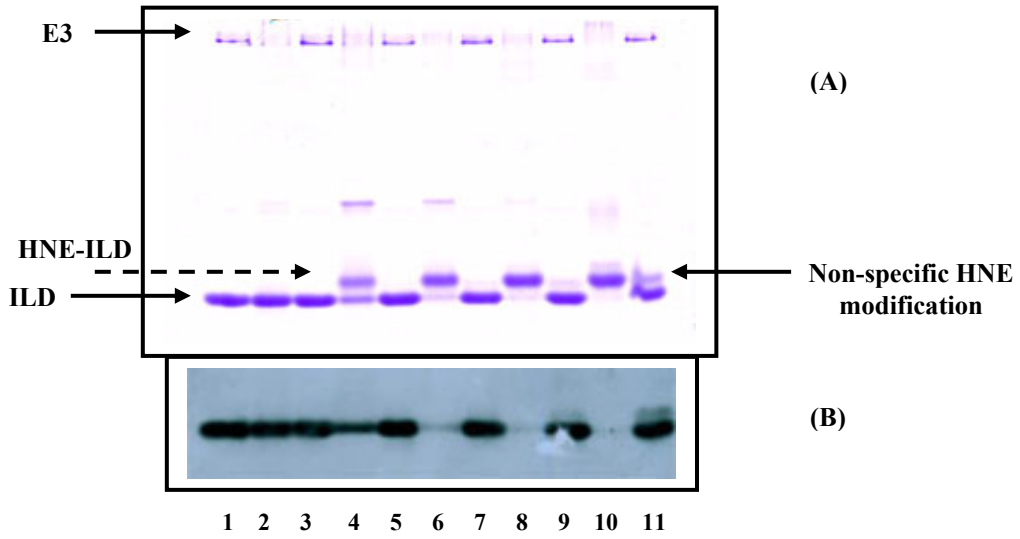

Figure 4-6 Modification of human ILD-PDC with HNE: effect on recognition by PD2
ILD-PDC (20µg) was modified chemically with increasing concentrations of HNE (0, 0.05, 0.1, 0.25, and 0.5mM) at 30°C for 1h after incubation with 0.1mM NADH and NAD^+ in 50mM KPi pH 7.4 as described in Materials & Methods, separated on 15% native gel (6µg or 3µg of modified proteins), and stained with Coomassie Brilliant Blue (A) or immunoblotted with PD2 antibody (B).

Lane 1, ILD-E2; **lane 2**, ILD-E2 plus NADH; **lane 3**, ILD-E2 plus NAD^+; **lane 4**, as lane 2 plus 0.05mM HNE; **lane 5**, 0.05mM HNE-ILD- PDC plus NADH; **lane 6**, as lane 2 plus 0.1mM HNE; **lane 7**, as lane 3 plus 0.1mM HNE; **lane 8**, as lane 2 plus 0.25mM HNE; **lane 9**, as lane 3 plus 0.5mM HNE; **lane 10**, as lane 2 plus 0.5mM HNE; and **lane 11**, as lane 3 plus 0.5mM HNE.

4.1.3.1.3 N-ethylmaleimide (NEM) modification

4.1.3.1.3.1 Modification of bovine PDC with NEM

Bovine PDC (bPDC) was treated with NEM (C6) (0, 0.5, and 1mM). The treatment was performed in the presence of NAD^+ and NADH at 25°C for 30min as described in Materials and Methods, section 2.5.8.1. After incubation, excess NEM was scavenged using DTT.

PDC assays were employed as described in Materials and Methods, 2.5.3.2 to check the activity of PDC after NEM modification (0.5mM) and to ensure maximal incorporation of NEM. Figure 4-7 shows that the overall bPDC activity decreased to 5% in the presence of NADH, although, there is also a minor decrease in bPDC activity in the presence of NAD^+. This results from NEM modification of accessible cysteine residues located on the E1α and E1β subunits (Hodgson *et al.*, 1986).

Bovine PDC modified with NEM (0, 0.5 and 1mM) in the presence of NAD^+ and NADH was blotted with PD2 (Figure 4-8, panel B). In parallel, SDS-PAGE of modified PDC samples was run and stained with Coomassie Brilliant Blue to confirm equality of loading (Figure 4-8, panel A). As shown in the immunoblotting analysis, the cross reactivity of PD2 to modified E3BP of bPDC was eliminated; however, only a partial reduction in the cross reactivity of PD2 with modified E2-bPDC was observed. In order to exclude the possibility that this partial response resulted from incomplete modification of E2-PDC lipoamide thiols by NEM, the study was extended to examine the effect of NEM modification on the human ILD-E2 (Figure 4-9).

4.1.3.1.3.2 Modification of recombinant ILD-E2 with NEM

Free sulphydryl groups of the ILD-E2 in the reduced form using NADH and E3 were chemically modified with NEM (0, 0.5, 1 and 2mM). Chemical modification was performed also in the presence of NAD^+ as a negative control under conditions described in Materials and Methods, section 2.5.8.1. Products of modification were analysed and visualised by means of gel shift assay on non-denaturating PAGE (15% gels) in which the modified protein exhibited a slower rate of migration (Figure 4-9, panel A). In parallel, non-denaturating PAGE of NEM-ILD-E2 was blotted with PD2 to check the cross reactivity with the modified protein (Figure 4-9, panel B). It was evident from the immunoblotting analysis that the decline in cross reactivity with PD2 resulted from modification of the sulphydryl groups of the dithiolane ring of the lipoamide

residue and that fully-modified lipoyl domains displayed no cross reactivity with this mAb.

Since the modification of human ILD-E2 by all these reagents, mPEG maleimide (M_r 5000 Da), HNE (C9) and NEM (C6) abolished cross reactivity with PD2, the effect of the smallest thiol group reagent available, iodoacetamide (C2) was tested

4.1.3.1.4 Modification of recombinant ILD-E2 with iodoacetamide

Free sulphydryl groups of the ILD-E2 in the reduced form using NADH and E3 were chemically modified with increasing concentrations of iodoacetamide (0, 1, 2, 5, 10, 15 and 100mM) at 25°C for 30min. After a 30min incubation, excess iodoacetamide was scavenged by using DTT.

Chemical modification was performed also in the presence of NAD^+ as a negative control under conditions described in Materials and Methods, section 2.5.8.1. LD products of iodoacetamide modification were analysed and visualised by means of gel shift assay on non-denaturating PAGE (15% gels) in which the modified protein exhibited a slight decrease in migration rate (Figure 4-10, panel A). In parallel, mPEG maleimide-ILD-E2 was blotted with PD2 to check its cross reactivity with the modified ILD (Figure 4-10, panel B). As previously the immunoblotting analysis revealed complete loss of recognition of ILD-E2 by PD2 following modification by iodoacetamide.

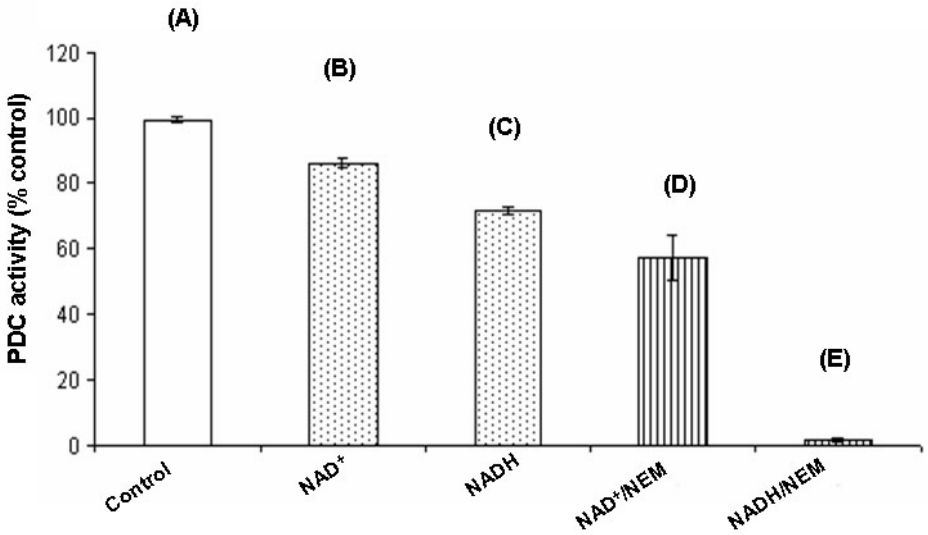

Figure 4-7 Activity of bovine PDC after modification with NEM
Purified bovine PDC was modified with 0.5mM NEM in the presence of 1mM NAD^+ or NADH. After NEM modification, the activity NEM modified bovine heart PDC was measured at 340nm (at 30°C) as described in Materials & Methods.

Column (A), bovine PDC as a control; **column (B)**, bovine PDC with NAD^+; **column (C)**, bovine PDC with NADH; **column (D)**, 0.5mM NEM-bPDC in the presence of NAD^+; and **column (E)**, 0.5mM NEM-bPDC in the presence of NADH.

Error bars indicate the extent of variation of duplicate readings.

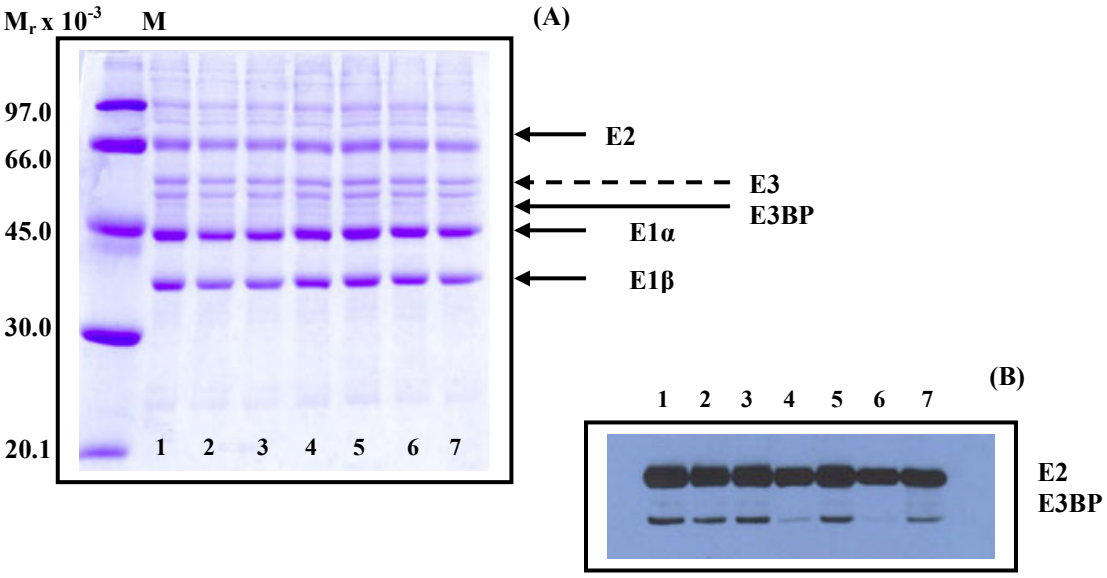

Figure 4-8 Modification of bovine PDC with NEM: effect on PD2 recognition
Purified bovine PDC was modified with 0.5 and 1mM NEM in the presence of NADH and NAD^+.

Bovine PDC was modified chemically with NEM at 25°C for 30min after incubation with 1mM NAD^+ or NADH in 50mM Tris-HCl pH 7.5 as described in Materials & Methods, samples were separated by reducing SDS-PAGE (15µg of modified proteins), stained with Coomassie Brilliant Blue (A) and immunoblotted with PD2 antibody (B).

Lane 1, bovine PDC; **lane 2**, bovine PDC plus NADH; **lane 3**, bovine PDC plus NAD^+; **lane 4**, as lane 2 plus 0.5mM NEM; **lane 5**, as lane 3 plus 0.5mM NEM; and **lane 6**, as lane 2 plus 1mM NEM; **lane 7**, as lane 3 plus 1mM NEM.

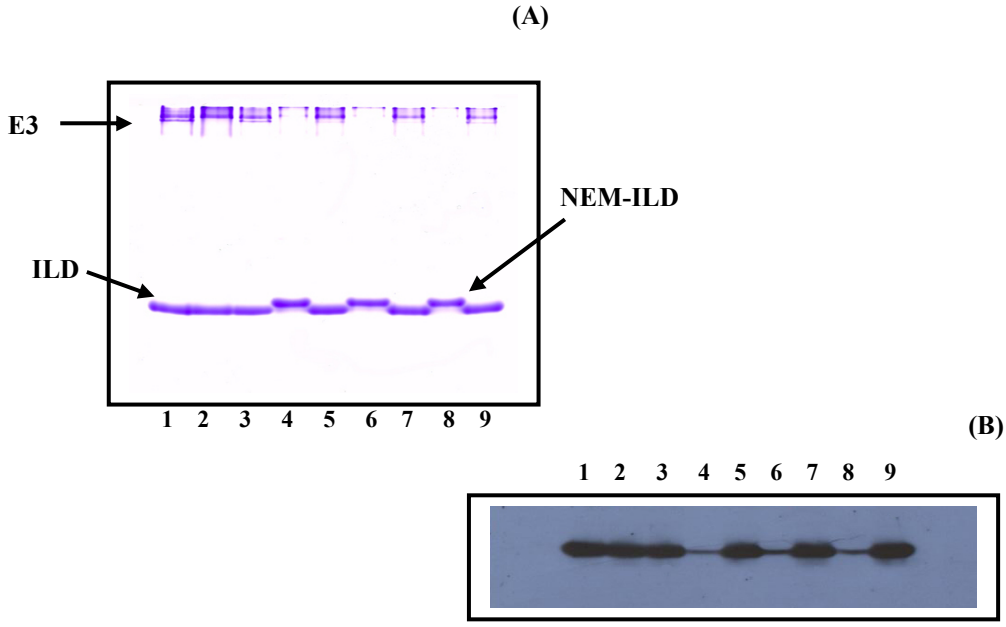

Figure 4-9 Modification of human ILD-E2 with NEM: effect on PD2 recognition
ILD-E2 (20µg) was modified chemically with increasing concentrations of NEM (0, 0.5, 1.0, and 2.0mM) at 25°C for 30min after incubation with 1mM NADH or NAD^+ and E3 in 50mM Tris-HCl pH 7.5. Samples were separated on 15% native gel (6µg or 3µg of modified proteins), stained with Coomassie Brilliant Blue (A) or immunoblotted with PD2 antibody (B).

Lane 1, ILD-E2; **lane 2**, ILD-E2 plus NADH; **lane 3**, ILD-E2 plus NAD^+; **lane 4**, as lane 2 in the presence of 0.5mM NEM; **lane 5**, as lane 3 in the presence of 0.5mM NEM; **lane 6**, as lane 2 plus 1mM NEM; **lane 7**, as lane 3 plus 1mM NEM; **lane 8**, as lane 2 plus 2mM NEM; and **lane 9**, as lane 3 plus 2mM NEM.

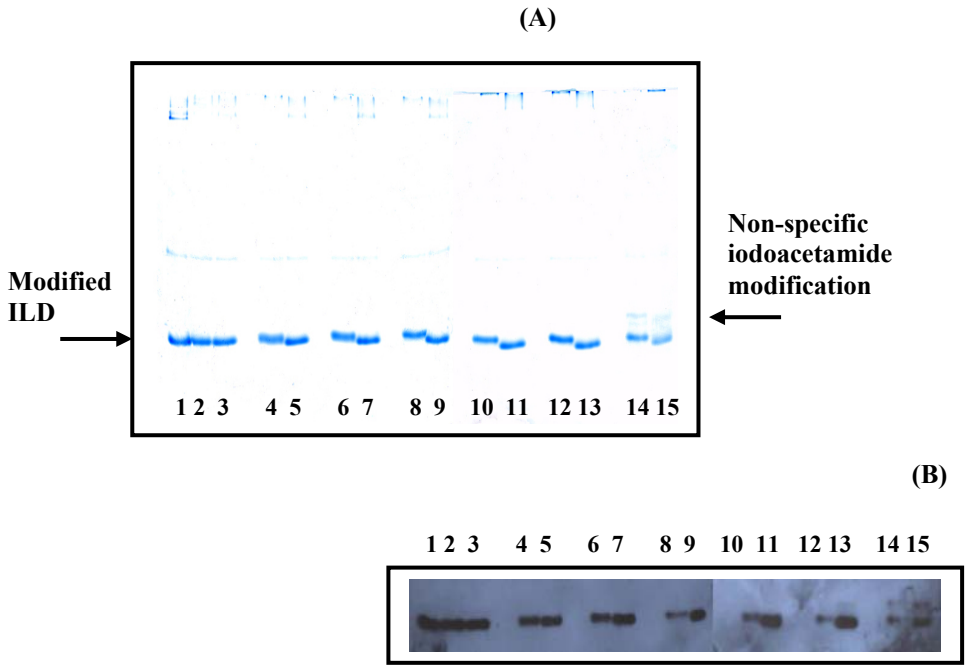

Figure 4-10 Modification of human ILD-E2 with iodoacetamide: effect on recognition by PD2

ILD-E2 (20µg) was modified chemically with increasing concentrations of iodoacetamide (0, 1, 2, 5, 10, 25, and 100mM) at 25°C for 30min after incubation with 1mM NADH and NAD^+ in 50mM Tris-HCl buffer pH 7.5, separated on a 15% native gel (4µg or 0.2µg of modified proteins), stained with Coomassie Brilliant Blue (A) or immunoblotted with PD2 antibody (B).

Lane 1, ILD-E2; **lanes 2 and 3**, ILD-PDC without iodoacetamide; **lanes 4 and 5**, ILD-PDC plus 1mM iodoacetamide; **lane 6 and 7**, 2mM iodoacetamide; **lanes 8 and 9**, 5mM iodoacetamide; **lanes 10 and 11**, 10mM iodoacetamide; **lanes 12 and 13**, 20mM iodoacetamide; and **lanes 14 and 15**, 100mM iodoacetamide.

Note: *lanes 2, 4, 6, 8, 10, 12* and *14* represent modification in the presence of NADH; *lanes 3, 5, 7, 9, 11, 13* and *15* represent modification in the presence of NAD^+.

4.1.4 Discussion

This phase of the project focused on the dithiolane ring and the involvement of the thiol groups of the lipoamide prosthetic group of bE2/E3BP-PDC and ILD-E2 in particular, in antibody recognition in PBC.

Previously it was shown in chapter 3 that the octanoylated domain elicited strong cross reactivity with mAbs PD1 and PD2, suggesting that lipoamide thiols were not necessary for Ab recognition. Moreover, the degree of cross reactivity of the octanoylated domain is equivalent to that of the lipoylated domain with PD1 and PD2. Fussey *et al.* found that bacterial octanoylated E2-PDC and E2-OGDC, produced by a mutant deficient in lipoate biosynthesis, were recognised by PBC patient sera, but not as efficiently as their lipoylated counterparts (Fussey *et al.*, 1990). In addition, Amano *et al.* demonstrated that octanoic acid was also recognised by PBC sera but to a lower extent once again (Amano *et al.*, 2005). However, Long *et al.* showed that an octanoylated 12 amino acid peptide of ILD-E2 (172-183) failed to react well with affinity purified PBC sera to recombinant E2-PDC (Long *et al.*, 2001). Contradictory results can be accounted for in previous studies as PBC sera have been used instead of mAbs.

In our study, an analysis was performed to determine the extent to which PD1 and PD2 were able to recognise lipoamide in which its dithiolane ring was modified by various thiol group reagents of different sizes and structures.

Thus E2 and E3BP of the native purified bPDC and the recombinant ILD-PDC were modified through the thiol groups of lipoamide employing mPEG maleimide (M_r 5000 Da), 4-hydroxy-2-nonenal (HNE) (C9), N-ethylmaleimide (NEM) (C6), and iodoacetamide (C2). Modified forms of bPDC and recombinant E2 was subjected to Western blotting to determine the influence of these specific treatments on cross reactivity with mAb PD2.

Chemical modification was performed in the presence of NAD^+ and NADH. It was observed that the oxidized and reduced forms of ILD-E2 and E2/E3BP-bPDC were equally immunogenic for mAbs. This result is not in agreement with an early study by Mendel-Hartvig *et al.* (Mendel-Hartvig *et al.*, 1985). This study showed that the PBC antigen recognised by PBC patient autoantibodies is sensitive to the redox potential of the preparation. The intensity of the PBC antigen (70 kDa) immunoblotting by PBC

patient antisera correlated with the concentration of the thiol reducing agent in the sample buffer added to purified PDC before SDS-PAGE, suggesting that PBC patient autoantibodies preferentially recognise E2-PDC in the reduced state (Mendel-Hartvig *et al.*, 1985).

The extent of modification of LDs of E2- and E3BP-bPDC was assessed by PDC activity. There is a correlation between the decrease of the enzyme activity and the modification of sulphydryl groups which occurred mostly in the presence of NADH, since thiol groups of the dithiolane ring are critical residues essential for domain function.

Modification of E2 and E3BP-bPDC as well as ILD-E2 was accompanied by a decrease in cross reactivity of these proteins with PD2. The lack of immunoreactivity of mAbs with modified-autoantigens agrees with a report by Odin *et al.* (Odin *et al.*, 2001), who studied the characteristics of the autoantibody recognition site and the effect of apoptosis on the immunogenecity of E2-PDC. They found that apoptotic cells (Hela, Jurkat T, and Caco-2 cells) presented a form of E2-PDC that became undetectable when probed with AMA (Odin *et al.*, 2001). This loss of recognition in apoptotic cells is not attributable to disappearance or degradation, but rather to a reversible structural change in the epitope(s) of E2-PDC as a result of a covalent modification of E2-PDC thiol group(s) by glutathione. Significantly, it was noticeable that this situation did not occur in the apoptotic cells pre-treated with the glutathione synthesis inhibitor, buthionine sulfoximine (BSO) which permitted the depletion of the glutathione pool before inducing apoptosis, thus preventing the loss of autoantibody recognition (Celli *et al.*, 1998; Odin *et al.*, 2001). Moreover, cholangiocytes and salivary gland epithelial cells, the cell types most frequently affected in patients with PBC, maintain the E2-PDC epitope(s) recognised by PBC patient autoantibodies after apoptosis due to the low level of GSH in these cells (Celli *et al.*, 1998).

In all cases, the cross reactivity of PD2 with the antigenic determinant located on the ILD-, OLD-E2-PDC and LD-E3BP antigen (s) was lost when their thiol groups were chemically-modified. Our interpretation of these observations is that these chemicals may block or mask the immunoreactivity of mAbs leading to steric hindrance of the interaction of mAb with its epitope in bovine E2 and/E3BP-PDC and human ILD-PDC.

4.2 Section 2

4.2.1 The lipoyl domain

The lipoyl domain plays a central role in the catalytic mechanism of the 2-oxoacid dehydrogenase complexes. Additionally, it is involved in two important recognition processes *in vivo*. Each lipoyl domain can be post-translationally modified covalently on a specific lysine residue by the lipoylating enzymes of the cell while the recognition of the lipoyl domain by its cognate E1 is a prerequisite for efficient catalysis.

Each lipoyl domain consists of approx 80 amino acids with each carrying a lipoic acid cofactor. The redox active disulphide bond of the lipoyl domain functions as a covalently bound carrier of reaction intermediates between active sites within these multienzyme complexes.

4.2.1.1 Structure of the Lipoyl Domain

The three-dimensional structure of the lipoyl domains of PDC of human (Howard *et al.*, 1998), *B. stearothermophilus* (Dardel *et al.*, 1993) and *E. coli* E2 (Green *et al.*, 1995a) have been solved by NMR spectroscopy. Owing to the high level of sequence similarity between lipoyl domains of 2-OADCs from many different species, all lipoyl domains are likely to have closely related structures.

The domain is composed of a flattened 8-stranded β-barrel consisting of two 4-stranded antiparallel β-sheets with the N- and C-termini close together in one sheet and the lipoyl-lysine residue prominently displayed at the tip of a tight type I β-turn in one of the β-sheets as shown in Figure 4-11 (Howard *et al.*, 1998).

This structural feature of the lipoyl domain is essential for correct post-translational modification by the lipoylating enzyme (Wallis & Perham, 1994). The lipoyl domain is recognised specifically by two enzymes: the lipoylating enzyme(s) of the cell and the E1 component of PDC. The lipoyl ligase attaches the lipoic acid to the domain, selecting both the domain and specific lysine residue within it which is to be lipoylated (Brookfield *et al.*, 1991).

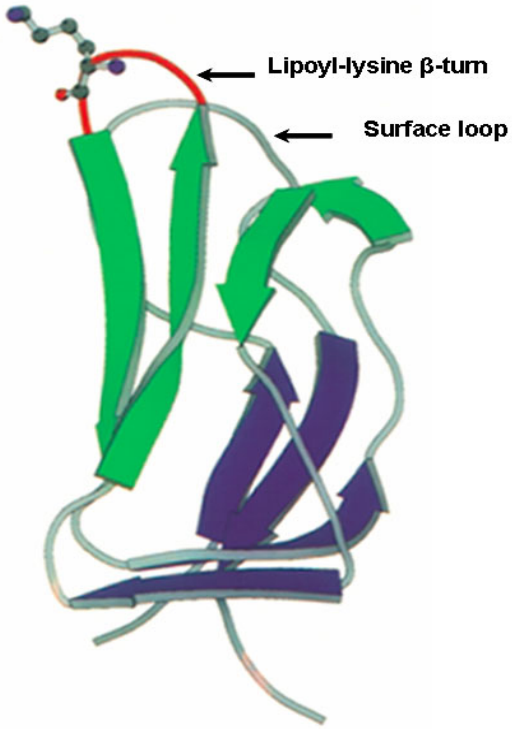

Figure 4-11 Schematic representation of the three-dimensional structure of the inner lipoyl domain from human E2-PDC
The β-sheet containing the lipoyl-lysine residue is shown in green. The β-sheet coloured blue contains the N-and C-terminal residues. The lipoyl-lysine β-turn is indicated in red. The surface loop linking the first and second β-sheet is shown in green.

The location of the lipoyl-lysine residue at the tip of a protruding β-turn is important for its presentation to the active site of E1 (Jones *et al.*, 2000a). However, no such specific molecular recognition appears to be necessary in E2 and E3 reactions since they can both utilise free lipoic acid as substrate with high efficiency (Wallis & Perham, 1994).

A DKA motif is widely conserved in the lipoyl-lysine β-turn in lipoyl domains from various PDCs (Dardel *et al.*, 1993; Green *et al.*, 1995a). However, neither the aspartate nor alanine residues appears to be a recognition signal for the lipoylating enzymes whereas changing the position of the target lysine residue in the β-turn has a crucial effect on lipoylation. In contrast, in *B. stearothermophilus* PDC, these residues flanking the lipoyl-lysine residue at position 42 are necessary for the reductive acetylation of the lipoyl group by the E1 component (Wallis & Perham, 1994; Green *et al.*, 1995a). Substitution of aspartate at position 41 with large residues eg. lysine or glutamate results in a decline in reductive acetylation by E1. Since this residue is at the mouth of a cleft in the structure (Dardel *et al.*, 1993), substitution by large residues may obstruct access to other residues within the cleft that are recognised by E1 (Wallis & Perham, 1994). In addition, the substitution of alanine at position 43 with polar residues also leads to a decrease in reductive acetylation, suggesting a hydrophobic interaction between the alanine residue and the E1 enzyme (Wallis & Perham, 1994).

4.2.2 The lipoic acid moiety

Lipoic acid (6, 8-thioctic acid) is a disulphide derivative of octanoic acid. It is a naturally occurring compound present as a prosthetic group in the 2-oxoacid dehydrogenase complexes (E2-PDC together with E3BP, E2-OGDC and E2-BCOADC) and the glycine cleavage system in most prokaryotic and eukaryotic organisms (Reed & Hackert, 1990).

The role of lipoic acid is dependent upon covalent attachment to specific lysine residues of the cognate enzymes. In each lipoyl domain, the lipoyl group is bound via an N^6-amide linkage to the €-amino group of a specific lysine residue, thus serving as a classical "swinging arm" for shuttling reaction intermediates between the different active sites (Perham, 2000).

Although the existence of lipoic acid has been known for almost 50 years, little is known about the endogenous pathway responsible for lipoic acid biosynthesis. In

mammals, lipoic acid has been found to be efficiently scavenged from dietary sources by the intestinal sodium-vitamin transporters (Prasad *et al.*, 1998).

In *E. coli,* there are two complementary pathways involving distinct enzyme systems for catalyzing the post-translational lipoylation of apoproteins with the lipoyl moiety as shown in Figure 4-12. **The first pathway** (endogenous pathway) is dependent on the *lipB* gene product, lipoyl (octanoyl)-[acyl-carrier-protein]-protein-N-lipoyltransferase (LipB). The *lipB* gene was isolated during selection for mutants defective in lipoate synthesis (Vanden Boom *et al.*, 1991). The (25kDa) LipB enzyme catalyses the transfer of endogenously synthesized lipoate or octanoate from lipoyl- or octanoyl-acyl carrier protein (ACP) to the relevant apoproteins (Vanden Boom *et al.*, 1991; Reed & Cronan, 1993; Morris *et al.*, 1995; Jordan & Cronan, 2003). This activity was also found in extracts of *E. coli lplA* null mutants and, unlike the LplA enzyme, it was not dependent on ATP whereas it was absent in *E. coli lipB* mutants (Cronan *et al.*, 2005). Octanoylated domains then become substrates for thiol insertion by the LipA enzyme (Zhao *et al.*, 2003). Genetic investigations have shown that a single *E .coli* gene *lipA,* encodes a protein of 36 kDa which is responsible for the sulphur-insertion steps of lipoate biosynthesis (Vanden Boom *et al.*, 1991; Reed & Cronan, 1993).

The second pathway in which exogenous lipoate or octanoate is transferred to non-lipoylated apoproteins in an ATP-dependent process catalysed by the *lplA* gene product, lipoate-protein ligase A (LplA) (Figure 4-12) (Brookfield *et al.*, 1991; Morris *et al.*, 1994; 1995). The *E. coli lplA* gene was the first lipoate protein ligase gene to be isolated and LplA enzyme was the first such ligase purified to homogeneity as a 38 kDa monomeric protein (Morris *et al.*, 1994; Green *et al.*, 1995b). LplA activity was described in *E. coli* by Brookfield *et al.* as two forms, LplA and LplB and subsequently reported in *E. coli* and in *E. faecalis* by Reed and coworkers (1958) (Brookfield *et al.*, 1991). They postulated that lipoate attachment was by a two-step ATP-dependent reaction with lipoyl-AMP as an activated intermediate and transfer to apoprotein with concomitant release of AMP (Brookfield *et al.*, 1991). In addition, the LplA enzyme has been shown to be capable of utilizing lipoate and several lipoate analogues (octanoate, selenolipoate, 6-thiooctanoate and 8-thiooctanoate) as donors for the post-translational modification of E2 apoproteins *in vivo* (Morris *et al.*, 1994; Green *et al.*, 1995b). This rather broad substrate specificity *in vivo* matches the similar broad substrate specificity observed *in vitro* (Brookfield *et al.*, 1991).

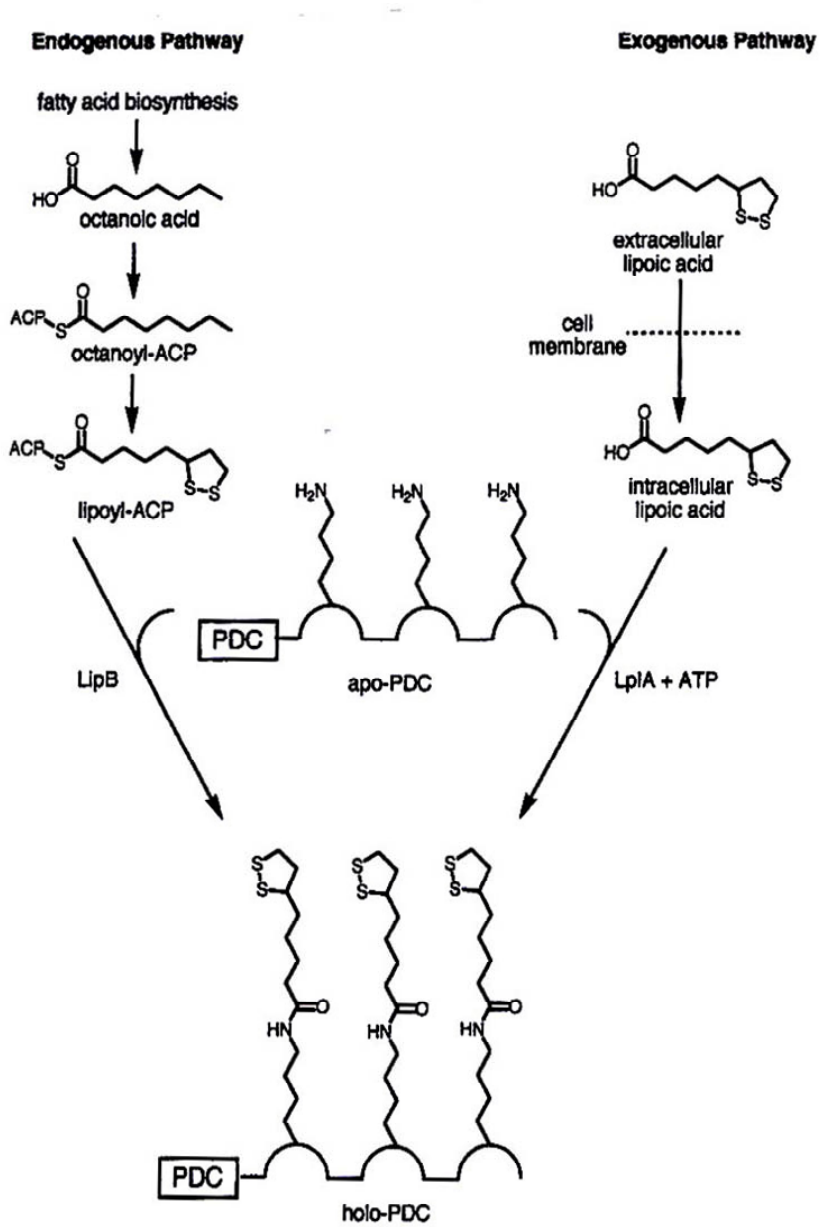

Figure 4-12 Complementary pathways of protein lipoylation in *E. coli*
(Taken from Miller *et al,* 2000)

Apo-PDC, unlipoylated protein; Holo-PDC, lipoylated protein.

In contrast to the situation in *E. coli,* the post-translational covalent attachment of lipoic acid to the apoprotein in mammalian cells seems to occur via one pathway in two successive steps involving two separate enzymes as follows:-

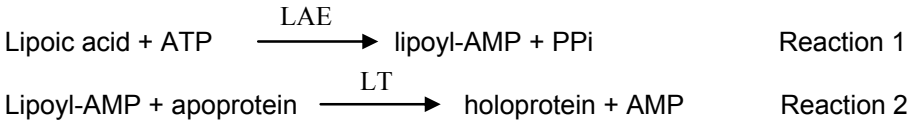

Firstly lipoic acid is activated to form lipoyl-AMP by lipoate-activating enzyme (LAE) (Fujiwara *et al.*, 2001). Secondly, the lipoyl moiety is transferred to a specific lysine residue in non-lipoylated apoproteins by the action of lipoyl-AMP:N^{ϵ}-lysine lipoyltransferase (LT) (Fujiwara *et al.*, 1994; Fujiwara *et al.*, 1996).

Both LAE and LT enzymes were initially purified, characterized and cloned from bovine liver (Fujiwara *et al.*, 1994; 2001). LAE purified from bovine liver has been shown to utilize GTP preferentially (in the presence of Mg^{2+}) at a 1000 fold higher rate than ATP for lipoic acid activation by forming lipoyl-GMP. Moreover, lipoyl-GMP is transferred more efficiently than lipoyl-AMP to non-lipoylated apoproteins containing the necessary "EXDKA" motif (Fujiwara *et al.*, 2001). In addition to lipoic acid, LAE has been found to utilize GTP to activate other fatty acid substrates (eg hexanoic, octanoic, decanoic, and dodecanoic acids) (Fujiwara *et al.*, 2001).

Furthermore, LAE promotes medium-chain acyl-CoA synthesis (eg hexanoic, octanoic, decanoic, and dodecanoic acids) with the highest specific activity with hexanoic acid (Fujiwara *et al.*, 2001). Nucleotide sequence analysis of cDNAs encoding LAE have confirmed the identity of the LAE sequence with bovine xenobiotic-metabolizing/medium-chain fatty acid:CoA ligase-III (XL-III) (Vessey *et al.*, 2000; Fujiwara *et al.*, 2001). This enzyme is one of three related enzymes that catalyze the activation of carboxylic acids to thioesters of CoA in an ATP-dependent reaction and are termed xenobiotic/medium-chain fatty acid:CoA ligase (XM-ligases). Therefore LAE exhibits broad substrate specificity in both acyl-CoA synthesis (used as a substrate for fatty acid β-oxidation) and acyl-GMP formation and is now regarded as a member of the family of carboxylic acid:CoA ligases (Vessey *et al.*, 1999).

Two isoforms of lipoyltransferase termed lipoyltransferase I and lipoyltransferase II, have been purified and characterized by Fujiwara *et al.* Both isoforms are unable to use lipoic acid plus Mg^{2+} and ATP as substrates in place of lipoyl-AMP (Fujiwara *et al.*, 1994). However, purified bovine LT also effectively catalyses the transfer of acyl groups (hexanoyl-, octanoyl, and decanoyl-AMP (-GMP)) to the lipoyl domain of the H-protein of the bovine glycine cleavage system (Fujiwara *et al.*, 1994).

4.2.3 RESULTS

4.2.3.1 Overexpression and purification of *E. coli* LplA

E. coli lipoate-protein ligase gene (*lplA*) cloned into the TM202 plasmid was kindly gifted by Dr. Ben Luisi, University of Cambridge (Morris *et al.*, 1994). *E. coli* BL21 (DE3) cells transformed with plasmid TM202, were grown in LB medium containing 50μg/ml ampicillin and induced at an A_{600} of 0.6-0.7 with 1mM IPTG. Initially, expression was performed at different temperatures, 37, 30 and 22°C for 6h to check the optimal conditions to obtain soluble protein in good yield. Expression of this protein at 30 and 37°C was suitable for this purpose (Figure 4-13).

The solubility of the lipoyl ligase was checked at different temperatures and it was observed that the protein was completely soluble at both 37 and 30 °C; however, protein production also occurred at 22°C with a lower level of expression (Figure 4-14).

Anion exchange chromatography was used initially to purify bacterial LplA ligase from the crude bacterial extract as described in Materials and Methods, section 2.5.2.4. The semi-purified enzyme was further fractionated using GFC in a prepacked HiPrep 16/60 Sephacryl S-300 High Resolution column as described in Materials and Methods, section 2.5.2.5 (data not shown).

4.2.3.2 Incorporation of various fatty acids and related compounds into ILD-E2 *in vitro* using *E. coli* LplA ligase

ILD-E2 expressed at 37°C in the absence of exogenous lipoic acid was purified by thrombin cleavage purification to release the GST-tag (Materials and Methods, sections 2.5.2.2). Purified ILD-PDC was used as a substrate for the LplA enzyme to incorporate various lengths of fatty acids and related compounds *in vitro*. These compounds were

divided into three groups according to the efficiency of the LplA ligase to promote their incorporation.

Group I

Two fatty acids, octanoic acid (C8) and decanoic acid (C10) were incorporated into purified non-modified ILD-E2 using *E. coli* LplA 0.1mg/ml as described in Materials and Methods, section 2.5.9. In parallel, lipoic acid modification was performed using the same concentration of *E. coli* LplA as a positive control whereas apodomain ILD-E2 substrate was incubated alone as a negative control. In addition, to check the purity of the lipoyl ligase, the enzyme (0.1mg/ml) was incubated with the substrate (ILD-E2). Successful post-translational modification was judged by gel-shift on non-denaturating PAGE (Figure 4-15, panel A).

To determine the cross reactivity of these prosthetic groups with PD1 and PD2, Western blot analysis of the ILD was performed after modification with lipoic, octanoic and decanoic acids. In addition, non-modified and endogenously modified ILD was analysed on the same native gel (Figure 4-15, panels B and C). It was noted that the purified lipoyl ligase contained a small amount of endogenous substrate that could be incorporated efficiently into the apodomain substrate.

It is clear from the native gel that both fatty acid substrates were efficiently incorporated into ILD to an equivalent extent to lipoic acid. The holodomain exhibited an increased rate of migration as a result of the modification the positively charged lysine residue. There was a significant enhancement in the reaction between ILD modified with added substrates and mAbs PD1 and PD2 compared to the endogenously modified ILD in all cases. Moreover, PD1 and PD2 showed equivalent or slightly greater cross reactivity with octanoylated and decanoylated ILD than with lipoylated domain. More precise quantitative analysis would be required to confirm the extent of this increased cross reactivity.

Group II

ILD-PDC expressed in the absence of exogenous lipoic acid was modified with hexanoic acid (C6) using *E. coli* LplA (0.3mg/ml) (Materials and Methods, section 2.5.9). A positive control was performed with lipoic acid whereas a negative control involved incubation of the apodomain substrate alone. Due to the contamination of the lipoyl ligase with endogenous substrate, ILD was modified using the same

concentration of enzyme to serve as a valid control. Modification was analysed by means of a native PAGE gel (15%) (Figure 4-16, panel A). In parallel, Western blot analysis was performed to check the cross reactivity of PD1 and PD2 with modified ILDs (Figure 4-16, panels B and C). Native PAGE analysis indicates that there is complete incorporation of hexanoic acid into ILD. However, Western blotting with PD1 and PD2 showed that there was no enhancement of the cross reactivity compared to the endogenously modified domain.

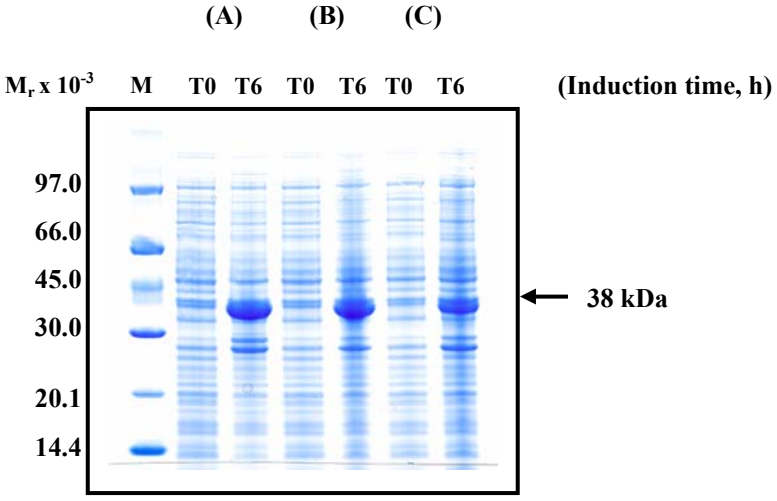

Figure 4-13 Overexpression of *E. coli* lipoyl ligase
Lipoyl ligase was expressed over 6h at 37°C, 30°C and 22°C in *E. coli* BL21 (DE3) cells. Samples were denatured in the presence of DTT (150mM) at 100°C for 5-10min prior to analysis on 12% SDS/polyacrylamide gels. Protein bands were stained with Coomassie Brilliant Blue. Molecular weight markers (M) are shown to the left of the gel. The arrow on the right of the gel denotes overexpressed recombinant enzyme.

Samples (A), (B) and (C), the expression of the bacterial lipoyl ligase before (T0) and after induction (T6) at 37°C, 30°C and 22°C respectively.

M: low molecular mass markers are shown to the left of the gel.

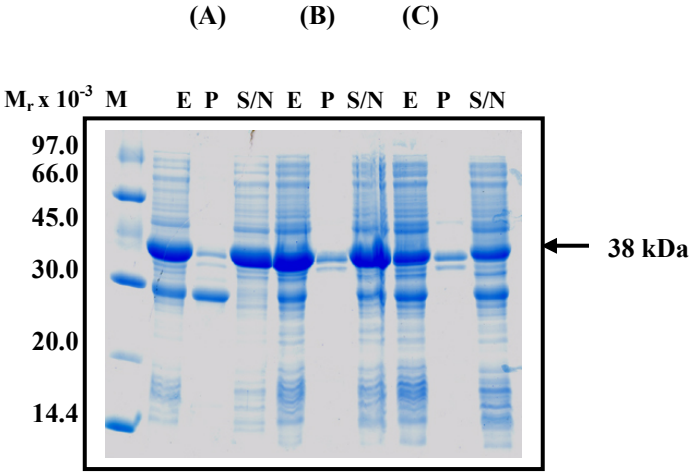

Figure 4-14 Solubility assessment of *E. coli* lipoyl ligase after overexpression at various temperatures

Following overexpression of the lipoyl ligase at 37, 30 and 22°C for 6h, the bacterial culture (50ml) was centrifuged and the pellet resuspended in 3ml PBS buffer pH 7.5. Cells were lysed by passage three times through a French Press at 750Psi. The cell extract (E) was separated into its soluble (S/N) and insoluble (P) fractions by centrifugation. Samples were prepared in Laemmli sample buffer and denatured for 5-10min at 100°C in the presence of DTT (150mM), prior to loading on a 12% SDS/polyacrylamide gel. Bands were stained with Coomassie Brilliant Blue.

Samples (A), (B) and (C) show the solubility of the protein at 37, 30 and 22°C respectively

E (cell extract), P (pellet) and S/N (supernatant)

The arrow indicates the lipoyl ligase.

M: low molecular mass markers are shown to the left of the gel.

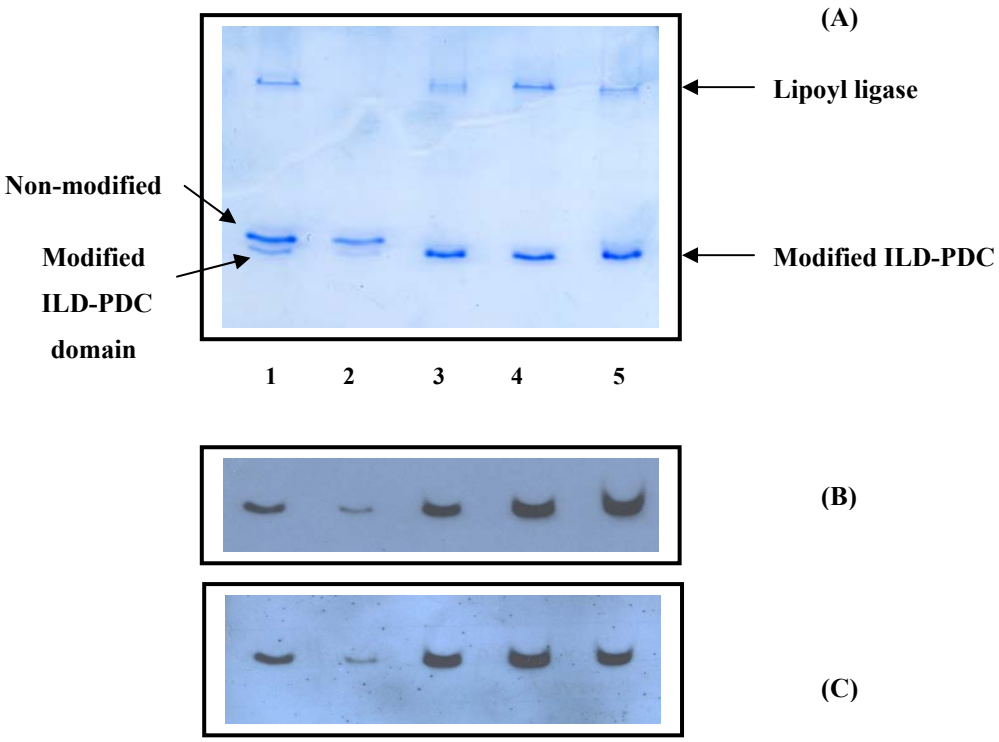

Figure 4-15 Post-translational modification of the human ILD-PDC *in vitro* by octanoic and decanoic acids
The apo-form of the human ILD-PDC (0.4mg/ml) was incubated with LplA (0.1mg/ml) under the conditions described in Materials and Methods. Samples were analysed by means of non-denaturating PAGE (15% gels). Samples (3µg) were stained with Coomassie Brilliant Blue on the first gel (A) while (0.5µg) samples on the second gel were blotted with PD1 and PD2 (B) and (C) respectively.

Lane 1, ILD-E2 with 0.1mg/ml LplA; **lane 2**, ILD-E2 as a negative control; **lane 3**, ILD-E2 plus 0.5mM lipoic acid as a positive control; **lane 4**, ILD-E2 plus 0.5mM octanoic acid; and **lane 5**, ILD-E2 with 0.5mM decanoic acid

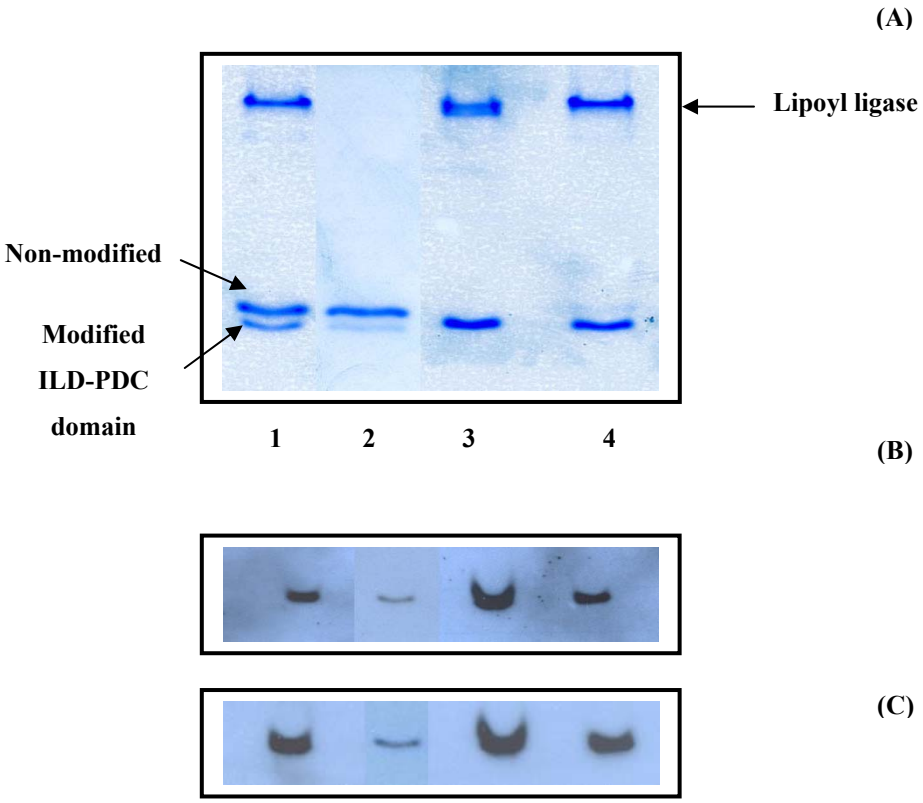

Figure 4-16 Post-translational modification of the human ILD-E2 *in vitro* by hexanoic acid
The apo-form of the human ILD-PDC (0.4mg/ml) was incubated with LplA (0.3mg/ml) under the conditions described in Materials and Methods. Samples were analysed by means of native PAGE (15% gels). Samples (3µg) were stained with Coomassie Brilliant Blue (A) while samples (0.5µg) were blotted with PD1 and PD2 (B) and (C) respectively.

Lane 1, ILD-E2 with 0.3mg/ml LplA as a control; **lane 2**, ILD-E2 as a control; **lane 3**, ILD-E2 with 0.5mM lipoic acid; **lane 4**, ILD-E2 with 0.5mM hexanoic acid.

Group III

Different lengths of fatty acids, acetic acid (C2), malonic acid (C3), butyric acid (C4), dodecanoic acid (C12) and tetradecanoic acid (C14) as well as the branched-chain fatty acid, valproic acid (C8) were incorporated into non-modified ILD-E2 using *E. coli* LplA (0.7mg/ml). A positive control (lipoylated ILD) using the same concentration of the enzyme and a negative control (non-modified ILD-E2) were prepared. In addition, an endogenous modification was conducted using the same concentration of the bacterial enzyme. The modification was checked by native PAGE gel (15%) (Figure 4-17 and Figure 4-18, panels A). In parallel, a native gel of modified substrates as well as controls was blotted with PD1 and PD2 (Figure 4-17 and Figure 4-18, panels B and C).

It is clear from the Coomassie Blue staining in Figure 4-17 that, apart from dodecanoic acid, all these fatty acids are unsuitable substrates for the lipoyl ligase even at high concentrations (0.7mg/ml). In addition, there was also minimal modification with valproic acid (Figure 4-18). Western blot analysis showed that there was an enhancement of the cross reactivity of dodecanoylated ILD with mAbs compared to the endogenously modified sample. In addition, even though the valproic acid is a poor substrate for the bacterial ligase, there is a clear enhancement of the valproated ILD signal with PD1 and PD2.

Group IV

ILD-E2 was modified with trans-2-nonenoic acid (C9) using three concentrations of bacterial ligase LplA (0.1, 0.3 and 0.7mg/ml) as described in Materials and Methods, section 2.5.9. As before, lipoic acid modification of ILD-E2 was carried out as a positive control whereas incubation of the apodomain alone was used as a negative control. To obtain a precise evaluation, endogenous modifications were employed using three concentrations of the bacterial enzyme owing to the presence of endogenous substrate.

Again successful post-translational modification was judged by gel-shift on non-denaturating PAGE. The modification was analysed by means of a native PAGE gel (15%) (Figure 4-19, panel A). In parallel, the cross reactivity of mAbs with modified domain was checked by Western blot analysis of the native gel (Figure 4-19, panels B and C).

It is clear from Coomassie Blue staining that this compound was readily incorporated into ILD; ILD was largely modified with tran-2-nonenoic acid using 0.1mg/ml and fully modified in the presence 0.3mg/ml lipoyl ligase. Western blot analysis shows that there is significant enhancement of mAb cross reactivity as a result of trans-2-nonenoic acid incorporation.

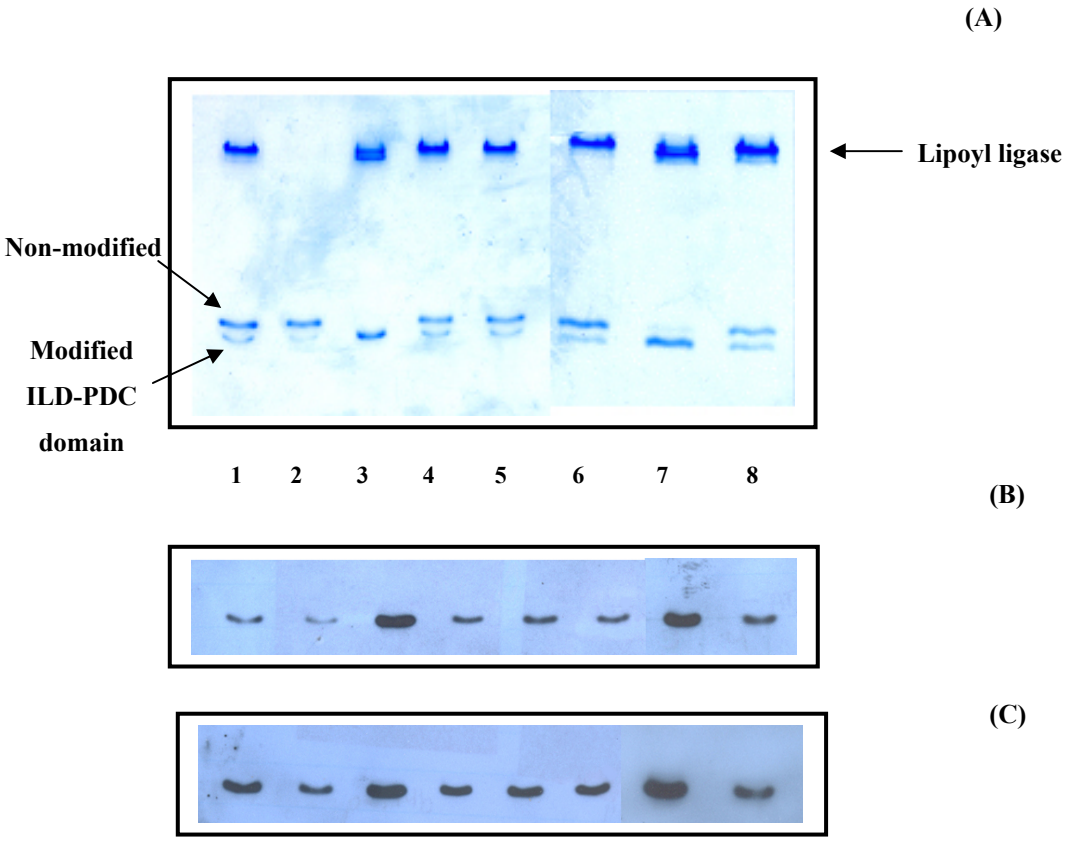

Figure 4-17 Post-translational modification of the human ILD-E2 *in vitro* by fatty acids of varying chain length

The apo-form of the human ILD-PDC (0.4mg/ml) was incubated with LplA (0.7mg/ml) under the condition described in Materials and Methods. Samples were analysed by means of native PAGE (15% gels). Samples (3µg) were stained with Coomassie Brilliant blue (A) or blotted (0.5µg) with PD1 and PD2 (B) and (C) respectively.

Lane 1, ILD-PDC with 0.7mg/ml LplA as a control; **lane 2**, ILD-PDC as a control; **lane 3**, ILD-PDC with 0.5mM lipoic acid; **lane 4**, ILD-PDC with 0.5mM acetic acid (C2); **lane 5**, ILD-PDC with 0.5mM malonic acid (C3); **lane 6**, ILD-PDC with 0.5mM butyric acid (C4); **lane 7**, ILD-PDC with 0.5mM dodecanoic acid (C12); and **lane 8**, ILD-PDC with 0.5mM tetradecanoic acid (C14).

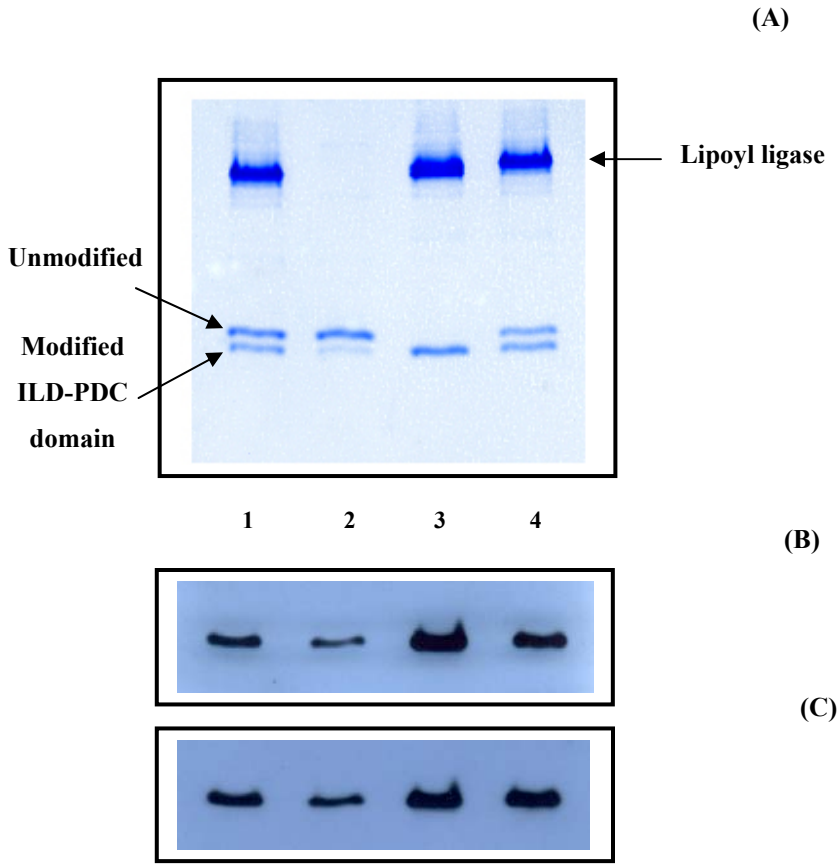

Figure 4-18 Post-translational modification of the human ILD-E2 *in vitro* with valproate as a substrate

The apo-form of the human ILD-PDC (0.4mg/ml) was incubated with LplA (0.7mg/ml) as described in Materials and Methods. Samples were analysed by means of native PAGE (15% gels). Samples (4µg) were stained with Coomassie Brilliant blue (A) or blotted (0.5µg) with antibodies PD1 and PD2 (B) and (C) respectively.

Lane 1, ILD-PDC with 0.7mg/ml LplA as a control; **lane 2**, ILD-PDC as a control; **lane 3**, ILD-PDC with 0.5mM lipoic acid; and **line 4**, ILD-PDC with 0.5mM valproic acid.

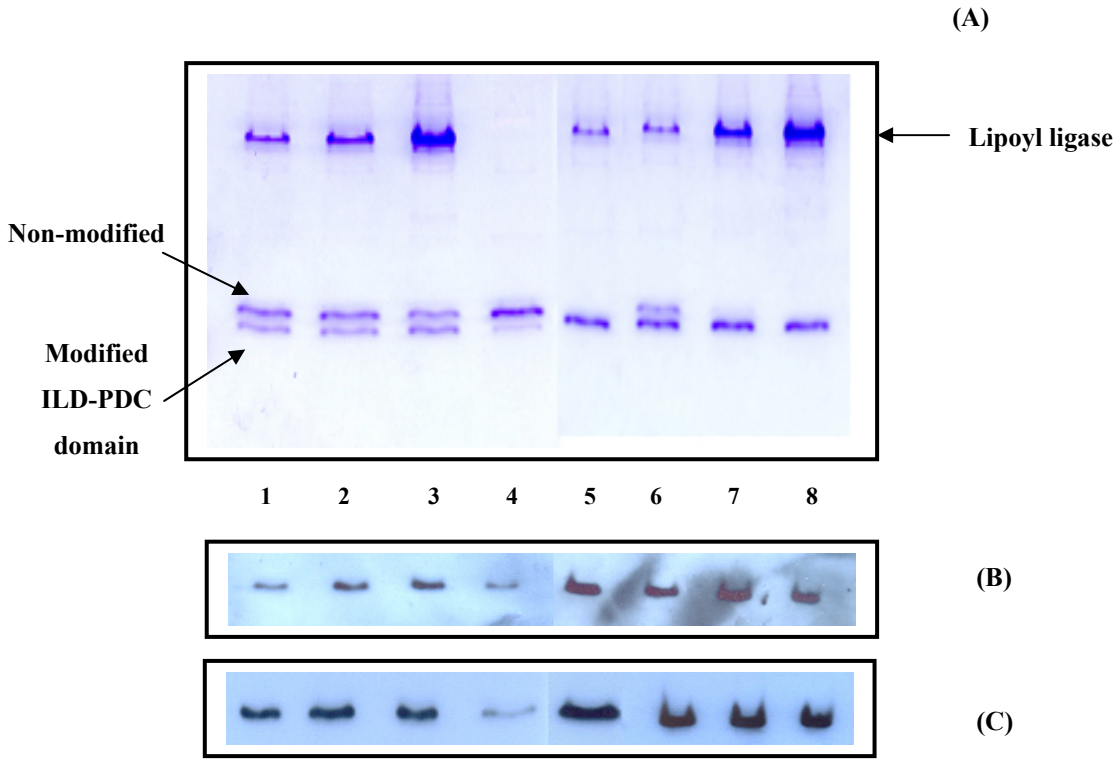

Figure 4-19 Post-translational modification of the human ILD-PDC *in vitro* with trans-2-nonenoic acid
The apo-form of the human ILD-PDC (0.4mg/ml) was incubated with LplA (0.1, 0.3 and 0.7mg/ml) under the conditions described in Materials and Methods. Samples were analysed by means of native PAGE (15% gels). Samples (3µg) were stained with Coomassie Brilliant Blue (A) whereas samples (0.5µg) were blotted with PD1 and PD2 (B) and (C) respectively.

Lane 1, ILD-E2 with 0.1mg/ml LplA as a control; **lane 2**, ILD-E2 with 0.3mg/ml as a control; **lane 3**, ILD-E2 with 0.7mg/ml as a control; **line 4**, ILD-E2 as a control; **lane 5**, ILD-E2 with 0.5mM lipoic acid and 0.1mg/ml ligase as a control; **lane 6**, ILD-E2 with 0.5mM nonenoic acid and 0.1mg/ml ligase; **lane 7**, ILD-E2 with 0.5mM nonenoic acid and 0.3mg/ml ligase; and **lane 8**, ILD-E2 with 0.5mM nonenoic acid and 0.7mg/ml ligase.

4.2.4 Discussion

Specific post-translational modification (lipoylation) is essential for the attainment of lipoyl domain function. Lipoylation of the key lysine residue is governed by precise protein-protein interactions between the folded lipoyl domain and the lipoylating enzyme(s) (Wallis *et al.*, 1996). However, lipoyl protein ligases do not require full length apo-proteins as substrates, being able to modify excised lipoyl domains but not short peptides (12-15 amino acids) based around the lipoylation site (Quinn *et al.*, 1993b). Thus a precise structural cue promotes lipoylation and not a specific sequence motif (Wallis & Perham, 1994). Accurate positioning of the target lysine residue in a tight type I β-turn in the structure is also essential for lipoylation (Wallis & Perham, 1994). Moreover, aspartic acid and alanine residues on either side of the key lysine in the highly-conserved DKA motif are not necessary for lipoyl domain recognition (Wallis & Perham, 1994).

Lipoyl protein ligase (LplA) has a broad specificity for lipoyl domains as it will lipoylate the E2-PDC and OGDC lipoyl domains of *E. coli*, as well as lipoyl domains from other species including yeast and human (Quinn *et al.*, 1993b; Wallis & Perham, 1994), which must have features in common for this to occur (Wallis & Perham, 1994). Therefore, it was possible in this study to use *E. coli* lipoyl protein ligase, LplA *in vitro* to incorporate lipoic acid into human ILD-E2.

The LplA ligase has been shown previously to be able to use several lipoate analogues (C8) as donors for the post-translational modification of E2 apoproteins *in vivo* as well as *in vitro* (Brookfield *et al.*, 1991; Morris *et al.*, 1994). However, the current work has shown for the first time that this incorporation is not exclusive to 8-carbon substrates and can be achieved with various fatty acid intermediates other than lipoic acid or octanoic acid (C8). In our case, LplA ligase was able to incorporate *in vitro* octanoate (C8), decanoate (C10) and, an unsaturated aliphatic compound, trans-2-nonenoic acid with high efficiency. In addition, hexanoate (C6) and dodecanoate (C12) were active as substrates but their incorporation was achieved at reduced efficiencies. Aliphatic fatty acids with less than 6 carbon atoms (acetic, malonic, and butyric) and more than 12 carbon atoms, tetradecanoic acid (C14) were ineffective as substrates for LplA ligase. Valproic acid, an eight carbon branched chain fatty acid could be incorporated into ILD-PDC to a very limited extent employing high concentrations of the bacterial lipoyl ligase.

The current work confirms studies by Fujiwara *et al* showing that the lipoate-activating enzyme (LAE) has an ability to activate different fatty acids via an ATP- or GTP-dependent pathway (Fujiwara *et al.*, 2001). In addition, it is important to note from our study and previous studies that the lipoyl domains can be a target for aberrant incorporation of a variety of carboxylic acids of appropriate chain length (Brookfield *et al.*, 1991; Reed *et al.*, 1994).

Although several laboratories have been involved in the identification of major autoantigens of PBC, the initial trigger leading to recognition of these self-proteins as immunogenic is not clear at present. It has been hypothesised that molecular mimicry between self-Ag (lipoylated E2-PDC) and xenobiotically modified E2-PDC may be a key event in promoting breakdown of tolerance and initiating AMA production (Bustamante *et al.*, 1998; Amano *et al.*, 2005). This idea was supported by the observation that AMA from patients with PBC were able to recognise xenobiotically modified E2-PDC peptides, mimicking lipoic acid (Long *et al.*, 2001; Amano *et al.*, 2005; Rieger *et al.*, 2006). Furthermore, rabbits and Guinea Pigs immunized with the lipoic acid mimic 6-bromohexanoate, conjugated to BSA, produced autoantibodies that react not only with the xenobiotic, but also with mitochondrial autoantigens recognised by autoimmune PBC sera (Leung *et al.*, 2003; 2007; Amano *et al.*, 2004). Our current work has also indicated that thiol groups of the dithiolane ring are not an integral part of the autoantigenic determinant for mAbs PD1 and PD2. However, non-lipoylated ILD is not a target for these mAbs even though the lysine side chain is available.

To further characterise the epitope of ILD-E2 and to find the optimal motif for mAb binding, the bacterial lipoyl ligase was employed in attempts to incorporate aliphatic saturated fatty acids of varying chain length (C2-C14), an aliphatic unsaturated compound, trans-2-nonenoic acid (C9), and the branched chain fatty acid, valproic acid (C8). Cross-reactivity of the modified human ILD-PDC with mAbs was studied via immunoblotting analysis. It was observed that there is an enhancement of mAb binding with increasing numbers of carbon atoms. Octanoylated, decanoylated and dodecanoylated ILDs produced a cross reactivity with mAbs equivalent to, if not greater than, the native holodomain. These data suggest a hydrophobic interaction between the aliphatic chain attached to the lysine of the ILD-PDC and the antigen binding site. As a result of the lack of appreciable incorporation with tetradecanoic acid, it was difficult to check the capacity of Ab recognition with a 14 carbon compound. A minimum aliphatic chain length of 8 carbons was required for this reactivity. Thus hexanoylated ILD (C6)

was not recognised by PD1 and PD2 although a report by Leung *et al.* involving the immunization of rabbits with 6-bromohexanoate demonstrated the development of rabbit antibodies that have the characteristics of human AMA with reactivity against the E2 subunits of PDC, OGDC and BCOADC and an ability to inhibit enzymatic activity (Leung *et al.*, 2003). In addition, this group found that aromatic structures derived from benzoic acid did not bind PBC sera, unless they were substituted predominantly in the para-position with halogens, trifluoromethyl, or alkyl groups (Amano *et al.*, 2005). Therefore, further studies are necessary to define the importance of halogens in Ab recognition. Our results are in accord with a study reported by Amano *et al.* who showed that the organic acid moiety attached to the lysine residue of the imunodominant E2-PDC peptide must preferably be of hydrophobic character and of a certain size (C8-C12) to be successfully recognised by the antigen binding sites of AMA (Amano *et al.*, 2005).

Another interesting finding is that the cross reactivity is not exclusive to unbranched aliphatic chains as there is also enhancement with the branched chain fatty acid derivative, valproate although it was not efficiently incorporated into ILD-E2. In fact, valproate, a simple 8-carbon branched chain fatty acid, is an effective anti-epileptic drug with occasional serious side effects including the accumulation of triacylglycerols within hepatocytes and reduction in serum protein concentrations as a result of liver damage (Bellringer *et al.*, 1988).

It was also realised that Ab recognition is not limited to saturated fatty acids chain as trans-2-nonenoic acid (C9) was incorporated into ILD and recognised by mAbs. Lipid peroxidation of cellular membranes is known to produce various aldehydic compounds that cause a range of pathological effects in humans. One of the possible mechanisms responsible for the increase of lipid peroxidation products is the increase of reactive oxygen species (ROS) such as superoxide and hydrogen peroxide which are produced by phagocytes during inflammation (Babior, 1984). Damaged bile ducts of PBC patients are surrounded by many inflammatory cells, including activated macrophages that can generate reactive species (Kawamura *et al.*, 2000) Another possible mechanism is that the accumulation of cytotoxic hydrophobic bile acids during cholestasis may contribute to the induction of lipid peroxidation by generation of reactive oxygen species; ROS production is attenuated by the presence of α-tocopherol, the major membrane associated, lipid antioxidant (Sokol *et al.*, 1995;2001).

Of particular interest to this study is HNE, a toxic lipid peroxidation product of n-6-polyunsaturated fatty acids (mainly arachidonate and linoleate). Since this aldehyde is electrophilic in nature, it readily reacts with nucleophiles, such as thiols and amines of proteins forming protein-HNE adducts. In fact, HNE-modified proteins has been detected immunohistochemically in the apical domain of the damaged bile ducts in 80% of PBC liver patients but not in controls in which there was a concomitant decrease in the level of glutathione, a major component of the antioxidant system (Paradis *et al.*, 1997; Tsuneyama *et al.*, 2002; Aboutwerat *et al.*, 2003).

As a consequence of the ability of HNE to form protein adducts, leading to selective alterations in cell signalling, protein and DNA damage, and cytotoxicity, mammalian cells are equipped with several enzymes to detoxify this aldehyde by different routes. One of these is the oxidation of HNE to form 4-hydroxy trans-2-nonenoic acid (HNA) by means of oxidative metabolism via aldehyde dehydrogenase (ALDH) (Haynes *et al.*, 2000; Choudhary *et al.*, 2003) Our current study has shown that its close relative, trans-2-nonenoic acid is a substrate for the lipoyl ligase and is readily attached to the lysine residue of the lipoyl domain. Therefore, HNA (the carboxylic acid form of HNE) is likely to be a suitable substrate for the lipoyl ligase.

The role of xenobiotics or biological compounds already present *in vivo* in the scenario of neoantigen triggering leading to PBC warrants further investigation. Naturally, these compounds may have the ability either to modify or to bind self-molecules, thus altering their recognition by the immune system. As the main detoxifying organ is the liver, this makes hepatocytes and BECs particularly prone to the action of these compounds. Mammalian (Fujiwara *et al.*, 2001) and bacterial lipoyl ligases exhibit a broad specificity for incorporating a variety of carboxylic acids related to lipoic acid, thereby potentially generating immunogenic neoantigens in genetically predisposed individuals. In this context, our novel postulate is that during detoxification of internally-produced lipid peroxidation compounds such as HNE, its acidic form, HNA can be incorporated into nascent non-lipoylated E2 components inside mitochondria by LAE forming neoantigens. This aberrant modification may lead to chronic PDC malfunction and metabolic damage as a result of energy depletion of the cell. This event may render these neoantigens accessible to the immune system thus breaking tolerance and initiating an autoimmune response against lipoylated E2 (Figure 4-20).

Apoptosis or necrosis may potentiate the autoimmune response even at a low level of aberrant modification of the nascent non-lipoylated E2 components. PBC is a cholestatic liver disease in which small (interlobular/septal) bile ducts are destroyed. Recently, it has been confirmed that there is link between apoptosis or necrosis and PBC. DNA fragmentation was noticed to be more frequently found in PBC than other liver diseases such as chronic viral hepatitis C (CVHC) and even more frequently than in the normal controls (Koga *et al.*, 1997). Moreover, Harada *et al.* suggested that apoptosis of the BECs in the liver of PBC might be triggered by the interaction of Fas ligand on the surrounding inflammatory cells and the Fas receptor on the BECs (Harada *et al.*, 1997b). Therefore, there is a possible concomitance between inflammation and apoptosis (Tinmouth *et al.*, 2002). In addition, hydrophobic bile acids accumulate intracellularly during cholestasis inducing the opening of the mitochondrial inner membrane permeability transition pore. This results in the collapse of the electrochemical gradient ($\Delta\psi$) across the inner membrane, uncoupling of oxidative phosphorylation and osmotic swelling of mitochondria. In addition, bile acids may interfere with normal mitochondrial electron transport, leading to inhibition of the activity of respiratory complexes I and III and consequently reducing ATP synthesis and leading to metabolic damage (Sokol *et al.*, 2001). Therefore, these mechanisms (necrosis or apoptosis) may play an important role in increasing aberrantly-modified E2-PDC availability to the immune system.

We have proposed an alternative model to the one hypothesised by Potter *et al* (Potter *et al* 2001). Our postulation suggests that the aberrant modification of the newly synthesised protein as a result of the broad specificity of the lipoyl ligase may trigger the disease. The excess of this aberrant modification in BECs causes a metabolic defect which in turn results in apoptosis or necrosis leading to BECs damage. This situation makes the abnormal modified protein (neoantigen) accessible to the immune system as a foreign compound that the immune system reacts to it accordingly. Consequently, the immune system recognises the self protein (self Ag) as a result of the epitope shifting from the neo- to the self-Ag. In comparison, Potter *et al* have postulated that the trigger of the disease may be a microbial infection in which Ab (IgM) on the surface of the naïve B-cell first recognises an unidentified antigen and then accumulation of the somatic mutations and molecular mimicry between the microbial and the self Ag result in an intermolecular epitope shift which has an effect on the E1/E3 binding domain. Further mutations result in the specificity being redirected to the ILD-E2 due to the intramolecular epitope shift (Potter *et al* 2001).

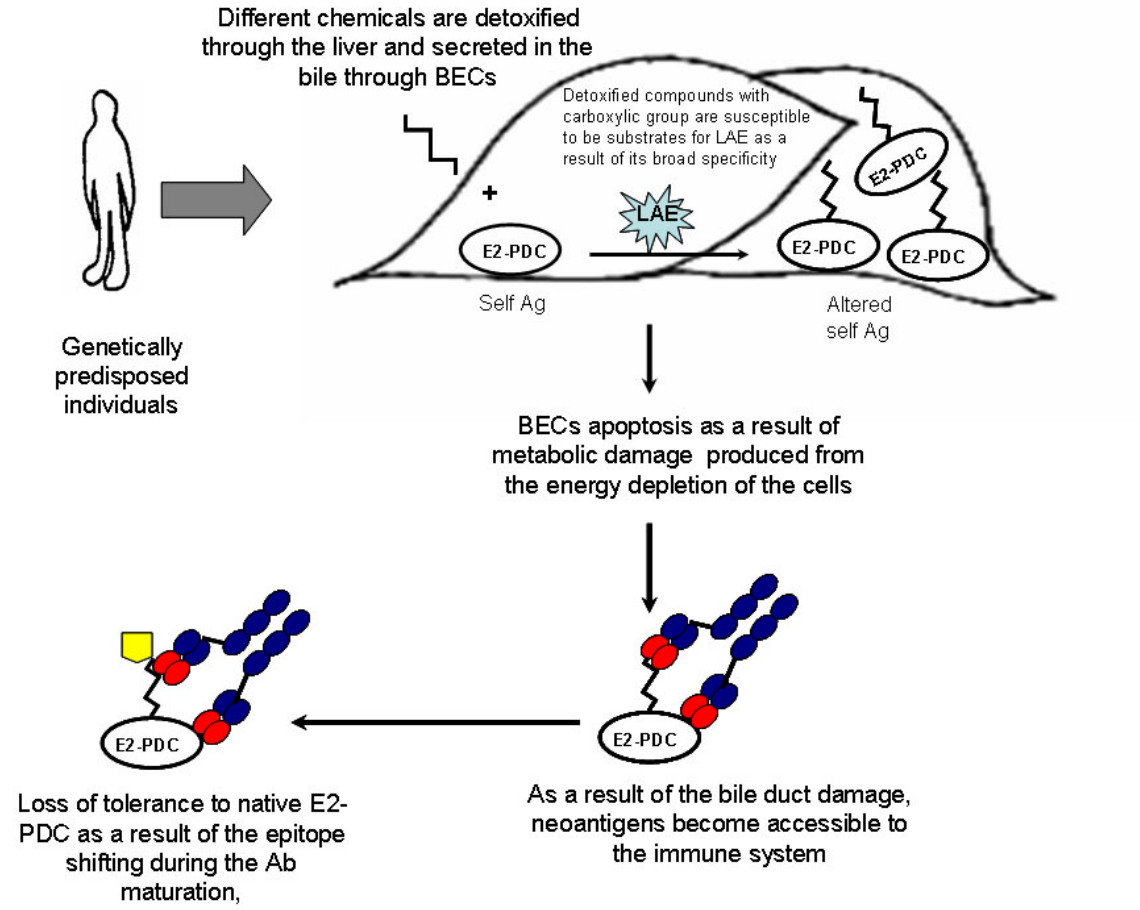

Figure 4-20 Hypothetical scheme reflecting the mechanism by which biological compounds may break tolerance and induce PBC

Immune system (Ab)

Alterd self Ag (neoantigen)

Lipoylated self Ag

Lipoate-activating enzyme (LAE)

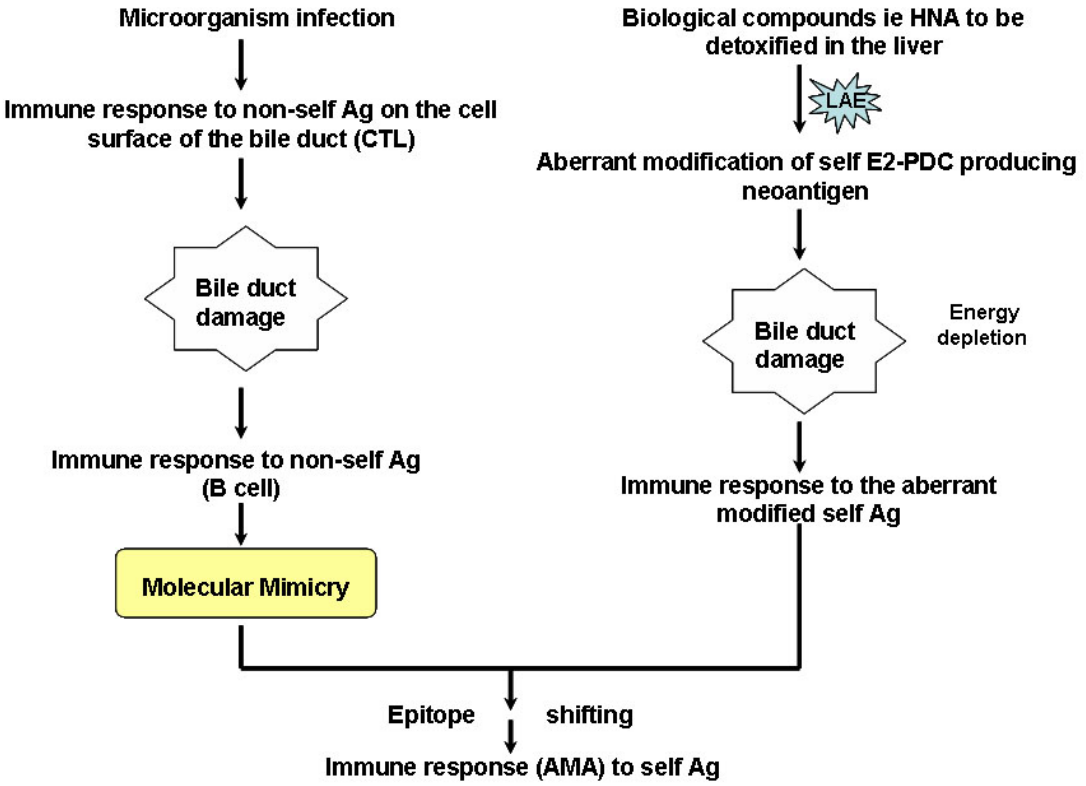

Figure 4-21 hypothetical scheme reflecting the mechanism by which microorganism infection or biological compounds may break the tolerance to native E2-PDC

Chapter 5

Molecular cloning and overexpression of E2, E3BP and E3 precursors as well as preliminary folding studies of E2 and E3BP precursors of human pyruvate dehydrogenase complex

5.1 Introduction

The individual components of the 2-oxoacid dehydrogenase complexes are all nuclear-encoded and hence are synthesized in the cytoplasmic compartment on soluble ribosomes as precursor forms possessing variable presequences, 24-86 amino acids in length. These are normally located at the N-terminus of the polypeptides (Glover & Lindsay, 1992). As the assembly of 2-oxoacid dehydrogenase complexes occurs in the matrix-inner mitochondrial membrane compartment, these cytoplasmically synthesized proteins must be delivered efficiently across both outer and inner membranes before reaching their final destination in the mitochondrial matrix (Maas & Bisswanger, 1990).

A series of immunological analyses have been conducted to study the biosynthesis, import and assembly of the mammalian 2-oxoacid dehydrogenase complexes and their constituent enzymes (Hunter & Lindsay, 1986; De Marcucci *et al.*, 1988; Lindsay, 1989; Clarkson & Lindsay, 1991). The transit time for movement of nascent precursor forms into the organelle is short, approximately 5-10 min, leading to difficulties in studying the properties of these transient precursors. In addition, it is known that translocation is an energy-linked process requiring both ATP (Chen & Douglas, 1987) and an intact electrochemical gradient, $\Delta\mu_H^+$, across the inner membrane (Gasser *et al.*, 1982). Thus by dissipating the electrochemical gradient necessary for translocation, it has been possible to study the properties of the precursors during their accumulation in the cytoplasmic compartment in the presence of uncouplers of mitochondrial energy production, e.g. 2,4-dinitrophenol or carbonyl cyanide *p*-trifluoromethoxyphenylhydrazone.

It was found using immunoprecipitation and fluorography analysis in different cultured cell lines such as pig kidney (PK-15), bovine kidney (NBL-1) and Buffalo rat liver (BRL) cells incubated with [^{35}S] methionine that all the constituent polypeptides of PDC, OGDC and BCOADC have signal sequences in the M_r range 1500-3000 except the precursors of E2 and E3BP that contain a long additional segment of 7000-9000. This observation has been verified subsequently by the availability of the human genome sequence that enables sequence comparison of the components of 2-OADCs and shows that the E2 and E3BP presequences are longer than those of the other components. Moreover, immunological data have revealed that the E2 precursor of OGDC was not recognized by anti-native E2-OGDC sera whereas it could be immunoprecipitated by antibodies raised against the denatured E2 subunit. These data

support the requirement for polypeptides to be maintained in an unfolded or loosely folded, "translocation-competent" state prior to import. Moreover, no interaction with other components of the complex was detected during this stage of protein targeting, again suggesting that there is a significant difference in the conformational states of pre-E2 and mature E2 molecules which are required to assemble into multi-molecular aggregates in the native complexes. Thus large extended presequences on E2 precursors may be necessary not only for targeting but also in preventing premature association of precursors as a secondary function before entry into the mitochondrial organelle and functional maturation into native complexes (Hunter & Lindsay, 1986; De Marcucci *et al.*, 1988; Lindsay, 1989; Clarkson & Lindsay, 1991). The M_r values and the numbers of amino acids present in the components of the 2-oxoacid dehydrogenase complexes and their precursors are listed in Table 5-1.

	Apparent M_r		No of amino acids		No of amino acids in presequences
	Mature form	Precursor form	Mature form	Precursor form	
Pyruvate dehydrogenase complex (PDC)					
E1α subunit	40229	43296	361	390	29
E1β subunit	36518	39249	335	359	24
E2	59621	68997	561	647	86*
E3BP	48040	54085	448	501	53*
2-oxoglutarate dehydrogenase complex (OGDC)					
E1	113003	115935	997	1023	26
E2	41390	48755	386	453	67*
Branched-chain 2-oxoacid dehydrogenase complex (BCOADC)					
E1α	45513	50471	400	445	45
E1β	37865	43123	342	392	50
E2	46630	53517	421	482	61*
E3 (PDC, OGDC and BCOADC)	50148	54150	474	509	35

Table 5-1 Comparison of M_r values of mature and precursor forms of constituent subunits of human PDC, OGDC and BCOADC
Precursor and mature **E1α-PDC,** (Dahl *et al.*, 1987; Koike *et al.*, 1990; Cullingford *et al.*, 1994); mature and precursor **E1β-PDC,** (Huh *et al.*, 1990); mature **E2-PDC,** (Coppel *et al.*, 1988; Thekkumkara *et al.*, 1988) whereas its precursor was identified by our group; mature and precursor **E3BP**, (Harris *et al.*, 1997); mature and precursor **E1-OGDC**, (Rice *et al.*, 1992); mature and precursor **E2-OGDC**, (Koike *et al.*, 2000); mature and precursor **E1α-BCOADC**, (Fisher *et al.*, 1991); mature and precursor **E1β-BCOADC**, (Nobukuni *et al.*, 1990); mature and precursor **E2-BCOADC**, (Lau *et al.*, 1992); and mature and precursor of **E3-PDC, OGDC** and **BCOADC**, (Pons *et al.*, 1988).

***** idicates a presequence of unusual lenght.

5.2 Aims of this study

(a) To describe the strategy used to clone various constructs of human PDC as follows:

- Full length E2 precursor (pre-E2) and its N-terminal truncate containing outer and inner lipoyl domains and adjacent subunit binding domain.
- N-terminal truncate of mature E2.
- Full length E3BP precursor (pre-E3BP).
- E2 presequence linked to mature E3 (pE2-E3) and E3 presequence linked to mature E2 (pE3-E2).
- Full length E3 precursor (pre-E3).

(b) To overexpress these recombinant precursors proteins in *E. coli.*

(c) To study the effect of the extended presequences on the expression, solubility and folding of these enzymes.

Plasmids

Plasmids used for the cloning of pre-E2 and N-terminal truncates of pre-E2 and its mature form, pre-E3BP and pre-E3 of human PDC were obtained from a variety of sources. pET-28b containing the full length E2 precursor sequence (previously cloned by our group) was used as a template to subclone full length pre-E2 and its N-terminal truncate. pET-14b containing the mature E2 (previously cloned in the laboratory and kindly provided by Dr. Audrey Brown) was used as a template to produce the N-terminal truncate of mature E2. Plasmids as IMAGE clones containing the cDNA for the full length E3 precursor (obtained from MRC Geneservice, Babraham, Cambridge) were used as templates to subclone this precursor. Plasmids as IMAGE clones containing the cDNA for full length E3BP precursor (obtained from MRC Geneservice, Babraham, Cambridge) were used to clone pre-EBP. All inserts (PCR products) were cloned into pET-14b as the expression plasmid.

5.3 RESULTS

5.3.1 General strategy for cloning E2, E3BP, E3 precursors, the N-terminal truncate of mature E2 and its precursor, pE2-E3 and pE3-E2

5.3.1.1 PCR amplification

The cDNA sequences of E3BP (Harris *et al.*, 1997) and E3 (Pons *et al.*, 1988) precursors have previously been published allowing the design of specific primers for PCR amplification.

Two groups have apparently cloned the entire sequence of the mammalian E2-PDC gene (Coppel *et al.*, 1988; Thekkumkara *et al.*, 1988). While the sequences for the mature enzyme are identical in both studies, the presequences show an obvious disparity. Only one of the sequences (Coppel *et al.*, 1988) contains an N-terminal methionine residue required for initiation. However, when this presequence was analysed by BLAST search, its N-terminal region was found to be almost identical to that of part of the aryl sulphatase A gene, suggesting that it is incorrect. The other sequence (Thekkumkara *et al.*, 1988) is apparently incomplete as it does not contain a methionine initiation codon. When the incomplete presequence together with part of mature E2 was analysed by BLAST search against the human genome sequence, several homologous Expressed Sequence Tags (ESTs) were found. The EST with the longest sequence upstream from the Thekkumkara sequence (IMAGE clone 2394617) was then matched against the human genome and mapped to several independent clones encoding a similar region on chromosome 11. Figure 5-1 shows the nucleotide sequence of the EST matched against one of these independent clones of chromosome 11 and its predicted primary sequence with the initiator methionine and start of the mature E2 enzyme shown in Figure 5-2.

```
>gi|9757502|dbj|AP000907.4|AP000907 Homo sapiens chromosome 11 clone RP11-708L7 map
11q23, WORKING DRAFT
          SEQUENCE, 24 unordered pieces
        Length = 177564

 Score =  644 bits (325), Expect = 0.0
 Identities = 332/333 (99%), Gaps = 1/333 (0%)
 Strand = Plus / Plus

Query: 53    accttctgatgcgggggaagactgtaatagcggcggccgggcgaccccaaaagctgcagc 112
              ||||||||||||||||||||||||||||||||||||||||||||||||||||||||||||
Sbjct: 73480 accttctgatgcgggggaagactgtaatagcggcggccgggcgaccccaaaagctgcagc 73539

Query: 113   agtaagcggttccgcggcgtggccccagaactgggggtccagccgcacagtgcccggacc 172
              ||||||||||||||||||||||||||||||||||||||||||||||||||||||||||||
Sbjct: 73540 agtaagcggttccgcggcgtggccccagaactgggggtccagccgcacagtgcccggacc 73599

Query: 173   ccgccataccctgtagtcacgctgttgcgacgagcgggagccgggccagatcgcgaggtc 232
              ||||||||||||||||||||||||||||||||||||||||||||||||||||||||||||
Sbjct: 73600 ccgccataccctgtagtcacgctgttgcgacgagcgggagccgggccagatcgcgaggtc 73659

Query: 233   actcgtggagttccgggtacctcctgcaaggccgtccaccggagcctcgagtcccgccca 292
              |||||||||||||||||||||||||||||||||||| ||||||||||||||||||||
Sbjct: 73660 actcgtggagttccgggtacctcctgcaaggccgtccacc-gagcctcgagtcccgccca 73718

Query: 293   tggggctacattctgagcccgtcgcgcacagacgcgccacatagtgccaccaacccccca 352
              ||||||||||||||||||||||||||||||||||||||||||||||||||||||||||||
Sbjct: 73719 tggggctacattctgagcccgtcgcgcacagacgcgccacatagtgccaccaacccccca 73778

Query: 353   caccccaaaaccaacgccgtctccggagtgacc 385
              |||||||||||||||||||||||||||||||
Sbjct: 73779 caccccaaaaccaacgccgtctccggagtgacc 73811
```

Figure 5-1 Nucleotide sequence of EST IMAGE clone 2394617 obtained from BLAST search matched against chromosome 11 clone RP11-708L7

```
73760 atgtggcgcgtctgtgcgcgacgggctcagaatgtagccccatgg
      M  W  R  V  C  A  R  R  A  Q  N  V  A  P  W
73715 gcgggactcgaggctcggtggacggccttgcaggaggtacccgga
      A  G  L  E  A  R  W  T  A  L  Q  E  V  P  G
73670 actccacgagtgacctcgcgatctggcccggctcccgctcgtcgc
      T  P  R  V  T  S  R  S  G  P  A  P  A  R  R
73625 aacagcgtgactacagggtatggcggggtccgggcactgtgcggc
      N  S  V  T  T  G  Y  G  G  V  R  A  L  C  G
73580 tggacccccagttctggggccacgccgcggaaccgcttactgctg
      W  T  P  S  S  G  A  T  P  R  N  R  L  L  L
73535 cagcttttggggtcgcccggccgccgctattacagtcttcccccg
      Q  L  L  G  S  P  G  R  R  Y  Y  S  L  P  P
73490 catcagaaggt
      H  Q  K  V
```

Figure 5-2 Amino acid sequence of the deduced E2-PDC presequence btained from BLAST search

The deduced 86-a.a. presequence is denoted by the broken underline and the sequence of the mature E2 is denoted by the solid underline.

The full length precursors of E2 and E3BP were amplified using primers designed to the 5' region upstream of the respective start codons and to the 3' regions downstream of the STOP codons. The N-terminal pre-E2 truncate was amplified using the same forward primer and a reverse primer to the 3' region downstream of the E2 lipoyl domains and adjacent subunit binding domain. In addition, the same reverse primer was employed to clone the mature form of the N-terminal E2 truncate; however, the forward primer was designed to the 5' region upstream of the start codon of mature E2. pE2-E3 was cloned by amplifying the E2 presequence and mature E3 separately prior to subsequent ligation whereas pE3-E2 was cloned by linking amplified E3 presequence to mature E2. Primers for the E2 and E3 presequences were designed to the 5' region upstream of the start codon of each precursor and to the relevant 3' region of the presequence. Primers for mature E3 and E2 were designed to the 5' regions upstream of the start codon of each mature protein and to the 3' region downstream of the STOP codon of the full length cDNA. All primers were generated with specific restriction sites to facilitate cloning into the chosen expression vector, pET-14b (see Materials and Methods, section 2.1.3.1 for primer sequences with incorporated restriction sites).

PCR reactions were generally performed using either Expand High Fidelity DNA Polymerase or $Vent_R^{®}$ DNA Polymerase as these enzymes have lower error rates (see Materials and Methods, section 2.3.2 for more details). PCR conditions were optimised as described in Materials and Methods, section 2.3.2.1. Samples of each PCR reaction (typically 5µl) were electrophoresed on a 1% (w/v) TAE agarose gel. Figure 5-3; Figure 5-5; Figure 5-8, panel A; and Figure 5-9, panel A illustrate the PCR products obtained. The presence of minor PCR products in some reactions may be due to the occurrence of non-specific priming events in early cycles. In each case, the major product was excised from an agarose gel and the DNA was then purified using QIAquick gel extraction kit (Qiagen) as described in Materials and Methods, section 2.3.6. An aliquot of the purified DNA was electrophoresed on a 1% (w/v) agarose gel to check the quality and quantity of the purified DNA (data not shown).

5.3.1.2 Ligation, transformation and identification of clones

The expression plasmid pET-14b (Novagen) was chosen as a suitable vector in which to clone the precursors for a number of reasons. The pET-14b vectors provide a convenient route for DNA cloning as they contain unique restriction sites in their multiple cloning region. In addition, pET-14b contains an N-terminal 6 Histidine-tag

which provides for routine purification of the protein of interest using metal chelate affinity column. The pET-14b vector also confers ampicillin resistance on the cloned product. Moreover, this vector has been employed successfully in our laboratory to obtain high level expression of fully-active mature human E2, E3BP and E3.

NdeI and BamHI sites were chosen for the directional cloning of pre-E2, N-terminal pre-E2 truncate and its mature form whereas pre-E3 and pre-E3BP, pE2-E3 and pE3-E2 were cloned non-directionally into BamHI restriction sites. GeneJocky software was used to check that these restriction sites were not present in any of the genes.

The TOPO TA cloning vector system was used as described in Materials and Methods, section 2.3.3 to facilitate cloning of PCR products of pre-E2, N-terminal pre-E2 truncate and its mature form, pre-E3 and pre-E3BP. However, pE2-E3 and pE3-E2 were cloned directly into pET-14b.

TOPO cloning or PCR products and pET-14b vector were subjected to restriction digestion by using specific restriction enzymes according to the clone of interest to generate cohesive ends for ligation. For the single restriction digests, the vector was treated with calf intestinal alkaline phosphatase to remove phosphate groups exposed by digestion and so prevent self-ligation. The dephosphorylation step helps to reduce the effort required to screen ampicillin-resistant colonies obtained after transformation. After digestion, PCR products either from the TOPO cloning vector or from direct amplification and pET-14b vector were purified using the QIAquick gel extraction kit (Qiagen) and DNA was eluted in 30µl elution buffer.

To check the quantity of DNA obtained, samples (5µl) of each were electrophoresed on a 1% (w/v) TAE agarose gel. For ligations to be successful a high insert:vector ratio was usually required. A series of ligation reactions were set up with varying ratios of insert:vector plus a control reaction without insert as described in Materials and Methods, section 2.3.8. The ligation mixes were left overnight at room temperature and transformed into *E. coli* DH5α cells the following day. The transformations were plated on LB-agar plates supplemented with 50µg/ml ampicillin and incubated overnight at 37°C.

Colonies were selected and cultured overnight in LB media supplemented with ampicillin (50µg/ml) at 37°C. Purification of plasmids was performed using the Wizard

SV Minipreps kit (Promega) and DNA was eluted in 100µl nuclease-free water as instructed by the manufacturer. To identify the clones containing the insert of interest, samples, typically 5µl, were electrophoresed on a 1% TAE agarose gel along with wild-type pET-14b (data not shown).

Putative positive clones were subjected to digestion using the appropriate restriction enzymes to assess if an insert of the correct size was present. Figure 5-4; Figure 5-6, panel A; Figure 5-7, lanes 2 and 5; Figure 5-8, panel B and Figure 5-9, panel B show the results of these digestions. *Nde*I and *Bam*HI were used to check the insert size in clones containing full length pre-E2, N-terminal pre-E2 truncate and its mature form. Figure 5-4, panel A shows that out of four colonies examined for putative full length pre-E2, three contained the insert (lanes 1, 2 and 4). Three and six positive clones were obtained successfully for the N-terminal truncates of pre-E2 and mature E2 respectively (Figure 5-4, panels B and C). *Bam*HI was used also to check the insert size of pE2-E3, pE3-E2, pre-E3 and pre-E3BP. For pE2-E3, one of two clones contained the insert (Figure 5-6, panel A, lane 1) while two clones for pE3-E2 were examined successfully (Figure 5-7, lanes 2 and 5). In the case of pre-E3, six clones were digested successfully with *Bam*HI (Figure 5-8, panel B). For the pre-E3BP, three of four clones were confirmed to have the insert using diagnostic digestion with *Bam*HI (Figure 5-9, panel B).

The orientation of the insert in non-directional clones was then checked by a further digestion with a suitable restriction enzyme, selected for its ability to cleave both the vector and also in the insert itself. *Eco*RI was used to check the orientation of the insert in the putative pE2-E3 and pE3-E2 clones. Figure 5-6, panel B and Figure 5-7, lanes 3 and 6 show the results of these digestions. In the case of pE2-E3, one colony was digested successfully (Figure 5-6, panel B, lane 1) while both clones containing pE3-E2 were found to have the insert in the correct orientation (Figure 5-7, lanes 3 and 6). The orientation of the pre-E3 sequence was examined using *Hind*III. Figure 5-8, panel C, lanes 1 and 4 show that two of the six possible pre-E3 clones were oriented correctly. In the case of pre-E3BP, *Nde*I was used to check the orientation of the insert. Figure 5-9, panel C shows that of the three clones examined, two contained the insert in the correct orientation (lanes 1 and 2). At this stage, clones containing insert in the correct orientation were transformed into competent *E. coli* BL21 (DE3) pLysS cells (Strategene) for overexpression of the proteins of interest.

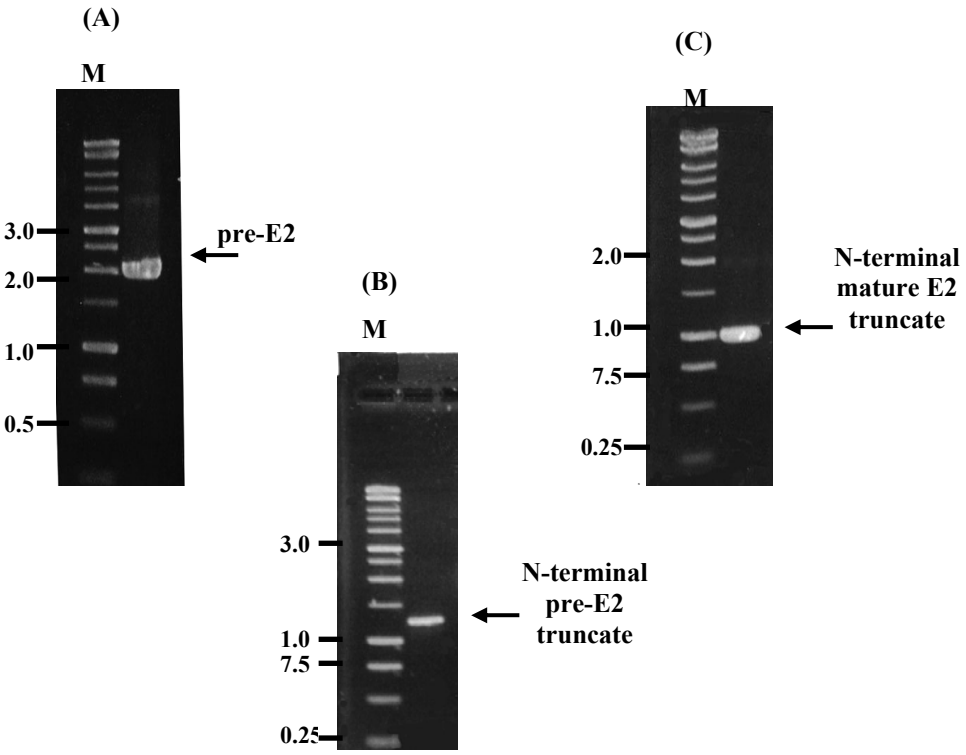

Figure 5-3 PCR products of full length pre-E2, N-terminal pre-E2 truncate and its mature form
PCR mixtures (5µl) were resolved on 1% agarose gels and the DNA viewed after staining with ethidium bromide (0.5µg/ml) under a UV light.

Panel A: PCR of full length pre-E2; a positive result was seen by the presence of a single band of 2kb (expected size 1944 bps).

Panel B: PCR of the N-terminal pre-E2 truncate; a positive result was seen by the presence of a single band of 1.2 kb (expected size 1221 bps).

Panel C: PCR of the N-terminal E2 truncate; a positive result was seen by the presence of a single band of 1kb (expected size 963 bps).

M: 1 kb DNA ladder markers.

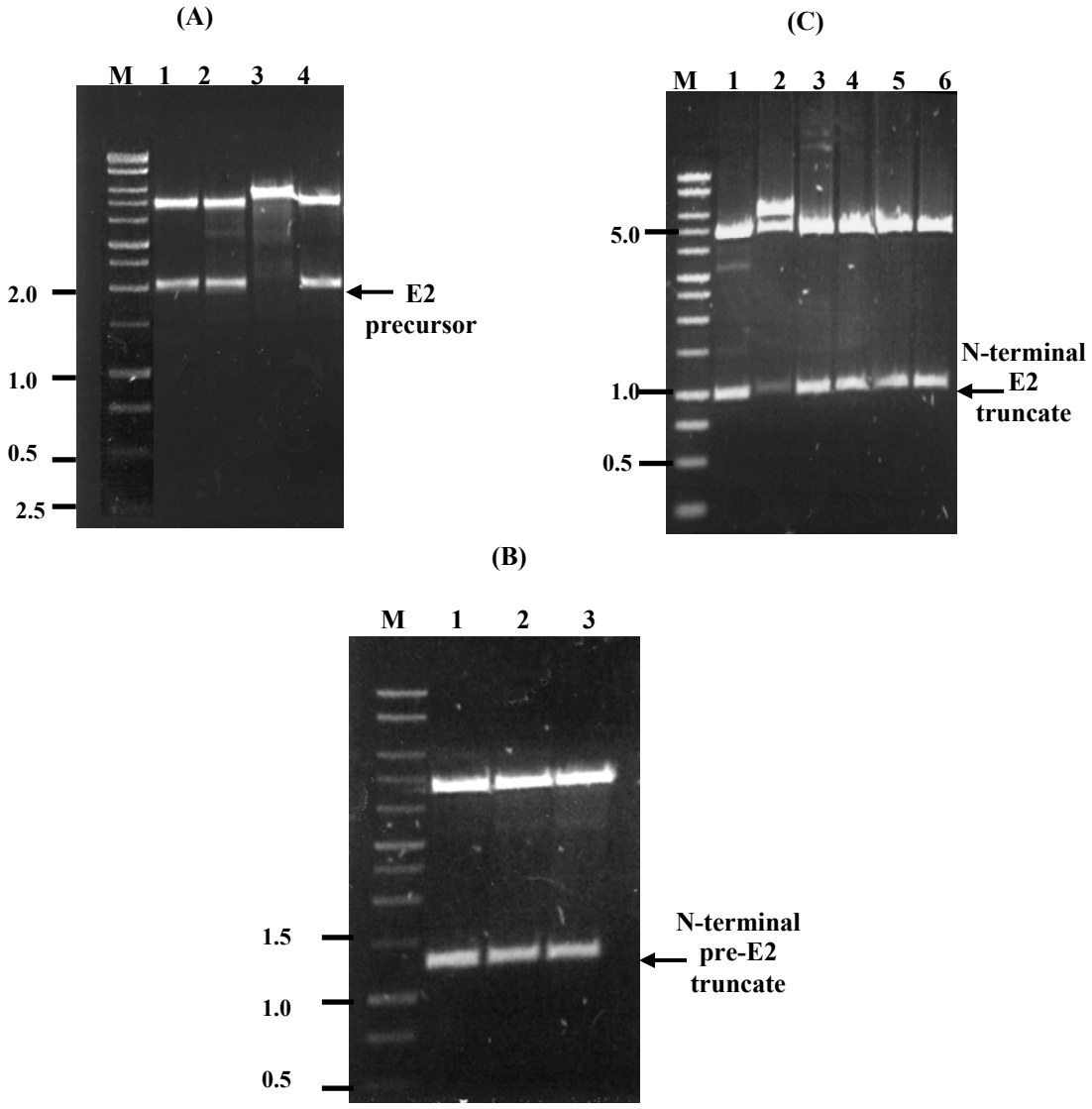

Figure 5-4 Restriction digestion of plasmids of pre-E2, N-terminal pre-E2 truncate and its mature form

Putative positive clones were subjected to restriction digestion by *Nde*I and *Bam*HI. A sample of the digestion of each clone was resolved on 1% (w/v) agarose gels and then stained with ethidium bromide and viewed under a UV transilluminator.

Panel A: three positive directional clones with an expected insert of 2kb encoding the full length pre-E2 (lanes 1, 2 and 4) were confirmed by NdeI and BamHI digestion.

Panel B: three positive directional clones with an expected insert of 1.2kb encoding the N-terminal pre-E2 truncate (lanes 1, 2 and 3) were confirmed by NdeI and BamHI digestion.

Panel C: Six positive colonies with an expected insert of 1kb encoding the N-terminal mature E2 truncate (lanes 1-6) were confirmed by NdeI and BamHI digestion.

M: 1 kb DNA ladder markers.

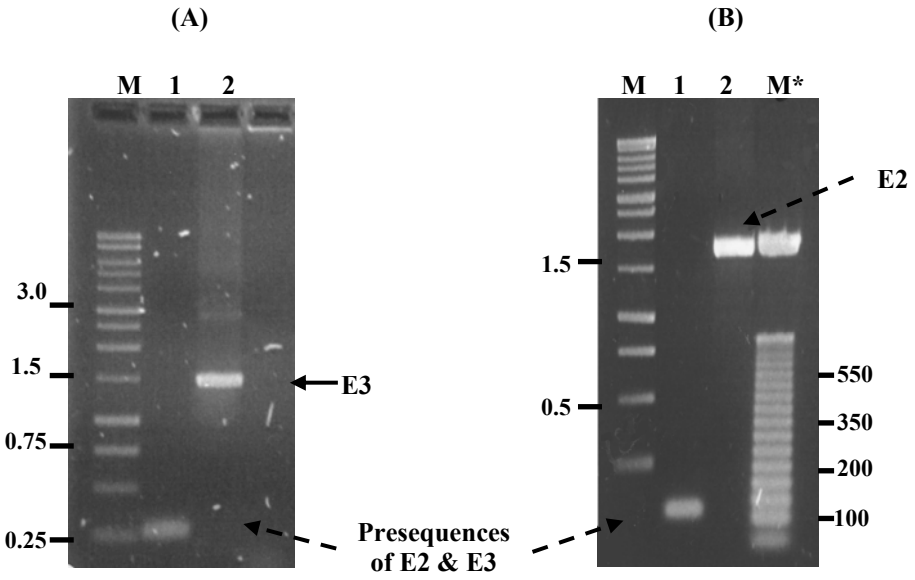

Figure 5-5 PCR amplification of presequences and mature forms of E2 and E3
Panel A: *lane 1*, PCR of E2 presequence with BamHI and SacI restriction sites. A positive result was seen by the presence of a single band of approximate size 0.25kb (expected size 258bps); *lane 2*, PCR of mature E3 with SacI and BamHI restriction sites. A positive result was seen by the presence of a single band of 1.5kb (expected size 1425 bps).

Panel B: *lane 1*, PCR of E3 presequence with BamHI and SacI restriction sites. A positive result was seen by the presence of a single band of approximate size 100 bps (expected size 105 bps); *lane 2*, PCR of mature E2 with SacI and BamHI restriction sites. A positive result was seen by the presence of a single band of 1.7kb (expected size 1686 bps).

M: 1 kb DNA ladder markers, M*: 50bp DNA ladder marker

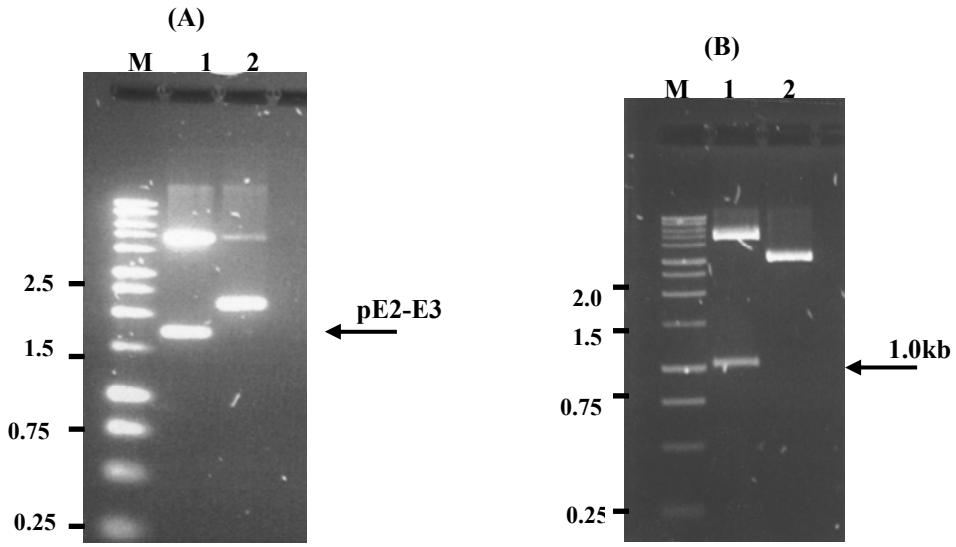

Figure 5-6 Restriction digestion of pE2-E3 plasmids
Putative positive clones containing insert were subjected to restriction digestion by *Bam*HI (panel A) or *Eco*RI (panel B). Samples of each digest (10µl) were analysed on 1% (w/v) agarose gels which were then stained with ethidium bromide and viewed under a UV transilluminator.

Panel A: BamHI restriction digestion of two clones, possibly containing insert, show that a band of approximate size 1.7kb is present in lane 1 (expected size 1682 bps).

Panel B: EcoRI restriction digestion of the same two clones shows that the clone 1 contains insert in the correct orientation as indicated by predicted sizes of the fragments. For a clone containing inserts in the correct orientation a digestion product 1kb in size was observed (expected size 1034 bps) while, for a clone containing insert in the wrong orientation, the digestion product should be 1.7kb.

M: 1 kb DNA ladder markers.

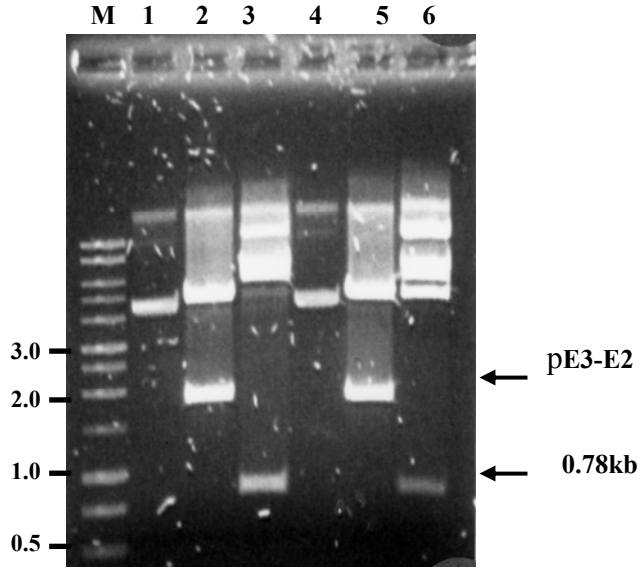

Figure 5-7 Restriction digestion of pE3-E2 plasmids
Putative positive clones containing insert were subjected to restriction digestion by *Bam*HI or *Eco*RI. 10µl samples of each digest were analysed on 1% (w/v) agarose gels which were then stained with ethidium bromide and viewed under a UV transilluminator.

Lanes 1 and 4: Two possible positive clones prior to digestion.

Lanes 2 and 5: BamHI restriction digestion of two clones, possibly containing insert, show that a band of approximate size 2kb is present in lanes 2 and 5 (expected size 1791 bps).

Lanes 3 and 6: EcoRI restriction digestion of the same two clones applied to check the orientation of the insert shows that they have pE3-E2 sequences inserted in the correct orientation as indicated by the predicted sizes of the fragments. For a clone containing inserts in the correct orientation, digestion products of 787 and 5675 bps in size were predicted, while a clone containing insert in the wrong orientation should yield fragments of 2028 and 4434 bps in size

M: 1 kb DNA ladder marker.

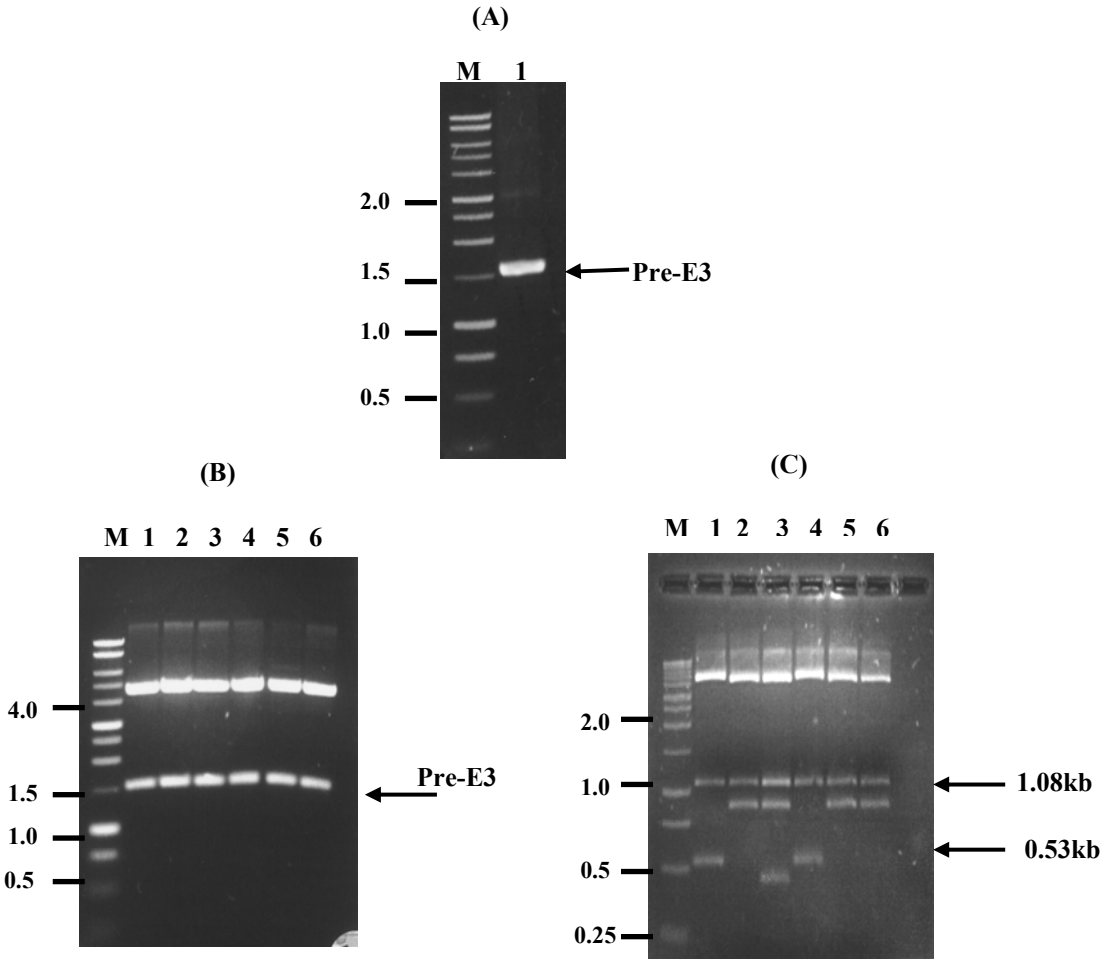

Figure 5-8 PCR amplification and restriction digestion of pre-E3 plasmids
PCR reaction and samples of each digest were run on a 1% (w/v) agarose gel and stained with ethidium bromide before visualizing on a UV transilluminator.

Panel (A): Amplified PCR (5µl) of full length pre-E3 with Bam HI restriction sites. A strong PCR product was obtained at an approximate size of 1.5kb (expected size 1530 bps).

Putative positive clones containing insert were subjected to restriction digestion with *Bam*HI or *Hind*III to check the orientation of pre-E3 fragments.

Panel (B): BamHI diagnostic digestion of 6 clones, possibly containing insert, show that a band of the expected size (1.5kb) is present in all lanes.

Panel (C): HindIII diagnostic digestion of the same clones applied to check the orientation of the insert, shows that out of the six clones which contain insert, clones in *lanes 1* and *4* have pre-E3 inserted in the correct orientation as indicated by the predicted sizes of the fragments. For a clone containing insert in the correct orientation, the expected sizes were 536, 1080, and 4585 bps. Clones in *lanes 2, 5* and *6* have insert in the wrong orientation producing restriction fragments as predicted of 875, 1080, 4246 bps.

M: 1Kb DNA ladder markers

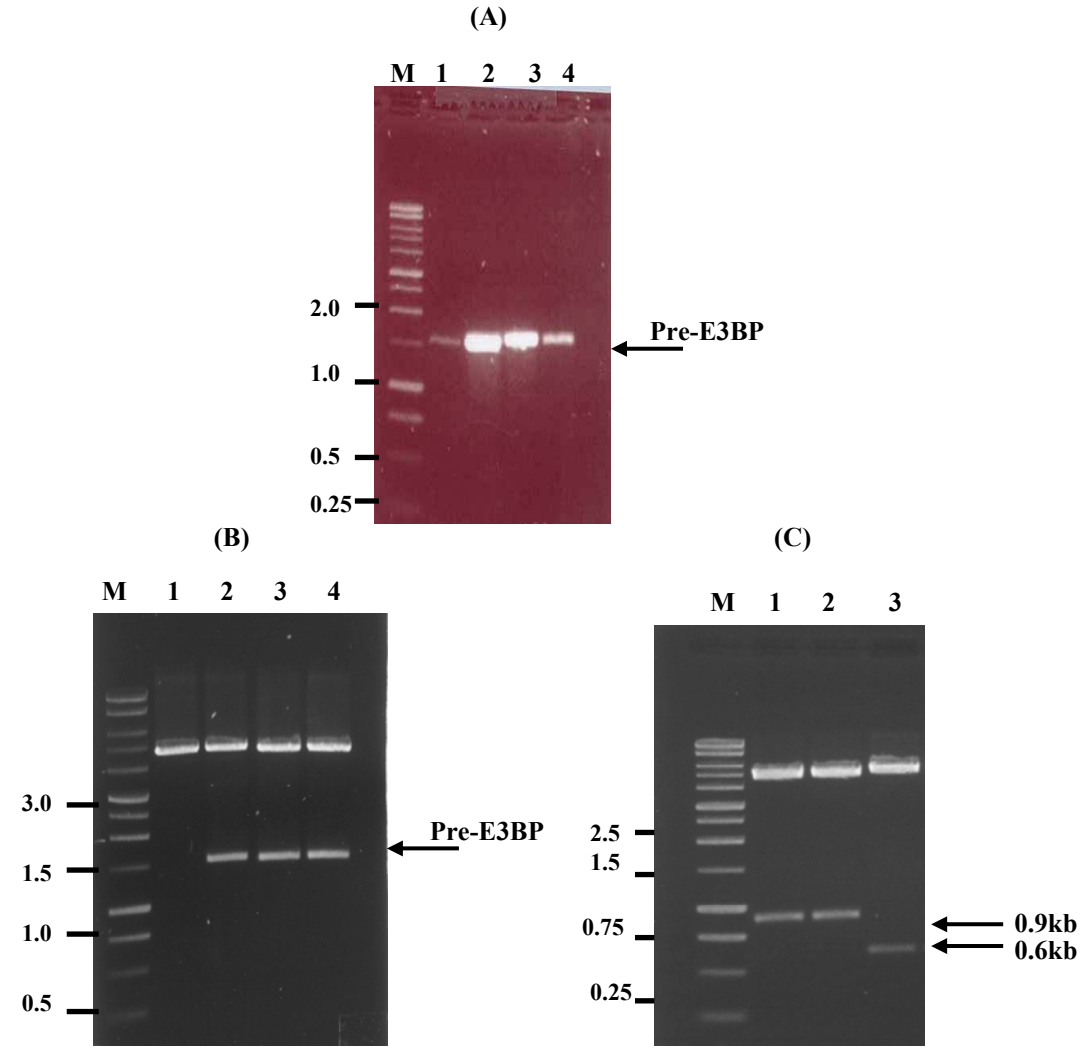

Figure 5-9 PCR amplification and restriction digest of pre-E3BP plasmids
PCR reaction and samples of each digest were run on a 1% (w/v) agarose gel and stained with ethidium bromide before visualizing on a UV transilluminator.

Panel (A): Amplified PCR (5µl) of full length pre-E3BP with Bam HI restriction sites. Pre-E3BP was amplified from four IMAGE clones and a strong PCR product was obtained at an approximate size of 1.5kb (expected size 1506 bps). The product of the second PCR reaction was employed for pre-E3BP cloning.

Putative positive clones containing inserts were subjected to restriction digestion with *Bam*HI, then *Nde*I to check the orientation of pre-E3BP fragments.

Panel (B): BamHI digestion of four clones, possibly containing insert, show that a band of the expected size (1.5kb) is present in *lanes 2, 3* and *4*.

Panel (C): NdeI restriction digestion of the three positive clones applied to check the orientation of the insert shows that clones in *lanes 1* and *2* have pre-E3BP inserted in the correct orientation as indicated by the predicted size of the fragments. For a clone containing insert in the correct orientation, a digestion product of 0.9kb in size was obtained (the predicted sizes 915 and 5262 bps) while a band of approximate size 0.6kb was obtained for a clone containing insert in the wrong orientation (the predicted sizes 615 and 5562 bps).

M: 1Kb DNA ladder markers.

5.3.2 Overexpression of precursor proteins at different temperatures

To study the effect of the presence of presequence on the expression and folding of E2 and E3BP, small-scale protein inductions were performed at 37, 30, and 22°C for 3, 4 and 6h respectively as described in Materials and Methods, section 2.3.11.1. Samples before and after induction were pelleted by centrifugation, resuspended in an appropriate volume of Laemmli sample buffer and analysed by SDS-PAGE.

All proteins cloned in this project; pre-E2, E3, E3BP, hybrid pE3-E2 and pE2-E3, as well as the N-terminal pre-E2 truncate and its mature form were successfully expressed using this system. In addition, the mature forms of each protein were expressed as positive controls. Initially, recombinant precursor proteins were overexpressed in *E. coli* BL21 (DE3) cells (data not shown). However, it was found that expression of heterologous protein using the BL21 (DE3) pLysS strain of *E. coli* was often more effective than the parent BL21 (DE3) strain (data not shown). In un-induced cells, low levels of transcription are often observed in the parent strain. It is therefore advantageous to use expression hosts carrying the pLysS plasmid that allows more control of basal levels of transcription by providing T7 lysozyme, a natural repressor of T7 RNA polymerase. This minimizes the possible toxic effects of heterologous protein expression prior to induction on addition of IPTG. In the presence of IPTG, T7 lysozyme is still present; however, due to the dramatic increase in T7 polymerase levels, rapid transcription of the target gene is initiated. In addition, T7 RNA polymerase is selective and extremely active so that almost all of the host cell resources are converted to the expression of the target gene.

Apart from pre-E2, overexpression of all precursors was performed successfully at variable levels over a range of temperatures, 37, 30 and 22°C compared to their mature forms. The overexpression of full length pre-E2 was attempted over a series of temperatures but it was very poor as seen in Figure 5-10 (panels A, B and C, samples a). As a result of poor expression, immunoblotting using anti-His-tag IgG was required to check successful expression of this enzyme (data not shown). In contrast high-level expression of its mature form was achieved successfully over a series of temperatures and 30°C deemed optimal (Figure 5-10, panel A, B and C, samples b). The N-terminal pre-E2 truncate also expressed successfully in good yield over different temperatures (Figure 5-10, panels A, B and C, samples c); however, the level of the expression of this

construct is still low compared to the expression of its mature form (Figure 5-10, panel A, B and C, samples d). Figure 5-11, panels A and B display the expression of pE2-E3 and pE3-E2 constructs over different temperatures and 22°C deemed optimal for both constructs. Interestingly, the successful expression of E3 ligated to the elongated E2 presequence was achieved at all the different temperatures used (Figure 5-11, panel A) whereas E2 ligated to the standard length of E3 presequence displayed poor expression in comparison to pE2-E3 (Figure 5-11, panel A) and its mature form, E2 (Figure 5-10, samples b). Overexpression of pre-E3 was also achieved successfully at various temperatures at high levels that were equivalent to or in occasions greater than its mature form (Figure 5-12, panels A and B). In addition, significant expression of pre-E3BP was readily observed but at a low level compared to its mature form (Figure 5-13, panels A and B).

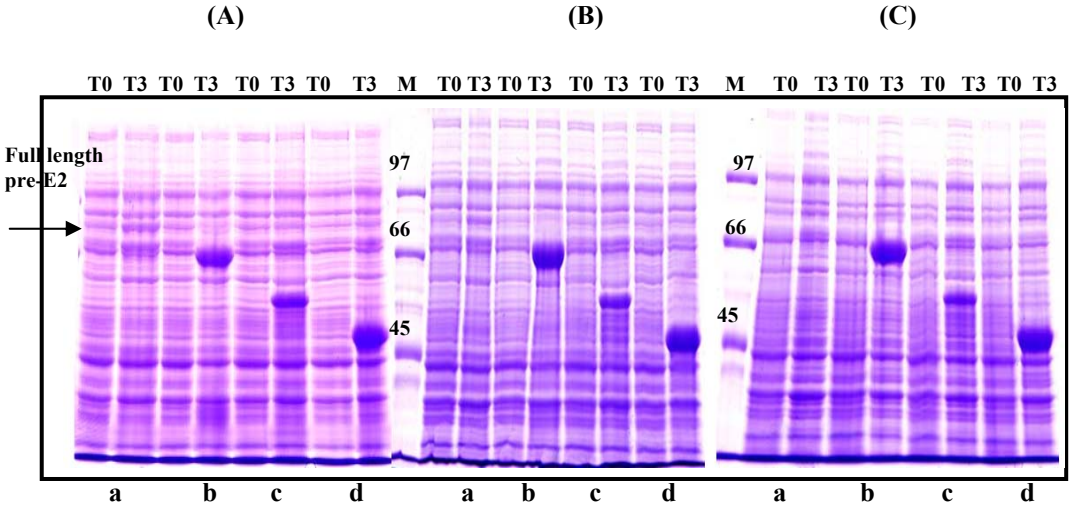

Figure 5-10 Overexpression of E2 precursor, mature E2 and their N-terminal truncated forms

Selected clones were transformed into competent BL21 (DE3) pLysS cells for protein expression at 37, 30 and 22°C. Samples were taken just before induction with IPTG (T_0), after 3h, 4h, or 6h 1mM IPTG induction at 37, 30 and 22°C (T_3, T_4 and T_6 respectively) and resolved by SDS-PAGE (8%) prior to staining with Coomassie Blue. All proteins were expressed in His-tagged form with approximate sizes of 86, 66, 50 and 45 kDa. Full length pre-E2, *samples a*; mature E2, *samples b*; N-terminal pre-E2 truncate, *samples c*; and N-terminal E2 truncate, *samples d*.

Panel (A): *Samples a*, expression of full length pre-E2; *samples b*, mature E2; *samples c*, N-terminal truncate pre-E2; and *samples d*; N-terminal mature E2 truncate at 37°C for 3h induction.

Panel (B): *Samples a*, expression of full length pre-E2; *samples b*, mature E2; *samples c*, N-terminal truncate pre-E2; and *samples d*, N-terminal mature E2 truncate at 30°C for 4h induction.

Panel (C): *Samples a*, expression of full length pre-E2; *samples b*, mature E2; *samples c*, N-terminal truncate pre-E2; and *samples* d, N-terminal mature E2 truncate at 22°C for 6h induction.

M (M_r x10^{-3}) low molecular mass marker

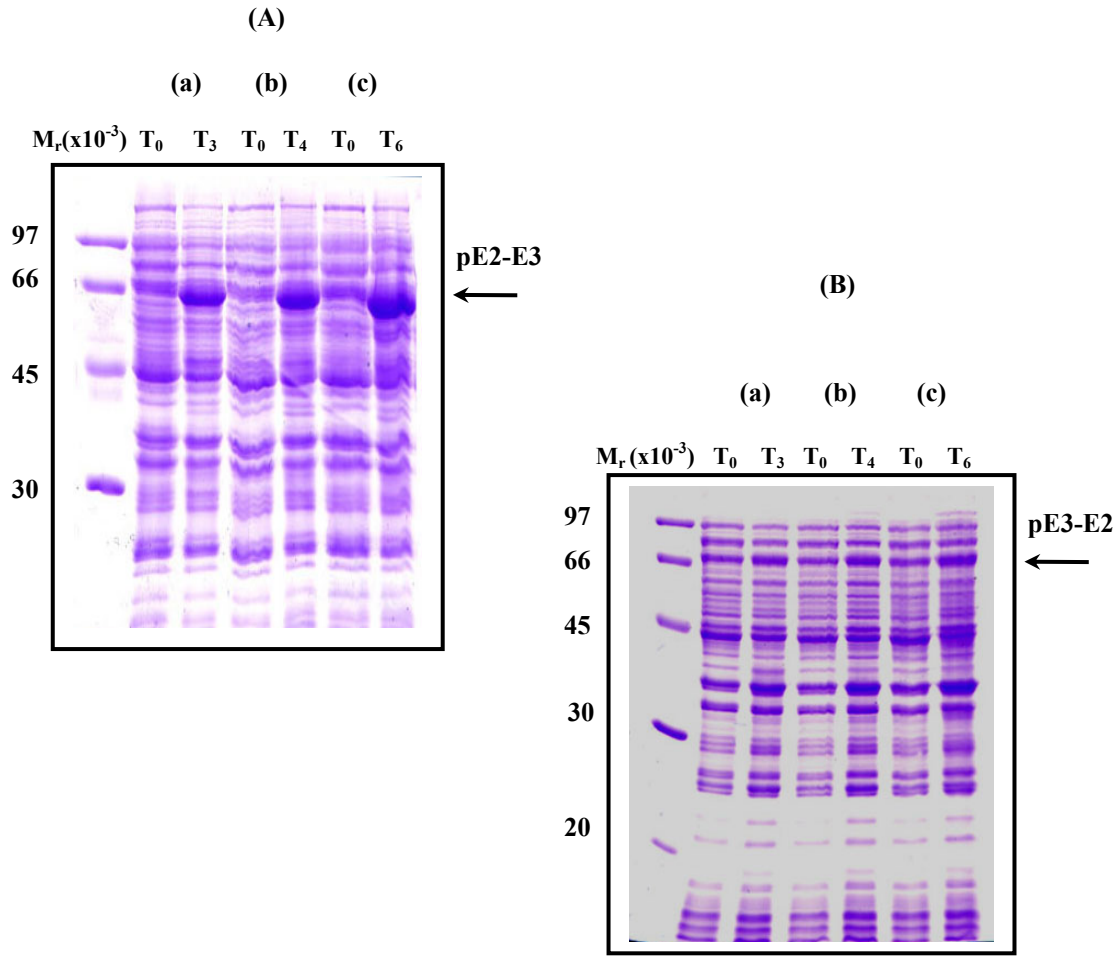

Figure 5-11 Overexpression of hybrid pE2-E3 and pE3-E2 at various temperatures
Recombinant plasmids containing pE2-E3 and pE3-E2 were transformed into competent *E. coli* BL21 (DE3) pLysS cells. Small scale protein inductions were carried out in LB media, at 37, 30, 22°C using 1mM IPTG induction for 3, 4, and 6h. Bacterial extracts taken just before induction, (T_0) and after 3, 4 and 6 hours (T_3, T_4 and T_6 respectively), were separated by SDS-PAGE on 12% gels and stained with Coomassie Blue.

Panel (A): *Samples a, b* and *c*, expression of pE2-E3 with approx. size of 60 kDa at 37°C, 30°C and 22°C.

Panel (B): *Samples a*, *b* and *c*, expression of pE3-E2 with approx. size of 70 kDa at 37°C, 30°C and 22°C.

M: relative molecular mass markers

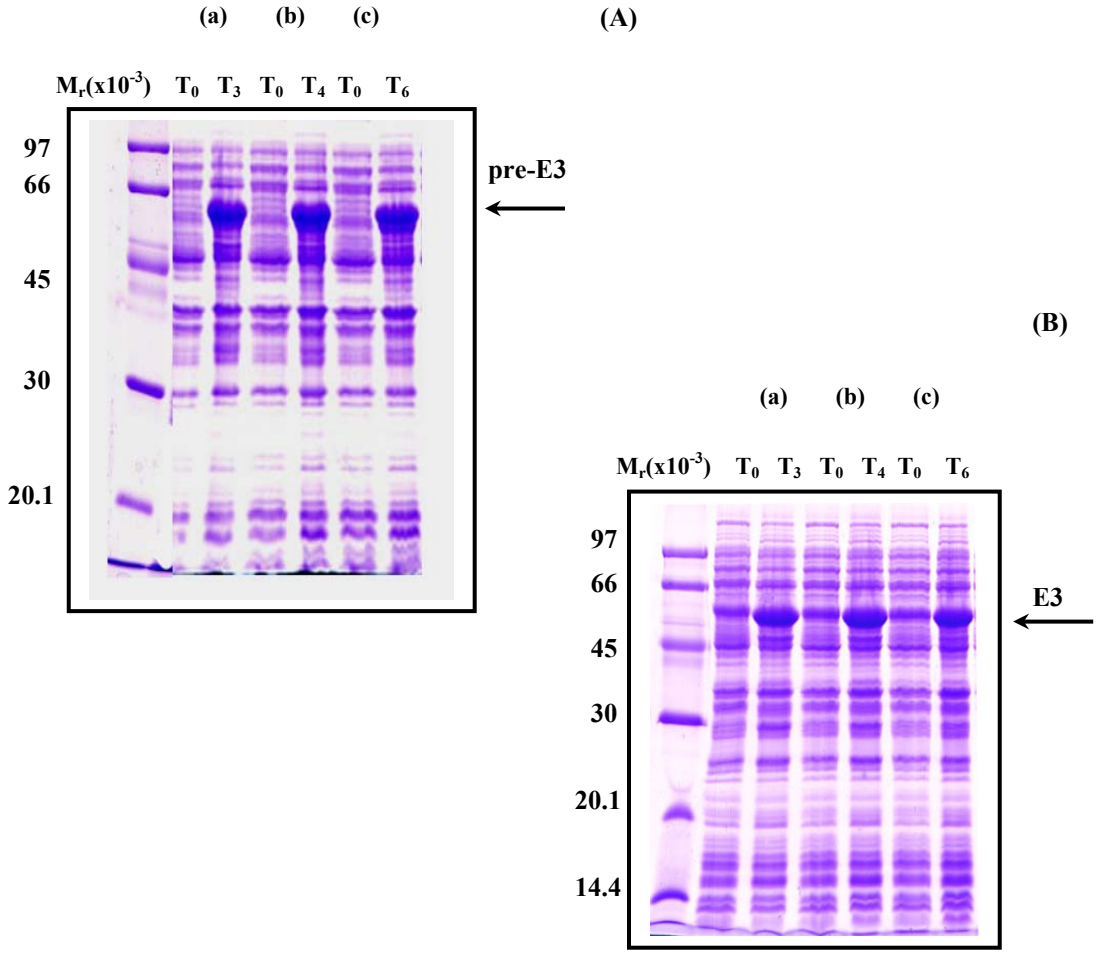

Figure 5-12 Overexpression of pre-E3 and its mature form at various temperatures
Clones of E3 precursor and its mature form were transformed into *E. coli* BL21 (DE3) pLysS cells. Expression was carried out on a small scale protein induction in LB media using 1mM IPTG at 37, 30, and 22°C for 3, 4, and 6h respectively. Bacterial extracts were taken just before IPTG induction (T_0) and after 3, 4 and 6 hours (T_3, T_4, and T_6) and then separated by SDS-PAGE on 12% gels and stained with Coomassie Blue.

Panel (A): *Samples a, b* and *c*, expression of pre-E3 with approximate size 59 kDa at 37, 30, and 22°C respectively.

Panel (B): *Samples a, b,* and *c*, expression of E3 with approximate size 55 kDa at 37, 30, and 22°C respectively.

M: relative molecular mass markers

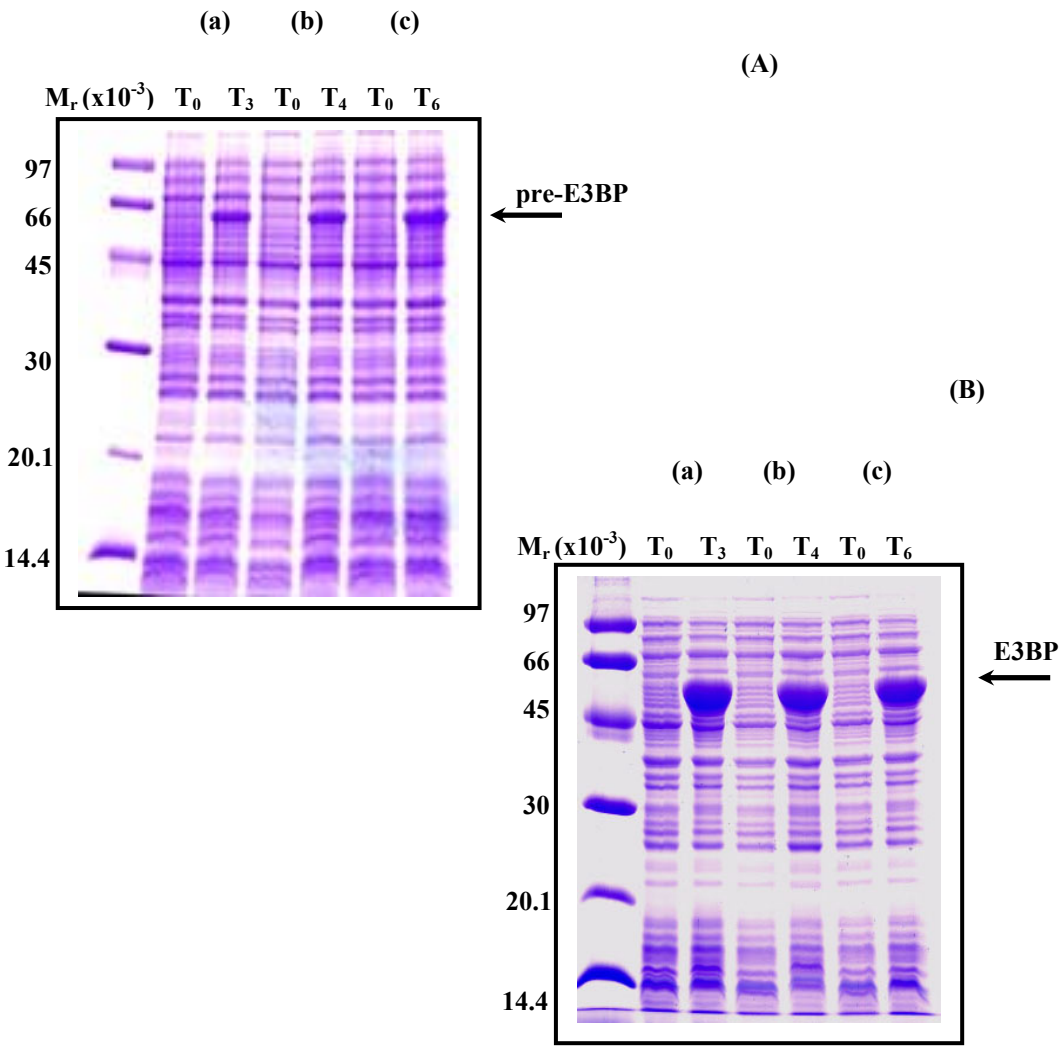

Figure 5-13 Overexpression of pre-E3BP and its mature form at various temperatures
Recombinant plasmid containing pre-E3BP and its mature were transformed into competent *E. coli* BL21 (DE3) pLysS cells for protein expression. Small scale protein inductions were carried out in LB media at 37, 30 and 22°C for 3, 4 and 6h respectively. Bacterial extracts taken just before induction with 1mM IPTG (T_0) and after 3, 4 and 6h (T_3, T_4 and T_6) were analysed by SDS-PAGE on 12% gels and stained with Coomassie blue.

Panel (A): *Samples a, b* and *c*, expression of pre-E3BP with approximate size of 57 kDa at 37, 30 and 22°C respectively.

Panel (B): *Samples a, b* and *c*, expression of E3BP with approximate size of 50 kDa at 37, 30 and 22°C respectively.

M: relative molecular mass markers

5.3.3 Checking the solubility of recombinant E2, E3BP and E3 constructs by immunoblotting

After successful cloning and expression of the recombinant polypeptides, the next essential step was to check the solubility of the proteins produced at different temperatures. This could be easily achieved by disrupting bacterial cells to release the soluble supernatant fraction and removal of insoluble cellular debris by centrifugation. Routinely, a French pressure cell treatment was used as described in Materials and Methods, section 2.3.12 to disrupt bacterial host cells.

To check the solubility of recombinant precursor proteins, aliquots of the cell extract, supernatant and pellet fractions were subjected to SDS/polyacrylamide gel electrophoresis and the solubility of the recombinant proteins was viewed by staining with Coomassie Blue as described in Materials and Methods, section 2.5.1 (data not shown).

Owing to poor expression of some precursor constructs such as pre-E2 and pE3-E2 as mentioned before, Western blot analysis was performed to study the level of expression and solubility of these precursors using an anti-His-tag IgG as described in Materials and Methods, section.2.5.6.2. Cell extract, pellet, and supernatant fractions for each precursor were blotted using a 1 in 2000 dilution of the anti-His tag antibody. In addition, parallel fractions of the equivalent mature proteins were also blotted to compare the solubility of the mature and the precursor forms of each construct.

Figure 5-14 (panels A, B, and C, samples a) shows that full length pre-E2 was completely insoluble at 37°C; however, by decreasing the temperature of expression, there was an improvement in the solubility of this construct as it became totally soluble at 22°C in low yield with noticeable degradation. In contrast, the majority of mature E2 was soluble at 37°C and completely soluble at 30 and 22°C (Figure 5-14, panels A, B and C, samples b). The N-terminal pre-E2 truncate was partially soluble at 37°C but became completely soluble at 30 and 22°C (Figure 5-15, panels A, B and C, samples a). In addition, all temperatures were suitable for production of soluble mature N-terminal E2 truncate (Figure 5-15, panels A, B and C, samples b). Figure 5-16, panels A and B shows the solubility of pE2-E3 and pE3-E2 respectively indicating that the pE2-E3 precursor was completely insoluble over this range of temperatures. Limited solubility of pE3-E2 was observed at 37°C and there was a slight improvement in the solubility on

decreasing the temperature of expression. Noticeable degradation was observed for pE3-E2 over the temperature range used. In addition, pre-E3 was completely insoluble but very limited solubility was observed on expression at 22°C (Figure 5-17, panel A). Interestingly, mature E3 was mostly insoluble at 37°C and partial solubilisation of this protein was achieved at 22°C (Figure 5-17, panel B). However, it was possible to produce totally soluble E3 in good yield by overnight expression at 15°C (data not shown). Pre-E3BP was mostly insoluble at 37°C compared to mature E3BP which was partially soluble under these conditions (Figure 5-18, panels A and B, sample a). However, improved solubility was achieved by decreasing the temperature in both cases; pre-E3BP became partially soluble whereas its mature form was expressed as a completely soluble protein at 22°C (Figure 5-18, panels A and B).

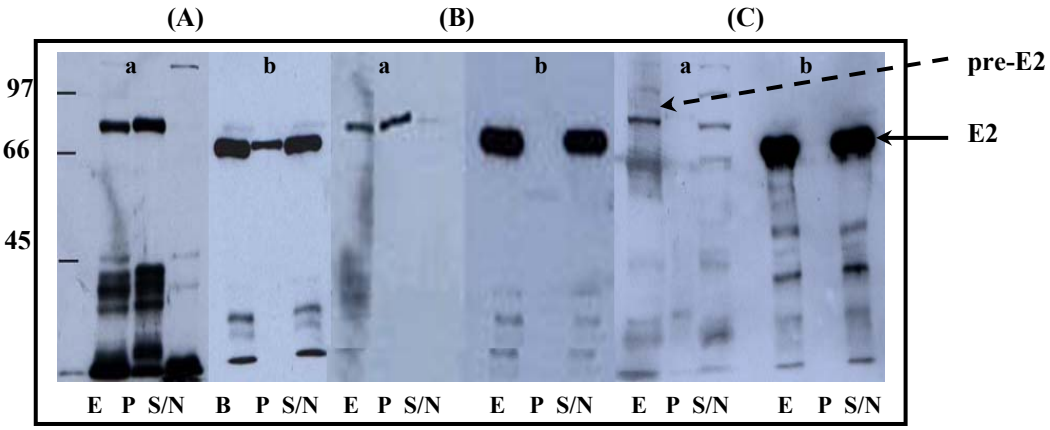

Figure 5-14 Western blot analysis of pre-E2 and its mature form expressed in *E. coli* to check solubility at different temperatures
Pellets of bacterial cells produced from the expression of E2 and its precursor at 37°C, *panel A*; 30°C, *panel B*; and 22°C, *panel C* were disrupted and centrifuged to produce bacterial cell extracts (E) pellet (P) and supernatant (S/N) fractions. All fractions of each protein were blotted using anti-His tag antibody (1 in 2000 dilution).

Samples a: Fractions of pre-E2

Samples b: Fractions of mature E2 (1 in 15 dilution).

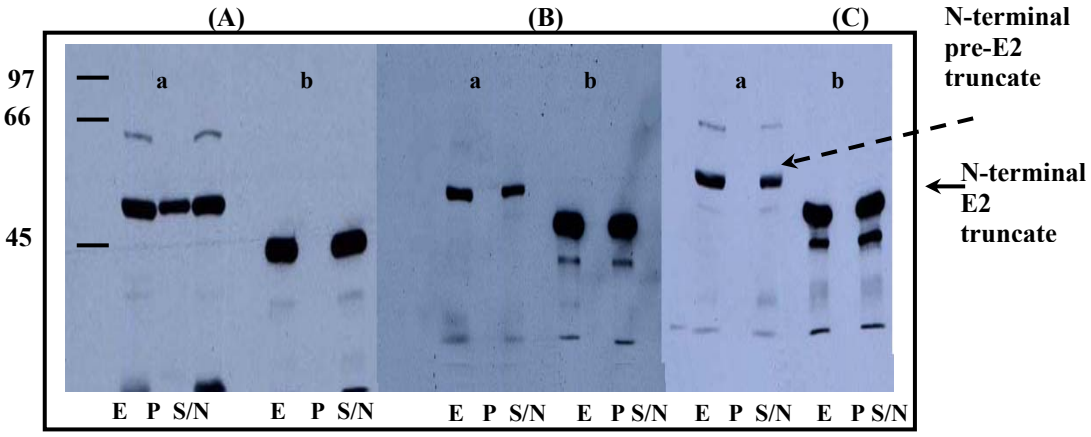

Figure 5-15 Western blot analysis of the N-terminal pre-E2 truncate and its mature E2 form to check the solubility at various temperatures
Pellets of bacterial cells produced from the expression of protein at 37°C, *panel A;* 30°C, *panel B*; and 22°C, *panel C* was disrupted and centrifuged to produce bacterial cell extracts (E) pellet (P) and supernatant (S/N) fractions. All fractions of each protein were blotted using anti-His tag Ab (1 in 2000 dilution).

Samples a: Fractions of N-terminal pre-E2 truncate

Samples b: Fractions of N-terminal mature E2 truncate (1 in 15 dilution).

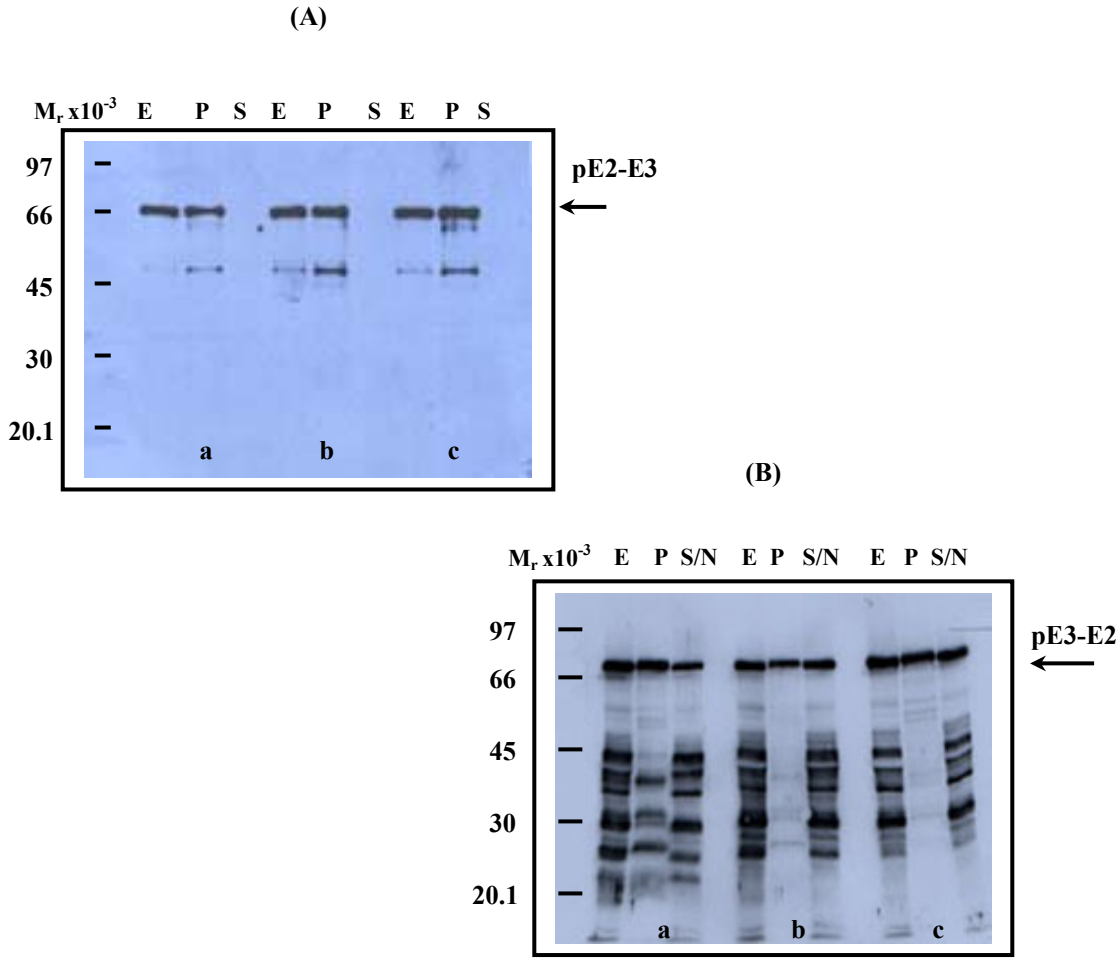

Figure 5-16 Western blot analysis of pE2-E3 and pE3-E2 expressed in *E. coli* to check solubility at various temperatures
Pellets of bacterial cells produced from the expression of pE2-E3 and pE3-E2 at 37°C, *samples a*; 30°C, *samples b*; and 22°C, *samples c* were disrupted and centrifuged to produce bacterial cell extracts (E) pellet (P) and supernatant (S/N) fractions. All fractions of each protein were blotted using anti-His tag Ab (1 in 2000 dilution).

Panel (A): Fractions of pE2-E3 (1 in 25 dilution).

Panel (B): Fractions of pE3-E2

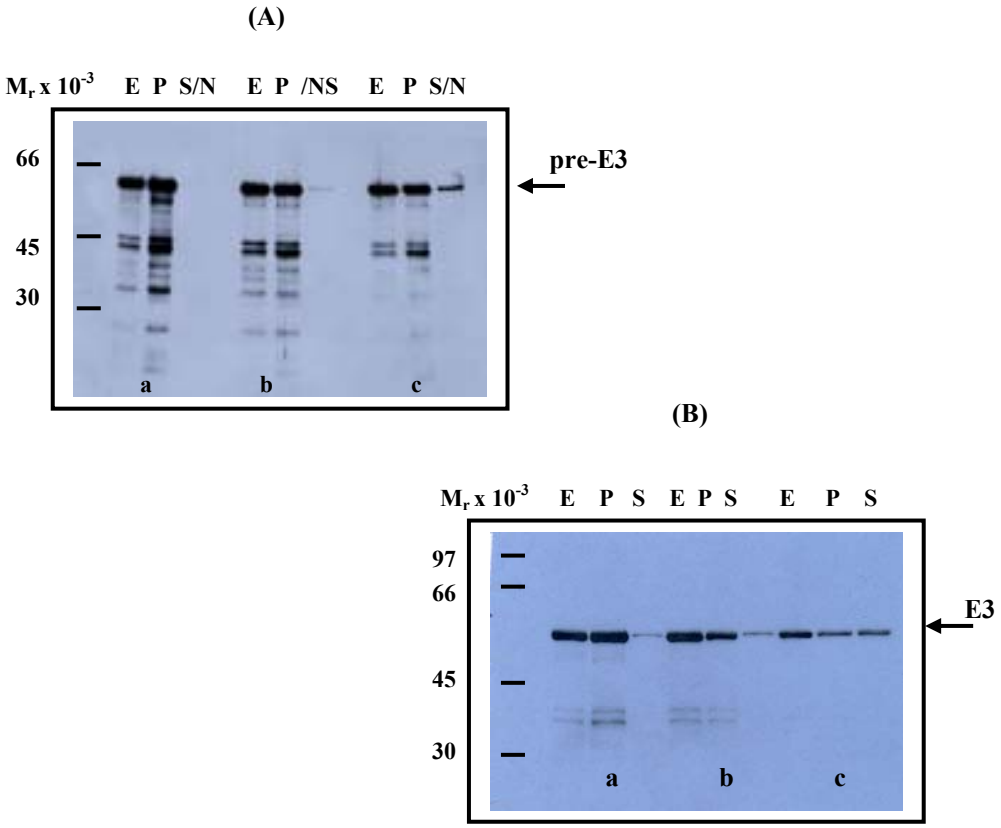

Figure 5-17 Western blot analysis of pre-E3 and its mature form expressed in *E. coli* at various temperatures
Pellets of bacterial cells produced from the expression of protein at 37, *samples a*; 30°C, *samples b*; and 22°C, *samples d* were disrupted and centrifuged to produce bacterial cell extracts (E) pellet (P) and supernatant (S/N) fractions. All fractions of each protein were blotted using anti-His tag Ab (1 in 2000 dilution).

Panel (A): fractions of pre-E3 (1 in 25 dilution)

Panel (B): Fractions of E3 (1 in 25 dilution)

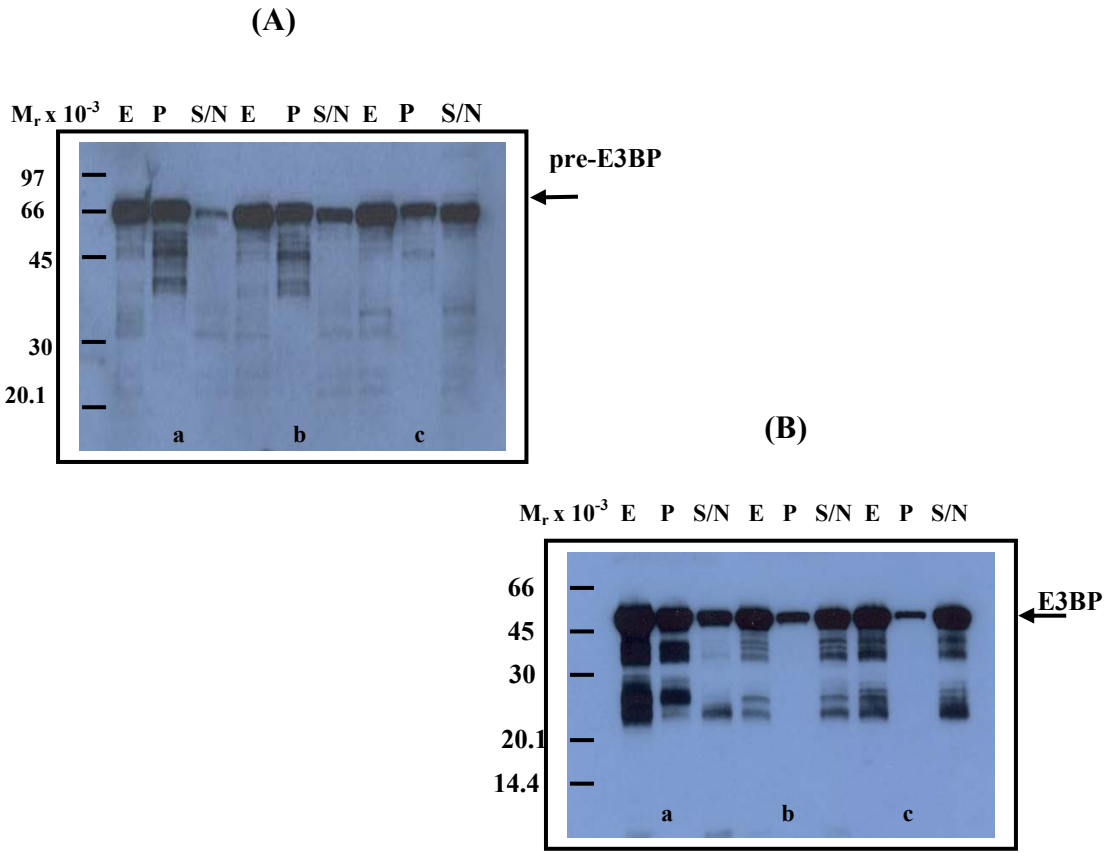

Figure 5-18 Western blot analysis of pre-E3BP and its mature form expressed in *E. coli* at various temperatures
Pellets of bacterial cells produced from the expression of protein at 37°C, *samples a*; 30°C, *samples b*; and 22°C, *samples c* were disrupted and centrifuged to produce bacterial cell extracts (E) pellet (P) and supernatant (S) fractions. All fractions of each protein were blotted using anti-His-tag Ab (1 in 2000 dilution).

Panel (A): fractions of pre-E3BP

Panel (B): Fractions of mature E3BP (1 in 10 dilution)

5.3.4 Checking the folding of precursors using immunoblot analysis

Incorporation of the essential lipoic acid prosthetic group by *E. coli* lipoyl ligase requires the presence of the correctly-folded apodomain in which the lipoyl-lysine residue is located on an exposed β-turn. This structural feature is essential for correct post-translational modification by the *E. coli* lipoylation system (Wallis & Perham, 1994). Access to monoclonal antibody PD2 that exclusively recognises the holodomain form of the human E2-PDC was generously provided by Prof. F. Stevenson, University of Southampton. This enabled us to study the folding status of the lipoyl domain by checking its level of lipoylation in both soluble and insoluble forms of mature and precursor E2 and E3BP.

To check the lipoylation of soluble and insoluble lipoyl domains; cell extract, pellet (insoluble) and supernatant (soluble) fractions from each precursor (pre-E2, its N-terminal truncate, pE3-E2 and pre-E3BP) were subjected to Western blot analysis using PD2. In parallel, fractions of the equivalent mature proteins were also blotted for comparison (Figure 5-19, Figure 5-20, Figure 5-21 and Figure 5-22).

It is clear from the results of immunoblot analysis that both soluble and insoluble fractions of precursor constructs display strong cross reactivity with mAb PD2 (Figure 5-19, samples a; Figure 5-20, samples a; Figure 5-21; and Figure 5-22, panel A). Considerable degradation of all precursor constructs was observed as judged by the appearance of multiple lower M_r value bands for the N-terminal pre-E2 truncate (Figure 5-20, samples a), pE3-E2 (Figure 5-21) and pre-E3BP (Figure 5-22, panel A) as compared to their equivalent mature forms, namely the N-terminal E2 truncate (Figure 5-20, samples b), mature E2 (Figure 4-19, samples b) and E3BP (Figure 5-22, panel B). Degradation of pre-E2 was not so apparent as its expression was very low making it difficult to visualise multiple lower M_r bands on the blot (Figure 5-19, samples a)

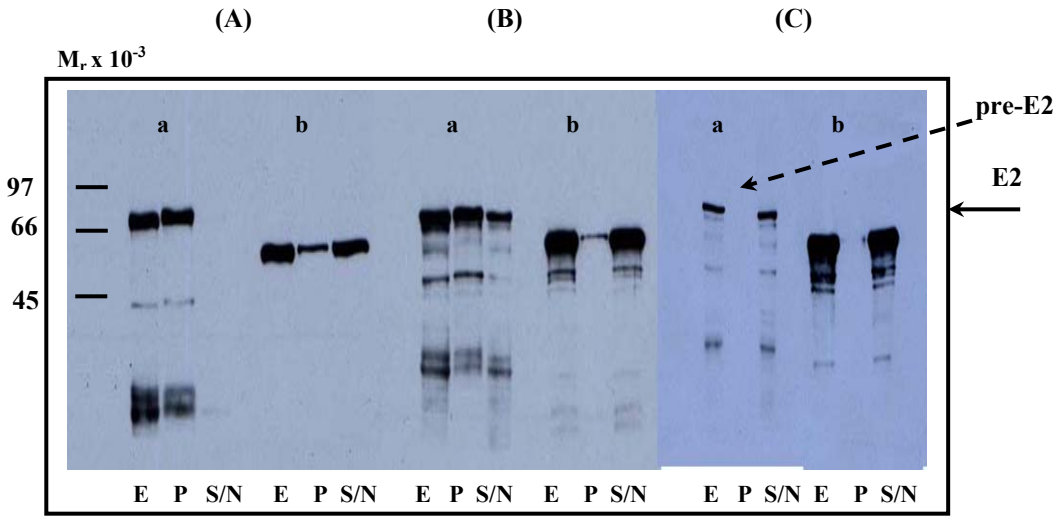

Figure 5-19 Western blot analysis of pre-E2 and its mature form expressed in *E. coli* at various temperatures
Pellets of bacterial cells produced from the expression of pre-E2 and its mature form at 37°C, *panel A*; 30°C, *panel B*; and 22°C, *panel C* were disrupted and centrifuged to produce bacterial cell extracts (E) supernatant (S) and pellet (P) fractions. All fractions of each enzyme were blotted using monoclonal antibody mAb PD2 (1 in 500 dilution).

Samples a: Fractions of pre-E2.

Samples b: Fractions of mature E2 (1 in 15 dilution).

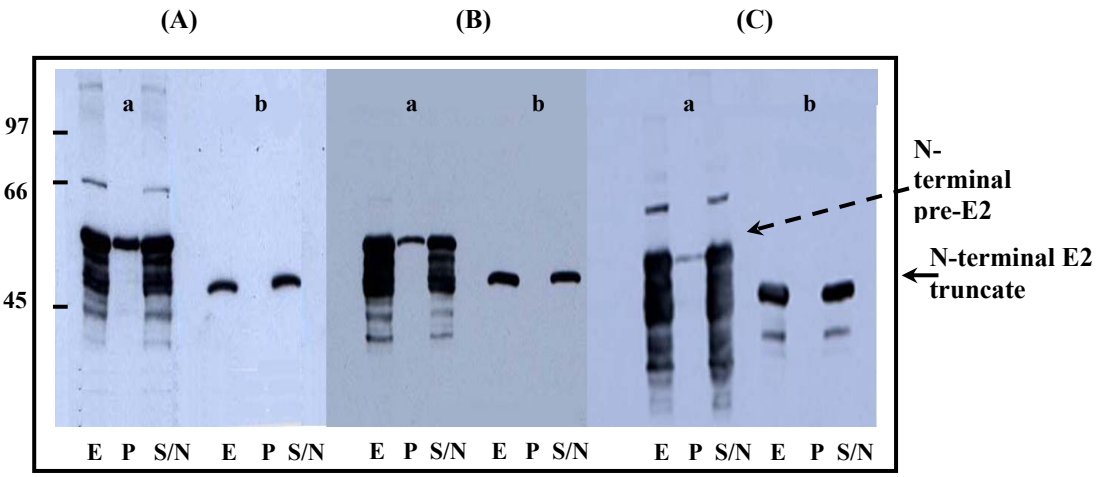

Figure 5-20 Western blot analysis of N-terminal pre-E2 truncate and its mature form expressed in *E. coli* at various temperatures
Pellets of bacterial cells produced from the expression of N-terminal pre-E2 and its mature truncate at 37°C, *panel A*; 30°C, *panel B*; and 22°C, *panel C* were disrupted and centrifuged to produce bacterial cell extracts (E) pellet (P), and supernatant (S/N) fractions. All fractions of each enzyme were blotted using mAb PD2 (1 in 500 dilution).

Samples a: Fractions of N-terminal pre-E2 truncate.

Samples b: Fractions of N-terminal E2 truncate (1 in 15 dilution)

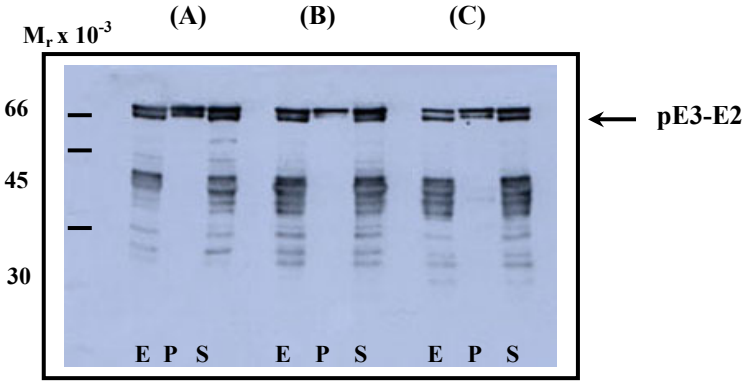

Figure 5-21 Western blot analysis of pE3-E2 expressed in *E. coli* at various temperatures
Pellets of bacterial cells produced from the expression of the hybrid precursor at 37°C, *panel A;* 30°C, *panel B;* and 22°C, *panel C* were disrupted and centrifuged to produce bacterial cell extracts (E) pellet (P) and supernatant (S/N) fractions of each protein were blotted using mAb PD2 (1 in 500 dilution)

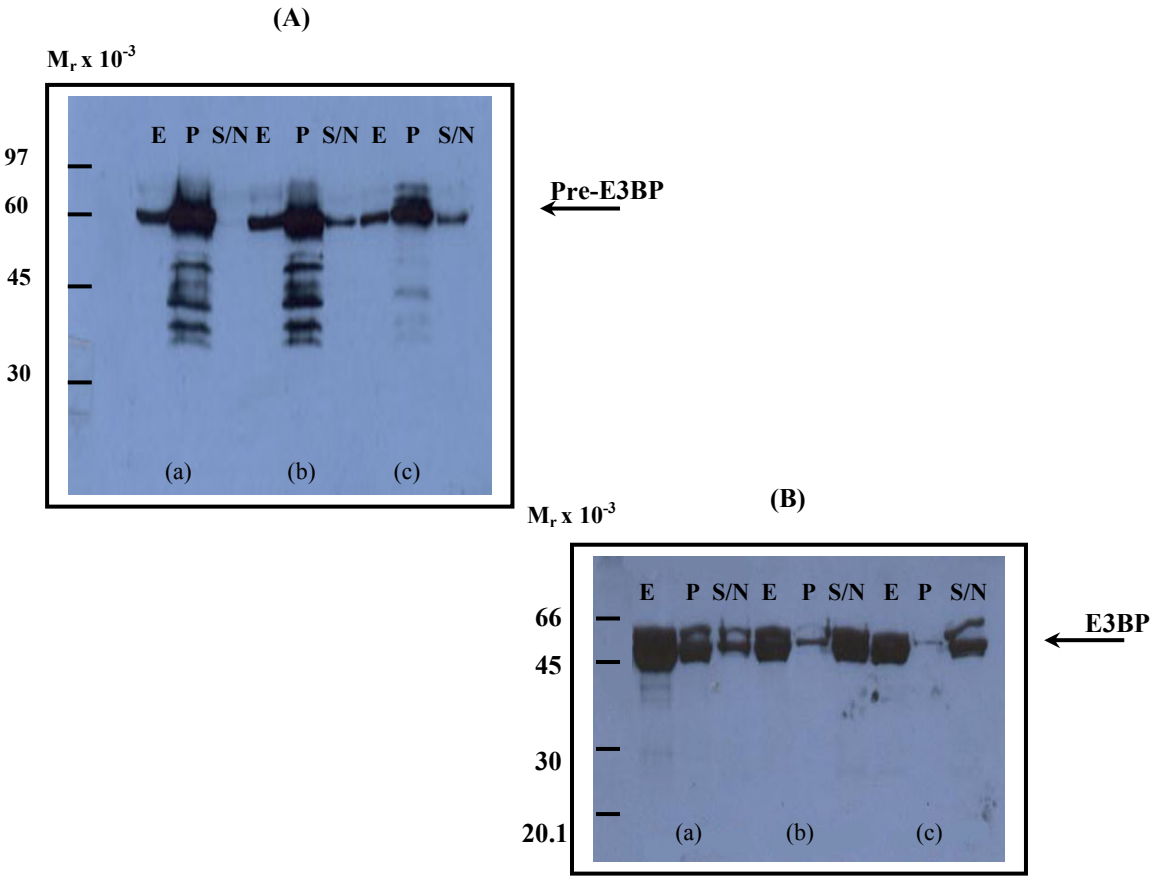

Figure 5-22 Western blot analysis of pre-E3BP and its mature form expressed at various temperatures

Pellets of bacterial cells produced from the expression of pre-E3BP and mature form at 37°C, *(a)*; 30°C, *(b)*; and 22°C, *(c)* were disrupted and centrifuged to produce bacterial cell extracts (E) pellet (P) and supernatant (S/N) fractions. All fractions of each protein were blotted using mAb PD2 (1 in 500 dilution).

Panel (A): fractions of pre-E3BP

Panel (B): fractions of E3BP (1 in 10 dilution)

5.4 Discussion

The E2 components of the 2-oxoacid dehydrogenase complexes have been shown to contain extended mitochondrial matrix targeting signals of 60-86 amino acids; moreover, E3BP also possesses a 53 amino acid presequence while other components of the 2-oxoacid dehydrogenase complexes have signal sequences in the range 24-50 amino acids in the length. These elongated E2 presequences suggest that they are not employed solely for targeting but may also play a role in maintaining this particular group of precursors in a loosely folded conformation distinct from the mature protein, thereby preventing premature association prior to import (Hunter & Lindsay, 1986; De Marcucci *et al.*, 1988; Lindsay, 1989; Clarkson & Lindsay, 1991).

The goal of this study was to investigate the effects of the elongated presequence on the expression, solubility and folding *in vivo* of human pre-E2, its N-terminal truncated form lacking the hydrophobic C-terminal domain and pre-E3BP by comparing them with human pre-E3 as a protein containing a standard mitochondrial targeting signal. Moreover, the work was extended to study the behaviour of the hybrid precursors, pE2-E3 and pE3-E2. In this chapter, the strategy has been described that has allowed us to generate the various constructs: human E2, E3BP, E3, pE2-E3 and pE3-E2 precursors plus N-terminal pre-E2 truncate and its mature form and then to achieve their successful and reproducible overexpression in *E. coli*.

Comparing the levels of expression of the various precursors at 37, 30 and 22°C with those of their mature forms, it can be noted that both presequences (extended and standard length) markedly reduced expression of E2 and E3BP but not E3. This effect was obvious in the expression of pre-E2 and pE3-E2 that were both greatly decreased compared to mature E2 as well as in the expression of pre-E3BP compared to its equivalent mature form but not with pre-E3 and pE2-E3 compared to their equivalent mature form. This is evidence that the nature of the mature protein as well as the presequence is important in moderating the level of protein expression. In the case of pre-E2, it was possible to improve its expression as an N-terminal truncate lacking the C-terminal core of the domain involved in self-assembly although it was still generated in low amounts as compared to its mature counterpart.

As a result of poor expression of precursor proteins, pre-E2 and pE3-E2, solubility checks were carried out by Western blot analysis using anti-His-tag IgG. Generally,

aggregation of non-native protein chains in *E. coli* is enhanced substantially by the effect of macromolecular crowding as a result of the rapid rates of polypeptide chain elongation (protein synthesis) occurring at higher temperatures (see Figure 5-23 for more details). However, aggregation phenomena can be limited by decreasing the rate of the protein synthesis employing lower temperatures for an extended period after induction to obtain soluble protein in good yield. The efficacy of this approach was apparent in the expression of the mature forms of E2, E3BP and E3. Thus, the partial solubility of both E2 and E3BP expressed at 37°C could be improved to full solubility by their expression at lower temperatures (30 and 22°C). Moreover, mature E2 polypeptide can be produced as a soluble protein over the entire range of temperatures used, when expressed as its monomeric N-terminal truncated form. The situation for E3 was slightly different as its overall level of the expression is much higher than that of E2 or E3BP. Therefore, expression of E3 at 30 or 22°C results only in the production of partially-soluble enzyme whereas complete solubility was achieved by overnight expression at 15°C (data not shown).

In this context, it was also noticed that protein aggregation was enhanced by the presence of the presequence. Both types of presequence (extended and standard length) have negative effects on protein solubility. Enhancement of aggregation by the presequences was observed clearly in the comparison of precursor solubility with their mature equivalents. Thus, whereas the E2 and E3BP precursors were completely insoluble at 37°C, their mature forms could be produced as partially soluble species at the same temperature. In addition, the largely insoluble E3 precursor at 22°C became partially soluble when expressed at the same temperature in its mature form. Moreover, the insolubility of pre-E2 could be improved when it was expressed as a monomeric N-terminal pre-E2 truncate.

Although both types of presequence have a negative effect on protein solubility, in our limited analysis, the extended E2 presequence appeared to induce aggregation to a greater extent than the standard E3 presequence. Thus, on comparison of the hybrid precursors pE2-E3 and pE3-E2 with their original precursors, pE2-E3 was insoluble over the entire range of temperatures employed while pre-E3 exhibited limited solubility at low temperature. However, pE3-E2 was shown to be partially soluble at 37°C and solubility was improved slightly by decreasing the temperature whereas pre-E2 was completely insoluble at 37°C and produced in very low yield as a soluble species with extensive degradation at 22°C.

Folding of proteins into their compact three-dimensional structures is the most fundamental and universal example of biological self-assembly. Information transfer from DNA to mRNA and from mRNA to the polypeptide involves molecular complementarity and the genetic code. Initially, it requires translation of the linear sequence of base triplets into a linear sequence of amino acids devoid of any biological activity. To become functionally active, newly synthesized protein must be changed from linear information to unique three dimensional structures through a complex series of folding/assembly events. Mature, correctly-folded proteins exhibit long-term stability in crowded biological environments and are able to interact selectively with their natural partners. In the case of the E2 enzymes of the 2-OADCs and E3BP, their N-terminal lipoyl domains are required to attain their native conformations in which the lipoyl-lysine is located on an exposed type-I β-turn for them to serve as substrates for the *E. coli* lipoylation system. Additionally, their C-terminal regions must then associate in an ordered, highly-specific fashion to form the vast 60:12-meric E2:E3BP pentagonal dodecahedral core assembly.

In this study it has been clearly established that the presence of an N-terminal mitochondrial matrix targeting signal has a pronounced negative impact on E2 or E3BP protein folding as judged by the enhanced generation of insoluble aggregates for most precursor states; however, their presence did not completely suppress the ability of precursors to achieve functional maturity as suggested by the improvement in precursor solubility at lower temperatures in many cases. Direct confirmation that E2 and E3BP precursor constructs have retained the ability to proceed along the correct folding pathway, at least in the initial stages, was demonstrated by using PD2, a lipoylation-dependent mAb that was able to detect lipoylated domains in both soluble and insoluble fractions indicating the presence of mature, folded holodomains. A similar result was observed with the N-terminal truncated pre-E2 form although extensive degradation of precursor forms was also detectable in all cases (as evidenced by the presence of multiple lower M_r bands) whereas little or no degradation of the equivalent mature polypeptides was apparent.

A unifying proposal to account for these observations is encompassed in the suggestion that the N-terminal matrix targeting signal of the precursor limits the rate of pre-E2 or pre-E3BP folding rather than preventing it completely. In this scenario, mitochondrial precursors are retained as ‘molten globule-like’ folding intermediates for prolonged periods (see Figure 5-23 for more details) such that these folding intermediates remain

susceptible to proteolysis and form inappropriate interactions via exposed hydrophobic surfaces leading to increased formation of insoluble aggregates. In mammalian cells, this limitation in the rate of protein folding may be necessary to permit interaction with cytosolic chaperones and other mitochondrial import factors that are required to maintain (and protect) the cytosolic precursor while in a 'loosely-folded' state that is a prerequisite for efficient import across both mitochondrial outer and inner membranes. At this stage, no major differences in the functional properties of the elongated and standard mitochondrial targeting sequences have been observed although it can be speculated that the increased length of presequence may either (a) allow binding of complex-specific, import factors/chaperones or (b) further limit the rate of assembly of this group of enzymes directly to prevent premature core formation prior to import as they all display a pronounced tendency to assemble rapidly into vast multimeric assemblies.

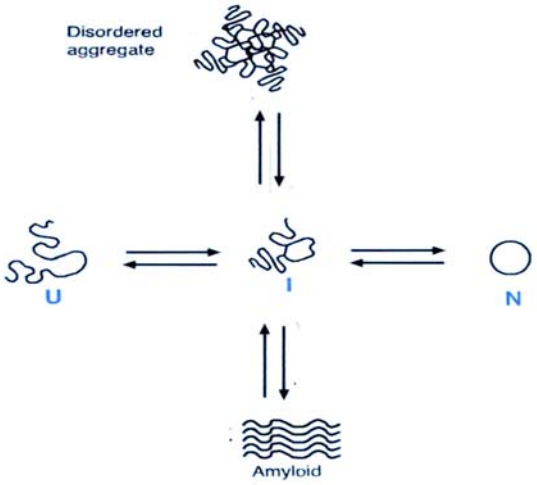

Figure 5-23 Aggregation of non-native protein chains as a side-reaction of the productive folding process
Folding of most proteins inside cells is not generally a spontaneous process and often inefficient especially in large proteins composed of multiple domains. Their folding often requires the participation of molecular chaperones that catalyze protein folding, by binding exposed hydrophobic patches and thus preventing aggregation into insoluble, non-functional inclusion bodies. Moreover, some molecular chaperones are able not only to protect proteins as they fold but also to rescue misfolded or aggregated proteins and enable them to have a second opportunity to assume their native 3-conformation. In a simple protein folding scheme, this process involves a three-state folding mechanism, U <-> I <-> N, where I represents an obligatory folding intermediate on a direct path between the unfolded and native states. Under physiological conditions, in particular with molecular crowding, proteins can be kinetically trapped at the folding intermediate stage and become susceptible to degradation or aggregation as inclusion bodies or amyloid fibrils, devoid of biological activity.

Further experiments are currently undergoing to directly test the effect of these presequences on the rate of protein folding and these will be described in the general discussion (chapter6)

Chapter 6

General discussion

The 2-oxoacid dehydrogenase family of multi-enzyme assemblies, loosely associated with the inner mitochondrial membrane, catalyse multi-step oxidative decarboxylation of several different 2-oxoacids. The three principal members of this family are the pyruvate dehydrogenase (PDC), 2-oxoglutarate dehydrogenase (OGDC) and branched-chain 2-oxoacid dehydrogenase (BCOADC) complexes. They are crucial to the operation of the glycolytic pathway, the tricarboxylic acid cycle and the metabolism of branched-chain amino acids as they catalyse major committed steps in intermediary metabolism. Their three constituent enzymes, E1, E2 and E3 contribute jointly to the overall catalytic mechanism, namely to oxidise their respective 2-oxoacid substrates to the corresponding acyl CoAs, with concomitant reduction of NAD^+ to NADH. The key to the structure and function of each of these complexes is their respective E2 component. In terms of their overall subunit organisation, mammalian E2s form a stable, symmetrical core of 60 subunits (PDC) or 24 subunits (OGDC and BCOADC) around which complex-specific E1 enzymes and a common E3 enzyme are assembled in a tight but non-covalent fashion. In the case of mammalian PDC, there is an additional subunit, termed E3BP that is tightly integrated into the E2 'core' where it is responsible for mediating E3 binding.

Importantly, all the constituent enzymes of these complexes are nuclear-encoded polypeptides so they are separately produced and imported individually into mitochondria as larger precursors in an energy-dependent fashion. Thus, these massive molecular 'machines' must be assembled *in situ* within the mitochondrial matrix-inner membrane compartment. Cofactor attachment is also considered to take place within the organelle, most notably the addition of the lipoic acid group to E2s and E3BP.

The E2 chains of PDC, OGDC and BCOADC as well as E3BP share a highly segmented organisation. Mammalian E2 and E3BP polypeptides fold into three distinct domains, the C-terminal core, SBD and the N-terminal lipoyl domain. The E2 polypeptide contains two tandemly repeated LDs whilst E3BP has a single LD. Defects in catalytic function, import and biogenesis of these complexes are implicated in a wide range of biochemical and genetic disorders, including various types of metabolic lactic acidosis, Alzheimer's disease and autoimmune conditions such as primary biliary cirrhosis (Patel & Harris, 1995; Young *et al.*, 1998; Gibson *et al.*, 2000; Ramadan *et al.*, 2004).

Primary biliary cirrhosis is an idiopathic hepatic disorder with autoimmune features, characterised by lymphoid infiltrates in the portal tracts, bile duct destruction, the presence of AMA and the progressive development of fibrotic chronic liver disease culminating in cirrhosis. Antimitochondrial antibodies (AMA) are present in 90-95% of patients with PBC. The principal targets of the AMA are E2s of 2-OADCs and E3BP. However, the most common reactivity is against E2-PDC and E3BP where the lipoic acid attached to the lipoyl domain itself appears to constitute an important part of the epitope. The role played by lipoic acid in the B cell autoepitope of E2-PDC has been confirmed in studies of the antigen specificity of human monoclonal antibodies PD1 and PD2 (Thomson *et al.*, 1998). These mAbs were found to be specific for lipoylated recombinant human E2 and E3BP-PDC with no binding being detected with non-lipoylated antigen.

Chapter 3 was concerned with investigation of the precise molecular basis for recognition of human E2-PDC and E3BP by mAbs PD1 and PD2 to gain a more detailed understanding of the aetiology of PBC. The chapter was divided into three sections. The first section involved the screening of different wt LDs from various sources and confirmed the hypothesis that although the extent of lipoylation is an important factor in PBC sera recognition, not all lipoylated domains are antigenic. Moreover, there was variation in the degree of antigenicity amongst cross-reactive lipoyl domains. By comparing the amino acid sequences of these LDs, it was evident that all cross-reacting lipoyl domains had a central block of 8 highly-conserved amino acids immediately adjacent to the lipoyl-lysine residue. Weakly cross-reacting LD-E3BP has a valine substitution at the C-terminal end of this central block. In addition, both the non-reacting LD of OGDC and *A. thaliana* plastid (Atpt) have several amino acid substitutions inside this central core region, predominantly towards its C-terminus.

The second section of chapter 3 involved mutation of the reactive lipoyl domain of human ILD-PDC, altering it systematically to be equivalent to the sequence of the non-reactive lipoyl domain of Atpt E2-PDC. This enabled investigation of the extent to which amino acid residues in the central region around the lipoyl-lysine play an integral part in the epitope recognised by PD1 and PD2. Western blot analysis either after SDS-PAGE or native gel separation was employed in this study. As these mAbs react specifically to the lipoylated form of E2-PDC and E3BP, two factors have to be taken into account: the extent of lipoylation and the presence of key residues that may be integral to mAb recognition. Therefore, native gel analysis was applied to investigate

the degree of lipoylation by separating lipoylated and non-lipoylated domains. In addition, mPEG maleimide modification facilitated the confirmation of the identity of the lipoylated species.

Interestingly, the expression of wt ILD-PDC in the absence of added lipoate produced approx. 20% octanoylated domain rather than the lipoylated form as this domain was not amenable to mPEG maleimide modification. This observation was consistent with previous studies reported by Ali *et al.* in which a lipoylation deficient strain of *E. coli* was used instead of the wt type host (Ali *et al.*, 1990). However, our current findings were contrary to a report by Quinn *et al.* who suggested that the apo and holodomains produced under these conditions and resolved by anion-exchange chromatography represented non-lipoylated and lipoylated ILD-PDC respectively (Quinn *et al.*, 1993a). Q-TOF mass spectrometry has confirmed the presence of octanoylated ILD-PDC in our case. Moreover, this work has demonstrated for the first time that the dithiols of the lipoic acid cofactor were not important in mAb recognition as octanoylated ILD-PDC also displayed strong cross reactivity.

The third section of chapter 3 dealt with the non-reactive domain, LD-OGDC in a complementary study designed to restore Ab recognition to that of ILD-PDC using site-directed mutagenesis. A series of 12 mutants of LD-OGDC were produced in attempts to investigate the key residues required for Ab recognition. The work was initiated by concentrating on the central block around the lipoyl-lysine residue. However, by changing the two non-conserved residues in the central block of LD-OGDC to be equivalent to that of ILD-PDC, negligible cross-reactivity was restored. Thus it was realised that the major epitope recognised by mAbs PD1 and PD2 did not solely involve this highly-conserved block of 8 amino acids. Subsequently, the work was expanded to other highly conserved residues in the adjacent N and C-terminal regions.

The possibility to restore the cross reactivity of LD-OGDC completely was proved in a stepwise fashion by introducing a series of amino acid replacements on the C-terminal side of the lipoylation site (outwith the central block) corresponding to conserved residues present in ILD-PDC. In fact, several conclusions can be drawn from this study: (a) mAbs PD1 and PD2 recognise a contiguous epitope involving the lipoic acid prosthetic group and a region of primary sequence approx 9-11 amino acids in length located C-terminal to the lipoylation site; (b) apart from the lipoyl-lysine itself, no specific amino acid has been identified as essential to Ab recognition; thus, both loss

and reappearance of cross-reactivity require the presence of two or more mutations; (c) significant restoration of Ab cross-reactivity with LD-OGDC was achieved only after generation of constructs containing Gln-47 and Val-48 replacements; however, these mutant constructs contained a total of 5 substitutions overall so it is likely that final reconstitution of the antigenic determinant stems from a cumulative effect of multiple substitutions; and (d) the epitope is confined to this region of primary sequence which can be inserted into different lipoyl domain backgrounds.

In terms of the lipoylation status of the various mutant domains of LD-OGDC, again it was apparent that, apart from lipoyl-lysine, there was no specific motif or amino acid that was essential for substrate recognition by the *E. coli* lipoylating system. In general, therefore, alterations in the extent of lipoylation, either positive or negative, were relatively minor following single amino acid replacements. The vast majority of multiple mutants were also partially or fully lipoylated indicating that the structural integrity of the domain was preserved in most cases. The extent of lipoylation of LD-OGDC mutants was also checked by native gel analysis and mPEG maleimide modification. In fact, wt LD-OGDC was a poorer substrate for the bacterial lipoylating enzymes than ILD-PDC; approx. 70% lipoylated LD-OGDC could be produced in the presence of exogenous lipoate whereas completely non-lipoylated domain was present in its absence. Moreover, it was observed that some amino acid replacements had a negative impact on the extent of lipoylation, some had no effect whereas the majority had a positive effect to give a full lipoylated domain. Perhaps, more precise quantitative analysis (competitive ELISA) would be considered to measure the absorbed of Ab reactivity by mutated ILD-PDC and LD-OGDC constructs.

In chapter 4, the lipoamide thiols of the reactive ILD-PDC as well as bovine PDC were modified with bulky substituents, mPEG, HNE, NEM and iodoacetamide in the presence of NAD^+ and NADH in order to investigate the role of the dithiolane ring of the lipoic acid prosthetic group in Ab recognition. The extent of modification was checked by a complex activity assay in the case of bPDC modification whereas native gel analysis as gel shift assay was employed in the case of ILD-PDC modification in which the modified proteins exhibited decreased rates of migration in the presence of NADH. Western blot analysis was employed to check the cross reactivity of these modified proteins with mAbs. It was found that this modification was accompanied by a decrease in Ab recognition. However, the loss of the recognition is not attributable to the importance of the dithiols in Ab recognition *per se* as the previous results (chapter

3) have shown that the octanoylated ILD-PDC lacking dithiols exhibits similar, if not identical, cross reactivity with these mAbs. Lack of cross reactivity of these modified domains was probably a result of steric hindrance.

A puzzling feature of PBC is that the autoimmune attack is predominantly organ specific, but the principal mitochondrial autoantigens are present in all nucleated cells and organs. One attractive theory, an extension of the original concept of molecular mimicry, is based on the principle that potential modifications of self-proteins by xenobiotics or natural agents may initiate an autoimmune response and subsequent immunopathology by generating autoreactive lymphocytes and/or antibodies that simultaneously recognise cross-reactive determinants from the original immunogen.

To address this hypothesis, *in vitro* modification of the non-lipoylated ILD-PDC generated in the absence of the lipoate was attempted with various lengths of fatty acids and their related compounds using bacterial LplA (chapter 4, second part). Two different aspects have been studied in this section: (a) investigating the specificity of the LplA by monitoring the incorporation of various fatty acids and related compounds into the non-lipoylated ILD-PDC employing native gel analysis; and (b) identifying the ability of these compounds to elicit an immune response with mAbs PD1 and PD2 following their incorporation. LplA displayed a broad specificity since its activity was not limited to C8 compounds such as lipoic and octanoic acid but included the C6, C10 and C12 saturated fatty acids. Moreover, activity was not restricted to linear, saturated fatty acids as it included the branched compound (valproic acid) but with low efficiency. In addition, a related compound to HNE (a major lipid peroxidation product), tran-2-nonenoic acid was shown to be incorporated into non-lipoylated ILD-PDC.

Screening modified ILD-PDCs with mAbs PD1 and PD2 using Western blot analysis revealed that 8-carbon atoms were the minimal chain length required to restore the antigenicity of the non-lipoylated domain. Moreover, this effect was not exclusive to lipoic acid or octanoic acid as C10 and C12 saturated fatty acids as well as valproate, a branched-chain fatty acid also elicited a strong immune response as did the ILD following trans-2-nonenoic acid incorporation. The importance of this compound is that it is readily formed from HNE, a harmful lipid peroxidation product generated after exposure of cells/tissues to oxidative stress. In this context, a novel postulate is that

nascent non-lipoylated E2 enzymes can potentially be aberrantly-modified by this route forming neo-antigen.

Previous studies have demonstrated that the E2s of 2-OADCs and E3BP are encoded initially as cytosolic precursor molecules containing elongated N-terminal presequence. Chapter 5 contained an analysis of how the presence of standard length and elongated presequences on E2, E3BP and E3 precursors affects their expression, solubility and folding. This investigation was approached by conducting comparative studies between the behaviour of pre-E2 and pre-E3BP as precursors containing extended presequences and the behaviour of pre-E3 as a precursor containing a standard presequence. It was observed that both types of presequence as well as the nature of mature protein affect the level of expression. Thus mature E3 linked either to E2 or E3 presequences displays a good level of protein expression compared to the mature form whereas mature E2 linked either to E2 or E3 presequences displays poor expression compared to the mature form. Generally, both types of presequence reduce the solubility of these constructs although the extended form appeared to have a greater effect. However, formation of insoluble aggregates was decreased by expression of precursors at lower temperatures.

Current evidence suggests that presequences inhibit the rate of precursor folding but do not prevent it completely. Thus nascent folding intermediates, whether soluble or insoluble, are more susceptible to degradation but are at least partially lipoylated.

Future work in this area is planned to analyse directly the rate of the folding of the N-terminal truncate of the E3BP precursor using its mature form as a positive control. This analysis will be carried out using stop-flow, CD and fluorescence techniques. In addition, protein-protein interaction analysis of the N-terminal E3BP precursor truncate and its partner E3 enzyme can be studied by gel filtration, ‘pull-down’ assay or surface plasmon resonance (SPR) to check if the entire truncated form of the precursor can attain its mature, native conformation. In addition, the study of pre-E3 folding can be achieved by assaying the activity of the precursor enzyme or by analysing the effect of flavin incorporation into the precursor protein.

References

A AE, Chuang JL, Wynn RM, Turley S, Chuang DT & Hol WG (2000) Crystal structure of human branched-chain alpha-ketoacid dehydrogenase and the molecular basis of multienzyme complex deficiency in maple syrup urine disease. *Structure* **8**, 277-91.

Aboutwerat A, Pemberton PW, Smith A, Burrows PC, McMahon RF, Jain SK & Warnes TW (2003) Oxidant stress is a significant feature of primary biliary cirrhosis. *Biochim Biophys Acta* **1637**, 142-50.

Aevarsson A, Seger K, Turley S, Sokatch JR & Hol WG (1999) Crystal structure of 2-oxoisovalerate and dehydrogenase and the architecture of 2-oxo acid dehydrogenase multienzyme complexes. *Nat Struct Biol* **6**, 785-92.

Ahrens EH, Jr., Payne MA, Kunkel HG, Eisenmenger WJ & Blondheim SH (1950) Primary biliary cirrhosis. *Medicine (Baltimore)* **29**, 299-364.

Ali ST, Moir AJ, Ashton PR, Engel PC & Guest JR (1990) Octanoylation of the lipoyl domains of the pyruvate dehydrogenase complex in a lipoyl-deficient strain of *Escherichia coli*. *Mol Microbiol* **4**, 943-50.

Amano K, Leung PS, Rieger R, Quan C, Wang X, Marik J, Suen YF, Kurth MJ, Nantz MH, Ansari AA, Lam KS, Zeniya M, Matsuura E, Coppel RL & Gershwin ME (2005) Chemical xenobiotics and mitochondrial autoantigens in primary biliary cirrhosis: identification of antibodies against a common environmental, cosmetic, and food additive, 2-octynoic acid. *J Immunol* **174**, 5874-83.

Amano K, Leung PS, Xu Q, Marik J, Quan C, Kurth MJ, Nantz MH, Ansari AA, Lam KS, Zeniya M, Coppel RL & Gershwin ME (2004) Xenobiotic-induced loss of tolerance in rabbits to the mitochondrial autoantigen of primary biliary cirrhosis is reversible. *J Immunol* **172**, 6444-52.

Arjunan P, Nemeria N, Brunskill A, Chandrasekhar K, Sax M, Yan Y, Jordan F, Guest JR & Furey W (2002) Structure of the pyruvate dehydrogenase multienzyme complex E1 component from *Escherichia coli* at 1.85 A resolution. *Biochemistry* **41**, 5213-21.

Babior BM (1984) The respiratory burst of phagocytes. *J Clin Invest* **73**, 599-601.

Bach N & Schaffner F (1994) Familial primary biliary cirrhosis. *J Hepatol* **20**, 698-701.

Baum H (1995) Mitochondrial antigens, molecular mimicry and autoimmune disease. *Biochim Biophys Acta* **1271**, 111-21.

Beddoe T & Lithgow T (2002) Delivery of nascent polypeptides to the mitochondrial surface. *Biochim Biophys Acta* **1592**, 35-9.

Behal RH, Browning KS, Hall TB & Reed LJ (1989) Cloning and nucleotide sequence of the gene for protein X from *Saccharomyces cerevisiae*. *Proc Natl Acad Sci U S A* **86**, 8732-6.

Behal RH, Buxton DB, Robertson JG & Olson MS (1993) Regulation of the pyruvate dehydrogenase multienzyme complex. *Annu Rev Nutr* **13**, 497-520.

Bellringer ME, Rahman K & Coleman R (1988) Sodium valproate inhibits the movement of secretory vesicles in rat hepatocytes. *Biochem J* **249**, 513-9.

Berg A, Westphal AH, Bosma HJ & de Kok A (1998) Kinetics and specificity of reductive acylation of wild-type and mutated lipoyl domains of 2-oxo-acid dehydrogenase complexes from *Azotobacter vinelandii*. *Eur J Biochem* **252**, 45-50.

Berg PA & Klein R (1986) Mitochondrial antigens and autoantibodies: from anti-M1 to anti-M9. *Klin Wochenschr* **64**, 897-909.

Berg PA & Klein R (1988) Molecular determination of the primary biliary cirrhosis-specific M2 antigen. *Hepatology* **8**, 200-1.

Berg PA & Klein R (1989) Heterogeneity of antimitochondrial antibodies. *Semin Liver Dis* **9**, 103-16.

Berg PA, Klein R & Lindenborn-Fotinos J (1986) Antimitochondrial antibodies in primary biliary cirrhosis. *J Hepatol* **2**, 123-31.

Bomsel M, Heyman M, Hocini H, Lagaye S, Belec L, Dupont C & Desgranges C (1998) Intracellular neutralization of HIV transcytosis across tight epithelial barriers by anti-HIV envelope protein dIgA or IgM. *Immunity* **9**, 277-87.

Bowker-Kinley M & Popov KM (1999) Evidence that pyruvate dehydrogenase kinase belongs to the ATPase/kinase superfamily. *Biochem J* **344 Pt 1**, 47-53.

Bowker-Kinley MM, Davis WI, Wu P, Harris RA & Popov KM (1998) Evidence for existence of tissue-specific regulation of the mammalian pyruvate dehydrogenase complex. *Biochem J* **329 (Pt 1)**, 191-6.

Bradford MM (1976) A rapid and sensitive method for the quantitation of microgram quantities of protein utilizing the principle of protein-dye binding. *Anal Biochem* **72**, 248-54.

Brautigam CA, Wynn RM, Chuang JL, Machius M, Tomchick DR & Chuang DT (2006) Structural insight into interactions between dihydrolipoamide dehydrogenase (E3) and E3 binding protein of human pyruvate dehydrogenase complex. *Structure* **14**, 611-21.

Brind AM, Bray GP, Portmann BC & Williams R (1995) Prevalence and pattern of familial disease in primary biliary cirrhosis. *Gut* **36**, 615-7.

Brivet M, Moutard ML, Zater M, Venet L, Chenel C, Mine M & Legrand A (2005) First characterization of a large deletion of the *PDHA 1* gene. *Mol Genet Metab* **86**, 456-61.

Brookfield DE, Green J, Ali ST, Machado RS & Guest JR (1991) Evidence for two protein-lipoylation activities in *Escherichia coli*. *FEBS Lett* **295**, 13-6.

Brown RM, Dahl HH & Brown GK (1989) X-chromosome localization of the functional gene for the E1 alpha subunit of the human pyruvate dehydrogenase complex. *Genomics* **4**, 174-81.

Brown RM, Head RA, Boubriak, II, Leonard JV, Thomas NH & Brown GK (2004) Mutations in the gene for the E1beta subunit: a novel cause of pyruvate dehydrogenase deficiency. *Hum Genet* **115**, 123-7.

Brown RM, Head RA, Morris AA, Raiman JA, Walter JH, Whitehouse WP & Brown GK (2006) Pyruvate dehydrogenase E3 binding protein (protein X) deficiency. *Dev Med Child Neurol* **48**, 756-60.

Bruggraber SF, Leung PS, Amano K, Quan C, Kurth MJ, Nantz MH, Benson GD, Van de Water J, Luketic V, Roche TE, Ansari AA, Coppel RL & Gershwin ME (2003) Autoreactivity to lipoate and a conjugated form of lipoate in primary biliary cirrhosis. *Gastroenterology* **125**, 1705-13.

Bustamante J, Lodge JK, Marcocci L, Tritschler HJ, Packer L & Rihn BH (1998) Alpha-lipoic acid in liver metabolism and disease. *Free Radic Biol Med* **24**, 1023-39.

Butler P, Hamilton-Miller J, Baum H & Burroughs AK (1995) Detection of M2 antibodies in patients with recurrent urinary tract infection using an ELISA and purified PBC specific antigens. Evidence for a molecular mimicry mechanism in the pathogenesis of primary biliary cirrhosis? *Biochem Mol Biol Int* **35**, 473-85.

Butler P, Valle F, Hamilton-Miller JM, Brumfitt W, Baum H & Burroughs AK (1993) M2 mitochondrial antibodies and urinary rough mutant bacteria in patients with primary biliary cirrhosis and in patients with recurrent bacteriuria. *J Hepatol* **17**, 408-14.

Cameron JM, Levandovskiy V, Mackay N, Tein I & Robinson BH (2004) Deficiency of pyruvate dehydrogenase caused by novel and known mutations in the E1alpha subunit. *Am J Med Genet A* **131**, 59-66.

Cate RL, Roche TE & Davis LC (1980) Rapid intersite transfer of acetyl groups and movement of pyruvate dehydrogenase component in the kidney pyruvate dehydrogenase complex. *J Biol Chem* **255**, 7556-62.

Celli A, Que FG, Gores GJ & LaRusso NF (1998) Glutathione depletion is associated with decreased Bcl-2 expression and increased apoptosis in cholangiocytes. *Am J Physiol* **275**, G749-57.

Cha S, Leung PS, Gershwin ME, Fletcher MP, Ansari AA & Coppel RL (1993) Combinatorial autoantibodies to dihydrolipoamide acetyltransferase, the major autoantigen of primary biliary cirrhosis. *Proc Natl Acad Sci U S A* **90**, 2527-31.

Chen WJ & Douglas MG (1987) Phosphodiester bond cleavage outside mitochondria is required for the completion of protein import into the mitochondrial matrix. *Cell* **49**, 651-8.

Chernushevich IV, Loboda AV & Thomson BA (2001) An introduction to quadrupole-time-of-flight mass spectrometry. *J Mass Spectrom* **36**, 849-65.

Choudhary S, Srivastava S, Xiao T, Andley UP, Srivastava SK & Ansari NH (2003) Metabolism of lipid derived aldehyde, 4-hydroxynonenal in human lens epithelial cells and rat lens. *Invest Ophthalmol Vis Sci* **44**, 2675-82.

Christen U, Quinn J, Yeaman SJ, Kenna JG, Clarke JB, Gandolfi AJ & Gut J (1994) Identification of the dihydrolipoamide acetyltransferase subunit of the human pyruvate dehydrogenase complex as an autoantigen in halothane hepatitis. Molecular mimicry of trifluoroacetyl-lysine by lipoic acid. *Eur J Biochem* **223**, 1035-47.

Chuang DT, Chuang JL & Wynn RM (2006) Lessons from genetic disorders of branched-chain amino acid metabolism. *J Nutr* **136**, 243S-9S.

Chuang JL, Cox RP & Chuang DT (1997) E2 transacylase-deficient (type II) maple syrup urine disease. Aberrant splicing of E2 mRNA caused by internal intronic deletions and association with thiamine-responsive phenotype. *J Clin Invest* **100**, 736-44.

Ciszak EM, Korotchkina LG, Dominiak PM, Sidhu S & Patel MS (2003) Structural basis for flip-flop action of thiamine pyrophosphate-dependent enzymes revealed by human pyruvate dehydrogenase. *J Biol Chem* **278**, 21240-6.

Ciszak EM, Makal A, Hong YS, Vettaikkorumakankauv AK, Korotchkina LG & Patel MS (2006) How dihydrolipoamide dehydrogenase-binding protein binds dihydrolipoamide dehydrogenase in the human pyruvate dehydrogenase complex. *J Biol Chem* **281**, 648-55.

Clarkson GH & Lindsay JG (1991) Immunology, biosynthesis and in vivo assembly of the branched-chain 2-oxoacid dehydrogenase complex from bovine kidney. *Eur J Biochem* **196**, 95-100.

Coppel RL, McNeilage LJ, Surh CD, Van de Water J, Spithill TW, Whittingham S & Gershwin ME (1988) Primary structure of the human M2 mitochondrial autoantigen of primary biliary cirrhosis: dihydrolipoamide acetyltransferase. *Proc Natl Acad Sci U S A* **85**, 7317-21.

Cronan JE, Zhao X & Jiang Y (2005) Function, attachment and synthesis of lipoic acid in *Escherichia coli. Adv Microb Physiol* **50**, 103-46.

Cullingford TE, Clark JB & Phillips IR (1994) The pyruvate dehydrogenase complex: cloning of the rat somatic E1 alpha subunit and its coordinate expression with the mRNAs for the E1 beta, E2, and E3 catalytic subunits in developing rat brain. *J Neurochem* **62**, 1682-90.

Dahl HH, Hunt SM, Hutchison WM & Brown GK (1987) The human pyruvate dehydrogenase complex. Isolation of cDNA clones for the E1 alpha subunit, sequence analysis, and characterization of the mRNA. *J Biol Chem* **262**, 7398-403.

Dardel F, Davis AL, Laue ED & Perham RN (1993) Three-dimensional structure of the lipoyl domain from *Bacillus stearothermophilus* pyruvate dehydrogenase multienzyme complex. *J Mol Biol* **229**, 1037-48.

Davies JM (2000) Introduction: Epitope mimicry as a component cause of autoimmune disease. *Cell Mol Life Sci* **57**, 523-6.

Davis PA, Leung P, Manns M, Kaplan M, Munoz SJ, Gorin FA, Dickson ER, Krawitt E, Coppel R & Gershwin ME (1992) M4 and M9 antibodies in the overlap syndrome of

primary biliary cirrhosis and chronic active hepatitis: epitopes or epiphenomena? *Hepatology* **16**, 1128-36.

De Groote J (1991) [Mitochondrial antigens and their antibodies]. *Acta Gastroenterol Belg* **54**, 19-26.

De Kok A, Hengeveld AF, Martin A & Westphal AH (1998) The pyruvate dehydrogenase multi-enzyme complex from Gram-negative bacteria. *Biochim Biophys Acta* **1385**, 353-66.

De Marcucci O & Lindsay JG (1985) Component X. An immunologically distinct polypeptide associated with mammalian pyruvate dehydrogenase multi-enzyme complex. *Eur J Biochem* **149**, 641-8.

De Marcucci OG, Gibb GM, Dick J & Lindsay JG (1988) Biosynthesis, import and processing of precursor polypeptides of mammalian mitochondrial pyruvate dehydrogenase complex. *Biochem J* **251**, 817-23.

De Marcucci OG, Hodgson JA & Lindsay JG (1986) The Mr-50 000 polypeptide of mammalian pyruvate dehydrogenase complex participates in the acetylation reactions. *Eur J Biochem* **158**, 587-94.

De Marcucci OL, DeBuysere MS & Olson MS (1995) Dissociation and reassembly of the dihydrolipoyl transacetylase component of the bovine heart pyruvate dehydrogenase complex. *Arch Biochem Biophys* **323**, 169-76.

De Marcucci OL, Hunter A & Lindsay JG (1985) Low immunogenicity of the common lipoamide dehydrogenase subunit (E3) of mammalian pyruvate dehydrogenase and 2-oxoglutarate dehydrogenase multienzyme complexes. *Biochem J* **226**, 509-17.

Deshaies RJ, Koch BD, Werner-Washburne M, Craig EA & Schekman R (1988) A subfamily of stress proteins facilitates translocation of secretory and mitochondrial precursor polypeptides. *Nature* **332**, 800-5.

Dey R, Mine M, Desguerre I, Slama A, Van Den Berghe L, Brivet M, Aral B & Marsac C (2003) A new case of pyruvate dehydrogenase deficiency due to a novel mutation in the *PDX1* gene. *Ann Neurol* **53**, 273-7.

Doyle HA & Mamula MJ (2001) Post-translational protein modifications in antigen recognition and autoimmunity. *Trends Immunol* **22**, 443-9.

Dubel L, Tanaka A, Leung PS, Van de Water J, Coppel R, Roche T, Johanet C, Motokawa Y, Ansari A & Gershwin ME (1999) Autoepitope mapping and reactivity of autoantibodies to the dihydrolipoamide dehydrogenase-binding protein (E3BP) and the glycine cleavage proteins in primary biliary cirrhosis. *Hepatology* **29**, 1013-8.

Eliasson E, Gardner I, Hume-Smith H, de Waziers I, Beaune P & Kenna JG (1998) Interindividual variability in P450-dependent generation of neoantigens in halothane hepatitis. *Chem Biol Interact* **116**, 123-41.

Endo T, Mitsui S, Nakai M & Roise D (1996) Binding of mitochondrial presequences to yeast cytosolic heat shock protein 70 depends on the amphiphilicity of the presequence. *J Biol Chem* **271**, 4161-7.

Farris AD, Keech CL, Gordon TP & McCluskey J (2000) Epitope mimics and determinant spreading: pathways to autoimmunity. *Cell Mol Life Sci* **57**, 569-78.

Fisher CR, Fisher CW, Chuang DT & Cox RP (1991) Occurrence of a Tyr393----Asn (Y393N) mutation in the E1 alpha gene of the branched-chain alpha-keto acid dehydrogenase complex in maple syrup urine disease patients from a Mennonite population. *Am J Hum Genet* **49**, 429-34.

Flannery GR, Burroughs AK, Butler P, Chelliah J, Hamilton-Miller J, Brumfitt W & Baum H (1989) Antimitochondrial antibodies in primary biliary cirrhosis recognize both specific peptides and shared epitopes of the M2 family of antigens. *Hepatology* **10**, 370-4.

Floreani A, Naccarato R & Chiaramonte M (1997) Prevalence of familial disease in primary biliary cirrhosis in Italy. *J Hepatol* **26**, 737-8.

Frank RA, Pratap JV, Pei XY, Perham RN & Luisi BF (2005) The molecular origins of specificity in the assembly of a multienzyme complex. *Structure (Camb)* **13**, 1119-30.

Fregeau DR, Davis PA, Danner DJ, Ansari A, Coppel RL, Dickson ER & Gershwin ME (1989) Antimitochondrial antibodies of primary biliary cirrhosis recognize dihydrolipoamide acyltransferase and inhibit enzyme function of the branched chain alpha-ketoacid dehydrogenase complex. *J Immunol* **142**, 3815-20.

Fregeau DR, Prindiville T, Coppel RL, Kaplan M, Dickson ER & Gershwin ME (1990a) Inhibition of alpha-ketoglutarate dehydrogenase activity by a distinct population of autoantibodies recognizing dihydrolipoamide succinyltransferase in primary biliary cirrhosis. *Hepatology* **11**, 975-81.

Fregeau DR, Roche TE, Davis PA, Coppel R & Gershwin ME (1990b) Primary biliary cirrhosis. Inhibition of pyruvate dehydrogenase complex activity by autoantibodies specific for E1 alpha, a non-lipoic acid containing mitochondrial enzyme. *J Immunol* **144**, 1671-6.

Frey N, Christen U, Jeno P, Yeaman SJ, Shimomura Y, Kenna JG, Gandolfi AJ, Ranek L & Gut J (1995) The lipoic acid containing components of the 2-oxoacid dehydrogenase complexes mimic trifluoroacetylated proteins and are autoantigens associated with halothane hepatitis. *Chem Res Toxicol* **8**, 736-46.

Fries M, Stott KM, Reynolds S & Perham RN (2007) Distinct modes of recognition of the lipoyl domain as substrate by the E1 and E3 components of the pyruvate dehydrogenase multienzyme complex. *J Mol Biol* **366**, 132-9.

Fujiwara K, Okamura-Ikeda K & Motokawa Y (1994) Purification and characterization of lipoyl-AMP:N epsilon-lysine lipoyltransferase from bovine liver mitochondria. *J Biol Chem* **269**, 16605-9.

Fujiwara K, Okamura-Ikeda K & Motokawa Y (1996) Lipoylation of acyltransferase components of alpha-ketoacid dehydrogenase complexes. *J Biol Chem* **271**, 12932-6.

Fujiwara K, Takeuchi S, Okamura-Ikeda K & Motokawa Y (2001) Purification, characterization, and cDNA cloning of lipoate-activating enzyme from bovine liver. *J Biol Chem* **276**, 28819-23.

Fukushima N, Nalbandian G, Van De Water J, White K, Ansari AA, Leung P, Kenny T, Kamita SG, Hammock BD, Coppel RL, Stevenson F, Ishibashi H & Gershwin ME (2002) Characterization of recombinant monoclonal IgA anti-PDC-E2 autoantibodies derived from patients with PBC. *Hepatology* **36**, 1383-92.

Furst SM, Luedke D & Gandolfi AJ (1997) Kupffer cells from halothane-exposed guinea pigs carry trifluoroacetylated protein adducts. *Toxicology* **120**, 119-32.

Fussey SP, Ali ST, Guest JR, James OF, Bassendine MF & Yeaman SJ (1990) Reactivity of primary biliary cirrhosis sera with *Escherichia coli* dihydrolipoamide acetyltransferase (E2p): characterization of the main immunogenic region. *Proc Natl Acad Sci U S A* **87**, 3987-91.

Fussey SP, Bassendine MF, Fittes D, Turner IB, James OF & Yeaman SJ (1989a) The E1 alpha and beta subunits of the pyruvate dehydrogenase complex are M2'd' and M2'e' autoantigens in primary biliary cirrhosis. *Clin Sci (Lond)* **77**, 365-8.

Fussey SP, Bassendine MF, James OF & Yeaman SJ (1989b) Characterisation of the reactivity of autoantibodies in primary biliary cirrhosis. *FEBS Lett* **246**, 49-53.

Fussey SP, Guest JR, James OF, Bassendine MF & Yeaman SJ (1988) Identification and analysis of the major M2 autoantigens in primary biliary cirrhosis. *Proc Natl Acad Sci U S A* **85**, 8654-8.

Fussey SP, Lindsay JG, Fuller C, Perham RN, Dale S, James OF, Bassendine MF & Yeaman SJ (1991) Autoantibodies in primary biliary cirrhosis: analysis of reactivity against eukaryotic and prokaryotic 2-oxo acid dehydrogenase complexes. *Hepatology* **13**, 467-74.

Gakh O, Cavadini P & Isaya G (2002) Mitochondrial processing peptidases. *Biochim Biophys Acta* **1592**, 63-77.

Gasser SM, Daum G & Schatz G (1982) Import of proteins into mitochondria. Energy-dependent uptake of precursors by isolated mitochondria. *J Biol Chem* **257**, 13034-41.

Geoffroy V, Fouque F, Benelli C, Poggi F, Saudubray JM, Lissens W, Meirleir LD, Marsac C, Lindsay JG & Sanderson SJ (1996) Defect in the X-lipoyl-containing component of the pyruvate dehydrogenase complex in a patient with neonatal lactic acidemia. *Pediatrics* **97**, 267-72.

Gerken G, Manns M, Ramadori G & Meyer zum Buschenfelde KH (1988) The target antigens of antimitochondrial antibodies (AMAs) in primary biliary cirrhosis. *Hepatology* **8**, 705-6.

Gershwin ME, Ansari AA, Mackay IR, Nakanuma Y, Nishio A, Rowley MJ & Coppel RL (2000) Primary biliary cirrhosis: an orchestrated immune response against epithelial cells. *Immunol Rev* **174**, 210-25.

Gershwin ME, Mackay IR, Sturgess A & Coppel RL (1987) Identification and specificity of a cDNA encoding the 70 kd mitochondrial antigen recognized in primary biliary cirrhosis. *J Immunol* **138**, 3525-31.

Ghadiminejad I & Baum H (1987a) Reaction pattern of mitochondrial antibodies of primary biliary cirrhosis (PBC) is species specific but not organ specific. *J Bioenerg Biomembr* **19**, 239-53.

Ghadiminejad I & Baum H (1987b) Evidence for the cell-surface localization of antigens cross-reacting with the "mitochondrial antibodies" of primary biliary cirrhosis. *Hepatology* **7**, 743-9.

Gibson GE, Park LC, Sheu KF, Blass JP & Calingasan NY (2000) The alpha-ketoglutarate dehydrogenase complex in neurodegeneration. *Neurochem Int* **36**, 97-112.

Gibson GE, Zhang H, Sheu KF, Bogdanovich N, Lindsay JG, Lannfelt L, Vestling M & Cowburn RF (1998) Alpha-ketoglutarate dehydrogenase in Alzheimer brains bearing the APP670/671 mutation. *Ann Neurol* **44**, 676-81.

Glover LA & Lindsay JG (1992) Targeting proteins to mitochondria: a current overview. *Biochem J* **284 (Pt 3)**, 609-20.

Goodnow CC (1996) Balancing immunity and tolerance: deleting and tuning lymphocyte repertoires. *Proc Natl Acad Sci U S A* **93**, 2264-71.

Graham LD, Packman LC & Perham RN (1989) Kinetics and specificity of reductive acylation of lipoyl domains from 2-oxo acid dehydrogenase multienzyme complexes. *Biochemistry* **28**, 1574-81.

Green JD, Laue ED, Perham RN, Ali ST & Guest JR (1995a) Three-dimensional structure of a lipoyl domain from the dihydrolipoyl acetyltransferase component of the pyruvate dehydrogenase multienzyme complex of *Escherichia coli*. *J Mol Biol* **248**, 328-43.

Green DE, Morris TW, Green J, Cronan JE, Jr. & Guest JR (1995b) Purification and properties of the lipoate protein ligase of *Escherichia coli*. *Biochem J* **309 (Pt 3)**, 853-62.

Green JD, Perham RN, Ullrich SJ & Appella E (1992) Conformational studies of the interdomain linker peptides in the dihydrolipoyl acetyltransferase component of the pyruvate dehydrogenase multienzyme complex of *Escherichia coli*. *J Biol Chem* **267**, 23484-8.

Guest JR, Angier SJ & Russell GC (1989) Structure, expression, and protein engineering of the pyruvate dehydrogenase complex of *Escherichia coli*. *Ann N Y Acad Sci* **573**, 76-99.

Guest JR, Lewis HM, Graham LD, Packman LC & Perham RN (1985) Genetic reconstruction and functional analysis of the repeating lipoyl domains in the pyruvate dehydrogenase multienzyme complex of *Escherichia coli*. *J Mol Biol* **185**, 743-54.

Gut J, Christen U, Frey N, Koch V & Stoffler D (1995) Molecular mimicry in halothane hepatitis: biochemical and structural characterization of lipoylated autoantigens. *Toxicology* **97**, 199-224.

Harada K, Van de Water J, Leung PS, Coppel RL, Ansari A, Nakanuma Y & Gershwin ME (1997a) In situ nucleic acid hybridization of cytokines in primary biliary cirrhosis: predominance of the Th1 subset. *Hepatology* **25**, 791-6.

Harada K, Ozaki S, Gershwin ME & Nakanuma Y (1997b) Enhanced apoptosis relates to bile duct loss in primary biliary cirrhosis. *Hepatology* **26**, 1399-405.

Harada K, Van de Water J, Leung PS, Coppel RL, Nakanuma Y & Gershwin ME (1997c) In situ nucleic acid hybridization of pyruvate dehydrogenase complex-E2 in primary biliary cirrhosis: pyruvate dehydrogenase complex-E2 messenger RNA is expressed in hepatocytes but not in biliary epithelium. *Hepatology* **25**, 27-32.

Harada K, Sudo Y, Kono N, Ozaki S, Tsuneyama K, Gershwin ME & Nakanuma Y (1999) In situ nucleic acid detection of PDC-E2, BCOADC-E2, OGDC-E2, PDC-E1alpha, BCOADC-E1alpha, OGDC-E1, and the E3 binding protein (protein X) in primary biliary cirrhosis. *Hepatology* **30**, 36-45.

Harris RA, Bowker-Kinley MM, Wu P, Jeng J & Popov KM (1997) Dihydrolipoamide dehydrogenase-binding protein of the human pyruvate dehydrogenase complex. DNA-derived amino acid sequence, expression, and reconstitution of the pyruvate dehydrogenase complex. *J Biol Chem* **272**, 19746-51.

Hasson MS, Muscate A, McLeish MJ, Polovnikova LS, Gerlt JA, Kenyon GL, Petsko GA & Ringe D (1998) The crystal structure of benzoylformate decarboxylase at 1.6 A resolution: diversity of catalytic residues in thiamine diphosphate-dependent enzymes. *Biochemistry* **37**, 9918-30.

Hawkins CF, Borges A & Perham RN (1989) A common structural motif in thiamine pyrophosphate-binding enzymes. *FEBS Lett* **255**, 77-82.

Haynes RL, Szweda L, Pickin K, Welker ME & Townsend AJ (2000) Structure-activity relationships for growth inhibition and induction of apoptosis by 4-hydroxy-2-nonenal in raw 264.7 cells. *Mol Pharmacol* **58**, 788-94.

Head RA, Brown RM, Zolkipli Z, Shahdadpuri R, King MD, Clayton PT & Brown GK (2005) Clinical and genetic spectrum of pyruvate dehydrogenase deficiency: dihydrolipoamide acetyltransferase (E2) deficiency. *Ann Neurol* **58**, 234-41.

Hendle J, Mattevi A, Westphal AH, Spee J, de Kok A, Teplyakov A & Hol WG (1995) Crystallographic and enzymatic investigations on the role of Ser558, His610, and Asn614 in the catalytic mechanism of *Azotobacter vinelandii* dihydrolipoamide acetyltransferase (E2p). *Biochemistry* **34**, 4287-98.

Hengeveld AF & de Kok A (2002) Structural basis of the dysfunctioning of human 2-oxo acid dehydrogenase complexes. *Curr Med Chem* **9**, 499-520.

Hipps DS, Packman LC, Allen MD, Fuller C, Sakaguchi K, Appella E & Perham RN (1994) The peripheral subunit-binding domain of the dihydrolipoyl acetyltransferase component of the pyruvate dehydrogenase complex of *Bacillus stearothermophilus*: preparation and characterization of its binding to the dihydrolipoyl dehydrogenase component. *Biochem J* **297 (Pt 1)**, 137-43.

Hiromasa Y, Fujisawa T, Aso Y & Roche TE (2004) Organization of the cores of the mammalian pyruvate dehydrogenase complex formed by E2 and E2 plus the E3-binding protein and their capacities to bind the E1 and E3 components. *J Biol Chem* **279**, 6921-33.

Hodgson JA, De Marcucci OG & Lindsay JG (1986) Lipoic acid is the site of substrate-dependent acetylation of component X in ox heart pyruvate dehydrogenase multienzyme complex. *Eur J Biochem* **158**, 595-600.

Homanics GE, Skvorak K, Ferguson C, Watkins S & Paul HS (2006) Production and characterization of murine models of classic and intermediate maple syrup urine disease. *BMC Med Genet* **7**, 33.

Hong YS, Kerr DS, Craigen WJ, Tan J, Pan Y, Lusk M & Patel MS (1996) Identification of two mutations in a compound heterozygous child with dihydrolipoamide dehydrogenase deficiency. *Hum Mol Genet* **5**, 1925-30.

Hong YS, Kerr DS, Liu TC, Lusk M, Powell BR & Patel MS (1997) Deficiency of dihydrolipoamide dehydrogenase due to two mutant alleles (E340K and G101del). Analysis of a family and prenatal testing. *Biochim Biophys Acta* **1362**, 160-8.

Horst M, Azem A, Schatz G & Glick BS (1997a) What is the driving force for protein import into mitochondria? *Biochim Biophys Acta* **1318**, 71-8.

Horst M, Oppliger W, Rospert S, Schonfeld HJ, Schatz G & Azem A (1997b) Sequential action of two hsp70 complexes during protein import into mitochondria. *Embo J* **16**, 1842-9.

Howard MJ, Fuller C, Broadhurst RW, Perham RN, Tang JG, Quinn J, Diamond AG & Yeaman SJ (1998) Three-dimensional structure of the major autoantigen in primary biliary cirrhosis. *Gastroenterology* **115**, 139-46.

Huang B, Gudi R, Wu P, Harris RA, Hamilton J & Popov KM (1998) Isoenzymes of pyruvate dehydrogenase phosphatase. DNA-derived amino acid sequences, expression, and regulation. *J Biol Chem* **273**, 17680-8.

Huh TL, Casazza JP, Huh JW, Chi YT & Song BJ (1990) Characterization of two cDNA clones for pyruvate dehydrogenase E1 beta subunit and its regulation in tricarboxylic acid cycle-deficient fibroblast. *J Biol Chem.* **265**, 13320-6.

Humphries KM & Szweda LI (1998) Selective inactivation of alpha-ketoglutarate dehydrogenase and pyruvate dehydrogenase: reaction of lipoic acid with 4-hydroxy-2-nonenal. *Biochemistry* **37**, 15835-41.

Humphries KM, Yoo Y & Szweda LI (1998) Inhibition of NADH-linked mitochondrial respiration by 4-hydroxy-2-nonenal. *Biochemistry* **37**, 552-7.

Hunter A & Lindsay JG (1986) Immunological and biosynthetic studies on the mammalian 2-oxoglutarate dehydrogenase multienzyme complex. *Eur J Biochem* **155**, 103-9.

Ichiki Y, Shimoda S, Ishibashi H & Gershwin ME (2004) Is primary biliary cirrhosis a model autoimmune disease? *Autoimmun Rev* **3**, 331-6.

Invernizzi P, Miozzo M, Selmi C, Persani L, Battezzati PM, Zuin M, Lucchi S, Meroni PL, Marasini B, Zeni S, Watnik M, Grati FR, Simoni G, Gershwin ME & Podda M (2005) X chromosome monosomy: a common mechanism for autoimmune diseases. *J Immunol* **175**, 575-8.

Ishibashi H, Nakamura M, Shimoda S & Gershwin ME (2003) T cell immunity and primary biliary cirrhosis. *Autoimmun Rev* **2**, 19-24.

Izard T, Aevarsson A, Allen MD, Westphal AH, Perham RN, de Kok A & Hol WG (1999) Principles of quasi-equivalence and Euclidean geometry govern the assembly of cubic and dodecahedral cores of pyruvate dehydrogenase complexes. *Proc Natl Acad Sci U S A* **96**, 1240-5.

Jilka JM, Rahmatullah M, Kazemi M & Roche TE (1986) Properties of a newly characterized protein of the bovine kidney pyruvate dehydrogenase complex. *J Biol Chem* **261**, 1858-67.

Jones DD, Horne HJ, Reche PA & Perham RN (2000a) Structural determinants of post-translational modification and catalytic specificity for the lipoyl domains of the pyruvate dehydrogenase multienzyme complex of *Escherichia coli*. *J Mol Biol* **295**, 289-306.

Jones DE (2000b) Autoantigens in primary biliary cirrhosis. *J Clin Pathol* **53**, 813-21.

Jones DE (2003) Pathogenesis of primary biliary cirrhosis. *J Hepatol* **39**, 639-48.

Jones DE, Palmer JM, Bennett K, Robe AJ, Yeaman SJ, Robertson H, Bassendine MF, Burt AD & Kirby JA (2002) Investigation of a mechanism for accelerated breakdown of immune tolerance to the primary biliary cirrhosis-associated autoantigen, pyruvate dehydrogenase complex. *Lab Invest* **82**, 211-9.

Jones DE, Palmer JM, James OF, Yeaman SJ, Bassendine MF & Diamond AG (1995) T-cell responses to the components of pyruvate dehydrogenase complex in primary biliary cirrhosis. *Hepatology* **21**, 995-1002.

Jones DE, Palmer JM, Yeaman SJ, Bassendine MF & Diamond AG (1997) T cell responses to natural human proteins in primary biliary cirrhosis. *Clin Exp Immunol* **107**, 562-8.

Jones DE, Watt FE, Metcalf JV, Bassendine MF & James OF (1999a) Familial primary biliary cirrhosis reassessed: a geographically-based population study. *J Hepatol* **30**, 402-7.

Jones DE, Palmer JM, Yeaman SJ, Kirby JA & Bassendine MF (1999b) Breakdown of tolerance to pyruvate dehydrogenase complex in experimental autoimmune cholangitis: a mouse model of primary biliary cirrhosis. *Hepatology* **30**, 65-70.

Joplin R, Lindsay JG, Hubscher SG, Johnson GD, Shaw JC, Strain AJ & Neuberger JM (1991) Distribution of dihydrolipoamide acetyltransferase (E2) in the liver and portal lymph nodes of patients with primary biliary cirrhosis: an immunohistochemical study. *Hepatology* **14**, 442-7.

Joplin R, Lindsay JG, Johnson GD, Strain A & Neuberger J (1992) Membrane dihydrolipoamide acetyltransferase (E2) on human biliary epithelial cells in primary biliary cirrhosis. *Lancet* **339**, 93-4.

Joplin R, Strain AJ & Neuberger JM (1989) Immuno-isolation and culture of biliary epithelial cells from normal human liver. *In Vitro Cell Dev Biol* **25**, 1189-92.

Joplin R, Strain AJ & Neuberger JM (1990) Biliary epithelial cells from the liver of patients with primary biliary cirrhosis: isolation, characterization, and short-term culture. *J Pathol* **162**, 255-60.

Joplin R, Wallace LL, Johnson GD, Lindsay JG, Yeaman SJ, Palmer JM, Strain AJ & Neuberger JM (1995) Subcellular localization of pyruvate dehydrogenase dihydrolipoamide acetyltransferase in human intrahepatic biliary epithelial cells. *J Pathol* **176**, 381-90.

Joplin RE, Johnson GD, Matthews JB, Hamburger J, Lindsay JG, Hubscher SG, Strain AJ & Neuberger JM (1994) Distribution of pyruvate dehydrogenase dihydrolipoamide acetyltransferase (PDC-E2) and another mitochondrial marker in salivary gland and biliary epithelium from patients with primary biliary cirrhosis. *Hepatology* **19**, 1375-80.

Joplin RE, Wallace LL, Lindsay JG, Palmer JM, Yeaman SJ & Neuberger JM (1997) The human biliary epithelial cell plasma membrane antigen in primary biliary cirrhosis: pyruvate dehydrogenase X? *Gastroenterology* **113**, 1727-33.

Jordan SW & Cronan JE, Jr. (2003) The *Escherichia coli lipB* gene encodes lipoyl (octanoyl)-acyl carrier protein:protein transferase. *J Bacteriol* **185**, 1582-9.

Jung HI, Cooper A & Perham RN (2002) Identification of key amino acid residues in the assembly of enzymes into the pyruvate dehydrogenase complex of *Bacillus stearothermophilus*: a kinetic and thermodynamic analysis. *Biochemistry* **41**, 10446-53.

Jung HI, Cooper A & Perham RN (2003) Interactions of the peripheral subunit-binding domain of the dihydrolipoyl acetyltransferase component in the assembly of the pyruvate dehydrogenase multienzyme complex of *Bacillus stearothermophilus*. *Eur J Biochem* **270**, 4488-96.

Kalia YN, Brocklehurst SM, Hipps DS, Appella E, Sakaguchi K & Perham RN (1993) The high-resolution structure of the peripheral subunit-binding domain of dihydrolipoamide acetyltransferase from the pyruvate dehydrogenase multienzyme complex of *Bacillus stearothermophilus*. *J Mol Biol* **230**, 323-41.

Kaplan MM (1996) Primary biliary cirrhosis. *N Engl J Med* **335**, 1570-80.

Kaplan MM & Gershwin ME (2005) Primary biliary cirrhosis. *N Engl J Med* **353**, 1261-73.

Karpova T, Danchuk S, Kolobova E & Popov KM (2003) Characterization of the isozymes of pyruvate dehydrogenase phosphatase: implications for the regulation of pyruvate dehydrogenase activity. *Biochim Biophys Acta* **1652**, 126-35.

Kawamura K, Kobayashi Y, Kageyama F, Kawasaki T, Nagasawa M, Toyokuni S, Uchida K & Nakamura H (2000) Enhanced hepatic lipid peroxidation in patients with primary biliary cirrhosis. *Am J Gastroenterol* **95**, 3596-601.

Kerr MA, Mazengera RL & Stewart WW (1990) Structure and function of immunoglobulin A receptors on phagocytic cells. *Biochem Soc Trans* **18**, 215-7.

Kiebler M, Becker K, Pfanner N & Neupert W (1993) Mitochondrial protein import: specific recognition and membrane translocation of preproteins. *J Membr Biol* **135**, 191-207.

Kim H & Patel MS (1992) Characterization of two site-specifically mutated human dihydrolipoamide dehydrogenases (His-452----Gln and Glu-457----Gln). *J Biol Chem* **267**, 5128-32.

Kita H, Lian ZX, Van de Water J, He XS, Matsumura S, Kaplan M, Luketic V, Coppel RL, Ansari AA & Gershwin ME (2002a) Identification of HLA-A2-restricted CD8(+) cytotoxic T cell responses in primary biliary cirrhosis: T cell activation is augmented by immune complexes cross-presented by dendritic cells. *J Exp Med* **195**, 113-23.

Kita H, Matsumura S, He XS, Ansari AA, Lian ZX, Van de Water J, Coppel RL, Kaplan MM & Gershwin ME (2002b) Quantitative and functional analysis of PDC-E2-specific autoreactive cytotoxic T lymphocytes in primary biliary cirrhosis. *J Clin Invest* **109**, 1231-40.

Kita H, Matsumura S, He XS, Ansari AA, Lian ZX, Van de Water J, Coppel RL, Kaplan MM & Gershwin ME (2002c) Analysis of TCR antagonism and molecular mimicry of an HLA-A0201-restricted CTL epitope in primary biliary cirrhosis. *Hepatology* **36**, 918-26.

Kleanthous C, Cullis PM & Shaw WV (1985) 3-(Bromoacetyl) chloramphenicol, an active site directed inhibitor for chloramphenicol acetyltransferase. *Biochemistry* **24**, 5307-13.

Klein R & Berg PA (1990) Anti-M9 antibodies in sera from patients with primary biliary cirrhosis recognize an epitope of glycogen phosphorylase. *Clin Exp Immunol* **81**, 65-71.

Klein R & Berg PA (1991) Anti-M4 antibodies in primary biliary cirrhosis react with sulphite oxidase, an enzyme of the mitochondrial inter-membrane space. *Clin Exp Immunol* **84**, 445-8.

Klein R, Wiebel M, Engelhart S & Berg PA (1993) Sera from patients with tuberculosis recognize the M2a-epitope (E2-subunit of pyruvate dehydrogenase) specific for primary biliary cirrhosis. *Clin Exp Immunol* **92**, 308-16.

Klingbeil MM, Walker DJ, Arnette R, Sidawy E, Hayton K, Komuniecki PR & Komuniecki R (1996) Identification of a novel dihydrolipoyl dehydrogenase-binding protein in the pyruvate dehydrogenase complex of the anaerobic parasitic nematode, *Ascaris suum*. *J Biol Chem* **271**, 5451-7.

Klyuyeva A, Tuganova A & Popov KM (2005) The carboxy-terminal tail of pyruvate dehydrogenase kinase 2 is required for the kinase activity. *Biochemistry* **44**, 13573-82.

Knapp JE, Mitchell DT, Yazdi MA, Ernst SR, Reed LJ & Hackert ML (1998) Crystal structure of the truncated cubic core component of the *Escherichia coli* 2-oxoglutarate dehydrogenase multienzyme complex. *J Mol Biol* **280**, 655-68.

Koga H, Sakisaka S, Ohishi M, Sata M & Tanikawa K (1997) Nuclear DNA fragmentation and expression of Bcl-2 in primary biliary cirrhosis. *Hepatology* **25**, 1077-84.

Koike K (1974) [Studies on pig heart 2-oxoglutarate dehydrogenase (author's transl)]. *Seikagaku* **46**, 325-35.

Koike K, Ishibashi H & Koike M (1998) Immunoreactivity of porcine heart dihydrolipoamide acetyl- and succinyl-transferases (PDC-E2, OGDC-E2) with primary biliary cirrhosis sera: characterization of the autoantigenic region and effects of enzymatic delipoylation and relipoylation. *Hepatology* **27**, 1467-74.

Koike K, Suematsu T & Ehara M (2000) Cloning, overexpression and mutagenesis of cDNA encoding dihydrolipoamide succinyltransferase component of the porcine 2-oxoglutarate dehydrogenase complex. *Eur J Biochem* **267**, 3005-16.

Koike K, Urata Y, Matsuo S & Koike M (1990) Characterization and nucleotide sequence of the gene encoding the human pyruvate dehydrogenase alpha-subunit. *Gene* **93**, 307-11.

Koike M & Koike K (1976) Structure, assembly and function of mammalian alpha-keto acid dehydrogenase complexes. *Adv Biophys*, 187-227.

Korotchkina LG & Patel MS (1995) Mutagenesis studies of the phosphorylation sites of recombinant human pyruvate dehydrogenase. Site-specific regulation. *J Biol Chem* **270**, 14297-304.

Korotchkina LG, Khailova LS & Severin SE (1995) The effect of phosphorylation on pyruvate dehydrogenase. *FEBS Lett* **364**, 185-8.

Laemli UK (1970) Cleavage of structural proteins during the assembly of the head of bacteriopage T4. *Nature,* **227**, 680-685.

Lane CS (2005) Mass spectrometry-based proteomics in the life sciences. *Cell Mol Life Sci* **62**, 848-69.

Lau KS, Chuang JL, Herring WJ, Danner DJ, Cox RP & Chuang DT (1992) The complete cDNA sequence for dihydrolipoyl transacylase (E2) of human branched-chain alpha-keto acid dehydrogenase complex. *Biochim Biophys Acta* **1132**, 319-21.

Lawson JE, Behal RH & Reed LJ (1991a) Disruption and mutagenesis of the *Saccharomyces cerevisiae* PDX1 gene encoding the protein X component of the pyruvate dehydrogenase complex. *Biochemistry* **30**, 2834-9.

Lawson JE, Niu XD & Reed LJ (1991b) Functional analysis of the domains of dihydrolipoamide acetyltransferase from *Saccharomyces cerevisiae*. *Biochemistry* **30**, 11249-54.

Lessard IA, Fuller C & Perham RN (1996) Competitive interaction of component enzymes with the peripheral subunit-binding domain of the pyruvate dehydrogenase multienzyme complex of *Bacillus stearothermophilus:* kinetic analysis using surface plasmon resonance detection. *Biochemistry* **35**, 16863-70.

Lessard IA & Perham RN (1994) Expression in *Escherichia coli* of genes encoding the E1 alpha and E1 beta subunits of the pyruvate dehydrogenase complex of *Bacillus stearothermophilus* and assembly of a functional E1 component (alpha 2 beta 2) in vitro. *J Biol Chem* **269**, 10378-83.

Lessard IA & Perham RN (1995) Interaction of component enzymes with the peripheral subunit-binding domain of the pyruvate dehydrogenase multienzyme complex of *Bacillus stearothermophilus*: stoichiometry and specificity in self-assembly. *Biochem J* **306 (Pt 3)**, 727-33.

Leung PS, Chuang DT, Wynn RM, Cha S, Danner DJ, Ansari A, Coppel RL & Gershwin ME (1995) Autoantibodies to BCOADC-E2 in patients with primary biliary cirrhosis recognize a conformational epitope. *Hepatology* **22**, 505-13.

Leung PS, Iwayama T, Coppel RL & Gershwin ME (1990) Site-directed mutagenesis of lysine within the immunodominant autoepitope of PDC-E2. *Hepatology* **12**, 1321-8.

Leung PS, Quan C, Park O, Van de Water J, Kurth MJ, Nantz MH, Ansari AA, Coppel RL, Lam KS & Gershwin ME (2003) Immunization with a xenobiotic 6-bromohexanoate bovine serum albumin conjugate induces antimitochondrial antibodies. *J Immunol* **170**, 5326-32.

Leung PS, Park O,Tsuneyama K, Kurth MJ, Lam KS, Ansari AA, Coppel RL & Gershwin ME.(2007) Induction of primary biliary cirrhosis in guinea pigs following chemical xenobiotic immunization. *J Immunol* **179**, 2651-7.

Leung PS, Van de Water J, Coppel RL, Nakanuma Y, Munoz S & Gershwin ME (1996) Molecular aspects and the pathological basis of primary biliary cirrhosis. *J Autoimmun* **9**, 119-28.

Liang B & Mamula MJ (2000) Molecular mimicry and the role of B lymphocytes in the processing of autoantigens. *Cell Mol Life Sci* **57**, 561-8.

Lindsay H, Beaumont E, Richards SD, Kelly SM, Sanderson SJ, Price NC & Lindsay JG (2000) FAD insertion is essential for attaining the assembly competence of the dihydrolipoamide dehydrogenase (E3) monomer from *Escherichia coli*. *J Biol Chem* **275**, 36665-70.

Lindsay JG (1989) Targeting of 2-oxo acid dehydrogenase complexes to the mitochondrion. *Ann N Y Acad Sci* **573**, 254-66.

Ling M, McEachern G, Seyda A, MacKay N, Scherer SW, Bratinova S, Beatty B, Giovannucci-Uzielli ML & Robinson BH (1998) Detection of a homozygous four base pair deletion in the protein X gene in a case of pyruvate dehydrogenase complex deficiency. *Hum Mol Genet* **7**, 501-5.

Linn TC, Pettit FH & Reed LJ (1969) Alpha-keto acid dehydrogenase complexes. X. Regulation of the activity of the pyruvate dehydrogenase complex from beef kidney

mitochondria by phosphorylation and dephosphorylation. *Proc Natl Acad Sci U S A* **62**, 234-41.

Lissens W, De Meirleir L, Seneca S, Benelli C, Marsac C, Poll-The BT, Briones P, Ruitenbeek W, van Diggelen O, Chaigne D, Ramaekers V & Liebaers I (1996) Mutation analysis of the pyruvate dehydrogenase E1 alpha gene in eight patients with a pyruvate dehydrogenase complex deficiency. *Hum Mutat* **7**, 46-51.

Lissens W, De Meirleir L, Seneca S, Liebaers I, Brown GK, Brown RM, Ito M, Naito E, Kuroda Y, Kerr DS, Wexler ID, Patel MS, Robinson BH & Seyda A (2000) Mutations in the X-linked pyruvate dehydrogenase (E1) alpha subunit gene (*PDHA1*) in patients with a pyruvate dehydrogenase complex deficiency. *Hum Mutat* **15**, 209-19.

Liu S, Baker JC & Roche TE (1995) Binding of the pyruvate dehydrogenase kinase to recombinant constructs containing the inner lipoyl domain of the dihydrolipoyl acetyltransferase component. *J Biol Chem* **270**, 793-800.

Long SA, Quan C, Van de Water J, Nantz MH, Kurth MJ, Barsky D, Colvin ME, Lam KS, Coppel RL, Ansari A & Gershwin ME (2001) Immunoreactivity of organic mimeotopes of the E2 component of pyruvate dehydrogenase: connecting xenobiotics with primary biliary cirrhosis. *J Immunol* **167**, 2956-63.

Long SA, Van de Water J & Gershwin ME (2002) Antimitochondrial antibodies in primary biliary cirrhosis: the role of xenobiotics. *Autoimmun Rev* **1**, 37-42.

Maas E & Bisswanger H (1990) Localization of the alpha-oxoacid dehydrogenase multienzyme complexes within the mitochondrion. *FEBS Lett* **277**, 189-90.

Macdonald P, Palmer J, Kirby JA & Jones DE (2004) Apoptosis as a mechanism for cell surface expression of the autoantigen pyruvate dehydrogenase complex. *Clin Exp Immunol* **136**, 559-67.

Machado RS, Clark DP & Guest JR (1992) Construction and properties of pyruvate dehydrogenase complexes with up to nine lipoyl domains per lipoate acetyltransferase chain. *FEMS Microbiol Lett* **79**, 243-8.

Mackay IR (1958) Primary biliary cirrhosis showing a high titer of autoantibody; report of a case. *N Engl J Med* **258**, 185-8.

Mackay IR, Whittingham S, Fida S, Myers M, Ikuno N, Gershwin ME & Rowley MJ (2000) The peculiar autoimmunity of primary biliary cirrhosis. *Immunol Rev* **174**, 226-37.

Maeng CY, Yazdi MA, Niu XD, Lee HY & Reed LJ (1994) Expression, purification, and characterization of the dihydrolipoamide dehydrogenase-binding protein of the pyruvate dehydrogenase complex from *Saccharomyces cerevisiae*. *Biochemistry* **33**, 13801-7.

Maeng CY, Yazdi MA & Reed LJ (1996) Stoichiometry of binding of mature and truncated forms of the dihydrolipoamide dehydrogenase-binding protein to the dihydrolipoamide acetyltransferase core of the pyruvate dehydrogenase complex from *Saccharomyces cerevisiae*. *Biochemistry* **35**, 5879-82.

Maj MC, Cameron JM & Robinson BH (2006) Pyruvate dehydrogenase phosphatase deficiency: orphan disease or an under-diagnosed condition? *Mol Cell Endocrinol* **249**, 1-9.

Malmborg AC, Shultz DB, Luton F, Mostov KE, Richly E, Leung PS, Benson GD, Ansari AA, Coppel RL, Gershwin ME & Van de Water J (1998) Penetration and co-localization in MDCK cell mitochondria of IgA derived from patients with primary biliary cirrhosis. *J Autoimmun* **11**, 573-80.

Mamula MJ (1998) Epitope spreading: the role of self peptides and autoantigen processing by B lymphocytes. *Immunol Rev* **164**, 231-9.

Mande SS, Sarfaty S, Allen MD, Perham RN & Hol WG (1996) Protein-protein interactions in the pyruvate dehydrogenase multienzyme complex: dihydrolipoamide dehydrogenase complexed with the binding domain of dihydrolipoamide acetyltransferase. *Structure* **4**, 277-86.

Marsac C, Stansbie D, Bonne G, Cousin J, Jehenson P, Benelli C, Leroux JP & Lindsay G (1993) Defect in the lipoyl-bearing protein X subunit of the pyruvate dehydrogenase complex in two patients with encephalomyelopathy. *J Pediatr* **123**, 915-20.

Martin J, Mahlke K & Pfanner N (1991) Role of an energized inner membrane in mitochondrial protein import. Delta psi drives the movement of presequences. *J Biol Chem* **266**, 18051-7.

Mato TK, Davis PA, Odin JA, Coppel RL & Gershwin ME (2004) Sidechain biology and the immunogenicity of PDC-E2, the major autoantigen of primary biliary cirrhosis. *Hepatology* **40**, 1241-8.

Matsui M, Nakamura M, Ishibashi H, Koike K, Kudo J & Niho Y (1993) Human monoclonal antibodies from a patient with primary biliary cirrhosis that recognize two distinct autoepitopes in the E2 component of the pyruvate dehydrogenase complex. *Hepatology* **18**, 1069-77.

Matsumura S, Van De Water J, Leung P, Odin JA, Yamamoto K, Gores GJ, Mostov K, Ansari AA, Coppel RL, Shiratori Y & Gershwin ME (2004) Caspase induction by IgA antimitochondrial antibody: IgA-mediated biliary injury in primary biliary cirrhosis. *Hepatology* **39**, 1415-22.

Mattevi A, Obmolova G, Kalk KH, Westphal AH, de Kok A & Hol WG (1993a) Refined crystal structure of the catalytic domain of dihydrolipoyl transacetylase (E2p) from *Azotobacter vinelandii* at 2.6 A resolution. *J Mol Biol* **230**, 1183-99.

Mattevi A, Obmolova G, Kalk KH, Teplyakov A & Hol WG (1993b) Crystallographic analysis of substrate binding and catalysis in dihydrolipoyl transacetylase (E2p). *Biochemistry* **32**, 3887-901.

Mattevi A, Obmolova G, Schulze E, Kalk KH, Westphal AH, de Kok A & Hol WG (1992) Atomic structure of the cubic core of the pyruvate dehydrogenase multienzyme complex. *Science* **255**, 1544-50.

Mazanec MB, Coudret CL & Fletcher DR (1995) Intracellular neutralization of influenza virus by immunoglobulin A anti-hemagglutinin monoclonal antibodies. *J Virol* **69**, 1339-43.

Mazanec MB, Kaetzel CS, Lamm ME, Fletcher D & Nedrud JG (1992) Intracellular neutralization of virus by immunoglobulin A antibodies. *Proc Natl Acad Sci U S A* **89**, 6901-5.

McCartney RG, Rice JE, Sanderson SJ, Bunik V, Lindsay H & Lindsay JG (1998) Subunit interactions in the mammalian alpha-ketoglutarate dehydrogenase complex. Evidence for direct association of the alpha-ketoglutarate dehydrogenase and dihydrolipoamide dehydrogenase components. *J Biol Chem* **273**, 24158-64.

McCartney RG, Sanderson SJ & Lindsay JG (1997) Refolding and reconstitution studies on the transacetylase-protein X (E2/X) subcomplex of the mammalian pyruvate dehydrogenase complex: evidence for specific binding of the dihydrolipoamide dehydrogenase component to sites on reassembled E2. *Biochemistry* **36**, 6819-26.

Medzhitov R & Janeway CA, Jr. (2000) How does the immune system distinguish self from nonself? *Semin Immunol* **12**, 185-8; discussion 257-344.

Mendel-Hartvig I, Nelson BD, Loof L & Totterman TH (1985) Primary biliary cirrhosis: further biochemical and immunological characterization of mitochondrial antigens. *Clin Exp Immunol* **62**, 371-9.

Meng M & Chuang DT (1994) Site-directed mutagenesis and functional analysis of the active-site residues of the E2 component of bovine branched-chain alpha-keto acid dehydrogenase complex. *Biochemistry* **33**, 12879-85.

Migliaccio C, Nishio A, Van de Water J, Ansari AA, Leung PS, Nakanuma Y, Coppel RL & Gershwin ME (1998) Monoclonal antibodies to mitochondrial E2 components define autoepitopes in primary biliary cirrhosis. *J Immunol* **161**, 5157-63.

Migliaccio C, Van de Water J, Ansari AA, Kaplan MM, Coppel RL, Lam KS, Thompson RK, Stevenson F & Gershwin ME (2001) Heterogeneous response of antimitochondrial autoantibodies and bile duct apical staining monoclonal antibodies to pyruvate dehydrogenase complex E2: the molecule versus the mimic. *Hepatology* **33**, 792-801.

Miles JS, Guest JR, Radford SE & Perham RN (1988) Investigation of the mechanism of active site coupling in the pyruvate dehydrogenase multienzyme complex of *Escherichia coli* by protein engineering. *J Mol Biol* **202**, 97-106.

Milne JL, Shi D, Rosenthal PB, Sunshine JS, Domingo GJ, Wu X, Brooks BR, Perham RN, Henderson R & Subramaniam S (2002) Molecular architecture and mechanism of an icosahedral pyruvate dehydrogenase complex: a multifunctional catalytic machine. *Embo J* **21**, 5587-98.

Mondino A, Khoruts A & Jenkins MK (1996) The anatomy of T-cell activation and tolerance. *Proc Natl Acad Sci U S A* **93**, 2245-52.

Morris HR, Paxton T, Panico M, McDowell R & Dell A (1997) A novel geometry mass spectrometer, the Q-TOF, for low-femtomole/attomole-range biopolymer sequencing. *J Protein Chem* **16**, 469-79.

Morris TW, Reed KE & Cronan JE, Jr. (1994) Identification of the gene encoding lipoate-protein ligase A of *Escherichia coli*. Molecular cloning and characterization of the *lplA* gene and gene product. *J Biol Chem* **269**, 16091-100.

Morris TW, Reed KE & Cronan JE, Jr. (1995) Lipoic acid metabolism in *Escherichia coli*: the *lplA* and *lipB* genes define redundant pathways for ligation of lipoyl groups to apoprotein. *J Bacteriol* **177**, 1-10.

Moteki S, Leung PS, Dickson ER, Van Thiel DH, Galperin C, Buch T, Alarcon-Segovia D, Kershenobich D, Kawano K, Coppel RL & et al. (1996) Epitope mapping and reactivity of autoantibodies to the E2 component of 2-oxoglutarate dehydrogenase complex in primary biliary cirrhosis using recombinant 2-oxoglutarate dehydrogenase complex. *Hepatology* **23**, 436-44.

Muller YA, Lindqvist Y, Furey W, Schulz GE, Jordan F & Schneider G (1993) A thiamine diphosphate binding fold revealed by comparison of the crystal structures of transketolase, pyruvate oxidase and pyruvate decarboxylase. *Structure* **1**, 95-103.

Mutimer DJ, Fussey SP, Yeaman SJ, Kelly PJ, James OF & Bassendine MF (1989) Frequency of IgG and IgM autoantibodies to four specific M2 mitochondrial autoantigens in primary biliary cirrhosis. *Hepatology* **10**, 403-7.

Nagatsu T (1997) Isoquinoline neurotoxins in the brain and Parkinson's disease. *Neurosci Res* **29**, 99-111.

Neagle J, De Marcucci O, Dunbar B & Lindsay JG (1989) Component X of mammalian pyruvate dehydrogenase complex: structural and functional relationship to the lipoate acetyltransferase (E2) component. *FEBS Lett* **253**, 11-5.

Neagle JC & Lindsay JG (1991) Selective proteolysis of the protein X subunit of the bovine heart pyruvate dehydrogenase complex. Effects on dihydrolipoamide dehydrogenase (E3) affinity and enzymic properties of the complex. *Biochem J* **278 (Pt 2)**, 423-7.

Nellis MM & Danner DJ (2001) Gene preference in maple syrup urine disease. *Am J Hum Genet* **68**, 232-7.

Neupert W (1997) Protein import into mitochondria. *Annu Rev Biochem* **66**, 863-917.

Nishio A, Keeffe EB & Gershwin ME (2001) Primary biliary cirrhosis: lessons learned from an organ-specific disease. *Clin Exp Med* **1**, 165-78.

Nishio A, Van de Water J, Leung PS, Joplin R, Neuberger JM, Lake J, Bjorkland A, Totterman TH, Peters M, Worman HJ, Ansari AA, Coppel RL & Gershwin ME (1997) Comparative studies of antimitochondrial autoantibodies in sera and bile in primary biliary cirrhosis. *Hepatology* **25**, 1085-9.

Nobukuni Y, Mitsubuchi H, Endo F, Akaboshi I, Asaka J & Matsuda I (1990) Maple syrup urine disease. Complete primary structure of the E1 beta subunit of human branched chain alpha-ketoacid dehydrogenase complex deduced from the nucleotide sequence and a gene analysis of patients with this disease. *J Clin Invest* **86**, 242-7.

Obermayer-Straub P, Strassburg CP & Manns MP (2000) Autoimmune hepatitis. *J Hepatol* **32**, 181-97.

Odievre MH, Chretien D, Munnich A, Robinson BH, Dumoulin R, Masmoudi S, Kadhom N, Rotig A, Rustin P & Bonnefont JP (2005) A novel mutation in the dihydrolipoamide dehydrogenase E3 subunit gene (DLD) resulting in an atypical form of alpha-ketoglutarate dehydrogenase deficiency. *Hum Mutat* **25**, 323-4.

Odin JA, Huebert RC, Casciola-Rosen L, LaRusso NF & Rosen A (2001) Bcl-2-dependent oxidation of pyruvate dehydrogenase-E2, a primary biliary cirrhosis autoantigen, during apoptosis. *J Clin Invest* **108**, 223-32.

Packman LC, Borges A & Perham RN (1988) Amino acid sequence analysis of the lipoyl and peripheral subunit-binding domains in the lipoate acetyltransferase component of the pyruvate dehydrogenase complex from *Bacillus stearothermophilus*. *Biochem J* **252**, 79-86.

Palmer JM, Jones DE, Quinn J, McHugh A & Yeaman SJ (1999) Characterization of the autoantibody responses to recombinant E3 binding protein (protein X) of pyruvate dehydrogenase in primary biliary cirrhosis. *Hepatology* **30**, 21-6.

Palmer JM, Robe AJ, Burt AD, Kirby JA & Jones DE (2004) Covalent modification as a mechanism for the breakdown of immune tolerance to pyruvate dehydrogenase complex in the mouse. *Hepatology* **39**, 1583-92.

Paradis V, Kollinger M, Fabre M, Holstege A, Poynard T & Bedossa P (1997) In situ detection of lipid peroxidation by-products in chronic liver diseases. *Hepatology* **26**, 135-42.

Patel MS & Harris RA (1995) Mammalian alpha-keto acid dehydrogenase complexes: gene regulation and genetic defects. *Faseb J* **9**, 1164-72.

Patel MS & Korotchkina LG (2001) Regulation of mammalian pyruvate dehydrogenase complex by phosphorylation: complexity of multiple phosphorylation sites and kinases. *Exp Mol Med* **33**, 191-7.

Patel MS & Korotchkina LG (2006) Regulation of the pyruvate dehydrogenase complex. *Biochem Soc Trans* **34**, 217-22.

Patel MS, Naik S, Wexler ID & Kerr DS (1995) Gene regulation and genetic defects in the pyruvate dehydrogenase complex. *J Nutr* **125**, 1753S-1757S.

Patel MS & Roche TE (1990) Molecular biology and biochemistry of pyruvate dehydrogenase complexes. *Faseb J* **4**, 3224-33.

Perham RN (1991) Domains, motifs, and linkers in 2-oxo acid dehydrogenase multienzyme complexes: a paradigm in the design of a multifunctional protein. *Biochemistry* **30**, 8501-12.

Perham RN (2000) Swinging arms and swinging domains in multifunctional enzymes: catalytic machines for multistep reactions. *Annu Rev Biochem* **69**, 961-1004.

Perham RN & Packman LC (1989) 2-Oxo acid dehydrogenase multienzyme complexes: domains, dynamics, and design. *Ann N Y Acad Sci* **573**, 1-20.

Pettit FH, Hamilton L, Munk P, Namihira G, Eley MH, Willms CR & Reed LJ (1973) Alpha-keto acid dehydrogenase complexes. XIX. Subunit structure of the *Escherichia coli* alpha-ketoglutarate dehydrogenase complex. *J Biol Chem* **248**, 5282-90.

Pettit FH, Roche TE & Reed LJ (1972) Function of calcium ions in pyruvate dehydrogenase phosphatase activity. *Biochem Biophys Res Commun* **49**, 563-71.
Pfanner N (2000) Protein sorting: recognizing mitochondrial presequences. *Curr Biol* **10**, R412-5.

Pfanner N & Wiedemann N (2002) Mitochondrial protein import: two membranes, three translocases. *Curr Opin Cell Biol* **14**, 400-11.

Pons G, Raefsky-Estrin C, Carothers DJ, Pepin RA, Javed AA, Jesse BW, Ganapathi MK, Samols D & Patel MS (1988) Cloning and cDNA sequence of the dihydrolipoamide dehydrogenase component human alpha-ketoacid dehydrogenase complexes. *Proc Natl Acad Sci U S A* **85**, 1422-6.

Popov KM, Hawes JW & Harris RA (1997) Mitochondrial alpha-ketoacid dehydrogenase kinases: a new family of protein kinases. *Adv Second Messenger Phosphoprotein Res* **31**, 105-11.

Popov KM, Kedishvili NY, Zhao Y, Shimomura Y, Crabb DW & Harris RA (1993) Primary structure of pyruvate dehydrogenase kinase establishes a new family of eukaryotic protein kinases. *J Biol Chem* **268**, 26602-6.

Potter KN, Thomson RK, Hamblin A, Richards SD, Lindsay JG & Stevenson FK (2001) Immunogenetic analysis reveals that epitope shifting occurs during B-cell affinity maturation in primary biliary cirrhosis. *J Mol Biol* **306**, 37-46.

Prasad PD, Wang H, Kekuda R, Fujita T, Fei YJ, Devoe LD, Leibach FH & Ganapathy V (1998) Cloning and functional expression of a cDNA encoding a mammalian sodium-dependent vitamin transporter mediating the uptake of pantothenate, biotin, and lipoate. *J Biol Chem* **273**, 7501-6.

Quinn J, Diamond AG, Palmer JM, Bassendine MF, James OF & Yeaman SJ (1993a) Lipoylated and unlipoylated domains of human PDC-E2 as autoantigens in primary biliary cirrhosis: significance of lipoate attachment. *Hepatology* **18**, 1384-91.

Quinn J, Diamond AG, Masters AK, Brookfield DE, Wallis NG & Yeaman SJ (1993b) Expression and lipoylation in *Escherichia coli* of the inner lipoyl domain of the E2 component of the human pyruvate dehydrogenase complex. *Biochem J* **289 (Pt 1)**, 81-5.

Rahmatullah M, Gopalakrishnan S, Andrews PC, Chang CL, Radke GA & Roche TE (1989) Subunit associations in the mammalian pyruvate dehydrogenase complex. Structure and role of protein X and the pyruvate dehydrogenase component binding domain of the dihydrolipoyl transacetylase component. *J Biol Chem* **264**, 2221-7.

Rahmatullah M, Jilka JM, Radke GA & Roche TE (1986) Properties of the pyruvate dehydrogenase kinase bound to and separated from the dihydrolipoyl transacetylase-

protein X subcomplex and evidence for binding of the kinase to protein X. *J Biol Chem* **261**, 6515-23.

Rahmatullah M, Radke GA, Andrews PC & Roche TE (1990) Changes in the core of the mammalian-pyruvate dehydrogenase complex upon selective removal of the lipoyl domain from the transacetylase component but not from the protein X component. *J Biol Chem* **265**, 14512-7.

Ramadan DG, Head RA, Al-Tawari A, Habeeb Y, Zaki M, Al-Ruqum F, Besley GT, Wraith JE, Brown RM & Brown GK (2004) Lactic acidosis and developmental delay due to deficiency of E3 binding protein (protein X) of the pyruvate dehydrogenase complex. *J Inherit Metab Dis* **27**, 477-85.

Rao T & Richardson B (1999) Environmentally induced autoimmune diseases: potential mechanisms. *Environ Health Perspect* **107 Suppl 5**, 737-42.

Reche P, Li YL, Fuller C, Eichhorn K & Perham RN (1998) Selectivity of post-translational modification in biotinylated proteins: the carboxy carrier protein of the acetyl-CoA carboxylase of *Escherichia coli*. *Biochem J* **329 (Pt 3)**, 589-96.

Reed KE & Cronan JE, Jr. (1993) Lipoic acid metabolism in *Escherichia coli:* sequencing and functional characterization of the *lipA* and *lipB* genes. *J Bacteriol* **175**, 1325-36.

Reed KE, Morris TW & Cronan JE, Jr. (1994) Mutants of *Escherichia coli* K-12 that are resistant to a selenium analog of lipoic acid identify unknown genes in lipoate metabolism. *Proc Natl Acad Sci U S A* **91**, 3720-4.

Reed LJ & Hackert ML (1990) Structure-function relationships in dihydrolipoamide acyltransferases. *J Biol Chem* **265**, 8971-4.

Reed LJ & Oliver RM (1968) The multienzyme alpha-keto acid dehydrogenase complexes. *Brookhaven Symp Biol* **21**, 397-412.

Rice JE, Dunbar B & Lindsay JG (1992) Sequences directing dihydrolipoamide dehydrogenase (E3) binding are located on the 2-oxoglutarate dehydrogenase (E1) component of the mammalian 2-oxoglutarate dehydrogenase multienzyme complex. *Embo J* **11**, 3229-35.

Rieger R, Leung PS, Jeddeloh MR, Kurth MJ, Nantz MH, Lam KS, Barsky D, Ansari AA, Coppel RL, Mackay IR & Gershwin ME (2006) Identification of 2-nonynoic acid, a cosmetic component, as a potential trigger of primary biliary cirrhosis. *J Autoimmun* **27**, 7-16.

Risch N (2000) Searching for genes in complex diseases: lessons from systemic lupus erythematosus. *J Clin Invest* **105**, 1503-6.

Robien MA, Clore GM, Omichinski JG, Perham RN, Appella E, Sakaguchi K & Gronenborn AM (1992) Three-dimensional solution structure of the E3-binding domain of the dihydrolipoamide succinyltransferase core from the 2-oxoglutarate dehydrogenase multienzyme complex of *Escherichia coli*. *Biochemistry* **31**, 3463-71.

Roise D (1997) Recognition and binding of mitochondrial presequences during the import of proteins into mitochondria. *J Bioenerg Biomembr* **29**, 19-27.

Rose NR (2000) Viral damage or 'molecular mimicry'-placing the blame in myocarditis. *Nat Med* **6**, 631-2.

Russell GC & Guest JR (1991) Sequence similarities within the family of dihydrolipoamide acyltransferases and discovery of a previously unidentified fungal enzyme. *Biochim Biophys Acta* **1076**, 225-32.

Saijo T, Naito E, Ito M, Yokota I, Matsuda J & Kuroda Y (1996) Stable restoration of pyruvate dehydrogenase complex in E1-defective human lymphoblastoid cells: evidence that three C-terminal amino acids of E1 alpha are essential for the structural integrity of heterotetrameric E1. *Biochem Biophys Res Commun* **228**, 446-51.

Sakaguchi S (2000) Animal models of autoimmunity and their relevance to human diseases. *Curr Opin Immunol* **12**, 684-90.

Sambrook J, Fritch EF & Maniatis T (1989) Molecular cloning. a laboratory manual. second edition. *Cold Spring Harbour Laboratory Press.*

Sanderson SJ, Miller C & Lindsay JG (1996a) Stoichiometry, organisation and catalytic function of protein X of the pyruvate dehydrogenase complex from bovine heart. *Eur J Biochem* **236**, 68-77.

Sanderson SJ, Khan SS, McCartney RG, Miller C & Lindsay JG (1996b) Reconstitution of mammalian pyruvate dehydrogenase and 2-oxoglutarate dehydrogenase complexes: analysis of protein X involvement and interaction of homologous and heterologous dihydrolipoamide dehydrogenases. *Biochem J* **319 (Pt 1)**, 109-16.

Sasaki M, Ansari A, Pumford N, van de Water J, Leung PS, Humphries KM, Szweda LI, Nakanuma Y, Roche TE, Coppel RL, Bach JF & Gershwin ME (2000) Comparative immunoreactivity of anti-trifluoroacetyl (TFA) antibody and anti-lipoic acid antibody in primary biliary cirrhosis: searching for a mimic. *J Autoimmun* **15**, 51-60.

Schleyer M, Schmidt B & Neupert W (1982) Requirement of a membrane potential for the posttranslational transfer of proteins into mitochondria. *Eur J Biochem* **125**, 109-16.

Schulze E, Benen JA, Westphal AH & de Kok A (1991) Interaction of lipoamide dehydrogenase with the dihydrolipoyl transacetylase component of the pyruvate dehydrogenase complex from *Azotobacter vinelandii*. *Eur J Biochem* **200**, 29-34.

Selmi C, Invernizzi P, Keeffe EB, Coppel RL, Podda M, Rossaro L, Ansari AA & Gershwin ME (2004) Epidemiology and pathogenesis of primary biliary cirrhosis. *J Clin Gastroenterol* **38**, 264-71.

Seyda A, McEachern G, Haas R & Robinson BH (2000) Sequential deletion of C-terminal amino acids of the E(1)alpha component of the pyruvate dehydrogenase (PDH) complex leads to reduced steady-state levels of functional E(1) alpha(2) beta(2) tetramers: implications for patients with PDH deficiency. *Hum Mol Genet* **9**, 1041-8.

Shany E, Saada A, Landau D, Shaag A, Hershkovitz E & Elpeleg ON (1999) Lipoamide dehydrogenase deficiency due to a novel mutation in the interface domain. *Biochem Biophys Res Commun* **262**, 163-6.

Sheffield WP, Shore GC & Randall SK (1990) Mitochondrial precursor protein. Effects of 70-kilodalton heat shock protein on polypeptide folding, aggregation, and import competence. *J Biol Chem* **265**, 11069-76.

Shimoda S, Nakamura M, Ishibashi H, Hayashida K & Niho Y (1995) HLA DRB4 0101-restricted immunodominant T cell autoepitope of pyruvate dehydrogenase complex in primary biliary cirrhosis: evidence of molecular mimicry in human autoimmune diseases. *J Exp Med* **181**, 1835-45.

Shimoda S, Nakamura M, Shigematsu H, Tanimoto H, Gushima T, Gershwin ME & Ishibashi H (2000) Mimicry peptides of human PDC-E2 163-176 peptide, the immunodominant T-cell epitope of primary biliary cirrhosis. *Hepatology* **31**, 1212-6.

Shimoda S, Van de Water J, Ansari A, Nakamura M, Ishibashi H, Coppel RL, Lake J, Keeffe EB, Roche TE & Gershwin ME (1998) Identification and precursor frequency analysis of a common T cell epitope motif in mitochondrial autoantigens in primary biliary cirrhosis. *J Clin Invest* **102**, 1831-40.

Smith DA & Germolec DR (1999) Introduction to immunology and autoimmunity. *Environ Health Perspect* **107 Suppl 5**, 661-5.

Smolle M, Prior AE, Brown AE, Cooper A, Byron O & Lindsay JG (2006) A new level of architectural complexity in the human pyruvate dehydrogenase complex. *J Biol Chem* **281**, 19772-80.

Sokol RJ, Straka MS, Dahl R, Devereaux MW, Yerushalmi B, Gumpricht E, Elkins N & Everson G (2001) Role of oxidant stress in the permeability transition induced in rat hepatic mitochondria by hydrophobic bile acids. *Pediatr Res* **49**, 519-31.

Sokol RJ, Winklhofer-Roob BM, Devereaux MW & McKim JM, Jr. (1995) Generation of hydroperoxides in isolated rat hepatocytes and hepatic mitochondria exposed to hydrophobic bile acids. *Gastroenterology* **109**, 1249-56.

Stanley CJ & Perham RN (1980) Purification of 2-oxo acid dehydrogenase multienzyme complexes from ox heart by a new method. *Biochem J* **191**, 147-54.

Starkov AA, Fiskum G, Chinopoulos C, Lorenzo BJ, Browne SE, Patel MS & Beal MF (2004) Mitochondrial alpha-ketoglutarate dehydrogenase complex generates reactive oxygen species. *J Neurosci* **24**, 7779-88.

Stepp LR, Pettit FH, Yeaman SJ & Reed LJ (1983) Purification and properties of pyruvate dehydrogenase kinase from bovine kidney. *J Biol Chem* **258**, 9454-8.

Stepp LR & Reed LJ (1985) Active-site modification of mammalian pyruvate dehydrogenase by pyridoxal 5'-phosphate. *Biochemistry* **24**, 7187-91.

Steussy CN, Popov KM, Bowker-Kinley MM, Sloan RB, Jr., Harris RA & Hamilton JA (2001) Structure of pyruvate dehydrogenase kinase. Novel folding pattern for a serine protein kinase. *J Biol Chem* **276**, 37443-50.

Stojanovski D, Johnston AJ, Streimann I, Hoogenraad NJ & Ryan MT (2003) Import of nuclear-encoded proteins into mitochondria. *Exp Physiol* **88**, 57-64.

Stoops JK, Cheng RH, Yazdi MA, Maeng CY, Schroeter JP, Klueppelberg U, Kolodziej SJ, Baker TS & Reed LJ (1997) On the unique structural organization of the *Saccharomyces cerevisiae* pyruvate dehydrogenase complex. *J Biol Chem* **272**, 5757-64.

Sugden MC & Holness MJ (2003) Recent advances in mechanisms regulating glucose oxidation at the level of the pyruvate dehydrogenase complex by PDKs. *Am J Physiol Endocrinol Metab* **284**, E855-62.

Sundin U & Sundqvist KG (1991) Plasma membrane association of primary biliary cirrhosis mitochondrial marker antigen M2. *Clin Exp Immunol* **83**, 407-12.

Surh CD, Coppel R & Gershwin ME (1990a) Structural requirement for autoreactivity on human pyruvate dehydrogenase-E2, the major autoantigen of primary biliary cirrhosis. Implication for a conformational autoepitope. *J Immunol* **144**, 3367-74.

Surh CD, Ahmed-Ansari A & Gershwin ME (1990b) Comparative epitope mapping of murine monoclonal and human autoantibodies to human PDH-E2, the major mitochondrial autoantigen of primary biliary cirrhosis. *J Immunol* **144**, 2647-52.

Surh CD, Roche TE, Danner DJ, Ansari A, Coppel RL, Prindiville T, Dickson ER & Gershwin ME (1989a) Antimitochondrial autoantibodies in primary biliary cirrhosis recognize cross-reactive epitope(s) on protein X and dihydrolipoamide acetyltransferase of pyruvate dehydrogenase complex. *Hepatology* **10**, 127-33.

Surh CD, Danner DJ, Ahmed A, Coppel RL, Mackay IR, Dickson ER & Gershwin ME (1989b) Reactivity of primary biliary cirrhosis sera with a human fetal liver cDNA clone of branched-chain alpha-keto acid dehydrogenase dihydrolipoamide acyltransferase, the 52 kDa mitochondrial autoantigen. *Hepatology* **9**, 63-8.

Tanaka A, Borchers AT, Ishibashi H, Ansari AA, Keen CL & Gershwin ME (2001) Genetic and familial considerations of primary biliary cirrhosis. *Am J Gastroenterol* **96**, 8-15.

Teague WM, Pettit FH, Wu TL, Silberman SR & Reed LJ (1982) Purification and properties of pyruvate dehydrogenase phosphatase from bovine heart and kidney. *Biochemistry* **21**, 5585-92.

Teoh KL, Mackay IR, Rowley MJ & Fussey SP (1994) Enzyme inhibitory autoantibodies to pyruvate dehydrogenase complex in primary biliary cirrhosis differ for mammalian, yeast and bacterial enzymes: implications for molecular mimicry. *Hepatology* **19**, 1029-33.

Thekkumkara TJ, Ho L, Wexler ID, Pons G, Liu TC & Patel MS (1988) Nucleotide sequence of a cDNA for the dihydrolipoamide acetyltransferase component of human pyruvate dehydrogenase complex. *FEBS Lett* **240**, 45-8.

Thomson RK, Davis Z, Palmer JM, Arthur MJ, Yeaman SJ, Chapman CJ, Spellerberg MB & Stevenson FK (1998) Immunogenetic analysis of a panel of monoclonal IgG and

IgM anti-PDC-E2/X antibodies derived from patients with primary biliary cirrhosis. *J Hepatol* **28**, 582-94.

Tinmouth J, Lee M, Wanless IR, Tsui FW, Inman R & Heathcote EJ (2002) Apoptosis of biliary epithelial cells in primary biliary cirrhosis and primary sclerosing cholangitis. *Liver* **22**, 228-34.

Toyoda T, Suzuki K, Sekiguchi T, Reed LJ & Takenaka A (1998) Crystal structure of eucaryotic E3, lipoamide dehydrogenase from yeast. *J Biochem (Tokyo)* **123**, 668-74.

Tretter L & Adam-Vizi V (2004) Generation of reactive oxygen species in the reaction catalyzed by alpha-ketoglutarate dehydrogenase. *J Neurosci* **24**, 7771-8.

Tsuji K, Watanabe Y, Van De Water J, Nakanishi T, Kajiyama G, Parikh-Patel A, Coppel R & Gershwin ME (1999) Familial primary biliary cirrhosis in Hiroshima. *J Autoimmun* **13**, 171-8.

Tsuneyama K, Harada K, Kono N, Sasaki M, Saito T, Gershwin ME, Ikemoto M, Arai H & Nakanuma Y (2002) Damaged interlobular bile ducts in primary biliary cirrhosis show reduced expression of glutathione-S-transferase-pi and aberrant expression of 4-hydroxynonenal. *J Hepatol* **37**, 176-83.

Tsuneyama K, Van De Water J, Van Thiel D, Coppel R, Ruebner B, Nakanuma Y, Dickson ER & Gershwin ME (1995) Abnormal expression of PDC-E2 on the apical surface of biliary epithelial cells in patients with antimitochondrial antibody-negative primary biliary cirrhosis. *Hepatology* **22**, 1440-6.

Tuaillon N, Andre C, Briand JP, Penner E & Muller S (1992) A lipoyl synthetic octadecapeptide of dihydrolipoamide acetyltransferase specifically recognized by anti-M2 autoantibodies in primary biliary cirrhosis. *J Immunol* **148**, 445-50.

Turner SL, Russell GC, Williamson MP & Guest JR (1993) Restructuring an interdomain linker in the dihydrolipoamide acetyltransferase component of the pyruvate dehydrogenase complex of *Escherichia coli. Protein Eng* **6**, 101-8.

Van de Water J, Ansari A, Prindiville T, Coppel RL, Ricalton N, Kotzin BL, Liu S, Roche TE, Krams SM, Munoz S & Gershwin ME (1995) Heterogeneity of autoreactive T cell clones specific for the E2 component of the pyruvate dehydrogenase complex in primary biliary cirrhosis. *J Exp Med* **181**, 723-33.

Van de Water J, Ansari AA, Surh CD, Coppel R, Roche T, Bonkovsky H, Kaplan M & Gershwin ME (1991) Evidence for the targeting by 2-oxo-dehydrogenase enzymes in the T cell response of primary biliary cirrhosis. *J Immunol* **146**, 89-94.

Van de Water J, Gershwin ME, Leung P, Ansari A & Coppel RL (1988a) The autoepitope of the 74-kD mitochondrial autoantigen of primary biliary cirrhosis corresponds to the functional site of dihydrolipoamide acetyltransferase. *J Exp Med* **167**, 1791-9.

Van de Water J, Fregeau D, Davis P, Ansari A, Danner D, Leung P, Coppel R & Gershwin ME (1988b) Autoantibodies of primary biliary cirrhosis recognize dihydrolipoamide acetyltransferase and inhibit enzyme function. *J Immunol* **141**, 2321-4.

Van de Water J, Ishibashi H, Coppel RL & Gershwin ME (2001) Molecular mimicry and primary biliary cirrhosis: premises not promises. *Hepatology* **33**, 771-5.

Van de Water J, Turchany J, Leung PS, Lake J, Munoz S, Surh CD, Coppel R, Ansari A, Nakanuma Y & Gershwin ME (1993) Molecular mimicry in primary biliary cirrhosis. Evidence for biliary epithelial expression of a molecule cross-reactive with pyruvate dehydrogenase complex-E2. *J Clin Invest* **91**, 2653-64.

Vanden Boom TJ, Reed KE & Cronan JE, Jr. (1991) Lipoic acid metabolism in *Escherichia coli*: isolation of null mutants defective in lipoic acid biosynthesis, molecular cloning and characterization of the *E. coli* lip locus, and identification of the lipoylated protein of the glycine cleavage system. *J Bacteriol* **173**, 6411-20.

Vessey DA, Kelley M & Warren RS (1999) Characterization of the CoA ligases of human liver mitochondria catalyzing the activation of short- and medium-chain fatty acids and xenobiotic carboxylic acids. *Biochim Biophys Acta* **1428**, 455-62.

Vessey DA, Lau E & Kelley M (2000) Isolation and sequencing of cDNAs for the XL-I and XL-III forms of bovine liver xenobiotic-metabolizing medium-chain fatty acid:CoA ligase. *J Biochem Mol Toxicol* **14**, 11-9.

Vilagut L, Vila J, Vinas O, Pares A, Gines A, Jimenez de Anta MT & Rodes J (1994) Cross-reactivity of anti-Mycobacterium gordonae antibodies with the major mitochondrial autoantigens in primary biliary cirrhosis. *J Hepatol* **21**, 673-7.

Voos W & Rottgers K (2002) Molecular chaperones as essential mediators of mitochondrial biogenesis. *Biochim Biophys Acta* **1592**, 51-62.

Walker JG, Doniach D, Roitt IM & Sherlock S (1965) Serological Tests in Diagnosis of Primary Biliary Cirrhosis. *Lancet* **39**, 827-31.

Wallis NG, Allen MD, Broadhurst RW, Lessard IA & Perham RN (1996) Recognition of a surface loop of the lipoyl domain underlies substrate channelling in the pyruvate dehydrogenase multienzyme complex. *J Mol Biol* **263**, 463-74.

Wallis NG & Perham RN (1994) Structural dependence of post-translational modification and reductive acetylation of the lipoyl domain of the pyruvate dehydrogenase multienzyme complex. *J Mol Biol* **236**, 209-16.

Weber P, Brenner J, Stechemesser E, Klein R, Weckenmann U, Kloppel G, Kirchhof M, Fintelmann V & Berg PA (1986) Characterization and clinical relevance of a new complement-fixing antibody--anti-M8--in patients with primary biliary cirrhosis. *Hepatology* **6**, 553-9.

Wynn RM, Chuang JL, Davie JR, Fisher CW, Hale MA, Cox RP & Chuang DT (1992) Cloning and expression in *Escherichia coli* of mature E1 beta subunit of bovine mitochondrial branched-chain alpha-keto acid dehydrogenase complex. Mapping of the E1 beta-binding region on E2. *J Biol Chem* **267**, 1881-7.

Yeaman SJ, Fussey SP, Danner DJ, James OF, Mutimer DJ & Bassendine MF (1988) Primary biliary cirrhosis: identification of two major M2 mitochondrial autoantigens. *Lancet* **1**, 1067-70.

Yeaman SJ, Hutcheson ET, Roche TE, Pettit FH, Brown JR, Reed LJ, Watson DC & Dixon GH (1978) Sites of phosphorylation on pyruvate dehydrogenase from bovine kidney and heart. *Biochemistry* **17**, 2364-70.

Yeaman SJ, Kirby JA & Jones DE (2000) Autoreactive responses to pyruvate dehydrogenase complex in the pathogenesis of primary biliary cirrhosis. *Immunol Rev* **174**, 238-49.

Young JC, Gould JA, Kola I & Iannello RC (1998) Review: *Pdha-2*, past and present. *J Exp Zool* **282**, 231-8.

Zhao X, Miller JR, Jiang Y, Marletta MA & Cronan JE (2003) Assembly of the covalent linkage between lipoic acid and its cognate enzymes. *Chem Biol* **10**, 1293-302.

Appendices

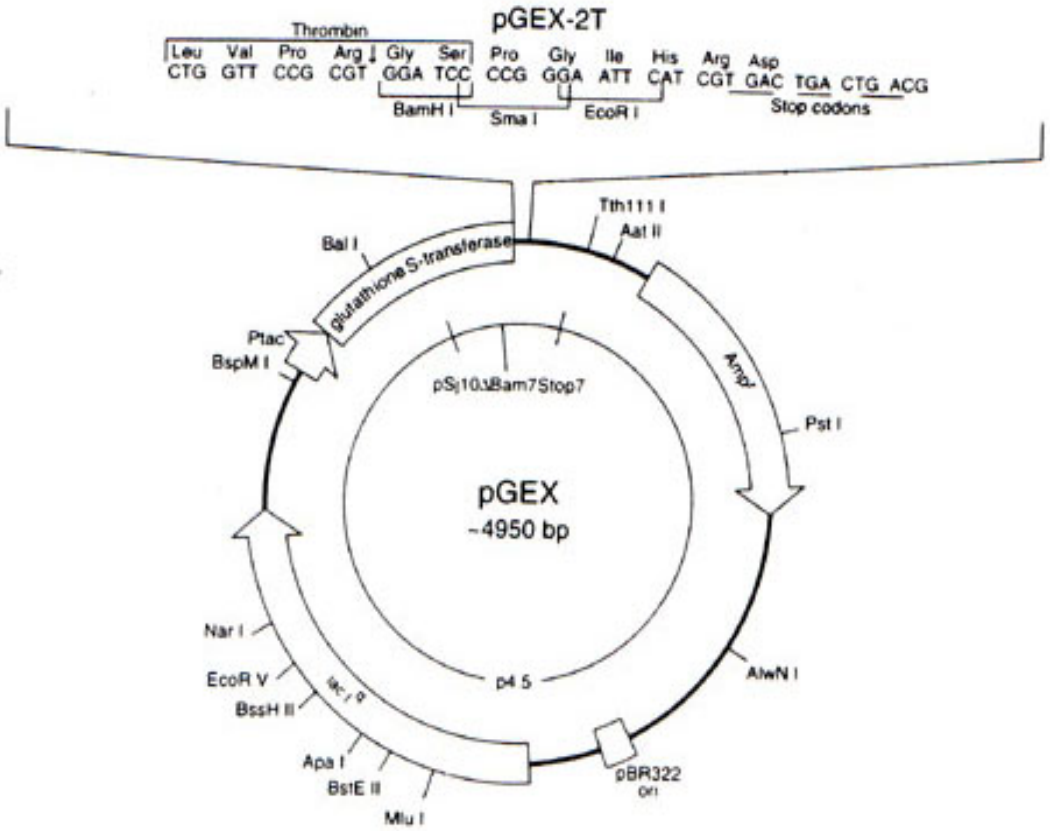

pGEX-2T sequence landmarks

tac promtor-10	205-211
tac promoter-35	183-188
GST gene region	258-918
Thrombin cleavage region	918-935
Multiple cloning sites	930-945
B-lactamase gene region	1309-2214
*lac*I^{q} gene region	3297-4377
Plasmid replication origion	2974

Appendix 1 Map of the glutathione S-transferase fusion vector pGEX-2T
pGEX-2T carries an N-terminal glutathione S-transferase-Tag sequence followed by a thrombin cleavage site and the multiple cloning site (BamHI-EcoRI). The cloning region is shown in detail above the plasmid

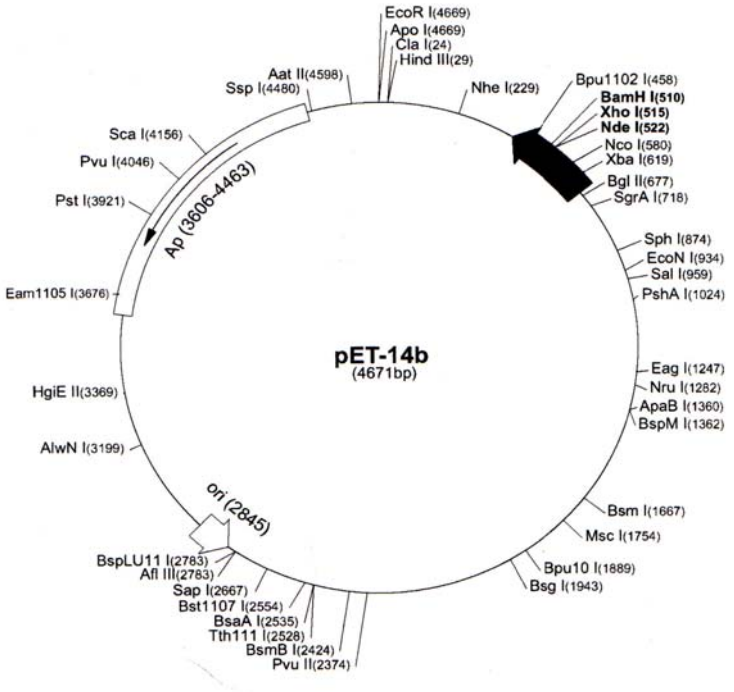

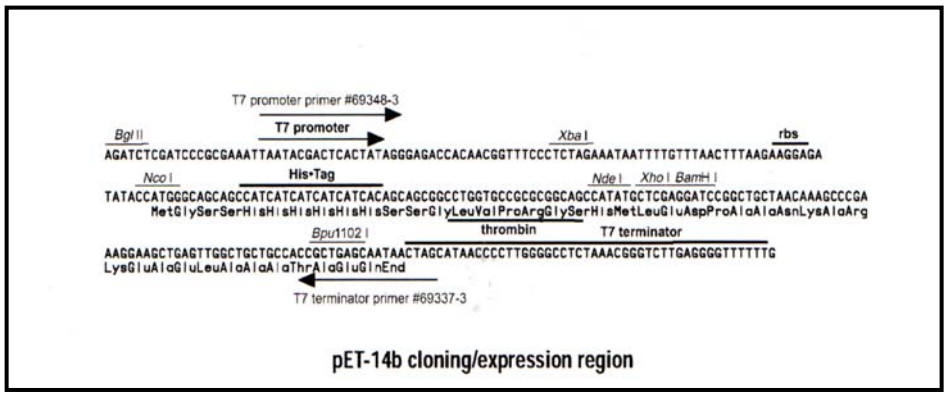

pET-14b sequence landmarks

T7 promoter	646-662
T7 transcription start	645
His-tag coding sequence	554-571
Multiple cloning sites	
(*Nde*I-*Bam*HI)	510-526
T7 terminator	404-450
pBR322 origion	2845
bla coding sequence	3606-4463

Appendix 2 Plasmid map of the pET-14b cloning/expression vector

The pET-14b vector carries an N-terminal His-tag sequence followed by a thrombin site and three cloning sites (NdeI-BamHI). Unique sites are shown on the circle map. The cloning/expression region of the coding strand transcribed bt T7 RNA polymerase is shown in more details in the box

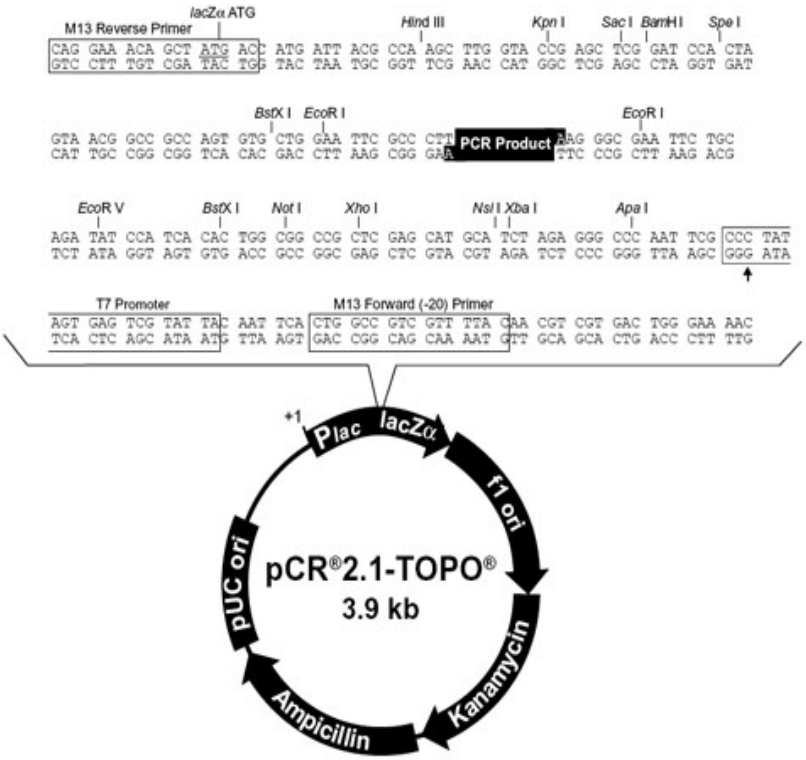

pCR®2.1 TOPO® 3931 nucleotides

LacZα fragment: bses	1-547
M13 reverse priming site: bases	205-221
Multiple cloning site: bases	234-357
T7 promoter/priming site: bases	364-383
M13 forward (-20) priming site: bases	391-406
F1 origion: bases	548-985
Kanamycin resistance ORF: bases	1319-2113
Ampicillin resistance ORF: bases	2131-2991
pUC origion: bases	3136-3809

Appendix 3 Map of the pCR® 2.1-TOPO® cloning vector

The map above shows the features of pCR®2.1-TOPO® and the sequence surrounding the TOPO® cloning site. Restriction sites are labelled to indicate the actual cleavage site. The arrow indicates the start of transcription for T7 polymerase.